Development and optimization of a workflow to enable mass-spectrometry based quantitative membrane proteomics of mature and tolerogenic dendritic cells

Matthew P. Buck

Thesis submitted for Doctor of Philosophy

Institute of Cellular Medicine, Newcastle University

March 2014

Abstract

Tolerogenic dendritic cells are monocyte-derived dendritic cells (DC) cultured such that they adopt an immunoregulatory phenotype. *In vitro*, these cells are able to induce and maintain T cell tolerance through deviation of naive T cells to an anti-inflammatory phenotype and induction of anergy in memory T cells. Equivalent cells suppress established arthritis in murine models and tolerogenic DC are presently the subject of a phase I safety and efficacy trial at Newcastle University as part of the AutoDeCRA study. However, in spite of these promising data, we are yet to rigorously explore the basis of the phenotype of tolerogenic DC and lack markers to unequivocally distinguish them from other types of DC.

This body of work is concerned with the development of a workflow to enable these questions to be addressed using mass spectrometry-based quantitative proteomics. Specifically, methods have been optimized and validated to enable **a)** enrichment and proteolytic digestion of membrane proteins, favouring their detection over more abundant cytoplasmic and nuclear proteins in LC/MS; **b)** differential stable isotope labelling of peptide N- and C-termini, enabling 'isobaric peptide termini labelling'-based relative quantitation at the MS2 level; **c)** pipette-tip based anion exchange fractionation of IPTL-labelled peptides prior to LC/MS analysis, broadening depth of proteome coverage. Efforts to apply aspects of the workflow to perform quantitative comparisons of the whole cell proteomes and qualitative profiling of the membrane proteomes of mature and tolerogenic DC are also documented.

It is envisaged that future application of this optimized workflow as a whole will enable the identification and relative quantitation of significant numbers of mature and tolerogenic DC plasma membrane proteins. Differentially expressed proteins of interest identified through this approach may then be further investigated for putative roles in tolerance induction.

Contents

Abstract ii
Figures and Tables xi
Abbreviations xxii

Chapter 1. Introduction 1

1.1. Proteomics 2
1.1.1. Top-down or bottom-up? 3
1.1.2. The Bottom-up Proteomics Workflow 4
1.1.2.1. Protein Extraction and Isolation 6
1.1.2.2. Protein Fractionation 6
1.1.2.3. Protein Digestion 7
1.1.2.4. Peptide Fractionation 8
1.1.2.5. Mass Spectrometry 9
1.1.2.5.1. Ion Sources 9
1.1.2.5.2. Mass Analysers 10
1.1.2.6. Mass Spectrometric Peptide Analysis 12
1.1.2.6.1. Peptide mass fingerprinting 12
1.1.2.6.2. Accurate mass and time tag 12
1.1.2.6.3. Tandem mass spectrometry 13
1.1.2.6.3.1. Precursor Ion Selection 15
1.1.2.6.3.2. Precursor Ion Fragmentation 15
1.1.2.6.3.3. Precursor Ion Identification 16
1.1.2.6.3.4. Protein Identification 18
1.1.3. Plasma Membrane Proteomics 19
1.1.3.1. Types of Membrane Protein 19
1.1.3.2. Challenges of Plasma Membrane Proteomics 20
1.1.3.3. Plasma Membrane Protein Enrichment 21
1.1.3.4. Plasma Membrane Protein Solubilization and Digestion 23
1.1.3.4.1. Detergents 23
1.1.3.4.2. Chaotropes 25
1.1.3.4.3. Solvents and Acids 25
1.1.3.4.4. Integrated Workflows 25
1.1.4. Quantitative Proteomics 27
1.1.4.1. Label-based Quantitative Proteomics (MS1) 29

1.1.4.1.1. Chemical Labelling 29
1.1.4.1.2. Enzymatic Labelling 29
1.1.4.1.3. Metabolic Labelling 30
1.1.4.2. Label-based Quantitative Proteomics (MS2) 31
1.1.4.3. Absolute Quantitation 32
1.1.4.4. Label Free Quantitative Proteomics 32
1.1.4.5. Quantitation Software 33

1.2. Dendritic Cells 35
1.2.1. Dendritic cells and immunological tolerance 35
1.2.2. Functional specialization of dendritic cell subsets 36
1.2.3. Dendritic cells in immunity and tolerance 37
1.2.3.1. Dendritic cells in immunity 37
1.2.3.2. Dendritic cells in tolerance 38
1.2.4. Mechanisms of tolerance induction 41
1.2.5. Molecules of tolerance induction 42
1.2.6. Using tolerogenic dendritic cells to treat autoimmune disease 43
1.2.7. Autologous Dendritic Cells for Rheumatoid Arthritis - the AuToDeCRA study at Newcastle University 45
1.2.8. Exploring the cell surface phenotype of tolerogenic dendritic cells 48
1.2.9. Previous dendritic cell proteomic studies 48
1.2.9.1. Proteomics of DC maturation 49
1.2.9.2. Proteomics of differentially matured DC 50

Chapter 2. Aims and Objectives 53

Chapter 3. Methods 55

3.1. Cell culture 56
3.1.1. Jurkat T cells 56
3.1.2. Isolation of cells from peripheral blood 56
3.1.3. Generation of dendritic cell populations 56
3.2. Protein extraction and isolation 57
3.2.1. Whole cell lysate preparation (in-solution digestion) 57
3.2.2. Whole cell lysate preparation (FASP) 57

3.2.3. Cell surface protein isolation with EZ-Link® Sulfo-NHS-SS Biotin and RevAmine 58
3.2.4. Membrane preparation using 'stepwise depletion' 59
3.3. Protein Digestion 61
3.3.1. Detergent removal from whole cell lysates for in-solution digestion 61
3.3.2. In-solution digestion of BSA / whole cell lysates 61
3.3.3. In-solution digestion of 'stepwise depletion' membrane preparations 62
3.3.4. FASP digestion of whole cell lysates and 'stepwise depletion' membrane preparations 63
3.4. Peptide Labelling 65
3.4.1. Desalting of digests prior to peptide labelling 65
3.4.2. C-terminal ^{18}O labelling 65
3.4.3. Lysine guanidination → N-terminal-specific succinylation 66
3.4.4. A novel isobaric peptide termini labelling protocol 69
3.5. Peptide Fractionation 70
3.5.1. Isoelectric Focussing 70
3.5.2. StageTip-based SAX fractionation 71
3.6. Desalting of peptides prior to LC-MS analysis 72
3.7. LC-MS/MS analysis 73
3.8. Data analysis 77
3.9. Miscellaneous 79
3.9.1. BSA labelling with EZ-Link® Sulfo-NHS-SS Biotin and RevAmine 79
3.9.2. MALDI-TOF-MS of EZ-Link® Sulfo-NHS-SS Biotin and RevAmine-labelled BSA 79
3.9.3. Fluorescence confocal microscopy of EZ-Link® Sulfo-NHS-SS Biotin and RevAmine-labelled cells 80

Chapter 4. Development and validation of a membrane enrichment and digestion protocol to favour mass spectrometric identification of membrane proteins 81

4.1. Introduction 82
4.1.1. Challenges of membrane proteomics 82

4.1.2. Criteria for evaluation of the effectiveness of a membrane protein enrichment and digestion strategy 83
4.1.3. Amine-directed biotinylation reagents 85
4.2. Results 89
4.2.1. Characterisation of RevAmine - a novel amine-directed biotinylation reagent 89
4.2.1.1. MALDI-TOF analysis demonstrates facile conjugation of RevAmine tag to intact BSA 89
4.2.1.2. LC-MS analysis demonstrates facile conjugation and traceless removal of RevAmine tag to and from intact BSA prior to tryptic digestion 91
4.2.1.3. Fluorescence confocal microscopy shows RevAmine and EZ-Link™ Sulfo-NHS-SS-Biotin are equally adept at biotinylating cell surface proteins in situ. 97
4.2.2. Evaluation of the suitability of amine-directed biotinylation reagents as tools for enrichment of cell surface proteins for analysis by mass spectrometry. 99
4.2.2.1. Filter-Aided Sample Preparation (FASP) performs as effectively as standard in-solution digestion for processing of whole cell lysates for LC-MS analysis. 100
4.2.2.2. Use of 'EZ-Link™' Sulfo-NHS-SS-Biotin and RevAmine to enrich for plasma membrane proteins prior to LC-MS analysis produces only a small increase in percentage of plasma membrane protein IDs 103
4.2.2.3. The limited enrichment of plasma membrane proteins in membrane fractions prepared using cell surface biotinylation-based approaches is likely due to biotinylation of intracellular proteins 110
4.2.3. Evaluation of the suitability of subcellular fractionation protocols for enrichment of cell surface proteins for analysis by mass spectrometry. 115
4.2.3.1. Crude membrane preparations processed using sequential extraction in high salt, high pH and urea-containing buffers yield a more significant increase in percentage of membrane protein IDs 115

4.2.3.2. Filter-Aided Sample Preparation (FASP) performs more effectively than standard in-solution digestion for processing of crude membrane fractions prepared using 'stepwise depletion' for LC-MS analysis 120
4.3. Discussion 122

Chapter 5. Development and validation of an isobaric peptide termini labelling-based method to facilitate relative quantitative proteomics between two samples 131

5.1. Introduction 132
5.1.1. Requirement for development and validation of alternative stable isotope labelling methods 132
5.1.2. Strategy for development and validation of alternative stable isotope labelling methods 133
5.2. ^{18}O Labelling 134
5.2.1. 'Optimal' ^{18}O Labelling 137
5.2.2. Results and Discussion 139
5.2.2.1. Development of a protocol for optimal C-terminal ^{18}O-labelling of peptides 139
5.2.2.2. Decoupling the carboxyl oxygen exchange reaction from hydrolysis and performing it at pH4.5 with soluble trypsin facilitates labelling of all peptides with two ^{18}O atoms. 139
5.2.2.3. Reducing and alkylating labelled samples with high concentrations of DTT and iodoacetamide prior to resuspension in ^{16}O-based buffers completely abrogates trypsin-catalysed back exchange in labelled peptides. 143
5.2.2.4. Low pH causes small amounts of acid-catalysed back exchange in labelled peptides completely independently of trypsin. 146
5.2.2.5. Optimised protocol for C-terminal ^{18}O labelling of peptides 148
5.2.2.6. Examination of the ability of C-terminal ^{18}O-labelling to quantify differences between labelled and unlabelled proteomic peptides across a wide dynamic range. 148
5.3. Isobaric Peptide Termini Labelling 158

5.3.1. 'Optimal' N-Terminal Labelling 160
5.3.2. Results and Discussion 161
5.3.2.1. Development of a protocol for optimal N-terminal succinylation of peptides 161
5.3.2.2. Peptides cannot be N-terminally succinylated whilst bound to a solid phase extraction column without significant succinylation of lysine side chains. 162
5.3.2.3. Peptides can be specifically guanidinated on lysine side chains whilst bound to a solid phase extraction column 165
5.3.2.4. Guanidination of lysine side chains renders subsequent succinylation N-terminal specific 167
5.3.2.5. Optimised protocol for N-terminal succinylation of peptides 170
5.3.2.6. Examination of the ability of isobaric peptide termini labelling employing both N-terminal succinylation and C-terminal ^{18}O labelling to quantify differences between labelled and unlabelled BSA and proteomic peptides across a wide dynamic range 170

Chapter 6. Evaluation of the suitability of OFFGEL fractionation and StageTip-based SAX fractionation as the first dimension of separation for analysis of complex mixtures of proteomic peptides 175

6.1. Introduction 176
6.2. OFFGEL Fractionation 177
6.2.1. Results 178
6.2.1.1. OFFGEL Fractionation can be used as the first dimension of separation for ^{18}O-based quantitative proteomic experiments. 178
6.2.1.2. OFFGEL Fractionation is less effective when used as the first dimension of separation for IPTL-based quantitative proteomic experiments. 181
6.3. StageTip-based SAX Fractionation 186
6.3.1. Results 187
6.3.1.1. Evaluation of StageTip-based SAX fractionation as an alternative to OFFGEL Fractionation for first-dimensional separation of succinylated peptides 187

6.3.1.2. StageTip-based SAX fractionation is an effective alternative to OFFGEL Fractionation for the first dimension of separation of unmodified and succinylated peptides 187
6.3.1.3. Peptides bound to anion exchange resin in StageTip-based SAX fractionation appear to interact with the polystyrene sorbent of the resin in addition to the quaternary ammonium functional groups 191
6.3.1.4. The ionic interactions of peptides with the resin in StageTip-based SAX fractionation that appears to vary with successive decreases in pH is strongly affected by the presence of acetonitrile in the buffer 195
6.4. Discussion 199

Chapter 7. Application of optimized quantitative and membrane proteomics methods to mature and tolerogenic dendritic cells 201
7.1. Introduction 202
7.2. ^{18}O-based quantitative profiling of the whole cell proteomes of mature and tolerogenic DC 203
7.3. IPTL-based quantitative profiling of the whole cell proteomes of mature and tolerogenic DC 207
7.4. Discussion (whole cell proteomes) 210
7.5. Qualitative profiling of the membrane proteomes of mature and tolerogenic DC 213
7.6. Discussion (membrane proteomes) 221

Chapter 8. General Discussion 225

References 2332

Figures and Tables

Figure 1: A general overview of the bottom-up proteomics workflow 5

Figure 2: MS/MS of a BSA-derived peptide with sequence HLVDEPQNLIK 14

Figure 3: Fragmentation nomenclature for peptide ion cleavages along the polypeptide backbone 16

Figure 4: Membrane protein nomenclature 20

Figure 5: Quantitative proteomic strategies 28

Figure 6: Dendritic cells in immunity and tolerance.....40

Figure 7: Generation of mature and tolerogenic dendritic cells in the immunotherapy group at Newcastle University 47

Figure 8: SPE cartridge configuration for succinylation of bound peptides 67

Figure 9: SPE cartridge configuration for guanidination of bound peptides 68

Figure 10: Biotinylation of proteins using EZ-Link™ Sulfo-NHS-SS-Biotin.....86

Figure 11: Biotinylation of proteins using RevAmine.....88

Figure 12: MALDI mass spectra showing intact mass measurements of a) unmodified BSA; b) BSA modified with EZ-Link™ Sulfo-NHS-SS Biotin; c) BSA modified with RevAmine 90

Figure 13: Unmodified and modified BSA peptides detected by LC-MS after tryptic digestion of EZ-Link™-modified BSA 93

Figure 14: Unmodified and modified BSA peptides detected by LC-MS after tryptic digestion of RevAmine-modified BSA.....94

Figure 15: Unmodified and modified BSA peptides detected by LC-MS after tryptic digestion followed by treatment with 0.1% (v/v) NH_3 of EZ-Link^{TM}-modified BSA 95

Figure 16: Unmodified and modified BSA peptides detected by LC-MS after tryptic digestion followed by treatment with 0.1% (v/v) NH_3 of RevAmine-modified BSA 96

Figure 17: *In situ* biotinylation of cell surface-exposed primary amine residues on Jurkat cells detected through staining with a Streptavidin – Alexa Fluor 568 conjugate followed by fluorescence confocal microscopy 98

Figure 18: Pie charts illustrating the distribution of cellular component ontologies of proteins identified from LC-MS analysis of a Jurkat whole cell lysate digested using a) in-solution digestion; b) FASP 102

Figure 19: Pie charts illustrating the distribution of cellular component ontologies of proteins identified from LC-MS analysis of Jurkat membrane fractions prepared using the Pierce Cell Surface Isolation Kit as per supplied protocol but with Pierce Lysis and Wash Buffers substituted for 0.1 M TRIS-HCl (pH 7.4) supplemented with a) 1% (w/v) SDS; b) 2% (w/v) SDS; c) 4% (w/v) SDS 105

Figure 20: Pie charts illustrating the distribution of cellular component ontologies of proteins identified from LC-MS analysis of a) unlabelled; b) EZ-Link^{TM}-labelled; c) RevAmine-labelled Jurkat membrane fractions prepared using the Pierce Cell Surface Isolation Kit as per supplied protocol (using Pierce Lysis and Wash Buffers) 108

Figure 21: Pie charts illustrating the distribution of cellular component ontologies of proteins identified from LC-MS analysis of a) unlabelled; b) EZ-Link^{TM}-labelled; c) RevAmine-labelled Jurkat membrane fractions prepared using the Pierce Cell Surface Isolation Kit with Pierce Lysis and Wash Buffers substituted for 0.1 M TRIS-HCl (pH 7.4) supplemented with 4% (w/v) SDS and increased incubation time for formation of the avidin-biotin interaction 109

Figure 22: Polyacrylamide gel electrophoresis of unprocessed, flow-through and eluate fractions of a) unlabelled Jurkat cell lysate; b) EZ-Link^{TM}-labelled Jurkat cell lysate processed using the Pierce Cell Surface Isolation Kit as per supplied protocol. 112

Figure 23: *In situ* biotinylation of cell surface-exposed primary amine residues on Jurkat cells detected through staining with a Streptavidin – Alexa Fluor 568 conjugate followed by fluorescence confocal microscopy. a) EZ-Link^{TM}-labelled cells. b) RevAmine-labelled cells. All cells were also stained with DAPI prior to imaging 114

Figure 24: Pie charts illustrating the distribution of cellular component ontologies of proteins identified from LC-MS analysis of Jurkat membrane fractions prepared using three iterations of the 'stepwise depletion' procedure originally described by Wisniewski *et al.* a) cells lysed using Dounce homogenization and procedure performed in standard microcentrifuge tubes; b) cells lysed using Dounce homogenization and procedure performed in siliconized microcentrifuge tubes; c) cells lysed using freeze-thaw lysis and lysates homogenized using QiaShredder spin columns, procedure performed in siliconized microcentrifuge tubes 119

Figure 25: Pie charts illustrating the distribution of cellular component ontologies of proteins identified from LC-MS analysis of Jurkat membrane fractions prepared using the 'stepwise depletion' procedure and digested using a) FASP; b) In-solution digestion. 121

Figure 26: The two reactions which occur during trypsin-catalysed digestion of proteins to peptides in $H_2{}^{18}O$ water 134

Figure 27: ^{18}O-labelling of a BSA-derived peptide with sequence HLVDEPQNLIK 136

Figure 28: Extent of incorporation of ^{18}O atoms at the carboxyl termini of 10 BSA peptides after a) 0 hours; b) 2 hours; c) 24 hours when the carboxyl

oxygen exchange reaction is carried out in 50 mM ammonium bicarbonate (^{18}O, pH 8) 141

Figure 29: Extent of incorporation of ^{18}O atoms at the carboxyl termini of 10 BSA peptides after a) 0 hours; b) 2 hours; c) 24 hours when the carboxyl oxygen exchange reaction is carried out in 50 mM ammonium bicarbonate (^{18}O, pH 4.5) 142

Figure 30: Extent of trypsin-catalysed back exchange of ^{18}O atoms for ^{16}O atoms at the carboxyl termini of 10 fully ^{18}O-labelled BSA peptides when vacuum-dried and resuspended in 50mM ammonium bicarbonate (^{16}O, pH 4.5) and left at room temperature for 24 hours after a) no treatment; b) incubation at 100ºC for 30 minutes; c) reduction with 20 mM DTT at 95ºC for 1 hour followed by alkylation with 40 mM iodoacetamide for 30 minutes 145

Figure 31: Extent of trypsin-catalysed back exchange of ^{18}O atoms for ^{16}O atoms at the carboxyl termini of 10 fully ^{18}O-labelled BSA peptides when vacuum-dried and resuspended in 50mM ammonium bicarbonate (^{16}O, pH 4.5), acidified with 1% TFA and left at room temperature for 24 hours after a) no treatment; b) incubation at 100ºC for 30 minutes; c) reduction with 20mM DTT at 95ºC for 1 hour followed by alkylation with 40 mM iodoacetamide for 30 minutes 147

Figure 32: Box and whisker plot showing distribution of protein ratios reported by Mascot Distiller when ^{18}O-labelled and unlabelled proteomic peptides derived from mature DC whole cell lysate are combined in ratios ranging from 5 parts labelled : 1 part unlabelled through to 1 part labelled : 5 parts unlabelled 150

Figure 33: Relative quantitation of a proteomic peptide with sequence SLYASSPGGVYATR derived from unlabelled and ^{18}O-labelled mature DC whole cell lysate combined in a 1:1 ratio 152

Figure 34: Box and whisker plot showing distribution of unfiltered peptide ratios for a) all peptides assigned to proteins; b) all peptides with MS1 signal intensity greater than 10^4 assigned to proteins; c) all peptides with MS1 signal intensity

greater than 10^5 assigned to proteins; reported by Mascot Distiller when ^{18}O-labelled and unlabelled proteomic peptides derived from mature DC whole cell lysate are combined in ratios ranging from 5 parts labelled : 1 part unlabelled through to 1 part labelled : 5 parts unlabelled 153

Figure 35: Box and whisker plot showing distribution of filtered peptide ratios for a) all peptides assigned to proteins; b) all peptides with MS1 signal intensity greater than 10^4 assigned to proteins; c) all peptides with MS1 signal intensity greater than 10^5 assigned to proteins; reported by Mascot Distiller when ^{18}O-labelled and unlabelled proteomic peptides derived from mature DC whole cell lysate are combined in ratios ranging from 5 parts labelled : 1 part unlabelled through to 1 part labelled : 5 parts unlabelled 154

Figure 36: Isobaric peptide termini labelling of a BSA-derived peptide with sequence HLVDEPQNLIK 159

Figure 37: Succinylation of 10 BSA peptides when reacted with 20 mM succinic anhydride in 200 mM sodium acetate / 20 mM sodium hydroxide (pH 7.6) for a) 5 minutes; b) 10 minutes; c) 15 minutes 163

Figure 38: Guanidination of 10 BSA peptides when reacted with ~1 M O-Methylisourea in 6.67% ammonia (pH ~11) at 65ºC for a) 10 minutes; b) 20 minutes; c) 30 minutes.....
.....166

Figure 39: Modification states of 10 BSA peptides when reacted with ~1 M O-Methylisourea in 6.67% ammonia (pH ~11) at 65ºC for 30 minutes and subsequently reacted with 20 mM succinic anhydride in 200 mM sodium acetate / 20 mM sodium hydroxide (pH 7.6) for 15 minutes 169

Figure 40: Mascot fragmentation data of the peptide with sequence YLYEIAR and a mass consistent with a) single succinylation; b) double succinylation...169

Figure 41: Box and whisker plot showing distribution of a) protein ratios; b) peptide ratios reported by Mascot when $^{13}C_4$-succinylated and $^{12}C_4$-succinylated

/ ^{18}O-labelled proteomic peptides derived from Jurkat whole cell lysate are combined in ratios ranging from 20:1 through to 1:20 172

Figure 42: OFFGEL fractionation of ~50 µg peptides derived from an unlabelled mature DC whole cell lysate combined 1:1 with ~50 µg peptides from an ^{18}O-labelled tolerogenic DC whole cell lysate and fractionated on a pH 3-10 IEF strip. a) Total and total unique peptides identified in each well; b) & c) Redundancy of unique peptide identification across all 12 wells represented as a bar graph and a pie chart respectively 180

Figure 43: OFFGEL fractionation of peptides derived from a $^{13}C_4$-succinylated mature DC whole cell lysate combined 1:1 with a $^{12}C_4$-succinylated / ^{18}O-labelled tolerogenic DC whole cell lysate and fractionated on a pH 3-10 IEF strip. a) Total and total unique peptides identified in each well; b) & c) Redundancy of unique peptide identification across all 12 wells represented as a bar graph and a pie chart respectively 182

Figure 44: OFFGEL fractionation of peptides derived from a $^{13}C_4$-succinylated mature DC whole cell lysate combined 1:1 with a $^{12}C_4$-succinylated / ^{18}O-labelled tolerogenic DC whole cell lysate and fractionated on a pH 3-6 IEF strip. a) Total and total unique peptides identified in each well; b) & c) Redundancy of unique peptide identification across all 10 wells represented as a bar graph and a pie chart respectively 185

Figure 45: First StageTip-based SAX fractionation of 25 µg unlabelled peptides derived from a Jurkat whole-cell lysate. a) Total and total unique peptides identified in each fraction; b) & c) Redundancy of unique peptide identification across all 7 fractions represented as a bar graph and a pie chart respectively 189

Figure 46: First StageTip-based SAX fractionation of 25 µg succinylated peptides derived from a Jurkat whole-cell lysate. a) Total and total unique peptides identified in each fraction; b) & c) Redundancy of unique peptide identification across all 7 fractions represented as a bar graph and a pie chart respectively 190

Figure 47: Second StageTip-based SAX fractionation of 25 µg unlabelled peptides derived from a Jurkat whole-cell lysate. a) Total and total unique peptides identified in each fraction and in an equivalent amount of unfractionated material; b) & c) Redundancy of unique peptide identification across all 8 fractions represented as a bar graph and a pie chart respectively 193

Figure 48: Second StageTip-based SAX fractionation of 25 µg succinylated peptides derived from a Jurkat whole-cell lysate. a) Total and total unique peptides identified in each fraction and in an equivalent amount of unfractionated material; b) & c) Redundancy of unique peptide identification across all 8 fractions represented as a bar graph and a pie chart respectively 194

Figure 49: Third StageTip-based SAX fractionation of 25 µg unlabelled peptides derived from a Jurkat whole-cell lysate. a) Total and total unique peptides identified in each fraction and in an equivalent amount of unfractionated material; b) & c) Redundancy of unique peptide identification across all 13 fractions represented as a bar graph and a pie chart respectively.....197

Figure 50: Third StageTip-based SAX fractionation of 25 µg succinylated peptides derived from a Jurkat whole-cell lysate. a) Total and total unique peptides identified in each fraction and in an equivalent amount of unfractionated material; b) & c) Redundancy of unique peptide identification across all 13 fractions represented as a bar graph and a pie chart respectively 198

Figure 51: Box and whisker plot showing distribution of a) protein ratios; b) peptide ratios reported by Mascot when $^{13}C_4$-succinylated mature DC proteomic peptides and $^{12}C_4$-succinylated / ^{18}O-labelled tolerogenic DC proteomic peptides are combined in a 1:1 ratio 209

Figure 52: Pie charts illustrating the distribution of cellular component ontologies of proteins identified from LC-MS analysis of a) mature DC membranes and b)

tolerogenic DC membranes prepared using the optimized stepwise depletion enrichment method described in Chapter 4 and digested using FASP 214

Figure 53: Total ion chromatograms from LC-MS analysis of a) mature DC membranes and b) tolerogenic DC membranes 215

Figure 54: Extracted ion chromatograms (XICs) and MS/MS spectra for the CD32-derived peptide of interest with sequence VTFFQNGK. a) Mature DC XIC, b) tolerogenic DC XIC; c) mature DC MS/MS spectrum; d) tolerogenic DC MS/MS spectrum 224

Table 1: Properties of mass analysers used for peptide analysis in bottom-up proteomics 11

Table 2: LC-MS settings used for experiments described in Chapters 4 - 7 75

Table 3: Number of unique CAMthiopropanoylated peptides and proteins detected from membrane fractions prepared using EZ-Link™ Sulfo-NHS-SS-Biotin and processed with Pierce lysis and wash buffers and 4% (w/v) SDS respectively 110

Table 4: Comparison of reported percentages of membrane protein identifications with percentages of membrane protein identifications computed from STRAP GO annotation and TMHMM transmembrane helix predication of protein lists supplied in supplementary data in publications citing high levels of membrane protein enrichment through various strategies 126

Table 5: Reaction conditions used in previously published ^{18}O-labelling proteomics papers 138

Table 6: Scheme for combining labelled and unlabelled proteomic peptides to examine whether ^{18}O-labelling is suitable for performing quantitative proteomic analyses.....148

Table 7: Scheme for combining differentially labelled proteomic peptides to examine whether isobaric peptide termini labelling is suitable for performing quantitative proteomic analyses.....170

Table 8: Proteins identified in ^{18}O-based quantitative profiling of whole cell proteomes of mature and tolerogenic DCs with twofold or greater expression in mature DCs.....205

Table 9: Proteins identified in ^{18}O-based quantitative profiling of whole cell proteomes of mature and tolerogenic DCs with twofold or greater expression in tolerogenic DCs 206

Table 10: Proteins identified in IPTL-based quantitative profiling of whole cell proteomes of mature and tolerogenic DCs with twofold or greater expression in one cell type relative to the other 209

Table 11: Proteins identified exclusively in mature DC membrane-enriched fraction 217

Table 12: Proteins identified exclusively in tolerogenic DC membrane-enriched fraction 218

Table 13: Proteins identified in both mature and tolerogenic DC membrane-enriched fractions with emPAI scores suggesting differential expression 219

Table 14: Proteins identified in both mature and tolerogenic DC membrane-enriched fractions with emPAI scores suggesting commensurate expression 220

Abbreviations

(16)BAC/SDS-PAGE	Benzyldimethyl-n-hexadecylammonium Chloride/SDS-PAGE
AA	Ammonium acetate
ABC	Ammonium bicarbonate
AMT	Accurate mass and time tag
AuToDeCRA	Autologous Tolerogenic Dendritic Cells for Rheumatoid Arthritis
BN/SDS-PAGE	Blue native SDS PAGE
BR	Britton-Robinson
BSA	Bovine serum albumin
BVR	Biliverdin reductase
C18	Octadecyl carbon chain
CAD	Collision-activated dissociation
CCL19	Chemokine (C-C motif) ligand 19
CCR7	Chemokine (C-C motif) receptor 7
CD103	Cluster of differentiation 103
CD14	Cluster of differentiation 14
CD150	Cluster of differentiation 150
CD154	Cluster of differentiation 154
CD163	Cluster of differentiation 163
CD1c	Cluster of differentiation 1c
CD25	Cluster of differentiation 25
CD29	Cluster of differentiation 29
CD299	Cluster of differentiation 299
CD303	Cluster of differentiation 303
CD317	Cluster of differentiation 317
CD32a	Cluster of differentiation 32a
CD32b	Cluster of differentiation 32b
CD4	Cluster of differentiation 4
CD40	Cluster of differentiation 40
CD44	Cluster of differentiation 44
CD45	Cluster of differentiation 45
CD49c	Cluster of differentiation 49c
CD50	Cluster of differentiation 50
CD63	Cluster of differentiation 63

CD74	Cluster of differentiation 74
CD8	Cluster of differentiation 8
CD80	Cluster of differentiation 80
CD83	Cluster of differentiation 83
CD86	Cluster of differentiation 86
cGMP	Current good manufacturing practice
CHAPS	3-[(3-cholamidopropanyl)dimethylammonio]-1-propanesulphonate
CIA	Collagen-induced arthritis
CID	Collision-induced dissociation
CLR	C-type lectin receptor
CMC	Critical micelle concentration
CTLA4	Cytotoxic T lymphocyte antigen 4
CXCR4	Chemokine (C-X-C motif) receptor 4
DAMP	Danger-associated molecular pattern
DAPI	4',6-diamidino-2-phenylindole
DC	Dendritic cell
DIGE	Difference gel electrophoresis
DMSO	Dimethyl sulfoxide
DTT	Dithiothreitol
EAE	Experimental autoimmune encephalitis
ECD	Electron capture dissociation
EDTA	Ethylenediaminetetraacetic acid
ELISA	Enzyme-linked immunsorbent assay
emPAI	Exponentially modified protein abundance index
ESI	Electrospray ionization
ETD	Electron transfer dissociation
FA	Formic acid
FACS	Fluorescence-activated cell sorting
FASP	Filter-aided sample preparation
FBS	Fetal bovine serum
FcγRI	High affinity immunoglobulin gamma Fc receptor I
FcγRIIA	Low affinity immunoglobulin gamma Fc receptor II-a
FcγRIIB	Low affinity immunoglobulin gamma Fc receptor II-b
FcγRIII	Low affinity immunoglobulin gamma Fc receptor III
FcεRIγ	Fc fragment of IgE, high affinity I, receptor for gamma polypeptide

FHA	Filamentous haemagglutinin
FoxP3	Forkhead box P3
FSL-1	Mycoplasmal diacylated LPT, S-(2,3-bispalmitoyloxypropyl)
FT-ICR	Fourier transform ion cyclotron resonance
GAPDH	Glyceraldehyde 3-phosphate dehydrogenase
GeLC-MS	1D SDS-PAGE followed by LC-MS
GM-CSF	Granulocyte macrophage colony-stimulating factor
GO	Gene Ontology
GPI	Glycosylphosphatidylinositol
HA	Haemagglutinin
HBSS	Hank's balanced salt solution
HEPES-NaOH	4-(-2-hydroxyethyl)-1-piperazineethanesulfonic acid sodium hydroxide
hESC	Human embryonic stem cell
HILIC	Hydrophilic interaction liquid chromatography
HIV-1	Human immunodeficiency virus type 1
HPLC	High performance liquid chromatography
ICAT	Isotope-coded affinity tag
ICR	Ion cyclotron resonance
IDO	Indoleamine 2,3-dioxygenase
IEF	Isoelectric focussing
IFNγ	Interferon gamma
IgE	Immunoglobulin E
IgG	Immunoglobulin G
IL-10	Interleukin 10
IL-12	Interleukin 12
IL-23	Interleukin 23
IL-27	Interleukin 27
IL-4	Interleukin 4
ILT	Immunoglobulin-like transcript
IMP	Integral membrane protein
IPG	Immobilized pH gradient
IPI	International protein index
IPTL	Isobaric peptide termini labelling
IT	Ion trap
iTRAQ	Isobaric tags for relative and absolute quantification

$_iT_{reg}$	'Adaptive' regulatory T cell
LC	Liquid Chromatography
LC-MS	Liquid chromatography – mass spectrometry
LCMV	Lymphocytic choriomeningitis virus
LPS	Lipopolysaccharide
LRS	Leukocyte reduction system
MALDI	Matrix-assisted laser desorption/ionization
MeOH	Methanol
MHC	Major histocompatibility complex
MLR	Mixed lymphocyte reaction
moDC	Monocyte-derived dendritic cell
MS	Mass spectrometry
MS/MS	Tandem mass spectrometry
MuDPIT	Multi-dimensional protein identification technology
MW	Molecular weight
MWCO	Molecular weight cut off
NF-κB	Nuclear factor-kappa B
NHS	N-Hydroxysuccinimide
NLR	NOD-like receptor
$_nT_{reg}$	'Naturally-occurring' regulatory T cell
PAGE	Polyacrylamide gel electrophoresis
PAMP	Pathogen-associated molecule pattern
PBMC	Peripheral blood mononuclear cell
PBS	Phosphate buffered saline
PEG	Polyethylene glycol
PMF	Peptide mass fingerprinting
PPAR	Peroxisome-proliferator activated receptor
PRR	Pattern recognition receptor
PS	Lysophosphatidylserine
PSAQ	Protein standard absolute quantification
PSM	Peptide-to-spectrum match
Q	Quadrupole
QconCAT	Quantification concatemer
RA	Retinoic acid
RALDH	Retinaldehyde dehydrogenase
Rf	Radiofrequency

RLR	Rig-I-like receptor
RPLC	Reversed phase liquid chromatography
SAX	Strong anion exchange chromatography
SCX	Strong cation exchange chromatography
SD	Standard deviation
SDC	Sodium deoxycholate
SDS	Sodium dodecyl sulphate
shRNA	Small hairpin RNA
SILAC	Stable isotope labelling by amino acids in cell culture
siRNA	Small interfering RNA
SIRP-β-1	Signal regulatory protein beta-1
SISCAPA	Stable isotope standards and capture by anti-peptide antibodies
SLAM	Selected lymphocyte antibody method
SOCS3	Suppressor of cytokine signalling 3
SPE	Solid phase extraction
SRM	Selected reaction monitoring
STAT-3	Signal transducer and activator of transcription 3
STAT-4	Signal transducer and activator of transcription 4
Sulfo-NHS-SS-Biotin	Sulfosuccinimidyl-2-(biotinamido)ethyl-1,2-dithiopropionate
TBS	Tris buffered saline
TCEP-HCl	Tris(2-carboxyethyl)phosphine hydrochloride
TcR	T cell receptor
TFA	Trifluoroacetic acid
TGF-β	Transforming growth factor beta
T_h1	Type 1 helper T cell
T_h2	Type 2 helper T cell
T_h17	T helper 17 cell
TIC	Total ion chromatogram
TLR	Toll-like receptor
TMD	Transmembrane domain
TMT	Tandem mass tags
TNFα	Tumour necrosis factor alpha
ToF	Time-of-flight
TRAIL	TNF-related apoptosis-inducing ligand
TRIS-HCl	Trs(hydroxymethyl)aminomethane hydrochloride

TRITC	Tetramethyl rhodamine isothiocyanate
WGA	Wheat germ agglutinin
XIC	Extracted ion chromatogram

Chapter 1. Introduction

1.1. Proteomics

The phrases ‘proteome’ and ‘proteomics’ first entered the scientific lexicon in 1996 (Wilkins *et al.*, 1996) and 1997 (James, 1997) respectively by way of analogy with the existing terms ‘genome’ and ‘genomics’. Each ‘omics’ is concerned with the study of a particular group of biological macromolecules and the ‘omics’ disciplines collectively share in common their conceptual approach of looking at these macromolecules through a holistic lens rather than a reductionist one (Kraj and Silberring, 2008). Thus genomics is the sequencing and analysis of genomes, whilst transcriptomics is the study of the transcription and post-transcriptional regulation of all mRNAs produced from a given genome. By extension, proteomics encompasses the study of the translation, function and post-translational regulation of all proteins produced from a given cellular complement of mRNAs.

With each successive transfer of information from DNA through RNA to protein comes a concurrent expansion in complexity of the nature of the subsequent class of macromolecules and an increased degree of difficulty in scrutinizing said class of macromolecules as a whole. Genomics, concerned solely with DNA sequencing, is now a mature and well-established discipline, with complete genome sequences available for 1153 organisms as of February 16th 2012 (Howald *et al.*, 2012). Proteomics, on the other hand, must account for alternative splicing (which in itself has been suggested to produce approximately 100000 protein isoforms from approximately 20000 genes of the human genome (Gstaiger and Aebersold, 2009)), post translational modifications (predicted to increase the number of mature protein species by a further order of magnitude (Jensen, 2004)) and dynamic ranges of expression which may span up to ten orders of magnitude (Hortin and Sviridov, 2010); not to mention subcellular localization, protein-protein interactions and turnover.

It is thus perhaps unsurprising that the comprehensive characterization of entire proteomes is a significantly more challenging proposition than the sequencing of entire genomes. In order to match up to this increased complexity, the development of proteomics-related techniques has had to move forward at an extraordinary rate. Advances in liquid chromatography (LC) and mass spectrometry (MS) over the past decade or so have invited comparison to Moore’s Law in some quarters (Mann, 2008). With the cutting edge

instrumentation available today it is possible to identify tens of thousands of peptides (many at sub-femtomole levels) (Thakur *et al.*, 2011) and obtain near-complete proteome coverage of simple model organisms (Nagaraj *et al.*, 2012) in a matter of hours. Consequently, LC-MS is now firmly established as the major facilitating technology for proteomics.

1.1.1. Top-down or bottom-up?

In the broadest sense, mass spectrometry-based proteomics workflows can be defined as being either 'bottom-up' or 'top-down'.

Top-down proteomics (Ge *et al.*, 2002) is concerned with the mass spectrometric analysis of intact proteins. It has proven possible to characterize intact proteins up to 200 kDa in size (Han *et al.*, 2006) and this approach thus has applicability in the analysis of isoforms, post-translational modifications and protein complexes (Zhou *et al.*, 2012a). Though identification of > 1000 proteins in a single study has previously been reported (Tran *et al.*, 2011); technical constraints pertaining to separation, ionization and fragmentation of whole proteins generally render complex samples less amenable to analysis via this route (Zhang *et al.*, 2013).

In contrast, bottom-up proteomics entails the proteolysis of proteins to peptides prior to LC-MS analysis. When performed on complex samples, this is known as shotgun proteomics (Yates, 1998) (by way of analogy with shotgun DNA sequencing (Staden, 1979)). Very briefly, peptides are fragmented, sequenced and the protein content of a sample inferred through assigning the peptide sequences to proteins. The advantages of the top-down approach are relinquished, but the concomitant returns in increased sensitivity and proteome coverage make shotgun proteomics the approach of choice for analysis of complex protein mixtures. A bottom-up approach was adhered to in all work presented within this thesis and the specifics of this approach will be outlined in greater detail below.

A recent addendum to the top-down / bottom-up paradigm is 'middle-down' proteomics (Wu *et al.*, 2005), which seeks to strike a compromise between the two extremes through analysis of large peptide fragments. These larger

fragments can provide more information on isoforms and post-translational modifications than the short peptides analysed in bottom-up proteomics and are considerably more tractable than the whole proteins analysed in the top-down approach.

1.1.2. The Bottom-up Proteomics Workflow

There are numerous variations on the theme of a bottom-up proteomics workflow, but a few aspects are common to all. As aforementioned, 'single-shot' analyses of entire proteomes are achievable but these are currently confined to a select few specialist laboratories and are not yet conceivable for more complex organisms. The central principle is one of 'divide and conquer'. The first step of any given workflow is thus extraction and isolation of a protein sample from the source of biological interest. The isolated protein sample is then digested to peptides, fractionated (though fractionation can also be performed at the protein level prior to digestion), ionized and subjected to mass spectrometric analysis. Bioinformatics tools are then employed to translate the information generated by the mass spectrometer into amino acid sequences of detected peptides and assign the peptides to proteins. These bottom-up workflows are outlined in **Fig. 1** and each stage is subsequently detailed further.

Figure 1

A general overview of the bottom-up proteomics workflow. Individual stages of the workflow are described in greater detail in the following pages.

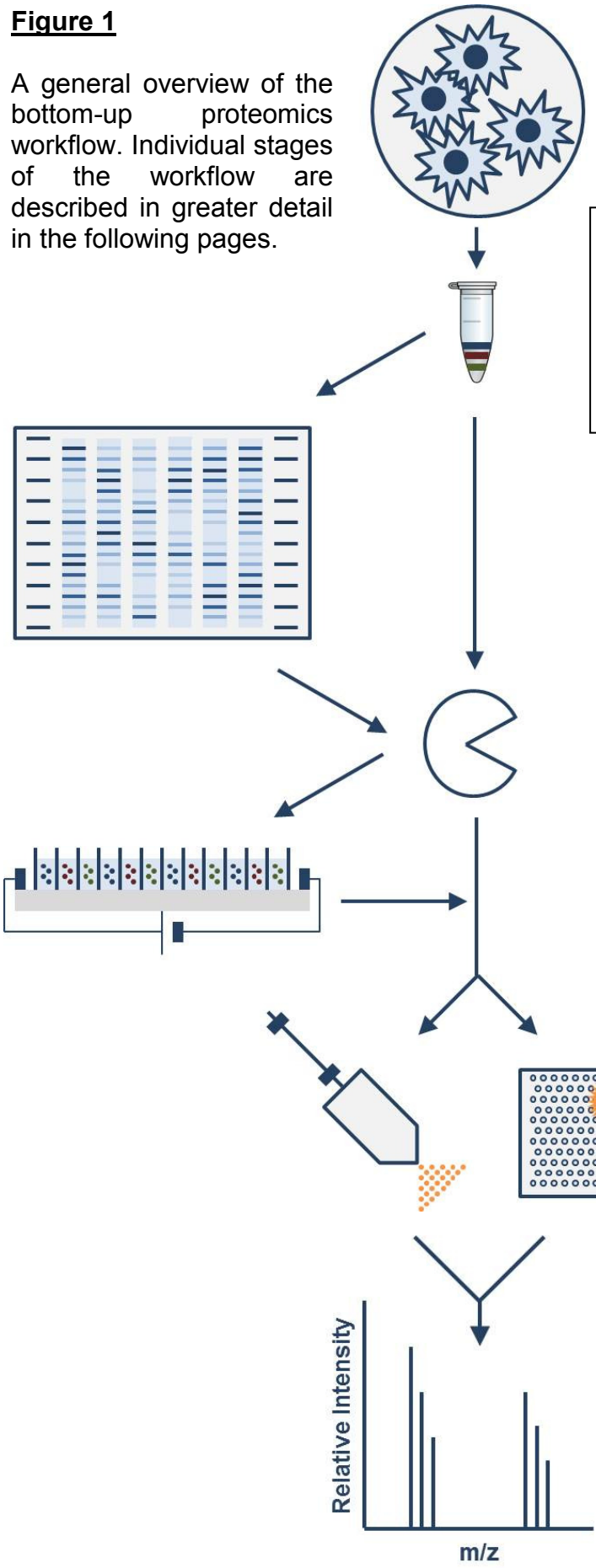

Starting Sample

Protein Extraction & Isolation

- *Subcellular Fractionation*
- Protein Depletion
- Protein Equalization

Protein Separation

- 2D PAGE
- *1D PAGE*
- Protein IEF

Protein Digestion

Peptide Separation

- On-line LC
- Off-line LC
- *Peptide IEF*

Ionization

- ESI
- MALDI

Mass Spectrometry

1.1.2.1. Protein Extraction and Isolation

The way in which a proteomic sample is extracted and isolated from the biological system under study can have important implications for stages further downstream in the workflow and its significance should not be underestimated. Even the most homogenous of biological systems (e.g. cells in culture) are still relatively complex with dynamic ranges of expression spanning many orders of magnitude. If certain sub-proteomes are of particular interest, subcellular fractionation techniques may be employed to decrease sample complexity. A case in point is the membrane proteome, whose low abundance and hydrophobic character relative to the rest of the proteome necessitates particular methodological considerations both at this stage and at the digestion stage. Since this body of work is concerned with characterization of the membrane proteomes of mature and tolerogenic dendritic cells, these considerations will be expanded upon in section **1.1.3.**

Secreted proteins represent something of a special case since the extracellular milieu into which they are secreted are not amenable to subcellular fractionation and are frequently even more complex than the cell from which the proteins originated. Accordingly, isolation approaches here are more geared towards depletion of highly abundant proteins (e.g. serum albumin), which alone constitutes over 50% of the total protein content of serum (Hortin and Sviridov, 2010).

1.1.2.2. Protein Fractionation

The majority of bottom-up workflows incorporating a protein fractionation step are gel-based. Indeed, the majority of early proteomics experiments utilized 2D-polyacrylamide gel electrophoresis (PAGE), a technique in which proteins are separated according to their isoelectric points in a first dimension pH gradient gel and their molecular masses in a second dimension PAGE (O'Farrell, 1975). The gel is then stained and imaged and spots of interest excised and analysed to confirm their identity. 2D-PAGE can therefore be used to look for differential protein expression in two (or more) samples run on two (or more) gels by examining differences in the protein spot profiles on the gel. However, the technique is hampered somewhat by low dynamic range, poor reproducibility, and a bias against both large and membrane proteins (Lopez, 2007); and is not

employed as regularly today as it once was. A more recent innovation is difference gel electrophoresis (DIGE), in which samples are differentially labelled with cyanine N-hydroxysuccinimide (NHS) esters prior to loading and quantified on a single gel, markedly alleviating the dynamic range and reproducibility issues (Alban *et al.*, 2003).

A simple and still commonly used protein fractionation method for proteomics is 1D-SDS-PAGE (Laemmli, 1970). In the context of a shotgun workflow, complex proteomic samples are resolved by size alone on a PAGE gel and the gel is divided into a number of slices. Each slice is then treated as a separate fraction, digested in-gel (Shevchenko *et al.*, 1996) and analysed by LC-MS. The entire workflow has thus been aptly termed GeLC-MS (Lundby and Olsen, 2011).

Proteins may also be fractionated according to their isoelectric points in the liquid phase (Zuo and Speicher, 2000), circumventing some of the problems associated with performing this mode of separation in-gel. This liquid phase isoelectric focusing has been combined with GeLC-MS, yielding increased proteome coverage and reproducibility in comparison to repeated runs of fractions processed using GeLC-MS alone (Wang *et al.*, 2010a).

1.1.2.3. Protein Digestion

Proteolytic digestion of proteins to peptides is a fundamental step central to all bottom-up workflows. Important considerations are the cleavage specificity of the enzyme/s used and the agent/s employed to aid solubilization and unfolding of proteins, affording the enzyme/s access to cleavage sites. These considerations are especially significant for membrane proteomics and will be discussed in greater detail in section **1.1.3.** Trypsin is the protease of choice for the majority of bottom-up workflows and is frequently combined with an initial Endoproteinase-LysC digestion in denaturing conditions.

1.1.2.4. Peptide Fractionation

Unfractionated and 1D-PAGE-fractionated proteomic material contain a highly complex mixture of peptide species and fractionation at the peptide level is thus a necessary prerequisite for in-depth mass spectrometric detection of a significant proportion of the proteome. In this regard, 2D-PAGE does not really fall within the realm of what is understood today as shotgun proteomics, since an excised spot of interest corresponds at most to a few proteins (and ideally to a single protein!)

Peptide separation can be performed off-line (whereby fractions are manually recovered prior to further analysis) or on-line (whereby fractionation is directly coupled to the mass spectrometer itself or a further dimension of downstream separation). All LC-MS workflows utilize at least one dimension of on-line chromatographic separation of peptides immediately prior to electrospray ionization (ESI). This allows large amounts of complex sample to be loaded onto the stationary phase of the chromatography column and continuously eluted over a pre-specified period of time by steadily increasing the concentration of the component in the mobile phase which favours displacement from the column. The specific physicochemical interaction of individual peptide species with the stationary phase determines the point at which they will be eluted.

Reversed phase liquid chromatography (RPLC) uses a hydrophobic stationary phase and an aqueous to organic mobile phase gradient to separate peptides on the basis of hydrophobicity, with hydrophilic and shorter peptides eluting early and hydrophobic and longer peptides later in the gradient. Its high separation efficiency, high resolving capacity and the compatibility of solvent buffers with ESI render it the most important form of chromatography for shotgun proteomics and it is almost exclusively used as the final dimension of peptide separation in LC-MS (Shen and Smith, 2002). A less commonly used alternative is hydrophilic interaction liquid chromatography (HILIC) (Alpert, 1990), which uses a hydrophilic stationary phase and an organic to aqueous mobile phase gradient and thus tends to invert the order in which peptides elute in RPLC.

These ESI-coupled chromatographic separations can be combined both on-line and off-line with many other forms of chromatography to further reduce sample complexity. The most common on-line separation upstream of RPLC is ion exchange chromatography, which uses a charged stationary phase and a mobile phase gradient of increasing ionic strength or changing pH; thereby separating peptides on the basis of charge. Strong cation exchange chromatography (SCX; negatively charged stationary phase, peptides loaded at low pH) is most frequently used, and the on-line coupling of SCX and RPLC has been dubbed Multi-dimensional Protein Identification Technology (MuDPIT) (Wolters *et al.*, 2001). Strong anion exchange chromatography (SAX; positively charge stationary phase, peptides loaded at high pH) has also been used in an on-line format (Dai *et al.*, 2009). Ion exchange chromatography can also be used for off-line separations by first collecting and then later analysing individual fractions with RPLC.

Electrophoretic separations initially conceived for fractionation at the protein level may also be applied for peptide fractionation upstream of RPLC. Peptide isoelectric focusing can be performed in-gel (Essader *et al.*, 2005) or in-solution (Heller *et al.*, 2005). Free flow electrophoresis has also been used to this end (Malmstrom *et al.*, 2006).

1.1.2.5. Mass Spectrometry

Mass spectrometry is the fundamental analytical technique underpinning proteomics and generates the raw data which will subsequently be used to identify proteins. All mass spectrometers consist of three basic components: an ion source which ionizes peptides and transfers them into the gas phase, a mass analyser which resolves sample components according to the mass-to-charge ratio (m/z) of each ionized peptide and an ion detector which records the number of ions at each m/z.

1.1.2.5.1. Ion Sources

Though developments in proteomic sample separation have undoubtedly helped further mass spectrometry-based proteomics in the past few years, the field as we know it would not even exist had it not been for the development of MALDI (matrix-assisted laser desorption ionization (Karas and Hillenkamp, 1988)) and ESI (electrospray ionization (Fenn *et al.*, 1989)) around 25 years

ago. The importance of these breakthroughs was recognized with the award of the 2002 Nobel Prize in chemistry to Koichi Tanaka and John Fenn for their parts in pioneering the usage of MALDI and ESI respectively to analyse biological macromolecules. MALDI and ESI are 'soft' ionization methods, and their development allowed for the facile transfer of proteins and peptides into the gas phase with minimal degradation (Yates *et al.*, 2009).

In MALDI, the analyte is co-crystallized with a low molecular mass organic matrix on a metal plate. The matrix absorbs the energy from a laser fired at the sample and transfers it to the analyte, causing ionization, sublimation and desorption from the plate of both matrix and analyte ions (Karas and Hillenkamp, 1988). MALDI ionization predominantly results in the production of singly charged peptide ions.

In ESI, samples are ionized as they elute from a chromatography capillary through the application of a high electric field generated via application of a voltage difference between the end of the capillary and the MS entrance. Liquid leaving the capillary is dispersed as an electrically charged aerosol. Positive ions accumulate at the surface of the droplets and as the solvent evaporates they are brought into closer and closer proximity with one another. When the surface tension of a droplet is exceeded by the forces of repulsion between the ions on its surface, the droplet 'explodes' into many smaller coulomb explosions. This occurs multiple times until all solvent has evaporated; leaving only ionized peptides in the gas phase (Fenn *et al.*, 1989). ESI produces a range of charged peptide ions, though doubly and triply charged ions are most frequently observed.

ESI is predominantly coupled to RPLC. Liquid chromatography has also previously been coupled to MALDI through automated deposition of column eluate onto MALDI plates (Miliotis *et al.*, 2000; Rejtar *et al.*, 2002; Wall *et al.*, 2002).

1.1.2.5.2. Mass Analysers

A variety of mass analysers are available. Time of flight (ToF) analysers compute m/z by accelerating the ions in a pulsed electric field and then measuring the time it takes for them to travel a fixed distance to the ion detector (Guilhaus, 1995). Quadrupole (Q) analysers are composed of two pairs of metal

rods and allow selectable ions of a particular m/z to reach the ion detector at any one time through application of oscillating radiofrequency (Rf) voltages to the rods such that all other ions are deflected (March, 1997). Ion trap (IT) analysers also utilize a quadrupolar field, but do so to 'trap' ions, such that ions of interest can be accumulated and then released from the trap according to their m/z value by varying the amplitude of the field (March, 1997). Finally, Fourier transform ion cyclotron resonance (FT-ICR) and Orbitrap analysers trap ions, measure ion oscillation frequencies and perform a Fourier transformation on the measured frequencies to derive m/z (Amster, 1996; Hu *et al.*, 2005). Mass analysers vary in the resolution and mass accuracy of their m/z measurements, in the sensitivity and dynamic range of their detection thresholds and in the speed of their scan rates; and different mass analysers thus lend themselves to different applications. The resolution, mass accuracy and dynamic range capabilities of the mass analysers described above are summarized in **Table 1** (adapted from (Zhang *et al.*, 2013))

Mass Analyser	Resolution	Mass Accuracy	Dynamic Range (Orders of Magnitude)
ToF	10 - 50 K	5 - 10 ppm	4
Quadrupole	1 - 2 K	~1‰	5 - 6
Ion Trap	1 - 2 K	~1‰	3 - 4
ICR	100 - 500 K	~100 ppb	3
Orbitrap	7.5 - 240 K	5 - 10 ppm	4

Table 1: Properties of mass analysers used for peptide analysis in bottom-up proteomics

Two (or more) mass analysers are frequently interfaced with one another for tandem mass spectrometry (described in more detail below) in order to exploit distinct advantageous properties of each of them. Ion trap analysers have been interfaced with FT-ICR (Syka *et al.*, 2004b) and Orbitrap (Yates *et al.*, 2006) analysers and quadrupole analysers with ToF (Steen *et al.*, 2001) and Orbitrap (Michalski *et al.*, 2011) analysers; combinations which can be used to take advantage of the greater sensitivity of the former instruments in combination with the higher resolution and mass accuracy of the latter.

1.1.2.6. Mass Spectrometric Peptide Analysis

The m/z of a peptide ion alone is insufficient information from which to determine its amino acid sequence. In order to identify individual peptide species present in a sample, the raw data must be searched against existing protein sequence databases. A number of approaches are available and the approach taken will depend upon the nature of the raw data generated.

1.1.2.6.1. Peptide mass fingerprinting

Peptide mass fingerprinting (PMF) was developed by a number of groups simultaneously in 1993 (Henzel *et al.*, 1993; James *et al.*, 1993; Mann *et al.*, 1993; Pappin *et al.*, 1993; Yates *et al.*, 1993). It identifies proteins by comparing the m/z values of the peptides detected in a given protein digest to databases of all theoretical peptide masses produced from an *in silico* digest. The principle behind this approach is that whilst a single m/z ratio may correspond to many peptide sequences, multiple m/z ratios corresponding to multiple peptide sequences known to be present in the same protein are increasingly unlikely to be observed by chance. This strategy can only identify proteins that are already in a database and rapidly becomes redundant as the number of proteins present in a sample increases. However, it is still a useful tool for analysis of single proteins and simple mixtures (differentially expressed spots on 2D gels for example).

1.1.2.6.2. Accurate mass and time tag

Accurate mass and time tag (AMT) identifies proteins in LC-MS by merit of both the m/z values of peptides and their retention time in liquid chromatography. The rationale here is that whilst multiple peptide species have the same m/z ratio, it is unlikely that they will also exhibit identical chromatographic behaviour. Retention time data thus constitutes an additional constraint, and it has been shown that when both constraints are used simultaneously, 88% of peaks on a mass spectrum can be matched to unique peptides (Lipton *et al.*, 2002). This approach however requires a complex database containing m/z ratios and elution times of previously identified peptides. It also requires that peptides are detected consistently across multiple LC-MS runs and that the retention time of these peptides doesn't drift from run to run.

1.1.2.6.3. Tandem mass spectrometry

Tandem mass spectrometry (MS/MS) is by far the most widespread strategy for protein identification in shotgun experiments and enables high throughput sequencing of peptide ions detected by LC-MS. Precursor ions of interest (typically doubly- or triply-charged) detected in an MS1 scan are selected and isolated. Isolated precursor ions are then fragmented and product ion m/z ratios recorded in an MS2 scan. The m/z differences between product ions derived from the same parent ion are diagnostic of the mass differences imparted by the distinct residue masses of individual amino acids in the fragments. The tandem mass spectrum of a given peptide therefore contains 'peptide sequence tags' (Mann and Wilm, 1994) which can be searched against theoretical fragmentation patterns of peptides present in sequence databases. This is outlined graphically in **Fig. 2**.

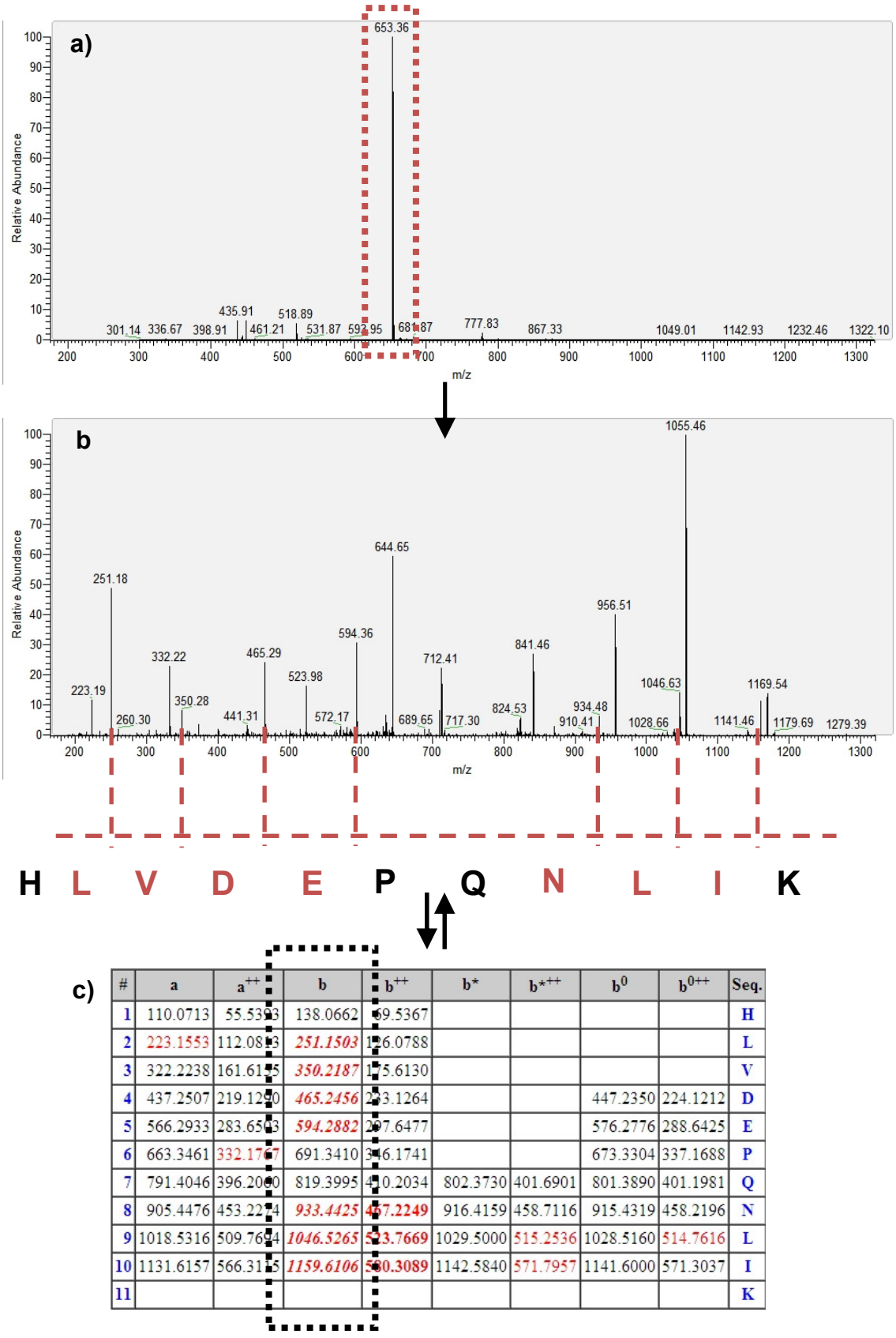

c)

#	a	a^{++}	b	b^{++}	b*	b^{*++}	b^{0}	b^{0++}	Seq.
1	110.0713	55.5393	138.0662	69.5367					H
2	223.1553	112.0813	*251.1503*	126.0788					L
3	322.2238	161.6155	*350.2187*	175.6130					V
4	437.2507	219.1290	*465.2456*	233.1264			447.2350	224.1212	D
5	566.2933	283.6503	*594.2882*	297.6477			576.2776	288.6425	E
6	663.3461	332.1767	691.3410	346.1741			673.3304	337.1688	P
7	791.4046	396.2060	819.3995	410.2034	802.3730	401.6901	801.3890	401.1981	Q
8	905.4476	453.2274	*933.4425*	467.2249	916.4159	458.7116	915.4319	458.2196	N
9	1018.5316	509.7694	*1046.5265*	523.7669	1029.5000	515.2536	1028.5160	514.7616	L
10	1131.6157	566.3115	*1159.6106*	580.3089	1142.5840	571.7957	1141.6000	571.3037	I
11									K

Figure 2: MS/MS of a BSA-derived peptide with sequence HLVDEPQNLIK. **a)** The precursor ion is selected and isolated owing to its intensity in the MS1 spectrum. **b)** The precursor ion is fragmented and product ion masses recorded in the MS2 spectrum. The peptide is sequenced by merit of the close correlation of the observed fragmentation spectrum with the theoretical fragmentation spectrum shown in **c)**.

1.1.2.6.3.1. Precursor Ion Selection

Precursor ions are usually selected for fragmentation in a 'data-dependent' manner on the basis of their observed intensity in a given MS1 scan. Data-dependent acquisition consists of repeated cycles of precursor ion scans followed by fragmentation of the n most intense ions in said scan. Highly abundant ions will generally be dynamically excluded from selection for a pre-determined period of time if they are repeatedly selected for fragmentation to allow less abundant ions to be fragmented (Mallick and Kuster, 2010). Automated 'exclusion lists' have also been used to prevent highly abundant ions from being excessively selected for fragmentation across technical replicates (Zhang, 2012) and to preclude the selection of ions corresponding to contaminant proteins (Hodge *et al.*, 2013). An alternative to the data-dependent paradigm is 'data-independent' acquisition, where the mass spectrometer is configured to sequentially cycle through small m/z 'windows' in the precursor ion scan; thus sampling lower abundance ions which would not otherwise be fragmented (Venable *et al.*, 2004).

1.1.2.6.3.2. Precursor Ion Fragmentation

Tandem mass spectrometry can be performed 'in space' or 'in time'. MS/MS 'in space' is carried out with two mass analysers separated by a collision chamber in which peptides are fragmented. The first analyser 'selects' ions of interest and enables them to pass into the collision chamber. Fragment m/z ratios are then recorded by the second analyser. MS/MS 'in time' is carried out with a single mass analyser able to isolate and fragment ions in a single chamber (e.g. quadrupole ion trap, FT-ICR and Orbitrap instruments).

Either way, the principle requirement to enable sequencing of the peptide is for individual precursor ions to undergo a single cleavage along the polypeptide backbone between amino acid residues. A standard notation exists for indicating whether the product ion incorporates the N- or the C- terminus, where along the backbone the fragmentation occurred and the number of amino acid residues in the fragment (Roepstorff and Fohlman, 1984). This is shown in **Fig. 3**.

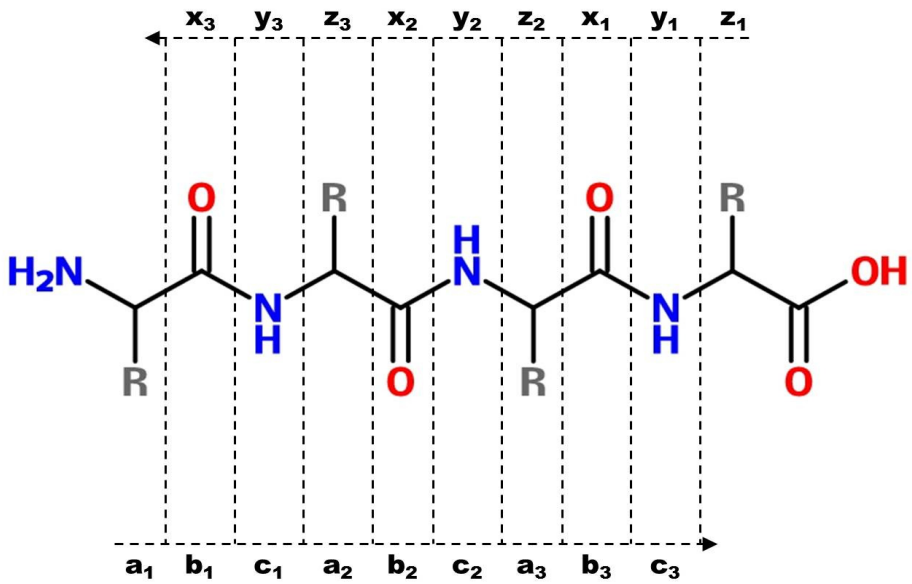

Figure 3: Fragmentation nomenclature for peptide ion cleavages along the polypeptide backbone. N-terminal fragment ions are notated a, b and c; C-terminal fragments are notated x, y and z. The numerical subscript indicates the number of amino acid residues present in the fragment ion.

The three most widely used means of inducing fragmentation in this manner are collision-induced/activated dissociation (CID/CAD), electron capture dissociation (ECD) and electron transfer dissociation (ETD). In CID/CAD, precursor ions of interest are accelerated to high kinetic energy and collided with an inert gas (usually helium, nitrogen or argon) (McLafferty and Bryce, 1967; Jennings, 1968). These collisions produce predominantly b- and y-series product ions (Roepstorff and Fohlman, 1984). ECD (Zubarev *et al.*, 1998) and ETD (Syka *et al.*, 2004a) entail bombarding precursor ions with low energy electrons and radical anions respectively to induce fragmentation, favouring production of c- and z-series product ions.

1.1.2.6.3.3. Precursor Ion Identification

As stated, the fragmentation spectrum of a peptide is diagnostic of its sequence. However, an experimental MS/MS spectrum may exhibit some degree of homology with multiple theoretical MS/MS spectra. Furthermore, manual interpretation of experimental spectra is time-consuming and impractical for complex samples. A pivotal development in the field was the development of software tools enabling experimental MS/MS spectra to be searched against theoretical MS/MS spectra derived from protein sequence databases. The theoretical spectra queried are delineated by search-specific parameters

pertaining to experimental and instrumentation-related constrains (e.g. enzyme used for digestion, fixed and variable peptide modifications, error window on experimental peptide m/z ratios). Experimental to theoretical spectral matches are ranked based on the probability that the match is genuine. A number of these tools are in use today; each differing slightly in the nature of the algorithm/s used to perform the ranking. A couple of the most widely used are described in more detail below.

The first software tool developed for this purpose was SEQUEST (Eng *et al.*, 1994). SEQUEST compares experimental fragmentation spectra of a given precursor ion to theoretical fragmentation spectra derived from precursor ions with similar m/z ratios and computes two statistics: XCorr (cross correlation of experimental and theoretical spectra) and ΔCN (difference between XCorr of highest ranking and second-highest ranking matches, assesses extent to which XCorr of highest ranking match deviates from stochastic matching).

Mascot (Perkins *et al.*, 1999) performs the same initial comparison but subsequently assigns all considered theoretical spectra a score dependent on the probability that the match between experimental and theoretical spectra is a random event, with low probability matches being assigned high scores and vice versa. The statistical significance of a match is ascertained by reference to a $P > 0.05$ threshold score determined from the data set and parameters under consideration. The probability of a peptide with a score identical to the threshold score being a random match is thus 1 in 20. The probability of a peptide with a score above the threshold score being a random match then decreases exponentially with increasing score.

Given the nature of these software tools, it is invariable that some experimental to theoretical fragmentation spectra matches will be false. The prevalence of these ‘false positives’ can be estimated through the use of decoy database searching (Elias and Gygi, 2007), whereby the protein database from which theoretical spectra are derived is randomized or reversed. Since no genuine matches should be expected from searching the decoy database, the matches which are found can be used to approximate the false discovery rate of a given experiment, imparting additional validation to genuine matches.

1.1.2.6.3.4. Protein Identification

The final stage in the bottom-up workflow is to assign all peptides identified in a given experiment to proteins. Mascot assigns all peptide matches to proteins regardless of their score. The scores of unique peptides assigned to each protein are then summed to arrive at a protein score. The output of a Mascot search is thus a list of proteins ranked on the basis of the summed scores of their peptides. The statistical significance of a protein hit is ascertained in a similar manner to that of peptide hits. The higher a protein score, the greater the confidence that that protein is present in the sample.

It is worth noting briefly here that assigning peptides to proteins is in itself a far from trivial process. Certain peptide sequences are present in various isoforms of the same protein or in various proteins with redundant function. However, information pertaining to the proteinaceous origins of these 'degenerate peptides' (Nesvizhskii *et al.*, 2003) is lost during the digestion step of a bottom-up workflow. This is known as the 'protein inference problem' (Nesvizhskii and Aebersold, 2005). The problem can be confronted in the simplest sense by applying the principle of parsimony. In cases where a given set of peptides maps to multiple proteins, Mascot reports the minimum set of proteins to which all observed peptide matches can be assigned. Where identical sets of peptides map to multiple proteins; these proteins are grouped as a single hit.

1.1.3. Plasma Membrane Proteomics

With regard to characterization of sub-proteomes, the plasma membrane proteome is frequently of considerable interest. Biological membranes demarcate intracellular compartments within cells and cells as a whole from their external environments. Since proteins are the principle mediators of all biological processes, it follows that membrane proteins govern the functionality of the membranes with which they are associated. Plasma membrane proteins act as receptors for propagation of signal transduction cascades; transporters and channels for movement of molecules and ions across the membrane; and adhesion molecules for contact-mediated cell-cell communication (Almen *et al.*, 2009). With 20% – 30% of genes in the majority of eukaryotic organisms encoding transmembrane proteins (Krogh *et al.*, 2001) and 60% of all existing drug targets possessing cell surface-exposed domains (Overington *et al.*, 2006); the origins of this aforementioned interest are evident.

1.1.3.1. Types of Membrane Protein

Membrane-associated proteins can be broadly divided into integral membrane proteins (IMPs) and peripheral membrane proteins depending on whether or not they possess domains which span the breadth of the membrane. IMPs may possess either α-helical or β-barrel transmembrane domains (TMD); with the former constituting nearly all of the aforementioned 20% - 30% eukaryotic transmembrane proteins. α-helical IMPs can be further subdivided into Type 1 (single TMD, cytoplasmic C-terminus), Type 2 (single TMD, cytoplasmic N-terminus and multi-pass (more than one TMD) (Kanapin *et al.*, 2003). Peripheral membrane proteins reside on either side of the membrane and interact with either IMPs themselves or with membrane lipids (Tan *et al.*, 2008). This is shown graphically in **Fig. 4**.

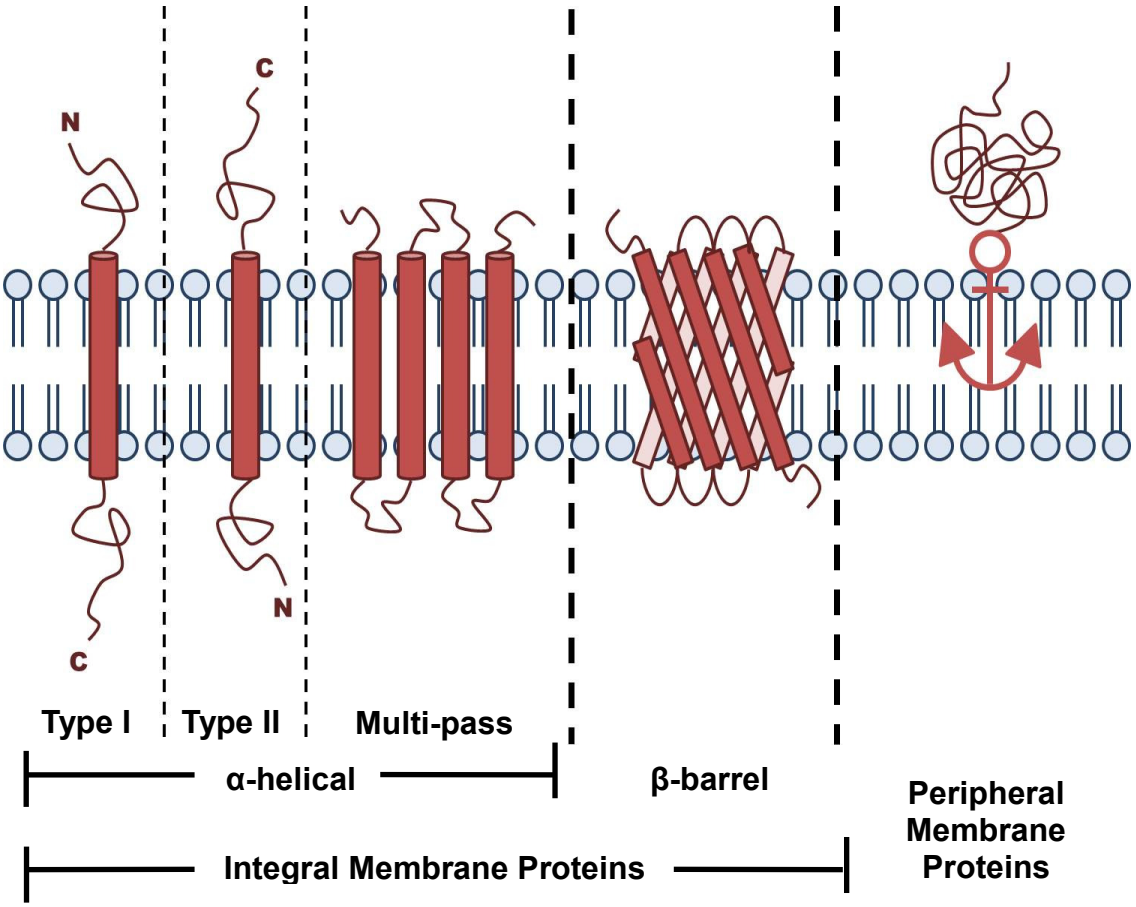

Figure 4: Membrane protein nomenclature. Membrane proteins are classed as either integral (IMPs) or peripheral depending on whether they possess transmembrane domains (TMDs). TMDs may have either α-helical or β-barrel secondary structure. α-helical IMPs are categorized as Type I, Type II or multi-pass depending on number of TMDs and orientation within the lipid bilayer. Peripheral membrane proteins do not span the bilayer but may be associated with IMPs or the membrane itself.

1.1.3.2. Challenges of Plasma Membrane Proteomics

Unfortunately, the characteristics of plasma membrane proteins which render them so interesting in theory also ensure that they are rather intractable to work with in practice. This is particularly true in bottom-up proteomic workflows; where their low abundance (approximately 2% relative to total cellular protein content (Rahbar and Fenselau, 2004)) and their comparative insolubility in the aqueous buffers which would typically be used throughout the workflow both pose significant obstacles to attaining comprehensive plasma membrane proteome coverage (Helbig *et al.*, 2010). A wide array of techniques has been developed in an effort to circumvent these obstacles. In the context of the bottom-up workflow outlined in **Fig. 1**, these techniques are predominantly concerned with membrane protein enrichment during the extraction/isolation

step and membrane protein solubilization to facilitate the continuation of the workflow thereafter.

1.1.3.3. Plasma Membrane Protein Enrichment

The rationale for performing membrane protein enrichment in plasma membrane-based proteomic studies is to increase the relative abundance of this particular class of proteins in a sample through depletion of proteins which would otherwise be present in far greater quantities (for instance cytoplasmic and nuclear proteins); thus increasing the probability that they are sampled during LC-MS. This can be achieved in a variety of ways, but the majority can be broadly divided into two categories: subcellular fractionation-based techniques which utilize some form of differential and/or density gradient centrifugation, and affinity purification-based techniques.

Differential centrifugation partitioning a crude cell lysate into soluble and insoluble fractions is probably the most simple form of subcellular fractionation and has been used successfully for membrane proteomics of simple prokaryotic organisms (e.g. (Goo *et al.*, 2003)) Sucrose density gradient centrifugation separates organelles on the basis of their buoyant density, is regarded as the classical subcellular fractionation technique and has previously been used for isolation of plasma membrane fractions of more complex organisms for proteomic analysis (e.g. (Zhang *et al.*, 2005)). Coating cells with cationic colloidal silica and crosslinking with polyacrylic acid results in formation of a dense pellicle, allowing plasma membrane sheets to be pelleted by differential centrifugation after lysis (Chaney and Jacobson, 1983) and collected for MS analysis (e.g. (Rahbar and Fenselau, 2004)). Aqueous-polymer two-phase partitioning with polyethylene glycol (PEG) and dextran causes membranes to preferentially segregate into the more hydrophobic PEG phase, and subsequent treatment of plasma membranes with wheat germ agglutinin (WGA) specifically apportions them into a clean dextran phase upon repeated partitioning (e.g. (Schindler *et al.*, 2006)).

Affinity purification-based enrichment strategies centre around the tagging of surface-exposed protein domains on intact cells and subsequent pull-down of tagged proteins with appropriate reagents. Biotinylation reagents incorporating reactive groups which target primary amines and sulfhydryl groups can all be

used to this end (Macher and Yen, 2007). Amine-directed biotinylation reagents are explored in more detail in **Chapter 4**. Cell surface glycoproteins can also be targeted in this manner using lectin affinity chromatography (e.g. (Ghosh *et al.*, 2004)). Alternatively, the *cis-diol* groups of glycan carbohydrates can be derivatized to aldehydes, allowing affinity capture of glycoproteins on immobilized hydrazide (e.g. (Zhang *et al.*, 2003)). Most recently, phospholipid coated superparamagnetic nanoparticles have been used to non-covalently coat the cell surface, enabling plasma membranes to be isolated magnetically after cell lysis (Thimiri Govinda Raj *et al.*, 2011).

A further consideration pertinent to both subcellular fractionation and affinity purification-based enrichment strategies is depletion of non-membrane proteins associated with proteins embedded within the membrane or the membrane itself. This can be achieved through washing membrane-enriched fractions with high salt buffers (disrupting interactions of membrane-associated proteins with phospholipid head groups (Hurwitz *et al.*, 2006)) and high pH buffers (converting closed membrane vesicles to open sheets and releasing trapped non-membrane proteins (Fujiki *et al.*, 1982)). Consecutive extractions of crude membrane extract in high salt, high pH and urea-containing buffers has been reported to provide effective membrane protein enrichment with no additional processing steps (Wisniewski *et al.*, 2009a) and will be examined further in **Chapter 4**.

Where the membrane fraction is recovered intact, depletion of membrane phospholipids themselves prevents their interference in downstream steps in the workflow. This is typically achieved by precipitating proteins whilst partitioning lipids into organic phases with, for instance, methanol/chloroform or acetone (Wessel and Flugge, 1984) .

A distinct approach is cell surface ‘shaving’, where intact cells are incubated in the presence of proteases. Extracellular protein domains with protease-accessible sites are cleaved and can be separated from cells and collected. Whilst conceptually attractive and somewhat fruitful for ‘surfaceome’ analysis of gram-positive bacteria (Rodriguez-Ortega *et al.*, 2006), cell lysis in the presence of proteases and release of intracellular proteins into the surrounding medium has thus far proven problematic for eukaryotic cells (De Palma *et al.*, 2010).

1.1.3.4. Plasma Membrane Protein Solubilization and Digestion

There are also a wide range of published strategies for membrane protein solubilization and digestion. The hydrophobic domains of membrane proteins cause them to aggregate and precipitate in aqueous buffers, rendering some means of solubilization essential to prevent protein losses and facilitate proteolysis (Speers and Wu, 2007). However, a key consideration is the extent to which the means of solubilization impacts upon the efficiency of digestion and LC-MS analysis. The two processes are thus frequently considered collectively in shotgun workflows.

Solubility issues are the underlying cause of the underrepresentation of membrane proteins in 2D-PAGE. A protein is at its least soluble in aqueous conditions at its isoelectric point and sparingly soluble membrane proteins thus tend to precipitate during first dimension isoelectric focussing (IEF), which prevents effective transfer into second dimension PAGE and severely hampers analysis (Klein *et al.*, 2005). Alternative two-dimensional separation strategies such as blue native (BN)/SDS-PAGE (Schagger and von Jagow, 1991) and benzyldimethyl-n-hexadecylammonium chloride (16-BAC)/SDS-PAGE (Hartinger *et al.*, 1996) alleviate these issues to some extent but 2D-PAGE is now rarely employed for membrane-based studies.

1.1.3.4.1. Detergents

The most effective way to solubilize membrane proteins is with the aid of detergents. Detergents are composed of a polar head group and a hydrophobic tail and these amphipathic characteristics enable them to self-associate and bind to hydrophobic surfaces, partially imitating the properties of the phospholipid bilayer (Garavito and Ferguson-Miller, 2001). At and above the critical micelle concentration (CMC) monomers will self-assemble into micelles; it is at this point that they can interact with and extract IMPs from the bilayer (le Maire *et al.*, 2000). Detergents come in a wide range of shapes and sizes and the physicochemical properties of each determine the concentration at which micellar formation is favoured. They are generally classified as being ionic, non-ionic or zwitterionic (Garavito and Ferguson-Miller, 2001), with bile acid salts being a class of ionic detergents with distinct structural properties (Seddon *et al.*, 2004).

The archetypal example of an ionic detergent is sodium dodecyl sulphate (SDS), widely regarded as the most powerful detergent available for solubilization and denaturation of proteins. Unfortunately for shotgun proteomics, it is also only compatible with tryptic digestion at minute (< 0.1%) concentrations (Zhang and Li, 2004) and severely interferes with RPLC (Bosserhoff *et al.*, 1989) and ESI (Loo *et al.*, 1994), necessitating near-complete removal prior to LC-MS. This is a topic of much research in the field and a variety of methods have been proposed to enable SDS depletion without incurring concurrent sample loss; these include dialysis (Nagaraj *et al.*, 2008), potassium chloride precipitation (Zhou *et al.*, 2012b) and SCX chromatography (Sun *et al.*, 2012). Commercially available resins which claim to quantitatively deplete SDS (amongst other detergents commonly used in shotgun workflows) have also been described (Antharavally *et al.*, 2011).

Non-ionic detergents (e.g. *n*-octyl glucoside), zwitterionic detergents (e.g. 3-[(3-cholamidopropyl)dimethylammonio]-1-propanesulfonate – CHAPS) and bile acid salts (e.g. sodium deoxycholate – SDC) do not possess the same solubilizing and denaturing power of SDS but compatibility with proteolytic enzymes at higher concentrations and/or increased ease of removal from samples mean they are also frequently employed in membrane-based proteomic workflows. For instance, *n*-octyl glucoside and CHAPS are both compatible with trypsin digestion at concentrations up to 1% (Zhang and Li, 2004) and both have a relatively high CMC, enabling them to be effectively depleted from samples by dialysis (Lorber *et al.*, 1990). Trypsin retains over three-quarters of its activity in concentrations of SDC up to 10% (Lin *et al.*, 2008), and SDC itself precipitates upon acidification with 0.1% trifluoroacetic acid (TFA), enabling removal by centrifugation (Zhou *et al.*, 2006).

Commercially available acid-labile detergents such as RapiGest™ (Yu *et al.*, 2003) (Waters) and PPS Silent® Surfactant (Norris *et al.*, 2003) (Protein Discovery) have been conceived specifically for mass spectrometric applications. They purport to exhibit solubilizing power on a par with SDS whilst being both compatible with proteolysis at higher concentrations and cleavable into non-surfactant breakdown products through sample acidification after digestion. However, it is acknowledged that hydrophobic peptides may co-precipitate with one of the RapiGest™ breakdown products (Yu *et al.*, 2003).

1.1.3.4.2. Chaotropes

Chaotropes such as urea, thiourea and guanidium chloride stabilize unfolded protein states through interference with higher order protein structure (Moglich *et al.*, 2005). Whilst chaotropes do not extract the majority of IMPs from the phospholipid bilayer itself (Wei *et al.*, 2005), they have applicability in the denaturation of otherwise inaccessible protein domains to facilitate proteolysis and are frequently employed in tandem with the detergent solubilization strategies described above. Whilst trypsin is inhibited at chaotrope concentrations required to disrupt TMDs, endoproteinase Lys-C is far more robust, retaining activity in up to 8 M urea. This enables Lys-C to cleave at lysine residues which would be inaccessible to trypsin at lower chaotrope concentrations, augmenting subsequent tryptic digestion (Thingholm *et al.*, 2008).

1.1.3.4.3. Solvents and Acids

Aqueous-organic solvent systems (acetonitrile / methanol – water) can disrupt phospholipid bilayers (Patra *et al.*, 2006) and denature proteins owing to their favourable interaction with nonpolar amino acid residues relative to purely aqueous buffers (Fink and Painter, 1987; Welinder, 1988); yet preserve sufficient trypsin activity to enable proteolysis to occur (Russell *et al.*, 2001) and can simply be evaporated prior to LC-MS analysis. Organic acids such as formic acid (FA) (Washburn *et al.*, 2001) and TFA (Zhong *et al.*, 2005) have also previously been used for the extraction and solubilization of IMPs. They have the advantage of complete compatibility with LC-MS but the disadvantage of incompatibility with tryptic digestion given the low pHs, necessitating the use of alternative modes of proteolysis (cyanogen bromide in (Washburn *et al.*, 2001) and acid-catalysed hydrolysis in (Zhong *et al.*, 2005)).

1.1.3.4.4. Integrated Workflows

It is evident from the multitude of approaches described above that the proteomics community has yet to hit upon an optimal strategy for comprehensive solubilization, digestion and shotgun analysis of the membrane proteome, largely due to the aforementioned difficulties in integrating various stages of the workflow as a cohesive whole. One recently described technique which seeks to do so is filter-aided sample preparation (FASP) (Wisniewski *et*

al., 2009b). In FASP, the protein sample of interest is completely solubilized in high concentrations of SDS (typically 4% (w/v)). The sample is then diluted with an excess of 8 M urea, dissociating detergent micelles from proteins whilst maintaining them in solution (Nagaraj *et al.*, 2008). The sample is then processed further in a molecular weight cut-off microcentrifuge spin column, enabling SDS monomers to be depleted whilst denatured proteins are retained and buffer exchanged into 8 M urea. Proteins are then digested first with Lys-C, then trypsin (after dilution) and released peptides pass through the molecular weight cut off (MWCO) filter and are then collected for LC-MS analysis. The applicability of the method to membrane-based studies has since been demonstrated with a crude membrane preparation extracted in high salt, high pH and urea-containing buffers as described in section **1.1.3.3.** (Wisniewski *et al.*, 2009a). FASP is explored further in **Chapter 4**.

1.1.4. Quantitative Proteomics

A straightforward shotgun strategy is well-suited to qualitative proteome analysis, though whether this information is valuable from a biological perspective is another question entirely. If proteome profiling is to be used to address biological questions, a reference point is needed. This typically entails comparing and contrasting the proteins present in two (or more) physiologically related (but not identical) states of a biological system. Even with such a reference point, a list of proteins present in each sample is likely to be of limited use; there would be very few (if any) proteins present in one proteome which were completely absent in the other. However, if the reference point could be used to infer the abundances of proteins present in each sample, this information would be of far greater biological worth. Protein abundance changes upon application of given stimuli hint at roles for the protein in question in response to the stimuli and can be indicative of potential drug targets and biomarkers for diagnosis and treatment of disease. This is the rationale behind quantitative proteomics. There are many methods available for performing quantitative proteomic analyses; however they can be broadly categorized as being either label-based or label-free.

Label-based approaches exploit the fact that proteins and peptides are able to incorporate stable isotopes into their amino acids which impart a measureable mass difference but do not significantly alter the physicochemical properties of the protein or peptide, such that both forms co-migrate or co-elute upon electrophoretic or chromatographic analysis respectively. This enables two or more samples to be labelled with differential mass tags and then combined prior to analysis. A peptide of given sequence present in differentially labelled forms in a single sample will produce discriminating peaks in a precursor or product ion scan. The relative intensities of the peaks can subsequently be compared to infer the relative quantities of differentially labelled peptide present in the sample. Label-based approaches can be further classified depending on whether quantitation is performed at the MS1 or MS2 level. In label-free approaches, quantitation is performed between samples rather than within them by comparing the ion intensity or the number of spectra acquired for a given peptide across all samples analysed. An overview of these various approaches is shown in **Fig. 5**.

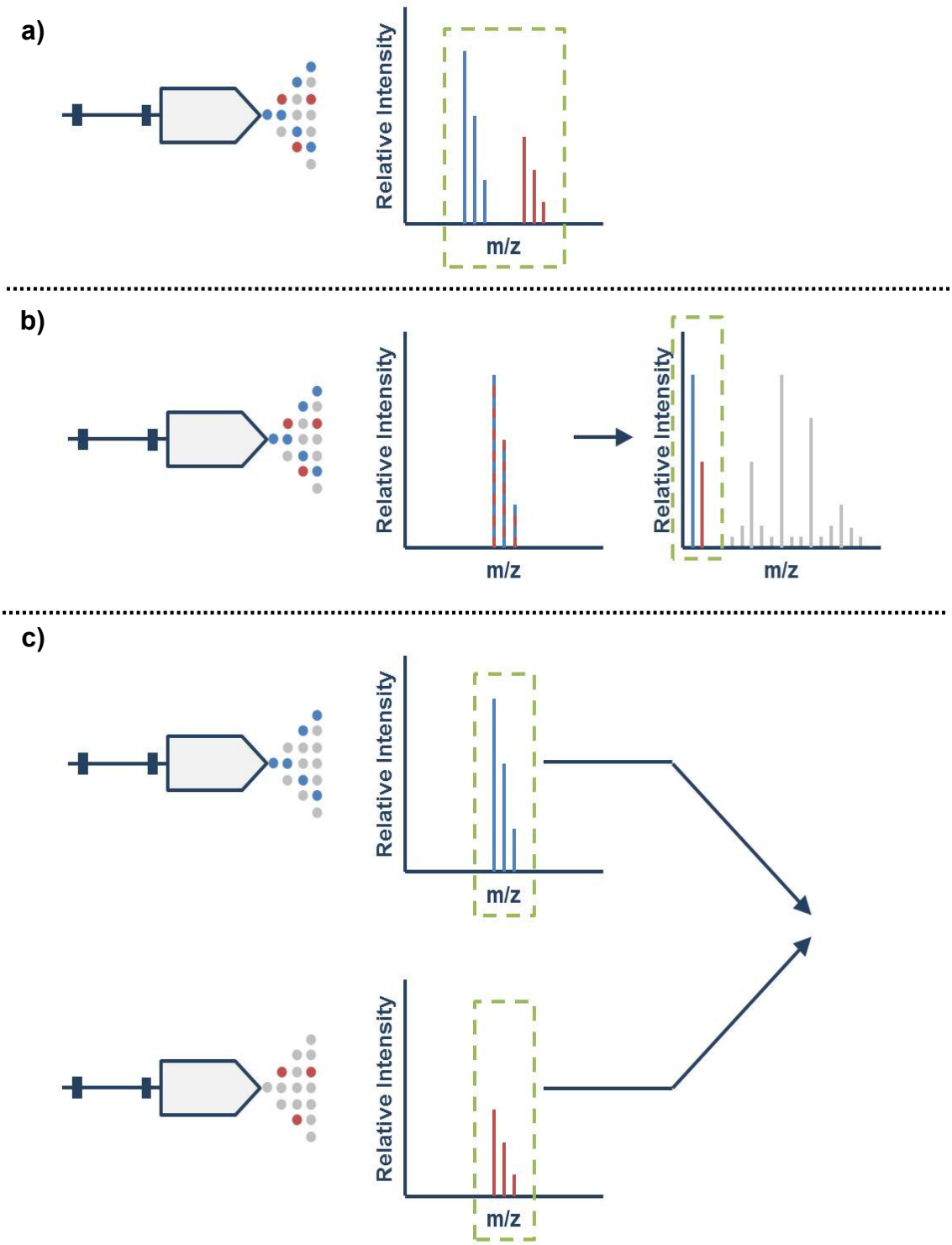

Figure 5: Quantitative proteomic strategies. **a)** Label-based quantitation at the MS1 level. Peptides are differentially labelled and relative abundances of differentially labelled precursor ions compared. **b)** Label-based quantitation at the MS2 level. Peptides are isobarically labelled and thus differentially labelled precursor ions have the same mass. Quantitation is performed by comparing relative abundances of reporter group ions which preferentially fragment from the peptide in the product scan. **c)** Label-free quantitation. Samples to be quantitatively compared are analysed separately and quantitation performed on the basis of their response in the mass spectrometer (total ion intensity in this instance). The dashed green areas bound the ions being quantitated.

1.1.4.1. Label-based Quantitative Proteomics (MS1)

1.1.4.1.1. Chemical Labelling

The first mass spectrometry-based quantitative proteomic methods were chemical in nature, with isotope-coded labels conjugated to various chemicals which target the reactive sites present on peptides (typically the N-terminus and the side chains of lysine and cysteine residues).

The first reagent developed with this purpose in mind was the isotope coded affinity tag (ICAT) (Gygi *et al.*, 1999), which is composed of a biotin affinity tag containing either eight hydrogen atoms (light tag) or eight deuterium atoms (heavy tag) and a thiol specific reactive group to target the tag to cysteine residues. The major drawbacks of this method are twofold. Firstly, only cysteine-containing peptides are recovered after tagging and cysteine is a relatively rare amino acid. Secondly, deuterium is known to affect retention time in RPLC, causing light and heavy-labelled peptides to elute at different times and complicating quantitation (Zhang *et al.*, 2001). This second issue has since been addressed by substituting the deuterated affinity tag with a ^{13}C-labelled tag (Hansen *et al.*, 2003; Li *et al.*, 2003; Oda *et al.*, 2003).

An alternative MS1-based chemical labelling strategy targeting primary amine residues is differential dimethyl labelling (Hsu *et al.*, 2003; Schmidt *et al.*, 2005). The mass shift is imparted by reacting peptides with different isotope-coded forms of formaldehyde and cyanoborohydride. This theoretically allows for many different mass shifts, though in practice a maximum of three are used (formaldehyde – cyanoborohydride, formaldehyde-d_2 – cyanoborohydride and formaldehyde-$^{13}c,d_2$ – cyanoborohydride-d_3), allowing for triplex labelling with each labelled species separated by 4 Da. Amine-targeted tagging enables increased proteome coverage relative to cysteinyl-targeted tagging but the deuterium retention time issue must once again be taken into consideration.

1.1.4.1.2. Enzymatic Labelling

Enzymatic labelling utilizes the hydrolytic addition of oxygen atoms to the carboxyl termini of peptides produced during proteolysis. Schnölzer et al. were the first group to show that tryptic digestion in $H^2{}_{18}O$ water imparts a 2 – 4 Da mass shift to the peptides produced relative to tryptic digestion in $H^2{}_{16}O$ water

(Schnolzer *et al.*, 1996). In practice, it is imperative to ensure that a 4 Da mass shift is imparted to all peptides as a 2 Da mass shift is insufficient to discriminate between the isotope envelopes of labelled and unlabelled peptides. ^{18}O labelling is examined in more detail in **Chapter 5**.

1.1.4.1.3. Metabolic Labelling

Metabolic labelling approaches exploit normal cell growth and division to introduce stable isotopes *in vivo* during protein synthesis. The most popular approach of this type is SILAC (stable isotope labelling by amino acids in cell culture) (Ong *et al.*, 2002), in which cells are cultured in media containing heavy or light isotopes of certain essential amino acids (typically arginine and lysine as this ensures that all peptides other than the C-terminal peptide will incorporate at least one heavy amino acid if trypsin is used for digestion). Near complete label incorporation can be achieved in as little as 5 cell cycles in replicative cell lines (Ong *et al.*, 2002). An alternative approach is to culture cells in media supplemented with Nitrogen-15 (Oda *et al.*, 1999); though this complicates data analysis considerably since different peptides will incorporate different amounts of isotope depending on the nitrogen content of their amino acid residues.

A major advantage of metabolic labelling is that the labels can be introduced and the samples mixed prior to any sample-handling steps, minimizing the introduction of variation due to parallel processing. A significant shortcoming is that the nature of the method limits the types of sample which can be labelled. Mice have been labelled with both SILAC (Kruger *et al.*, 2008) and ^{15}N (McClatchy *et al.*, 2007) by feeding with labelled diets for a number of generations but this is prohibitively expensive for large scale experiments. This can be overcome to some extent by using a labelled reference proteome as a 'spike-in' standard for comparison with multiple experimental proteomes and then quantifying the differences between the experimental proteomes on the basis of the quantitative data obtained from individual comparisons with the reference proteome. This approach has previously been used for quantitative proteomics of primary cultured neurons through comparison with a 15N-labelled rat brain (Liao *et al.*, 2012) and of human carcinoma tissue through comparison of a mixture of SILAC-labelled cell lines ('super-SILAC') (Geiger *et al.*, 2010).

Metabolic labelling also has applications in investigations into rates of protein turnover. In 'pulsed' SILAC, cells are cultured in light SILAC media and then transferred to differentially-labelled heavy SILAC media upon the imposition of differential stimuli (Schwanhausser *et al.*, 2009). Differences in protein turnover are ascertained by comparing the ratios of differential heavy labelling between samples.

1.1.4.2. Label-based Quantitative Proteomics (MS2)

MS2 level label-based quantitative proteomics differs from all of the approaches described above in that the quantitative measurement itself is performed in the product ion scan rather than the precursor ion scan. The best known MS2 level labelling reagents are the isobaric tags for relative and absolute quantification (iTRAQ) (Ross *et al.*, 2004) and the tandem mass tags (TMT) (Thompson *et al.*, 2003). The main advantage of these reagents is that the tags themselves are isobaric but incorporate reporter groups which fragment during MS/MS to produce a series of diagnostic 'signature' ions that can be quantitated. This circumvents the inherent limitations of MS spectra complexity associated with mass difference tags and enables significantly more scope for multiplexing within a single experiment (up to 8-plex for iTRAQ (Ow *et al.*, 2008) and 6-plex for TMT (Dayon *et al.*, 2008)). However, the reagents cannot be used for quantitation with all ion trap mass spectrometers owing to the well-known '1/3 cut-off rule' limitation which prevents detection of fragment ion masses which are approximately less than a third that of the precursor ion mass (with tryptic peptides this often includes the iTRAQ and TMT reporter ions). In addition, quantitative accuracy can be compromised if multiple peptide species with similar m/z ratios and retention times are selected for fragmentation at the same time (Ow *et al.*, 2009).

A less well known MS2 level quantitation strategy is isobaric peptide termini labelling (IPTL) (Koehler *et al.*, 2009), where two samples are rendered isobaric through incorporation of identical mass shifts to the N-termini of the peptides present in the first sample and the C-termini of the peptides present in the second sample. Quantitation is performed on the differentially N- and C-terminally labelled fragment ions themselves rather than with the aid of reporter ions. IPTL will be discussed in more detail in **Chapter 5**.

1.1.4.3. Absolute Quantitation

The labelling methods described so far all facilitate relative quantitative inferences to be made within a single sample. Absolute quantitation is also possible in a manner similar to the 'spike-in' metabolic labelling approach by using limited numbers of stable isotope labelled peptides or proteins of known concentration. Absolute quantitative approaches usually make use of selected reaction monitoring (SRM), where pre-defined 'transitions' (m/z values corresponding to pairs of precursor and fragment ions of interest) are monitored throughout the course of the experiment irrespective of precursor ion intensity. This targeted approach permits considerable increases in sensitivity and dynamic range for chosen ions over standard data dependent acquisition (Gallien *et al.*, 2011).

The first reagents conceived for absolute quantitation were the AQUA peptides (Gerber *et al.*, 2003), which are simply chemically synthesized stable isotope-labelled peptides of known concentration corresponding to a protein of interest. This concept has since been extended with the QconCAT (quantification concatemer) peptides (Beynon *et al.*, 2005), where an artificial protein comprised of a number of concatenated tryptic peptides corresponding to multiple proteins of interest is synthesized, affinity purified and introduced to the experimental sample prior to proteolysis. Design of AQUA and QconCAT constructs needs to be considered carefully to ensure optimal ionization and fragmentation behaviour of reference peptides within the mass spectrometer. In addition, neither technique is compatible with workflows incorporating protein fractionation steps owing to incomplete sample recovery for AQUA quantitation and the fact that the artificial protein construct does not correspond with any endogenously expressed protein for QconCAT quantitation (Havlis and Shevchenko, 2004). This shortcoming can be overcome using PSAQ (protein standard absolute quantification) stable isotope labelled proteins (Brun *et al.*, 2007), which can be spiked into samples at the beginning of the proteomics workflow and provide multiple peptide standards for a single protein of interest.

1.1.4.4. Label Free Quantitative Proteomics

Label-free approaches seek to use the mass spectrometer itself as a quantitative tool, alleviating the need to label and combine samples prior to

analysis and theoretically allowing an unlimited number of experiments to be compared. Peptide abundance can be inferred either directly or indirectly. Direct label free quantitation entails integrating the areas under the curves of extracted ion chromatograms (XICs) and comparing the signal responses of individual peptides (which are linear over around four orders of magnitude) between LC-MS runs (Bondarenko *et al.*, 2002; Chelius and Bondarenko, 2002). Indirect label free quantitation exploits the fact that the number of peptide-to-spectrum matches (PSMs) obtained for a given peptide consistently correlates with abundance over around two orders of magnitude (Liu *et al.*, 2004a). This is routinely reported as emPAI (exponentially modified protein abundance index, the exponent of the number of peptide-to-spectrum matches for a given protein divided by the number of theoretically observable peptides that the protein could produce (Ishihama *et al.*, 2005)).

A few factors pertaining to instrumentation need to be considered if quantitative inferences are to be made between runs. In direct label free approaches, the identification and quantitation of a peptide are decoupled and it is thus vital that the two are correctly reconciled. A mass spectrometer with high resolution and mass accuracy is of considerable utility here (Bantscheff *et al.*, 2012). Narrow peak widths aid in resolution of individual peptide species and retention time stability across runs can increase confidence that an XIC corresponds to a peptide in the absence of MS/MS data in all runs, thus a robust LC setup is also essential for accurate label free quantitation.

1.1.4.5. Quantitation Software

Whether label-based or label-free, intensity-based protein quantitation requires some degree of additional data processing on top of that used to for protein identification. For MS2 level label-based quantitation, the quantitative calculations are performed concurrently with peptide and protein identification and ratios are reported within the software tools themselves (where the quantitation method in question is supported). Mascot supports the commonly employed reporter ion chemistries (iTRAQ and TMT) and quantitation protocols are also customizable to allow for use of more exotic chemistries. For other modes of intensity-based quantitation, a number of open-source (e.g. MaxQuant (Cox and Mann, 2008)) and commercial (e.g. Mascot Distiller)

software tools are available to detect, align, normalise and compare peptide features of interest both within and across LC-MS runs.

1.2. Dendritic Cells

1.2.1. Dendritic cells and immunological tolerance

The term immunological tolerance refers to *"a state of indifference or non-reactivity towards a substance that would normally be expected to elicit an immunological response"* (Medawar, 1960). Such a state was first demonstrated *in vivo* in the transplantation immunology field using skin grafts between different strains of mice (Wood *et al.*, 2010); work for which Sir Peter Medawar and Sir Frank McFarlane Burnett were jointly awarded the Nobel Prize in Medicine in 1960. Today, we have a much greater appreciation of the importance of immunological tolerance and a more comprehensive understanding of the mechanisms which bring it to pass. T cell receptor gene rearrangement is an extremely effective means of generating a sizeable and diverse repertoire of receptors (Arstila *et al.*, 1999) but its stochastic nature inevitably ensures a significant percentage of productive rearrangements recognize endogenous antigens (van Meerwijk *et al.*, 1997). The processes underpinning immunological tolerance serve to prevent these self-reactive T cells from contributing to autoimmunity. The vast majority of self-reactive cells are deleted during their development through negative selection in the thymus. This is known as central tolerance (Palmer, 2003). However, a small number of cells evade this process and migrate from the thymus; these cells must be kept in check in the periphery by a process known as peripheral tolerance (Walker and Abbas, 2002).

Dendritic cells (referred to hereafter as DCs) are 'professional' antigen presenting cells, potent activators of other leukocytes and orchestrators of adaptive immunity (Trinchieri, 2007). Their presence as a constituent of murine peripheral lymphoid tissue (Steinman and Cohn, 1973) and purpose in performing the processes described above was first documented and defined by Ralph Steinman and collaborators; work which garnered a posthumous Nobel Prize in Medicine for Steinman in 2011. However, more recent work has shown that DCs are also important in the establishment and maintenance of central and peripheral tolerance. Their role in central tolerance was first established by Brocker *et al.*, who targeted expression of major histocompatibility complex (MHC) class II I-E molecules specifically to DCs in a transgenic mouse model and showed that its expression on thymic DCs was

sufficient to negatively select cognate cluster of differentiation (CD)4^+ T cells (Brocker *et al.*, 1997). Their role in peripheral tolerance was demonstrated by Probst *et al*., who generated transgenic mice in which DC expression and presentation of lymphocytic choriomeningitis virus (LCMV) peptide epitopes to $CD8^+$ T cells could be induced via Cre/Lox recombination in response to administration of Tamoxifen (Probst *et al.*, 2003). Co-administration of Tamoxifen with an antibody against CD40 caused the epitopes to be presented in an immunogenic context and led to antigen-specific $CD8^+$ T cell activation and expansion, whilst Tamoxifen alone caused the epitopes to presented in the steady state and led to antigen-specific $CD8^+$ T cell tolerance which endured upon subsequent challenge with LCMV. An extensive discussion of central tolerance is not pertinent to this body of work and it will not be considered further. The capacity of DCs to induce and maintain peripheral tolerance is examined in more detail below.

1.2.2. Functional specialization of dendritic cell subsets

All human DCs express high levels of MHC Class II and can be distinguished from blood lymphocytes through the absence of lineage-specific markers (Collin *et al.*, 2013). However, it is now clear that there are a number of DC subsets which differ in their locations throughout the body, their migratory pathways and their precise immunological function. Recent convention conceived to facilitate comparison of human and murine DC populations broadly divides human DCs into three subsets: $CD1c^+$ myeloid DCs, $CD141^+$ myeloid DCs and plasmacytoid DCs (Ziegler-Heitbrock *et al.*, 2010). $CD1c^+$ DCs comprise the major population of myeloid DCs. Present in peripheral tissues, lymphoid tissues and blood; they perform the processes of antigen uptake, transport and presentation to $CD4^+$ T cells with which DCs are typically associated (Reis e Sousa, 2001). $CD141^+$ DCs represent a small sub-population of myeloid DCs, distinguished by their considerably enhanced capacity to cross-present antigen to $CD8^+$ T cells and initiate cytotoxic effector responses (Bachem *et al.*, 2010; Crozat *et al.*, 2010; Jongbloed *et al.*, 2010; Poulin *et al.*, 2010). Plasmacytoid DCs are primarily present in blood and are uniquely specialized in their ability to produce vast quantities of type I interferons in response to viral challenge (Siegal *et al.*, 1999).

Additional subsets of DCs with distinct functional specializations are also recognized. For instance, human dermal and epidermal tissue contains $CD1a^+$ and $CD14^+$ 'dermal' DCs and Langerhans cells with structural and functional features specific to the environment in which they reside (Klechevsky *et al.*, 2008). Novel populations of DC not present in steady state conditions also appear in response to inflammation and are thought to differentiate from $CD14^+$ monocytes (Shortman and Naik, 2007). Derivation of these 'inflammatory' DCs is well characterized *in vitro* through culture of $CD14^+$ monocytes in the presence of interleukin 4 (IL-4) and granulocyte macrophage colony stimulating factor (GM-CSF) followed by exposure to a variety of inflammatory stimuli (e.g. tumour necrosis factor alpha (TNFα) (Sallusto and Lanzavecchia, 1994)). There is also evidence that it occurs *in vivo* through experiments in which monocytes were adoptively transferred into recipient mice and their fates followed upon introduction of inflammatory stimuli (Geissmann *et al.*, 2003; Serbina *et al.*, 2003).

1.2.3. Dendritic cells in immunity and tolerance

The molecular mechanisms which govern the function of myeloid DCs are now well known. In the steady state, peripheral tissue-resident DCs exist in an 'immature' state and act as 'immune sentinels'; surveying their surroundings through a variety of endocytic mechanisms and perpetually capturing, processing and presenting antigenic material to T cells (Sallusto *et al.*, 1995). The seemingly diametrically opposed outcomes of immunity and tolerance are both initiated through T cell recognition of cognate antigen presented by DCs. The question of whether the T cell is subsequently activated or tolerised is context-specific and determined by cues emanating from the microenvironment in which the DC itself encounters the antigen.

1.2.3.1. Dendritic cells in immunity

If an infectious agent is present, antigen uptake is coupled with the detection of 'danger signals' by pattern recognition receptors (PRRs). DCs are now known to express a number of PRRs (Takeuchi and Akira, 2010) (including Toll-like receptors (TLRs), C-type lectin receptors (CLRs), NOD-like receptors (NLRs) and RIG-I-like receptors (RLRs)) capable of recognizing exogenous pathogen-associated molecular patterns (PAMPs) such as peptidoglycan and

lipopolysaccharide (LPS) (Kadowaki *et al.*, 2001) and endogenous danger-associated molecular patterns (DAMPs) derived from stressed, injured or necrotic cells, such as heat shock proteins (Gallucci and Matzinger, 2001). Detection of these danger signals can contribute to inducing DC maturation (Macagno *et al.*, 2007). Maturing DCs cease to sample their extracellular environment (Garrett *et al.*, 2000) whilst upregulating the expression of MHC class II molecule / peptide complexes (signal 1) (Cella *et al.*, 1997), co-stimulatory molecules such as CD80 and CD86 (signal 2) (Caux *et al.*, 1994) and chemokine receptors CCR7 and CXCR4 (Sallusto *et al.*, 1998); enabling them to migrate out of peripheral tissues and towards lymph nodes to activate naïve T cells. Concurrent with activation, DCs provide T cells with immune-polarizing cues (signal 3) (Kalinski *et al.*, 1999) which direct their differentiation into an appropriate subtype. For example, DC production of IL-12 concomitant with stimulation instructs T cells to adopt a T_h1 phenotype (Macatonia *et al.*, 1995).

1.2.3.2. Dendritic cells in tolerance

If no infectious agent is present, antigen uptake is not coupled with the aforementioned danger signals and DCs remain immature. They continue to process and present self-antigens, but since uptake of these antigens is not (typically) coupled with danger signals, they express neither the chemokine receptors necessary to migrate from the periphery nor the co-stimulatory molecules necessary to activate T cells. This ensures that any potentially self-reactive T cells encountered in the periphery are not activated.

It was thus initially thought that mature DCs induce immunity and immature DCs induce tolerance (Probst *et al.*, 2003). However, it has since become evident that the situation is a little more equivocal: there are a number of reported instances in which activated ‘mature’ DCs induce T cell tolerance. For instance, DCs matured in the presence of PAMPs such as filamentous haemagglutinin (FHA) from *B. pertussis* (McGuirk *et al.*, 2002) or lysophosphatidylserine (PS) from *S. mansoni* (van der Kleij et al., 2002) adopt a mature surface phenotype but produce IL-10 and induce naïve T cells to adopt an IL-10-producing regulatory phenotype. DCs cultured in the presence of anti-inflammatory cytokines (IL-10 and transforming growth factor beta (TGF-β)) (Lan *et al.*, 2006) or corticosteroids (de Jong *et al.*, 1999) and matured with LPS exhibit a more

immature surface phenotype than would be expected upon LPS stimulation and expand regulatory T-cells and T_h2-polarized T-cells respectively (though the authors of the second study concede that T_h2 polarization can cause undesirable side effects due to elevated levels of Immunoglobulin E (IgE) and eosinophils). As touched upon above, it is now generally accepted that DCs can be ‘alternatively activated’ by certain signals they receive during maturation and subsequently exhibit similar T cell stimulatory capacity to that of mature DCs but generate tolerance in the same manner as immature DCs. This significant plasticity in the function of DCs is illustrated in **Fig. 6** overleaf.

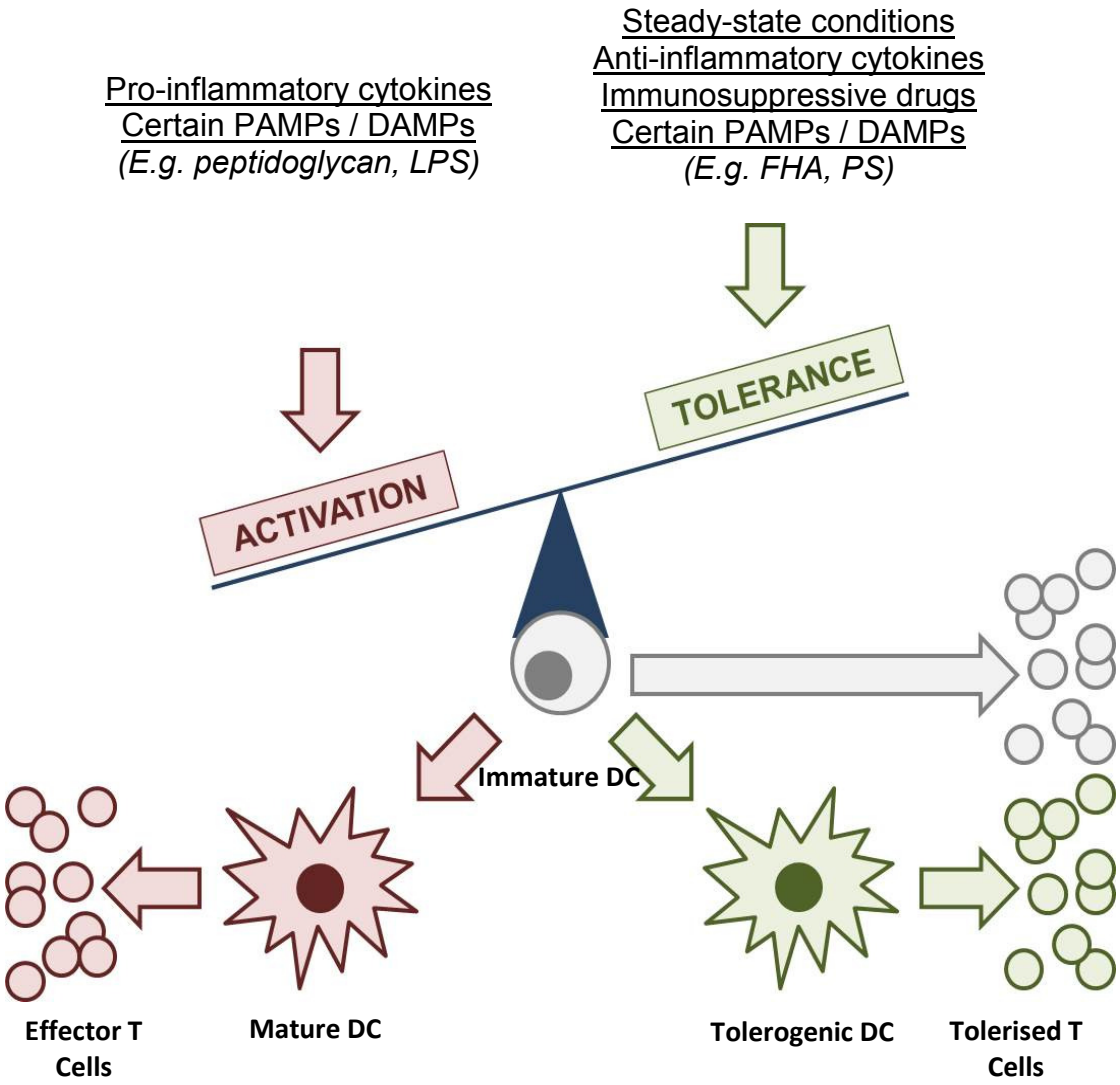

Figure 6: Dendritic cells in immunity and tolerance

DCs integrate antigen uptake, processing and presentation with the signals which they receive from the extracellular milieu to determine whether they will activate or tolerise cognate T cells. If antigen uptake takes place in the presence of danger signals (pro-inflammatory cytokines and pathogen/danger-associated molecular patterns such as peptidoglycan and lipopolysaccharide), DCs mature and activate effector T cells. If antigen uptake takes place in the steady-state, DCs remain immature and tolerise T cells. If antigen uptake takes place in the presence of anti-inflammatory cytokines, immunosuppressive drugs or pathogen/danger-associated molecular patterns such as filamentous haemagglutinin and lysophophatidylserine; DCs may assume a mature-like phenotype but retain the ability to tolerise T cells.

1.2.4. Mechanisms of tolerance induction

Several mechanisms have been outlined through which DCs mediate tolerance in the periphery. These include clonal anergy and clonal deletion of autoreactive T cells, polarization of autoreactive T cell cytokine profiles and induction and/or expansion of regulatory T cells (Hilkens *et al.*, 2010).

Clonal anergy is a hyporesponsive state assumed by T cells after recognizing their antigen in the absence of co-stimulation (Jenkins and Schwartz, 1987). Induction of clonal anergy upon stimulation with immature DCs has been demonstrated both *in vivo* and *in* vitro. Hawiger *et al.* injected mice with a monoclonal antibody to the DC endocytic receptor DEC-205 and engineered to contain a hen egg lysozyme peptide in steady-state conditions. T cells which recognized the peptide began to proliferate, but most of them were subsequently deleted. The small number which did remain did not respond to rechallenge with the same peptide (Hawiger *et al.*, 2001). Waithman *et al.* reported DC-mediated clonal deletion of ovalbumin-specific T cells in steady-state conditions in a transgenic mouse engineered to express membrane-bound ovalbumin on keratinocytes (Waithman *et al.*, 2007).

The T_h1/T_h2 paradigm postulates that T_h1 $CD4^+$ T cells will tend to promote more immunogenic cell-mediated immune responses, whilst T_h2 $CD4^+$ T cells will tend to promote more tolerogenic cell-mediated immune responses (Strom *et al.*, 1996). This is exploited for immune evasion by a number of pathogens whose PAMPs signal through PRRs which program DCs to induce T_h2 responses. Examples include recognition of the bacterial lipopeptide Pam-3-cys by TLR-2 (Agrawal *et al.*, 2003; Dillon *et al.*, 2004); and recognition of *Mycobacterial* ManLAM (Geijtenbeek *et al.*, 2003), *H. pylori* LPS Lewis antigens (Bergman *et al.*, 2004) and *L. acidophilus* surface layer A protein (Konstantinov *et al.*, 2008) by the CLR DC-SIGN. Skewing the effector T cell response has also been leveraged for therapeutic benefit. Li *et al.* transduced DCs with suppressor of cytokine signalling 3 (SOCS3) (a potent inhibitor of transcription of T_h1-specific genes by signal transducer and activator of transcription (STAT) 3 and 4). Transduced cells exhibited reduced MHC class II and CD86 expression, produced low levels of IL-12 and interferon gamma (IFN-γ) but high levels of IL-10 and suppressed experimental autoimmune encephalitis (EAE), a T_h1-mediated mouse model of multiple sclerosis *in vivo* (Li *et al.*, 2006).

Induction and expansion of regulatory T cells is perhaps the most widely reported mechanism through which DCs maintain immune tolerance. There are two major groups of regulatory T cells; 'naturally occurring' forkhead box $P3^+$ ($FoxP3^+$) $CD4^+$ $CD25^+$ regulatory T cells ($_nT_{regs}$) which constitute around 5% of all T cells which survive negative selection in the thymus (Itoh *et al.*, 1999) and 'adaptive' $FoxP3^+$ $CD4^+$ $CD25^-$ regulatory T cells ($_iT_{regs}$) which can be induced through stimulation of naïve T cells in the periphery (Chen *et al.*, 2003). Mature DCs are capable of expanding and sustaining antigen-specific populations of $_nT_{regs}$ in a mixed lymphocyte reaction (MLR), though this seems to depend less on the phenotype of the DCs and more on the phenotype of the $_nT_{regs}$ (Yamazaki *et al.*, 2006). In a study similar to that described by Hawiger *et al,* Bruder *et al.* injected a T cell receptor (TcR) transgenic mouse model of diabetes with an α-DEC-205-HA conjugate (Bruder *et al.*, 2005). The mice were engineered such that they expressed haemagglutinin (HA) under the control of the insulin promoter. Newborn mice injected with the conjugate did not develop disease and the induction of HA-specific $FoxP3^+$ $_iT_{regs}$ was observed.

1.2.5. Molecules of tolerance induction

Many studies documenting the induction of T cell tolerance by DCs identify certain molecules which appear to be important in both programming DCs themselves to a tolerogenic phenotype and enabling them to induce T cell tolerance. Expression of the tryptophan-catabolizing enzyme indoleamine 2,3-dioxygenase (IDO) by DCs activated with CD40 ligand (CD40L) and IFNγ inhibits the proliferation of autologous T cells in co-culture experiments through tryptophan starvation (Hwu *et al.*, 2000). IDO expression in DCs is coupled with upregulation of immunoglobin-like transcripts (ILTs) 3 and 4, resulting in impaired T cell stimulatory capacity (which can be rescued by ILT3 blockade) and enhanced induction of $_iT_{regs}$ (Brenk *et al.*, 2009). *In vivo*, treatment of mice with abatacept (cytotoxic T lymphocyte antigen 4 (CTLA4)-Ig) induces IDO expression in a subset of splenic DCs, which subsequently suppress the expansion of adoptively transferred T cells specific for murine MHC class I (Mellor *et al.*, 2003). TGF-β and retinoic acid (RA) act in a synergistic manner to induce differentiation of naïve T cells into $_iT_{regs}$ as opposed to T_h17 cells (Mucida *et al.*, 2007). Concurrent with this observation, $CD103^+$ lamina propria-resident DCs express high levels of retinal dehydrogenase (RALDH, which converts

retinaldehyde to retinoic acid) and induce FoxP3$^+$ T_{regs} in a RA and TGF-β-dependent manner (Coombes *et al.*, 2007; Sun *et al.*, 2007), an important mechanism for the maintenance of oral tolerance in the face of constant exposure of gut-associated lymphoid tissue to oral antigens. High RALDH expression in these DCs may be maintained through constitutive signalling through the Wnt-β-catenin pathway (Manicassamy *et al.*, 2010). Galectins may represent another important class of tolerogenic molecules. Exogenous and endogenous galectin-1 activates a STAT-3 mediated regulatory program in DCs, imparting a phenotype characterized by production of high levels of IL-27 (Ilarregui *et al.*, 2009). These DCs induce IL-10-producing T_{regs} and suppress inflammation in mice with EAE. Interestingly, it has been shown that galectin-1 is highly expressed by T_{regs} themselves (Garin *et al.*, 2007), alluding to cross-talk between T_{regs} and tolerogenic DC as a potential mechanism to perpetuate tolerance. The balance between expression of and signalling through activating and inhibitory Fcγ receptors on DCs also appears important, with signalling through FcγRI and FcγRIII favouring DC activation and maturation and signalling through FcγRIIB curtailing it. As such, FcγRIIB knockout mice exhibit increased DC activation and autoimmune inflammation upon nasal challenge with ovalbumin (Samsom *et al.*, 2005). A recent study has demonstrated that TLR-2 signalling in murine macrophages upregulates cell surface expression of FcγRIIB (Abdollahi-Roodsaz *et al.*, 2013). It is worth noting that whilst these are all undoubtedly important tolerogenic molecules in the context in which they were studied, a 'unifying theory' of tolerance induction is yet to be elucidated.

1.2.6. Using tolerogenic dendritic cells to treat autoimmune disease

With the accumulating evidence that DCs could engender tolerance in autoreactive T cells came increasing excitement that it might be possible to harness these properties to treat allergic and autoimmune disorders and promote transplantation tolerance (Steinman and Banchereau, 2007). A clinical trial which utilized autologous mature DCs to stimulate immune responses against tumours in patients with B cell lymphoma had already hinted at the tremendous potential that DCs held as biological therapeutics (Hsu *et al.*, 1996). Proof of principle that they could also be manipulated to induce tolerance *in vivo* in humans was provided in a similar manner through injection of a single dose of autologous immature DCs pulsed with influenza matrix peptide. This led to

the inhibition of $CD8^+$ T cell-mediated cytotoxity and the appearance of IL-10 producing T cells specific for the influenza matrix peptide (Dhodapkar *et al.*, 2001). These IL-10 producing cells were subsequently shown to be able to inhibit influenza matrix peptide-specific effector $CD8^+$ T cells generated from peripheral blood mononuclear cells (PBMCs) isolated prior to DC injection (Dhodapkar and Steinman, 2002).

Research groups all over the world have since dedicated a great deal of time and resources to developing means to manipulate DCs *ex vivo* such that they subsequently induce tolerance *in vivo*. Numerous studies have been conducted, differing in terms of the autoimmune diseases they are intended to treat and the manner in which the cells are manipulated. Tolerogenic DCs have previously been generated through: a) Inhibition of nuclear factor-kappa B (NF-κB)-mediated transcription of genes necessary for DC maturation, with immunomodulatory agents such as dexamethasone (e.g. (Matasic *et al.*, 1999)), 1-Alpha,25-dihydroxyvitamin D3 (e.g. (Penna and Adorini, 2000)) and BAY 11-7082 (e.g. (Martin *et al.*, 2007)); or transfection with MicroRNA-23b (Zheng *et al.*, 2012); b) genetic modification to upregulate expression of immunosuppressive molecules such as CTLA-4 (e.g. (Lu *et al.*, 1999)), IL-4 (e.g. (Kim *et al.*, 2001)) and IL-10 (e.g. (Coates *et al.*, 2001)); or apoptosis-inducing molecules such as Fas ligand (e.g. (Min *et al.*, 2000)) and TNF-related apoptosis-inducing ligand (TRAIL) (e.g. (Liu *et al.*, 2003)); or to downregulate expression of immunostimulatory molecules such as CD80/86 (e.g. (Liang *et al.*, 2003)) and IL-12 (e.g. (Xu *et al.*, 2006)); c) treatment with immunosuppressive cytokines or drugs such as IL-10 (e.g. (Steinbrink *et al.*, 1997)), TGF-β (e.g. (Yarilin *et al.*, 2002)) or rapamycin (e.g. (Turnquist *et al.*, 2007)); d) treatment with Wnt ligands to increase Wnt signalling (Valencia *et al.*, 2011); and finally e) short-term exposure to LPS (Salazar *et al.*, 2008).

An important consideration in *ex vivo* generation of tolerogenic DCs for treatment of autoimmune disease is that the cells must be maturation-resistant. In sites of autoimmune inflammation, endogenous danger signals are present in the absence of infection and there is an abundance of self-antigen for DCs to process and present. In these circumstances, mature DCs are at least as potent in perpetuating autoimmunity as tolerogenic DCs are in preventing it. 'Semi-mature' DCs generated through treatment of immature DCs with TNF-α have

been shown to mature further and become immunogenic *in vivo* upon exposure to inflammatory stimuli in murine EAE (Voigtlander *et al.*, 2006) and through increasing the inoculant number in murine collagen-induced arthritis (CIA) (Lim *et al.*, 2009).

1.2.7. Autologous Dendritic Cells for Rheumatoid Arthritis - the AuToDeCRA study at Newcastle University

Prophylactic and therapeutic efficiency of tolerogenic DCs has now been established in a number of the models described above and two Phase I human studies in type I diabetes and rheumatoid arthritis have recently been conducted with no adverse effects of treatment reported (Hilkens and Isaacs, 2013).

Here at Newcastle University, a robust method has been developed for the generation of human tolerogenic DCs from monocytes through treatment with dexamethasone and vitamin D_3 and maturation with LPS **(Fig. 7)**. These DCs exhibit a semi-mature phenotype relative to mature DCs characterized by: a) high MHC class II expression; b) intermediate expression of co-stimulatory molecules CD80 / CD86 and low expression of maturation markers CD40 / CD83; and c) an anti-inflammatory cytokine profile with high levels of IL-10 / TGF-β and low levels of IL-12, IL-23 and TNFα (Anderson *et al.*, 2008; Anderson *et al.*, 2009). They are limited in their capacity to activate naïve and memory $CD4^+$ T cells and modulate naïve and memory responses in distinct ways. Naïve cells primed by these DCs retain proliferative capacity but are deviated to an anti-inflammatory phenotype characterized by high expression of IL-10 and low expression of IFN-γ (Anderson *et al.*, 2008). Memory cells primed by these DCs do not exhibit a polarized cytokine profile but are rendered hyporesponsive to subsequent restimulation (Anderson *et al.*, 2008). LPS maturation of these DCs increases both their migratory capacity in response to the CCR7 ligand CCL19 and their ability to present an antigenic peptide from type II collagen relative to equivalent cells which do not receive a maturation stimulus (but still in a tolerogenic context) (Anderson *et al.*, 2009). Intravenous injection of equivalent mouse DCs pulsed with type II collagen significantly inhibits disease severity and progression in murine CIA (Stoop *et al.*, 2010).

Several translational issues have had to be addressed in order to bring these tolerogenic DCs into compliance with current good manufacturing practice

(cGMP) and enable the initiation of clinical trials. ‘Clinical grade’ DCs are cultured using CellGroDC (a cGMP compliant serum-free medium) (Napoletano *et al.*, 2007) and matured using monophosphoryl lipid A (a low toxicity derivative of the lipid A portion of LPS) (Makkouk and Abdelnoor, 2009). Tolerogenic DCs generated from the monocytes of rheumatoid arthritis patients in this manner exhibit a comparable phenotype to the DCs described above and are resistant to maturation when placed in a pro-inflammatory environment (Harry *et al.*, 2010), an important consideration if they are to be used to treat established rheumatoid arthritis.

These clinical grade tolerogenic DCs are presently the subject of a randomized, unblinded, placebo-controlled, dose-escalation Phase 1 safety trial as part of the Autologous Tolerogenic Dendritic Cells for Rheumatoid Arthritis (AuToDeCRA) study; in which RA patient monocytes are isolated, differentiated *ex vivo*, loaded with autologous synovial fluid and injected intra-articularly into an inflamed knee joint. Whilst the primary objective of the trial is to assess safety and acceptability, synovial biopsies are also collected to ascertain the effects of the treatment on local and systemic disease activity and to check for the presence of prospective response biomarkers (Hilkens and Isaacs, 2013).

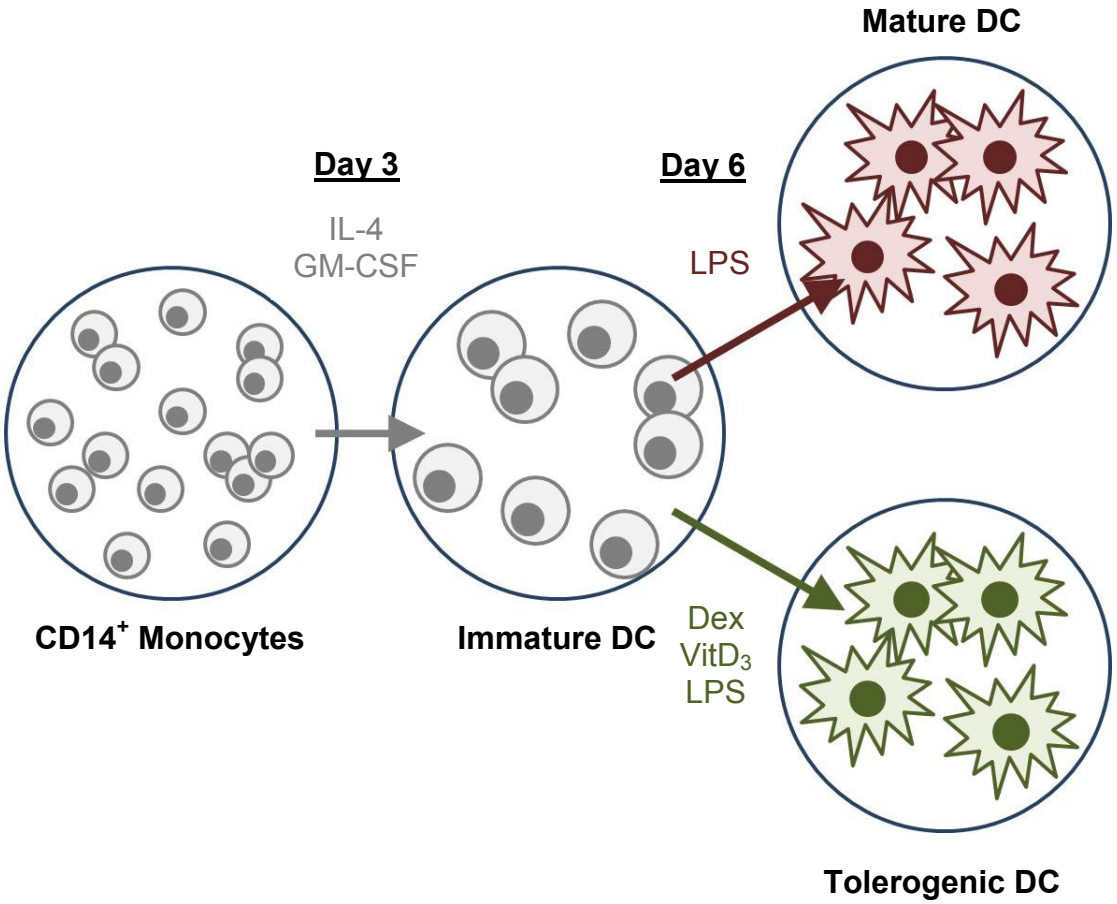

Figure 7: Generation of mature and tolerogenic dendritic cells in the immunotherapy group at Newcastle University

CD14+ monocytes are cultured for six days in the presence of IL-4 and GM-CSF to induce differentiation into immature DC. These are matured for a further 24 hours with LPS. To generate tolerogenic dendritic cells, monocytes are additionally supplemented with dexamethasone on days 3 and 6 and vitamin D_3 on day 6.

1.2.8. Exploring the cell surface phenotype of tolerogenic dendritic cells

The *in vitro* and *in vivo* evidence accumulated to date suggests that these tolerogenic DCs hold considerable immunotherapeutic promise. However, whilst it is known that they induce tolerance in part through a TGF-β dependent mechanism which inhibits T cell proliferation and IFN-γ production (Anderson and Hilkens; unpublished data), the basis of their phenotype and precisely what it is that makes them tolerogenic has yet to be systematically explored. This would be valuable information to possess in itself and the findings may also help to expedite their progression from bench to bedside.

A hitherto imperfectly addressed requirement in advancing tolerogenic DC-based therapy for the treatment of RA is the identification of 'quality control' (QC) markers which unambiguously exemplify the tolerogenic phenotype (Hilkens and Isaacs, 2013). Ideally, such markers need to be robust, readily assayable and indicative of tolerogenic function. With this in mind, the QC markers currently in use are low CD83 expression, indiscernible IL-12 production and high IL-10 production (Hilkens and Isaacs, 2013). TLR-2 is known to exhibit 3-4 fold greater expression on tolerogenic DCs than on mature or immature DCs (Harry *et al.*, 2010), though it is as yet unclear whether this correlates directly with their tolerogenic function. It is possible that as yet uncharacterized markers with more exclusive expression and/or more directly associated with function are yet to be discovered. The discipline of proteomics is well suited to pursue this particular line of enquiry.

1.2.9. Previous dendritic cell proteomic studies

The importance in fully comprehending the molecular processes underpinning the functional properties of human DCs in immunity and tolerance is reflected in the number of proteomic studies of which they have been the focus since the turn of the century (Ferreira *et al.*, 2010). The earliest studies were largely gel-based and focused largely on the differentiation and maturation process of monocyte-derived DCs (moDCs). Advances in the field have since facilitated comparative studies between different types of moDC and more in-depth investigation of individual organelles such as the plasma membrane.

1.2.9.1. Proteomics of DC maturation

The first human DC proteomic studies employed 2D-PAGE in an effort to characterize proteome-wide changes in response to differentiation and maturation, frequently in tandem with array-based transcriptome profiling to enable comparison of the two.

Angenieux *et al.* compared transcriptome and proteome profiles of monocytes and mature DCs (Angenieux *et al.*, 2001). A significant proportion of genes induced by maturation corresponded to surface expressed proteins with known functions in antigen processing and presentation. Intracellular components of the antigen processing machinery were also upregulated at the protein level; together with proteins with roles in cytoskeletal remodelling and the mitochondrial oxidative stress response. Le Naour *et al.* performed a similar study (Le Naour *et al.*, 2001), identifying 255 differentially expressed transcripts and 37 differentially expressed proteins. Differentially expressed genes corresponded largely to secreted proteins or proteins involved in cell adhesion and signalling; whilst differentially expressed proteins had roles in calcium and fatty acid-binding, chaperone activities associated with antigen processing and presentation, and cell motility. Pereira *et al.* used 2D-PAGE to examine differential protein expression during both differentiation and maturation (Pereira *et al.*, 2005), identifying 56 differentially expressed spots in immature DCs and 50 differentially expressed proteins in mature DCs. These spots corresponded to 36 proteins, 11 of which were present as 38 electrophoretic isoforms. As with the previously described studies, differentially expressed proteins corresponded predominantly to known biological alterations occurring during differentiation and maturation such as cytoskeletal remodelling, chaperone activities and intracellular antigen processing. Finally, Ferriera *et al*. used 2D-DIGE to examine differential protein expression during maturation (Ferreira *et al.*, 2008), identifying 74 differentially expressed spots corresponding to 41 proteins; many of which were once again involved in cytoskeletal modelling, cell motility and antigen processing.

A couple of trends emerge through collective consideration of these studies. Whilst differentially expressed genes and proteins in all of the studies can be broadly reconciled with the processes of DC differentiation and maturation, the two studies in which both transcriptome and proteome analysis were performed

note that little correlation was observed between the two datasets. Angenieux *et al*. attribute this to difficulties in analysing membrane proteins using 2D gels for the differentially expressed transcripts not identified by proteomics and to post-transcriptional and post-translational control of protein expression for the upregulated proteins not identified by transcriptomics. The latter proposition would appear to fit with the identification of numerous differentially expressed isoforms of individual proteins by Pereira *et al*. and Ferriera *et al*. This is corroborated by a more recent shotgun study by Buschow *et al*. examining transcriptome and proteome changes during DC maturation (Buschow *et al.*, 2010). Little correlation was observed between differentially expressed transcripts and proteins *per se*, but correlation was considerably greater when the transcripts and proteins were mapped to maturation-related pathways. The five pathways identified with considerable overlap between mRNA and protein levels were cell adhesion, cell motility, cytokine receptor interaction and the peroxisome proliferator-activated receptor (PPAR) and TLR signalling pathways. It is also noted that whilst differentially expressed proteins can be broadly reconciled with the processes of DC differentiation and maturation, there are very few differentially expressed proteins identified in common across the gel-based studies. It is suggested that differences in gel-based platforms and differentiation/maturation stimuli used may be partly responsible for this variation.

1.2.9.2. Proteomics of differentially matured DC

More recent human DC proteomic studies have focused less on the maturation process itself and more on differentially expressed proteins in DC matured with distinct stimuli and exhibiting discrete mature phenotypes.

Gundacker et al. compared differences in the cytoplasmic and secreted proteomes of immature DCs with DCs which had been either classically activated with LPS, alternatively activated with OxPAPC (an oxidized phospholipid) or tolerised with human rhinovirus (Gundacker *et al.*, 2009). They identified significant cytoplasmic and secretome changes in LPS-matured DCs relative to the other two cell types, most notably upregulation of a significant number of interferon-induced proteins, proteins involved in cell motility and secreted cytokines and chemokines. Few changes were noted in alternatively activated or tolerised DCs. It is possible that this is due to alternatively activated

/ tolerised DCs more closely resembling immature DCs than LPS-matured DCs, though it is also worth noting that an unusual metabolic labelling strategy was used in which DCs were matured for 6 hours in media containing ^{35}S-labelled methionine and cysteine.

In a follow up study to that described in (Ferreira *et al.*, 2008), Ferreira et al. examined the effects of adding TX527 (a structural analogue of vitamin D) (Ferreira *et al.*, 2009) on days 3 and 6 on the expression profiles of immature and mature DCs. The proteins differentially expressed between mature DCs and TX527-treated mature DCs could be categorized into three main groups. Proteins involved in cytoskeletal remodelling (e.g. fascin, actin polymerizing proteins) were downregulated, whilst proteins involved in mitochondrial oxidative metabolism (e.g. periredoxin, superoxide dismutase) were upregulated. TX527 treatment also had significant effects on antigen processing pathways. Proteins with a role in MHC class I antigen processing (e.g. cytosomal aminopeptidase, proteasome activator complex subunit 2) were downregulated, whilst proteins with a role in MHC class II antigen processing (e.g. cathepsins D and S) were upregulated.

The group has since published a further study which examines the effects of dexamethasone, vitamin D_3 and a combination of the two on the expression profiles of mature DCs (Ferreira *et al.*, 2012). The culture protocol differs slightly from both that employed at Newcastle and that employed in the previous study: the group treats DCs with vitamin D3 from day 0 and matures through co-culture on cells expressing CD154 for 48 hours. Nevertheless, the phenotype of DCs cultured in the presence of both reagents is broadly similar to that documented in the TX527 study, though the earlier supplementation of vitamin D3 seems to have an additional effect on a number of metabolic proteins, with fructose 1,6 biphosphate and carbonic anhydrase being particularly strongly induced.

Most recently, Zimmer *et al*. performed a label-free proteome-wide comparison of immature DCs, LPS-matured DCs (DC1), PGN-matured DCs (DC2) and dexamethasone-treated DCs (DCreg) in an effort to identify candidate response biomarkers to allergen immunotherapy (Zimmer *et al.*, 2012). Nine proteins were identified which were upregulated in DCreg relative to the other types of

DC; namely annexin A1, complement C1q subcomponent subunits B and C, dipeptidyl peptidase 1, coagulation factor XIII A chain, chloride intracellular channel protein 2, peptidyl-prolyl-cis-trans-isomerase, macrophage mannose receptor 1 and stabilin-1. Both complement C1q subcomponent subunits and stabilin-1 were subsequently validated as predictors of tolerogenic response to immunotherapy. Interestingly, none of the upregulated proteins identified in this study were also identified as upregulated in the dexamethasone-treated DCs in the study by Ferreira *et al.* Indeed, of the nine, only one (annexin A1) was detected in both studies at all. It is possible that this is again due to the different proteomic platforms utilized. It will be interesting to see if any of the differentially expressed proteins in either study are also detected in the current body of work.

Chapter 2. Aims and Objectives

The principle aim of this body of work entails the development of a mass spectrometry-based proteomics workflow to enable quantitative plasma membrane proteomics of mature and tolerogenic dendritic cells. This overall aim will be realised through the optimization and validation of several elements of the proteomics sample preparation process described in section **1.1.2.** such that the biological questions at hand can be addressed effectively. These elements pertain primarily to two active areas of research within the field, each of which has been the subject of a great deal of research to date.

- The first objective is to develop a technique to extract, isolate and digest the DC plasma membrane proteome which enables the detection of substantial numbers of this relatively scarce and biochemically recalcitrant class of proteins in LC-MS analysis.

- The second objective is to develop a means of stable isotope labelling the proteomic peptides of mature and tolerogenic DC to enable their respective protein complements to be quantified relative to one another.

The difficulties posed by these two considerations, in particular the latter, are in part imposed by the nature of the cells under study and the LC-MS instrumentation available and are detailed in the introductions of the respective chapters of which they are the focus.

Upon completion, it is envisaged that future application of the optimized elements of the sample preparation workflow in sequence will enable the identification and relative quantitation of significant numbers of mature and tolerogenic DC plasma membrane proteins. However, individual elements of the workflow should also prove applicable to the examination of mature and tolerogenic DC biology (and beyond in general proteomics).

- The third objective is thus to appropriate these elements as such for quantitative comparisons of their unfractionated proteomes in the absence of membrane enrichment, and qualitative profiling of their plasma membrane proteomes in the absence of stable isotope-based quantitation.

These investigations will both inform development of the overall workflow and may also be of interest from a biological perspective in their own right.

Chapter 3. Methods

All reagents were sourced from Sigma-Aldrich (St. Louis, MO, USA) unless otherwise stated.

3.1. Cell culture

3.1.1. Jurkat T cells

Jurkat T cells were cultured in RFI0 (RPMI 1640; Lonza, Basel, Switzerland) with 10% (v/v) fetal bovine serum (FBS; Lonza), 2 mM glutamine, 100 U/ml penicillin and 100 µg/ml streptomycin) at 37°C with 5% CO_2. Cells were split 1 in 10 twice a week and expanded as required.

3.1.2. Isolation of cells from peripheral blood

Human samples were obtained with informed consent and following a favourable ethical opinion from North Tyneside Research Ethics Committee (UK). PBMCs were isolated from leukocyte reduction system (LRS) cones through density gradient centrifugation on Lymphoprep (Axis-Shield Diagnostics, Dundee, UK). $CD14^+$ monocytes were isolated from PBMCs through positive selection with anti-CD14 microbeads (Miltenyi Biotec, Bergisch Gladback, Germany).

3.1.3. Generation of dendritic cell populations

$CD14^+$ monocytes were cultured in RF10 supplemented with 50 ng/ml IL-4 and 50 ng/ml GM-CSF (Immunotools, Friesoythe, Germany). Cells were cultured at 0.5×10^6 cells/ml for 6 days with fresh media and cytokines on day 3 to induce differentiation into immature DCs. Immature DCs were matured through the addition of 0.1 µg/ml LPS (Sigma-Aldrich) for a further 24 hours on day 6. Tolerogenic DCs were additionally supplemented with 10^{-6} M dexamethasone (Sigma-Aldrich) on days 3 and 6 and 10^{-10} M 1α,25-dihydroxyvitamin D3 (Leo-Pharma, Ballerup, Denmark) on day 6. All cells were cultured at 37°C with 5% CO_2.

3.2. Protein extraction and isolation

3.2.1. Whole cell lysate preparation (in-solution digestion)

Jurkat T cells were harvested at approximately 95% confluence. Mature and tolerogenic DCs were harvested on day 7, 24 hours after addition of LPS. All cells were resuspended in Hank's balanced salt solution (HBSS; Lonza) / 1% (v/v) FBS and washed three times; then resuspended in 1 ml phosphate buffered saline (PBS) / 1 mM ethylenediaminetetraacetic acid (EDTA), transferred to low binding microcentrifuge tubes (Sorensen Bioscience, Salt Lake City, UT, USA) and washed a further three times to remove residual serum proteins which would otherwise contaminate downstream LC-MS analysis. After washing, cells were resuspended in lysis buffer (1% (v/v) *n*-octyl-β-D-glucoside, 0.1% (w/v) SDC, 150 mM sodium chloride (NaCl), 50 mM tris(hydroxymethyl)aminomethane hydrochloride (Tris-HCl, pH ~7.5), 1 mM EDTA; supplemented with complete mini EDTA-free protease inhibitor cocktail (Roche Applied Science, Penzburg, Germany). The volume of lysis buffer used was calculated such that protein concentration in the lysates would be approximately 2 µg/µl assuming a yield of 100 picograms of protein per cell. Samples were thoroughly vortexed and incubated on ice for 30 minutes. To ensure complete lysis, cells were then subjected to 3 freeze-thaw cycles consisting of a sequence of 2 minutes in liquid nitrogen, 2 minutes in a 37°C water bath and 1 minute of thorough vortexing. Lysates were cleared by centrifugation at 1000*g* for 10 minutes at 4°C. Total protein concentration in clarified lysates was assayed using a Micro BCA assay kit (Thermo Fisher Scientific, Waltham, MA, USA) as per user instructions. Lysates were subsequently transferred to fresh low binding tubes and stored as 100 µg aliquots at -80ºC if not required immediately.

3.2.2. Whole cell lysate preparation (FASP)

Jurkat T cells and mature/tolerogenic DCs were harvested and washed with HBSS / 1% (v/v) FCS and PBS / 1% (v/v) EDTA as described above. After washing, cells were resuspended in 4% (w/v) SDS / 0.1 M Tris-HCl (pH ~7.5) and incubated for 5 minutes at 95°C. The volume of lysis buffer used was calculated as before. Lysates were homogenized by passage through QiaSHREDDER microcentrifuge spin columns (Qiagen, Hilden, Germany) at

16000*g* for 2 minutes at room temperature, transferred to low binding microcentrifuge tubes and cleared by centrifugation at 16000*g* for 5 minutes at room temperature. Total protein concentration in clarified lysates was assayed using a NanoDrop 1000 spectrophotometer (Thermo Fisher Scientific). Lysates were subsequently transferred to new low binding tubes and stored as 100 µg aliquots at -80ºC if not required immediately.

3.2.3. Cell surface protein isolation with EZ-Link® Sulfo-NHS-SS Biotin and RevAmine

Jurkat T cells were harvested and washed with HBSS / 1% (v/v) FCS and PBS / 1% (v/v) EDTA as described above. After washing, cells were resuspended in 1 ml PBS at a volume of 1×10^7 cells/ml. 10 µl of EZ-Link® Sulfo-NHS-SS Biotin (Thermo Fisher Scientific) or RevAmine (25 µg/µl, reconstituted in dimethyl sulfoxide (DMSO)) was added. 10 µl of DMSO alone was added to cells which would serve as unbiotinylated controls. Tubes were incubated for 30 minutes at 4ºC with end-over-end agitation. Biotinylation reactions were quenched through addition of 50 µl of 'quenching solution' (Thermo Fisher) and incubation for a further minute at 4ºC with end-over-end agitation. Biotinylated cells were spun down, resuspended in 25 mM Tris buffered saline (TBS) and washed three times.

Biotinylated and unbiotinylated cells were subsequently resuspended in either 100 µl of 'Lysis Buffer' (Thermo Fisher, proprietary formulation) or 100 µl of 1% (w/v), 2% (w/v) or 4% (w/v) SDS / 0.1 M Tris-HCl (pH ~7.5) supplemented with HALT EDTA-free protease inhibitor cocktail (Thermo Fisher Scientific) and 1 mM EDTA. Cells resuspended in Lysis Buffer were sonicated for 1 minute in a sonicating water bath at 4ºC and incubated on ice for 30 minutes with vortexing for 5 seconds every 5 minutes. Lysates were cleared by centrifugation at 10000*g* for 2 minutes at 4ºC. Clarified supernatant was transferred to new low binding tubes and stored at -80ºC if not required immediately. Cells resuspended in SDS / 0.1 M Tris-HCl were incubated for 5 minutes at 95ºC. Lysates were homogenized using a 25 gauge needle and syringe and cleared by centrifugation at 16000*g* for 5 minutes at room temperature. Clarified supernatant was processed and stored as described above if not required immediately.

For cell surface protein isolation, 100 µl of NeutrAvidin™ agarose resin (Thermo Fisher Scientific) was added to a 0.8 ml centrifuge column (Thermo Fisher Scientific) and washed three times. Resin which was to be used for isolation of cell surface proteins from cells lysed with Lysis Buffer was washed with 500 µl of 'Wash Buffer' (Thermo Fisher Scientific, proprietary formulation). Resin which was to be used for isolation of cell surface proteins from cells lysed with 1% (w/v), 2% (w/v) or 4% (w/v) SDS / 0.1 M Tris-HCl was washed with 500 µl of the corresponding SDS solution. Biotinylated and unbiotinylated lysates were added to the resin and incubated for 1 hour or overnight at room temperature with end-over-end agitation. After incubation, resin was washed four times with 500 µl of the buffer which had been used to equilibrate the resin prior to addition of lysates, supplemented with HALT EDTA-free protease inhibitor cocktail and 1 mM EDTA.

Proteins biotinylated with EZ-Link® Sulfo-NHS-SS Biotin were liberated from the resin through addition of 100 µl of 4% (w/v) SDS / 0.1 M Tris-HCl / 0.1 M dithiothreitol (DTT) and incubation for 1 hour at room temperature with end-over-end agitation. Proteins biotinylated with RevAmine were liberated from the resin through addition of 0.1% (v/v) ammonia solution and incubation for 1 hour at room temperature, followed by addition of 100 µl of 4% (w/v) SDS / 0.1 M Tris-HCl / 0.1 M DTT and incubation as described above. SDS eluates from EZ-Link®-biotinylated samples were collected in low binding microcentrifuge tubes. Ammonia eluates from RevAmine-biotinylated samples were collected in low binding microcentrifuge tubes and evaporated under vacuum prior to addition of SDS solution. SDS eluates were subsequently collected in the same tubes.

3.2.4. Membrane preparation using 'stepwise depletion'

Jurkat T cells and mature/tolerogenic DCs were harvested and washed with HBSS / 1% (v/v) FCS and PBS / 1% (v/v) EDTA respectively as described above. After washing, cells were resuspended in 1 ml hypotonic lysis buffer (10 mM NaCl, 10 mM 4-(2-hydroxyethyl)-1-piperazineethanesulfonic acid – sodium hydroxide (HEPES-NaOH) (pH ~7.5), 1 mM EDTA; supplemented with HALT EDTA-free protease inhibitor cocktail) and allowed to swell on ice for 10 minutes. Swollen cells were transferred to a pre-chilled Dounce homogenizer (2ml) and lysed using 50 strokes with a tight pestle. Lysates were cleared by centrifugation at 1000*g* for 10 minutes at 4ºC. Salt concentration in clarified

lysates was adjusted to 2 M NaCl. Alternatively, cells were resuspended in 200 µl isotonic lysis buffer (150 mM NaCl, 10 mM HEPES-NaOH (pH ~7.5), 1 mM EDTA; supplemented with HALT EDTA-free protease inhibitor cocktail) and subjected to 3 freeze-thaw cycles as described in section **3.2.1.** Volume and salt concentration of crude lysates was adjusted to 500 µl and 2 M NaCl respectively. Lysates were homogenized by three passages through QIAshredder microcentrifuge spin columns as described in section **3.2.2.** The volume of the clarified lysates was adjusted to 1 ml through addition of 500 µl hypertonic buffer (2 M NaCl, 10 mM HEPES-NaOH (**pH ~7.5**), 1 mM EDTA; supplemented with HALT EDTA-free protease inhibitor cocktail).

Crude membrane preparations were subsequently prepared using the 'stepwise depletion of non-membrane molecules' method described in (Wisniewski *et al.*, 2009a) with a few modifications. 1 ml volumes of clarified lysate prepared by either of the two methods described above were transferred to 1 ml siliconized microcentrifuge tubes (Sigma-Aldrich) and crude membranes pelleted by centrifugation at 21100*g* for 30 minutes at 4ºC. Supernatant was discarded and pellets extracted in 1 ml carbonate buffer (0.1 M Na_2CO_3 (pH 11.3), 1 mM EDTA; supplemented with HALT EDTA-free protease inhibitor cocktail). Pellet dispersal was aided by sonication for 1 minute in a sonicating water bath at 4ºC. Membranes were pelleted by centrifugation and extracted as described a further two times with carbonate buffer and one final time with urea-containing buffer (4 M urea, 100 mM NaCl, 10 mM HEPES-NaOH (pH ~7.5), 1 mM EDTA). The supernatant was carefully removed and discarded and the membrane pellets stored at -80ºC if not required immediately.

3.3. Protein Digestion

3.3.1. Detergent removal from whole cell lysates for in-solution digestion

Detergent was removed from whole cell lysates generated as described in section **3.2.1.** using detergent removal spin columns (Thermo Fisher) as per manufacturer instructions. Briefly, the columns were washed and equilibrated 3 times with 50 mM Tris-HCl (pH ~7.5). 100 µg aliquots of whole cell lysate were made up to 50 µl with 50 mM Tris-HCl (pH ~7.5), transferred onto columns and incubated at room temperature for 2 minutes. Columns were then centrifuged at 1500*g* for 2 minutes at room temperature and the eluate was collected in low binding microcentrifuge tubes.

3.3.2. In-solution digestion of BSA / whole cell lysates

50 µl volumes of bovine serum albumin (BSA) (Sigma-Aldrich) reconstituted in 50 mM Tris-HCl (pH ~7.5) to a final concentration of 200 ng/µl or 50 µl volumes of whole cell lysate depleted of detergent as described above were transferred to PCR tubes (STARLAB, Hamburg, Germany). RapiGest™ SF (Waters, Manchester, UK) was reconstituted in 10 mM TRIS-HCl to a stock concentration of 2% (w/v) and added to samples at a final concentration of 0.1% (w/v) (for experiments described in sections **5.2.**, **6.2.1.1.** and **7.2.**) Alternatively, ProteaseMAX™ (Promega, Fitchburg, WI, USA) was reconstituted in 10 mM TRIS-HCl (pH ~7.5) to a stock concentration of 1% (w/v) and added to samples at a final concentration of 0.03% (w/v) (for experiments described in sections **4.2.2.1.**, **4.2.3.2.**, **6.2.1.2.**, **6.3.** and **7.3.**) All samples were reduced by addition of Tris(2-carboxyethyl)phosphine hydrochloride (TCEP-HCl) to 1 mM and incubation for 30 minutes at 56ºC. Cysteine residues were then alkylated by addition of iodoacetamide to 5 mM and incubation for 1 hour at room temperature in the dark. Excess iodoacetamide was scavenged by addition of DTT to 4 mM and incubation for 30 minutes at room temperature. All samples were digested overnight at 37ºC with sequencing grade modified trypsin (Promega) (enzyme-to-substrate ratio 1:50 (w/w)). Upon digestion completion, RapiGest™-containing samples were acidified with 1/20th volume 10% (v/v) TFA, incubated at 37ºC for a further 45 minutes and centrifuged at 13000*g* for 10 minutes at room temperature to precipitate and pellet RapiGest™ breakdown products. ProteaseMAX™-containing samples were acidified with

1/20th volume 10% (v/v) TFA, incubated at room temperature for 5 minutes and centrifuged at 13000*g* for 10 minutes at room temperature to precipitate and pellet ProteaseMAX™ breakdown products. All supernatants were then transferred to new PCR tubes and stored at -20ºC if not required immediately.

3.3.3. In-solution digestion of 'stepwise depletion' membrane preparations

Crude membrane pellets were resuspended in 200 µl buffer (100 mM NaCl, 10 mM HEPES-NaOH (pH ~7.5), 1 mM EDTA), to which four volumes of ice cold acetone were added. Samples were vortexed for 1 minute, incubated at -20ºC for 1 hour and centrifuged at 15000*g* for 10 minutes at 4ºC. Supernatant was carefully decanted and protein pellets left to air-dry for 30 minutes at room temperature. ProteaseMAX™ was reconstituted in 50 mM ammonium bicarbonate to a stock concentration of 1% (w/v). Protein pellets were solubilized with 15 µl 8 M urea / 20 µl 0.2% (v/v) ProteaseMAX™, vortexed for 2 minutes, placed in a Thermomixer® (Eppendorf, Hamburg, Germany) set to 300 rpm and agitated at room temperature for a further hour. 50 mM ammonium bicarbonate was added to a final volume of 93.5 µl. Samples were reduced by addition of 1 µl 0.5 M DTT and incubation for 20 minutes at 56ºC. Cysteine residues were alkylated by addition of 2.7 µl 0.55 M iodoacetamide and incubation for 15 minutes at room temperature in the dark. A further 1 µl of 1% (v/v) ProteaseMAX™ was added and samples were digested overnight at 25°C with sequencing grade modified trypsin (Promega) (enzyme-to-substrate ratio 1:50 (w/w), added to make final sample volume up to 100 µl). Total protein concentration in the samples was not assayed directly but inferred from total protein concentration in crude membrane pellets prepared in the same way with the same number of cells which were solubilized in 4% (w/v) SDS / 0.1 M Tris-HCl and assayed using a NanoDrop 1000 spectrophotometer by UV versus blank. Upon digestion completion, ProteaseMAX™ breakdown products were precipitated and pelleted as described above and supernatants transferred to new low binding tubes and stored at -20ºC if not required immediately.

3.3.4. FASP digestion of whole cell lysates and 'stepwise depletion' membrane preparations

Crude membrane pellets were solubilized in 30 µl 4% (w/v) SDS / 0.1 M Tris-HCl (pH ~7.4) and incubated for 5 minutes at 95ºC. 3 µl of solubilized membrane protein was removed and total protein concentration assayed using a NanoDrop 1000 spectrophotometer as before.

Whole cell lysates and crude membrane pellets to be digested using FASP were reduced by addition of 1/10th volume 1 M DTT made up in 4% (w/v) SDS / 0.1 M Tris-HCl (pH ~7.4) and incubated for a further 5 minutes at 95ºC. FASP was subsequently carried out as described in (Wisniewski *et al.*, 2009b) with a few modifications. 30 µl volumes of reduced protein sample were diluted with 200 µl UA buffer (8 M urea, 0.1 M Tris-HCl (pH ~8.5)); vortexed for 1 minute and transferred to Microcon® YM-30 MWCO spin filters (Merck-Millipore, Billerica, MA, USA). Columns were centrifuged at 14000*g* for 40 minutes at 20ºC. A further 200 µl of UA buffer was added to the filters and centrifugation repeated as described above. Cysteine residues were alkylated through addition of 100 µl UA buffer containing 50 mM iodoacetamide. Filters were placed in a Thermomixer® set to 600 rpm and agitated at 20ºC for 1 minute, incubated at 20ºC without agitation for a further 20 minutes and then centrifuged at 14000*g* for 30 minutes at 20°C. Three 100 µl volumes of UB buffer (8 M urea, 0.1 M Tris-HCl (pH ~8)) were then passed through the filters by centrifugation at 14000*g* for 40 minutes at 20°C.

Samples were digested on-filter by addition of 30 µl UB buffer containing endoproteinase Lys-C (Promega) (enzyme-to-substrate ratio 1:50 (w/w)). Filters were agitated in a Thermomixer® as described above and incubated overnight at 25°C in a wet chamber. The filters were subsequently transferred to new collection tubes and the 30 µl UB buffer diluted through addition of 120 µl 50 mM ammonium bicarbonate (pH ~7.5) containing sequencing grade modified trypsin (Promega) (enzyme-to-substrate ratio 1:100 (w/w)). Filters were agitated in a Thermomixer® as described above and incubated over a second night at 25°C. Upon digestion completion, filters were centrifuged at 14000*g* for 40 minutes at 20°C. Finally, one volume of 50 µl 0.5 M NaCl was passed through the filters by centrifugation at 14000*g* for 20 minutes at 20°C. The combined eluates from the final two centrifugation steps were transferred to new low

binding tubes, acidified with 1/20th volume 10% (v/v) TFA and stored at -20ºC if not required immediately.

3.4. Peptide Labelling

3.4.1. Desalting of digests prior to peptide labelling

Digests performed using the methods described in sections **3.3.3.** and **3.3.4.** needed to be desalted prior to peptide stable isotope labelling. This was performed using Empore™ C18-SD solid phase extraction (SPE) cartridges (3M, St. Paul, MN, USA). Whole cell lysate digests were desalted with 3 ml cartridges (80 µg binding capacity) and membrane digests were desalted with 1 ml cartridges (25 µg binding capacity). Cartridges were conditioned with acetonitrile and equilibrated with 0.1% (v/v) TFA (500 µl for 3 ml cartridges, 200 µl for 1 ml cartridges). Acidified digests were passed through the cartridges. Bound peptides were washed with three volumes of 0.1% (v/v) TFA (3 ml for 3 ml cartridges, 1 ml for 1 ml cartridges) and eluted with 80% (v/v) acetonitrile / 0.1% (v/v) TFA (200 µl for 3 ml cartridges, 100 µl for 1 ml cartridges). Desalted peptides were stored at -20ºC if not required immediately.

3.4.2. C-terminal ^{18}O labelling

C-terminal ^{18}O labelling was initially optimized using in-solution BSA digests prepared in section **3.3.2.** The optimization process itself is described in **Chapter 5**. Optimized conditions were subsequently used for C-terminal labelling of in-solution and FASP digests of whole cell lysates and membrane preparations.

BSA peptides were dried under vacuum and reconstituted in either a) 50 µl of 50 mM ammonium bicarbonate (pH 8.0) or b) 50 µl of 50 mM ammonium acetate (pH 4.5), both of which had been prepared in $H_2{}^{18}O$ water (Isotec / Sigma). Peptides were sonicated in an ultrasonic bath for 1 minute at room temperature and vortexed briefly to aid resuspension. Trypsin was reconstituted in 50 mM acetic acid (prepared using $H_2{}^{18}O$ water) such that addition of 5 µl to peptides resulted in an enzyme-to-substrate ratio of 1:20 (w/w). Labelling reactions were allowed to proceed for either a) 2 hours or b) 24 hours at 37°C in a thermal cycler. Reaction termination was tested by either a) no manipulation, b) incubating reactions at 100°C for 30 minutes and then rapidly cooling to -20°C or c) performing reducing and alkylating reactions through addition of 1 M DTT to a final concentration of 20 mM and incubation at 95°C for 1 hour followed by addition of 1 M iodoacetamide to a final concentration of 40 mM and

incubation at 60°C for 30 minutes. Finally, labelled peptide storage conditions were tested by either: a) acidifying immediately through addition of 1/10th volume 10% (v/v) TFA or b) not acidifying the labelling reaction at all.

Optimized ^{18}O labelling conditions were subsequently established as: -

- Reconstitution of vacuum-dried peptides in 50 µl of 50 mM ammonium acetate (pH 4.5) prepared in $H_2{}^{18}O$ water.
- Incubation of peptides with trypsin (enzyme-to-substrate ratio of 1:20 (w/w)) for 24 hours at 37°C in a thermal cycler.
- Inactivation of trypsin by reducing and alkylating labelling reactions as described above.
- Storage of reduced / alkylated labelling reactions without acidification at -20°C until required for downstream processing or LC-MS analysis.

These conditions were used for the subsequent C-terminal ^{18}O labelling of all proteomic peptides.

3.4.3. Lysine guanidination → N-terminal-specific succinylation

As with C-terminal ^{18}O labelling, N-succinylation and lysine guanidination were initially optimized using the in-solution BSA digests described in section **3.3.2.** The two reactions were optimized separately and then consolidated as a single procedure; the net result rendering succinylation N-terminal-specific. The optimization process itself is described in **Chapter 5.** Optimized conditions were used for N-terminal labelling of in-solution and FASP digests of whole cell lysates and membrane preparations.

For non-specific succinylation, 1 ml Empore™ C18-SD SPE cartridges were conditioned and equilibrated as described in section **3.4.1.** Acidified digests were made up to 200 µl with 1% (v/v) TFA and passed through the cartridges. Bound BSA peptides were washed with 1 ml of 0.1% (v/v) TFA, followed by 1 ml of water, followed by 1 ml 200 mM sodium acetate (pH 7.6). Peptides were succinylated through addition of 1 ml of 20 mM succinic anhydride made up in 200 mM sodium acetate / 20 mM sodium hydroxide (pH 7.6). The SPE cartridges were attached to a 'Visi-1' SPE tube processor (3M) as shown below **(Fig. 8)**, which was configured such that the reaction buffer passed through the cartridges at a uniform rate over the course of a) 5 minutes, b) 10 minutes or c) 15 minutes. Upon completion, residual reaction buffer was expelled from the cartridge using the plunger on the processor. Peptides were washed with 1 ml of 200 mM sodium acetate (pH 7.6), followed by 1 ml of water, followed by 1 ml of 0.1% (v/v) TFA, followed by 1 ml of 0.2% (v/v) formic acid (FA), and eluted with 100 µl 80% (v/v) acetonitrile / 0.2% (v/v) FA. Succinylated peptides were dried under vacuum and stored at -20°C if not required immediately.

Figure 8: SPE cartridge configuration for succinylation of bound peptides.

For lysine guanidination, 1 ml Empore™ C18-SD SPE cartridges were conditioned, equilibrated and acidified digests passed through as described above. Bound BSA peptides were washed with 0.1% (v/v) TFA and water as above, followed by 1 ml of 6.67% (v/v) ammonia solution. Peptides were guanidinated through addition of 1 ml of 1 M O-Methylisourea made up in of 6.67% (v/v) ammonia solution. The end of the SPE cartridges were plugged using SPE tube adaptors attached to fully depressed 5 ml syringes as shown below **(Fig. 9)** and the cartridges were incubated at 65°C for a) 10 minutes, b) 20 minutes or c) 30 minutes. Upon completion, residual reaction buffer that had not passed through the cartridges was removed by inverting the cartridges and discarded. Peptides were washed with 1 ml of 6.67% (v/v) ammonia solution followed by water, 0.1% (v/v) TFA and 0.2% (v/v) FA as above; and eluted with 100 µl 80% (v/v) acetonitrile / 0.2% (v/v) FA. Guanidinated peptides were dried under vacuum and stored at -20°C if not required immediately.

Figure 9: SPE cartridge configuration for guanidination of bound peptides.

For combined lysine guanidination followed by N-terminal-specific succinylation, the lysine guanidination procedure described above was followed for 30 minutes. After removal of residual reaction buffer, peptides were washed with 1 ml of 6.67% (v/v) ammonia solution, followed by 1 ml 0.1% (v/v) TFA, followed by 1 ml water, followed by 1 ml 200 mM sodium acetate (pH 7.6). The non-specific succinylation procedure also described above was then followed, with the reaction allowed to proceed for 15 minutes. This was established as the optimized procedure for N-terminal-specific succinylation and used for N-terminal labelling of all proteomic peptides.

3.4.4. A novel isobaric peptide termini labelling protocol

Finally, C-terminal ^{18}O labelling and N-terminal-specific succinylation were consolidated as an integrated workflow, allowing two sets of proteomic peptides to be differentially isobarically labelled. C-terminal labelling was always carried out prior to N-terminal labelling. In the C-terminal labelling step, one set of peptides was ^{18}O labelled as described in section **3.4.2.** The other set of peptides was treated in exactly the same manner but all buffers used were made up using ^{16}O water. In the N-terminal labelling step, the ^{18}O-labelled set of peptides was guanidinated and succinylated with $^{12}C_4$ succinic anhydride as described in section **3.4.3.** The other set of peptides was treated in exactly the same manner but succinylated with $^{13}C_4$ succinic anhydride (Cambridge Isotope Laboratories, Tewksbury, MA, USA).

3.5. Peptide Fractionation

3.5.1. Isoelectric Focussing

Total peptide concentration in samples to be focused was first assayed using a NanoDrop 1000 spectrophotometer. Approximately 50 µg of a differentially labelled mixture mature and tolerogenic DC peptides were combined in a 1:1 ratio and separated into fractions using an Agilent 3100 OFFGEL Fractionator (Agilent, Santa Clara, CA, USA). For the experiments described in sections **6.2.1.1.**, **6.2.1.2.** (first experiment) and **7.2.**, 12 well frames and pH 3-10 immobilized pH gradient (IPG) strips (13 cm) (GE Healthcare, Buckinghamshire, UK) were assembled as per manufacturer instructions. For the experiments described in sections **6.2.1.2.** (second experiment) and **7.3.**, 12 well frames were converted into 11 well frames as described in (Berkelman *et al.*, 2011) and used in tandem with pH 3-6 IPG strips (11 cm) (Bio-Rad, Hercules, CA, USA). GE strips were rehydrated for 15 minutes with 40 µl / well IPG buffer (water, 5% (v/v) glycerol, 0.5% (v/v) pH 3-10 IPG amphyolytes (GE)). Bio-Rad strips were rehydrated in the same manner using Bio-Rad ampholytes instead of GE ampholytes. Combined samples were made up to 360 µl with water and then to 1.8 ml with 1.44 ml IPG buffer. For the experiments described in sections **6.2.1.1.**, **6.2.1.2.** (first experiment) and **7.2.**, 150 µl of sample was added to each of the 12 wells. For the experiments described in sections **6.2.1.2.** (second experiment) and **7.3.**, 163 µl of sample was added to each of the 11 wells. The wells were sealed using the cover strips provided and 10 µl distilled water was applied to the electrode pads. 200 µl of mineral oil was applied to the anode end of the frame, 1 ml to the cathode end, and the electrodes were attached. Peptides were focused for 20 kVh with a maximum current of 50 mA and power of 200 mW. After 24 hours the upper electrode pads were replaced and a further 200 µl mineral oil was applied to both electrodes. Focusing typically completed in around 36 hours. Focussed peptides were recovered from the wells, concentrated to approximately 50 µl under vacuum and stored at -20°C if not required immediately.

3.5.2. StageTip-based SAX fractionation

StageTip-based SAX fractionation was performed as described in (Wisniewski *et al.*, 2009a) with a few modifications. Anion exchanger columns were constructed by stacking 6 × approx. 1 mm diameter disks of Empore™ Anion-SR SPE resin (3M) in a 200 µl pipette tip (assuming a single disc had binding capacity of approx. 5 µg peptides). All steps were performed by passage of solutions through the tips using a room temperature microcentrifuge at 3000*g*. Equilibration, loading and elution steps were performed with Britton-Robinson (BR) buffer (20 mM acetic acid, 20 mM phosphoric acid, 20 mM boric acid; titrated to the desired pH with 1 N NaOH) Tips were conditioned with 50 µl acetone for 1 minute (spin time), followed by 50 µl methanol for 2 minutes, then 50 µl water for 4 minutes, then 50 µl 1 N NaOH for 5 minutes, then 50 µl water for 5 minutes; and finally equilibrated with 50 µl BR buffer (pH 11) for 5 minutes. Peptides to be fractionated were reconstituted in a final volume of 50 µl BR buffer (pH 11). Peptides were loaded onto tips for 5 minutes. Flow-through was recovered and the loading repeated a further two times, then reserved as the pH 11 fraction. For the experiments described in section **6.3.1.1.**, bound peptides were subsequently eluted through sequential passage of 50 µl volumes of BR buffer solutions of pH 7, 6, 5, 4, 3 and 2 respectively. For the experiment described in section **6.3.1.2.**, an additional final elution was performed with BR buffer (pH 2) / 50% (v/v) acetonitrile. For the experiment described in section **6.3.1.3.**, additional elutions were performed before every pH decrement with BR buffer of the corresponding pH / 50% (v/v) acetonitrile. Fractionated peptides were stored at -20°C if not required immediately.

3.6. Desalting of peptides prior to LC-MS analysis

All samples analysed by LC-MS other than those described in sections **5.3.2.**, **6.2.1.2.**, **6.3.1.** (succinylated samples) and **7.3.** (all in which desalting was achieved concurrent with peptide guanidination and/or succinylation) were desalted using StageTips as described in (Rappsilber *et al.*, 2003). Briefly, StageTips were constructed by stacking up to 5 × approx. 1 mm diameter discs of Empore™ C18-SR SPE resin (3M) in a 10 µl pipette tip (assuming a single disc had binding capacity of approx. 5 µg peptides). All steps were performed by passage of solutions through the tips using a syringe. Tips were wetted with 20 µl acetonitrile and equilibrated with 20 µl 0.1% (v/v) TFA. Samples were acidified with 1/10th volume 10% (v/v) TFA and passed through the tips. Bound peptides were washed twice with 50 µl 0.1% (v/v) TFA, twice with 50 µl 0.2% (v/v) FA and eluted with 10 µl 80% (v/v) acetonitrile / 0.2% (v/v) FA. Desalted peptides were dried under vacuum and stored at -20°C if not required immediately.

3.7. LC-MS/MS analysis

Peptides were reconstituted in 0.2% (v/v) FA and chromatographically resolved using a NanoACQUITY UltraPerformance LC® system (Waters, Manchester, UK). Buffer A was 0.1% (v/v) aqueous FA and buffer B was 0.1% (v/v) FA in acetonitrile.

Approximately 100 ng of BSA peptides or 1 µg proteomic peptides were loaded onto a 0.18 X 20 mm C18 Symmetry (5 µm) trapping column (Waters) in buffer A. The trap was then switched in-line with a self-packed column (100 µm internal diameter) of Reprosil-Pur C18-AQ 3 µm resin (Dr Maisch, Ammerbuch, Baden-Württemberg, Germany). Peptides were eluted with segmented gradients of buffer B. Ion source, trapping duration, flow rate, column length and temperature, chromatographic gradient duration and flow rate were varied across multiple experiments and are summarized in **Table 2**.

Peptides eluting from the capillary column were analysed by LC-MS using a Finnigan LTQ-FT mass spectrometer equipped with either a Finnigan Nanospray ion source (ThermoElectron, Bremen, Germany) or an Advance MS Source (Bruker, Billerica, MA, USA). All analysis was performed in positive ion mode. Eluate was sprayed using an uncoated 20 µm I.D. SilicaTip (New Objective, Woburn, MA, USA) at a spray voltage of 2 kV when using the Nanospray ion source and using an Advance Spraytip Assembly (Bruker) when using the Advance ion source. The ion source used varied across experiments and is summarized in **Table 2**.

Top 5 data-dependent acquisition was performed as follows. Survey MS scans were performed over the mass range m/z = 300 – 1500 in data-dependent mode. Data was acquired with a FT-MS resolution setting of 100,000 at m/z = 400 and a Penning trap injection target value of 1,000,000. The top five ions in the survey scan were automatically subject to collision-induced dissociation MS/MS in the linear ion trap region of the instrument at an injection target value of 100,000, using a normalized collision energy of 30% and an activation time of 30 ms (activation Q = 0.25). Precursor ion charge state screening was enabled and singly charged; quadruple charged (or greater) and unassigned charge states were rejected. Dynamic exclusion was enabled and precursor masses were selected for MS/MS with a repeat count of 2 (within 15 s), then excluded

from further selection for a duration of 20 s. The maximum number of precursor masses allowed on the exclusion list at any one time was 500. Inspection of mass spectrum plots and MS/MS fragmentation data was performed using QualBrowser software (ThermoElectron).

Sections	4.2.1.2., 4.2.2.2., 5.2.2.2., 5.2.2.3., 5.2.2.4., 5.2.2.6., 5.3.2.2., 5.3.2.3., 5.3.2.4., 6.2.1.2. (Fig. 43)

Gradient

Ion Source	Advance
Trapping Time	2 mins
Trapping Flow Rate	15 µl / min
Column Length	15 cm
Column Temp.	60°C
Gradient Length	50 mins
Gradient Flow Rate	1 µl / min

Time	% A	% B
0:00	99.9	0.1
0:06	93.0	7.0
31:00	60.0	40.0
32:00	20.0	80.0
34:00	20.0	80.0
34:30	99.9	0.1

Sections	4.2.3.1. (Fig 24a), 5.3.2.6.

Gradient

Ion Source	Advance
Trapping Time	3 mins
Trapping Flow Rate	10 µl / min
Column Length	15 cm
Column Temp.	60°C
Gradient Length	50 mins
Gradient Flow Rate	0.6 µl / min

Time	% A	% B
0:00	99.9	0.1
0:06	85.0	15.0
31:00	60.0	40.0
32:00	20.0	80.0
34:00	20.0	80.0
34:30	99.9	0.1

Sections	4.2.3.1. (Fig 24b & 24c), 4.3.2.3.

Gradient

Ion Source	Advance
Trapping Time	4 mins
Trapping Flow Rate	7.5 µl / min
Column Length	20 cm
Column Temp.	60°C
Gradient Length	50 mins
Gradient Flow Rate	0.5 µl / min

Time	% A	% B
0:00	99.9	0.1
0:06	88.0	12.0
30:00	60.0	40.0
32:00	20.0	80.0
34:00	20.0	80.0
34:30	99.9	0.1

Sections	6.2.1.2. (Fig. 44), 7.3

Gradient

Ion Source	Advance
Trapping Time	4 mins
Trapping Flow Rate	7.5 µl / min
Column Length	20 cm
Column Temp.	60°C
Gradient Length	90 mins
Gradient Flow Rate	1 µl / min

Time	% A	% B
0:00	99.9	0.1
0:06	90.0	10.0
70:00	50.0	50.0
72:00	20.0	80.0
74:00	20.0	80.0
74:30	99.9	0.1

Table 2: LC-MS settings used for experiments described in Chapters 4 - 7

Sections	6.2.1.1., 7.2

Ion Source	Finnigan Nanospray
Trapping Time	1 mins
Trapping Flow Rate	15 µl / min
Column Length	15 cm
Column Temp.	60°C
Gradient Length	85 mins
Gradient Flow Rate	0.5 µl / min

Gradient		
Time	% A	% B
0:00	99.9	0.1
1:00	95.0	5.0
62:00	55.0	45.0
67:00	15.0	85.0
70:00	15.0	85.0
70:30	99.9	0.1

Sections	4.2.1.1.

Ion Source	Finnigan Nanospray
Trapping Time	4 mins
Trapping Flow Rate	7.5 µl / min
Column Length	20 cm
Column Temp.	40°C
Gradient Length	50 mins
Gradient Flow Rate	0.4 µl / min

Gradient		
Time	% A	% B
0:00	99.9	0.1
0:06	85.0	15.0
30:00	65.0	35.0
32:00	20.0	80.0
34:00	20.0	80.0
34:30	99.9	0.1

Sections	6.3.1.2., 6.3.1.3., 6.3.1.4., 7.5.

Ion Source	Finnigan Nanospray
Trapping Time	4 mins
Trapping Flow Rate	7.5 µl / min
Column Length	50 cm
Column Temp.	40°C
Gradient Length	100 mins
Gradient Flow Rate	0.5 µl / min

Gradient		
Time	% A	% B
0:00	99.0	0.1
0:06	91.0	9.0
66:00	65.0	35.0
67:00	20.0	80.0
69:00	20.0	80.0
69:06	99.9	0.1

Table 2 (cont.): LC-MS settings used for experiments described in Chapters 4 - 7

3.8. Data analysis

Protein identifications were performed using the Mascot search engine (Matrix Science Ltd, London, UK). The peptide mass tolerance was limited to 10 ppm, the fragment mass tolerance to 0.6 Da and searches were performed against the UniProt protein sequence database (sprot release 20-04-2010; 516603 sequences; 181919312 residues). Searches were limited to human sequences for proteomic samples and sequences for all mammals other than primates and rodents for BSA samples. Cysteine carbamidomethylation was specified as a fixed modification, whilst methionine oxidation and pyroglutamate formation from N-terminal glutamine residues were taken into account as variable modifications. We routinely allow for potentially one missed trypsin cleavage and all proteins present in the database are taken into account without any p*I* or *M*r restrictions. Proteins with scores in excess of the 95% confidence limit ($P < 0.05$) are accepted as significant hits.

Protein quantitation in ^{18}O-labelled proteomic samples was carried out by performing Mascot searches as described above using the Mascot Distiller software package (Matrix Science) with C-terminal labelling with two ^{18}O atoms specified as an additional variable modification. For quantitation itself, Distiller calculates the areas under the precursor peak elution traces for unlabelled and labelled peptide pairs identified in the Mascot search and reports this as the abundance ratio of heavy peptide to that of light peptide. Individual peptide peak area ratios are collated into groups which correspond to individual protein hits and an average ratio is calculated for each identified protein, weighted using the signal intensities of each peptide peak. A minimum of two unique peptide ratios was specified as a requirement to report an average ratio for a protein. Upon completion, protein quantitation reports were exported to Excel for sorting and filtering of matches.

Protein quantitation in IPTL-labelled proteomic samples was carried out by performing Mascot searches as described above with lysine guanidination specified as an addition fixed modification and C-terminal labelling with two ^{18}O atoms, N-terminal succinylation with $^{12}C_4$-succinic anhydride and N-terminal succinylation with $^{13}C_4$-succinic anhydride specified as additional variable modifications. For quantitation, Mascots in-built multiplex quantitation protocol calculates the relative intensities of both $^{12}C_4$-labelled versus $^{13}C_4$-labelled b-

series product ions and unlabelled versus ^{18}O-labelled y-series product ions in a given product ion scan. Each peptide-to-spectrum match (PSM) is thus reported with an overall ratio derived from the summed ratios of each $^{12}c_4$ / $^{13}c_4$ and unlabelled / ^{18}O-labelled product ion pair. Individual PSM ratios are consolidated in instances where more than one PSM is obtained for a given peptide, and further consolidated as peptides are assigned to proteins. The final ratios are weighted using product ion signal intensities for all PSMs assigned to a given protein. A minimum of two unique peptide ratios was specified as a requirement to report an average ratio for a protein. Upon completion, protein and peptide reports were exported to Excel for sorting and filtering of matches.

Protein gene annotation and transmembrane helix prediction in membrane-enriched fractions was performed using the STRAP (Bhatia *et al.*, 2009) (http://www.bumc.bu.edu/cardiovascularproteomics/cpctools/strap/) and TMHMM (Krogh *et al.*, 2001) (http://www.cbs.dtu.dk/services/TMHMM/) algorithms respectively and described in more detail in **Chapter 4**.

3.9. Miscellaneous

3.9.1. BSA labelling with EZ-Link® Sulfo-NHS-SS Biotin and RevAmine

BSA (Sigma-Aldrich) was reconstituted in 1 ml PBS in low binding microcentrifuge tubes (Sorensen Bioscience) and reacted with 10 µl of either EZ-Link® Sulfo-NHS-SS Biotin (Thermo Fisher Scientific) or RevAmine, both at 25µg/µl, in DMSO). The amount of BSA reconstituted was calculated such that addition of 10 µl of either reagent would result in a 20-fold molar excess of reagent over that of BSA. 10 µl of DMSO alone was also added to BSA to serve as an unbiotinylated control. Tubes were vortexed for 1 minute and incubated for 1 hour at room temperature. Biotinylation reactions were quenched through addition of 50 µl of 'quenching solution' (Thermo Fisher) with incubation for a further minute at room temperature. Biotinylated BSA was desalted using PD SpinTrap™ Sephadex™ G-25 microcentrifuge spin columns (GE Healthcare). Columns were equilibrated with four 500 µl volumes of water and centrifuged at 800g for 1 minute at room temperature. 150 µl of BSA solution was applied to the resin, incubated at room temperature for 1 minute and then collected by centrifugation as described.

3.9.2. MALDI-TOF-MS of EZ-Link® Sulfo-NHS-SS Biotin and RevAmine-labelled BSA

Samples of desalted biotinylated and unbiotinylated control BSA were acidified through addition of 1/10th volume 10% (v/v) TFA and 1 µl (approximately 1 µg) protein solution was spotted onto a MALDI plate and allowed to air dry. Sample spots were then overlaid with 1 µl of sinapinic acid matrix (10 mg/ml in 50% (v/v) acetonitrile containing 0.1% (v/v) TFA) and allowed to air dry once more. Analysis was performed by matrix-assisted laser desorption ionization-time of flight mass spectrometry (MALDI-TOF-MS) using a Voyager DE-STR (Applied Biosystems, Foster City, CA, USA). Spectra were acquired in positive ion linear mode (25 kV accelerating voltage, 250 ns delay time) over a mass range of 40000 Da – 90000 Da with 50 laser shots per spectrum. External calibration was performed against the unbiotinylated BSA control.

3.9.3. Fluorescence confocal microscopy of EZ-Link® Sulfo-NHS-SS Biotin and RevAmine-labelled cells

Jurkat T cells were harvested, washed and biotinylated as described in section **3.2.3.** After quenching of biotinylation reactions and washing with TBS, biotinylated and control cells were resuspended in fluorescence-activated cell sorting (FACS) buffer (PBS / 0.5% (v/v) BSA / 0.01% (v/v) sodium azide) containing a streptavidin - Alexa Fluor® 568 conjugate (Life Technologies, Carlsbad, CA, USA). Cells were incubated at 4°C in the dark for 1 hour, washed three times with FACS buffer and fixed with FACS buffer / 1% (v/v) paraformaldehyde. 1×10^5 fixed cells were transferred to microscope slides using a Cytospin for 3 minutes at 1000 rpm and mounted using VECTASHIELD mounting media with 4',6-diamidino-2-phenylindole (DAPI) counterstain (Vector Laboratories, Burlingame, CA, USA). Cells were visualized by immunofluorescence using a Leica TCS SP2 UV laser-scanning confocal microscope set up to detect tetramethyl rhodamine isothiocyanate (TRITC) (excitation 547 nm, emission 572 nm) and DAPI (excitation 345 nm, emission 455 nm). Baseline TRITC emission levels were set using unlabelled cells and all labelled cells imaged using these settings.

Chapter 4. Development and validation of a membrane enrichment and digestion protocol to favour mass spectrometric identification of membrane proteins

4.1. Introduction

4.1.1. Challenges of membrane proteomics

As discussed in **Chapter 1**, bottom-up mass-spectrometry based proteomics of membrane proteins poses particular challenges owing to their low abundance relative to the rest of the proteome and their decreased solubility in the aqueous buffers typically used throughout the proteomic workflow prior to LC-MS analysis. The first of these challenges necessitates performing some form of membrane protein enrichment prior to analysis whilst the second requires the adoption of novel strategies to solubilize and digest membrane proteins whilst avoiding the use or retention of substances which negatively impact upon the activity of the protease/s used for digestion and the process of LC-MS analysis itself.

Mass spectrometry is essentially a concentration-dependent technique and the probability of sampling membrane proteins during LC-MS is substantially increased if proteins present in far greater quantities (for instance cytoplasmic and nuclear proteins) are first depleted from the sample. There are a variety of ways to enrich membrane proteins relative to non-membrane proteins in a sample, with the majority either utilising differential or density gradient centrifugation or affinity purification with tagging reagents which target surface-exposed protein domains on intact cells. It was initially intended that an enrichment strategy which fell into the second of these categories was pursued with a novel amine-directed biotinylation reagent (RevAmine), which will be discussed in more detail later.

There are also a wide range of published strategies for membrane protein solubilization and digestion. A key consideration here is the extent to which the means of solubilization impacts upon the efficiency of digestion and subsequent analysis. A case in point is SDS, which is widely regarded as the most powerful detergent available for solubilization of proteins, but is only compatible with tryptic digestion at minute (< 0.1% (w/v)) concentrations and must be completely removed prior to LC-MS. An ‘ideal’ strategy for solubilization and digestion would thus be one which employed a powerful solubilizing agent with negligible repercussions on downstream processing. FASP (Wisniewski *et al.*, 2009b) appears to be well-suited in this regard. In addition, the final elution step

of the affinity purification which would be required were a cell surface biotinylation strategy for membrane protein enrichment to be adopted would segue nicely into the initial solubilization step of FASP, and it was thus selected as the first-line digestion strategy to pursue.

4.1.2. Criteria for evaluation of the effectiveness of a membrane protein enrichment and digestion strategy

There exist a number of means for inferring which proteins identified in an LC-MS run are likely to be membrane proteins. A commonly employed approach in the literature is to use Gene Ontology annotations. The Gene Ontology (GO) is a major bioinformatics initiative which seeks to annotate all genes and gene products with a controlled vocabulary of attributes pertaining to the 'biological processes' in which they partake, the 'molecular functions' which they possess and the 'cellular components' in which they reside (Ashburner *et al.*, 2000). Membrane localization can thus be inferred through examining which of the identified proteins have a membrane-related cellular component annotation.

That said, GO annotation is by no means an infallible system for determining whether a given protein is likely to be a *bona fide* membrane protein. The nature of the controlled vocabulary and the fact that many annotations are assigned via software through inference from sequence or structural similarity to other proteins means that membrane annotations are often assigned to proteins which would not typically be considered membrane proteins and would almost certainly not be considered of interest in the context of this particular project. For instance, glyceraldehyde 3-phosphate dehydrogenase (GAPDH) has a plasma membrane annotation. The converse is also true, genuine membrane proteins which have not been annotated as such will clearly not be identified as such. This may occur with proteins that are poorly annotated. For instance, signal-regulatory protein beta-1 (SIRP-β-1) and SIRP-β-1 isoform 3 are both transcribed from the same gene and share 87% sequence identity but only the former has a plasma membrane GO annotation.

An alternative approach is to examine the primary amino acid sequences of the proteins identified for structural motifs synonymous with membrane localization. Motifs of interest are stretches of sequence which assume a membrane-spanning α-helical conformation, accumulation of amphiphilic residues at each

end of said α-helical stretches and cytoplasmic loop regions between helices. α-Helices are a very common structural motif but transmembrane helices are composed largely of hydrophobic amino acids and must be at least 15 residues in length in order to span the lipid bilayer (Punta *et al.*, 2007). The presence of amphiphilic amino acids at each end of a membrane-spanning helix ensure that the helical region itself resides entirely within the bilayer (Schiffer *et al.*, 1992; Reithmeier, 1995; Braun and von Heijne, 1999; Ridder *et al.*, 2000). Cytoplasmic loop regions contain a relatively high proportion of charged residues to prevent translocation of these regions across the lipid bilayer when the protein is inserted into the membrane, giving rise to the so called 'positive-inside' rule (von Heijne and Gavel, 1988; Nilsson *et al.*, 2005). These motifs can be used to develop algorithms to predict membrane protein topology (Punta *et al.*, 2007).

One such algorithm is TMHMM (Krogh *et al.*, 2001), which takes hydrophobicity, net charge, helix length and topological constraints into consideration when predicting presence and topology of transmembrane domains TMHMM performs very well in the analysis of the membrane protein content of a given dataset, misclassifying less than 1% of soluble proteins as membrane proteins whilst correctly identifying 97 – 98% of legitimate transmembrane helices. As an aside, SIRP-β-1 and SIRP-β-1 isoform 3 are both predicted to possess a single transmembrane helix in exactly the same place by TMHMM, lending further weight to the assertion that the latter is also a plasma membrane protein.

In evaluating the effectiveness of the various membrane enrichment and digestion strategies explored here, both GO annotation and the TMHMM algorithm have been employed; increasing confidence that any purported enrichment in membrane protein identifications are genuine and allowing the two software tools to be compared and contrasted.

4.1.3. Amine-directed biotinylation reagents

The interaction of avidin and biotin is among the strongest non-covalent interactions known, exhibiting a dissociation constant in the order of 10^{-15} M (Green, 1975). The native structure of avidin is resistant to harsh conditions such as extremes of temperature (up to 132ºC), pH (between pH 2 and pH 13) and strong denaturants (up to 8 M urea or 3 M guanidine hydrochloride) (Green, 1963). Interaction with biotin stabilizes the complex further, an avidin-biotin complex is stable in 8 M guanidine at pH 5.2, and complete dissociation requires at least 6 M guanidine at pH 1.5 (Cuatrecasas and Wilchek, 1968; Bodanszky and Bodanszky, 1970). There is also evidence that the complex can be formed and maintained in the presence of a wide range of detergents, including 1% (w/v) SDS (Waner *et al.*, 2004).

The properties of this interaction have facilitated its use in a plethora of biological applications. Biotinylated molecules will bind streptavidin conjugates with high affinity and specificity even in complex mixtures. A vast array of reagents are now available for biotinylation of biomolecules of interest, all of which are typically composed of a biotin moiety and a reactive group separated by a spacer arm.

A common reactive group used in such reagents is an NHS-ester, which will react covalently with primary amines to form a stable amide bond. One such reagent is sulfosuccinimidyl-2-(biotinamido)ethyl-1,2-dithiopropionate (EZ-Link™ Sulfo-NHS-SS-Biotin, Thermo Fisher) **(Fig. 10)**. This reagent incorporates a disulphide bridge in the spacer arm, enabling biotinylated biomolecules of interest to be released under reducing conditions without employing the harsh reagents required to disrupt the avidin-biotin interaction itself. The negative charge imparted to the reagent by the sulfonate group counterbalances the poor solubility imparted by the biotin moiety, enabling the reagent to be dissolved directly in aqueous buffers (Hermanson, 2008). This negative charge character should also prevent it from penetrating the plasma membrane of viable cells; indeed it was this property for which it was initially employed (Hurley *et al.*, 1985; Cole *et al.*, 1987; Meier *et al.*, 1992; Altin and Pagler, 1995). These properties theoretically make EZ-Link™ Sulfo-NHS-SS-Biotin ideal for targeting cell surface proteins.

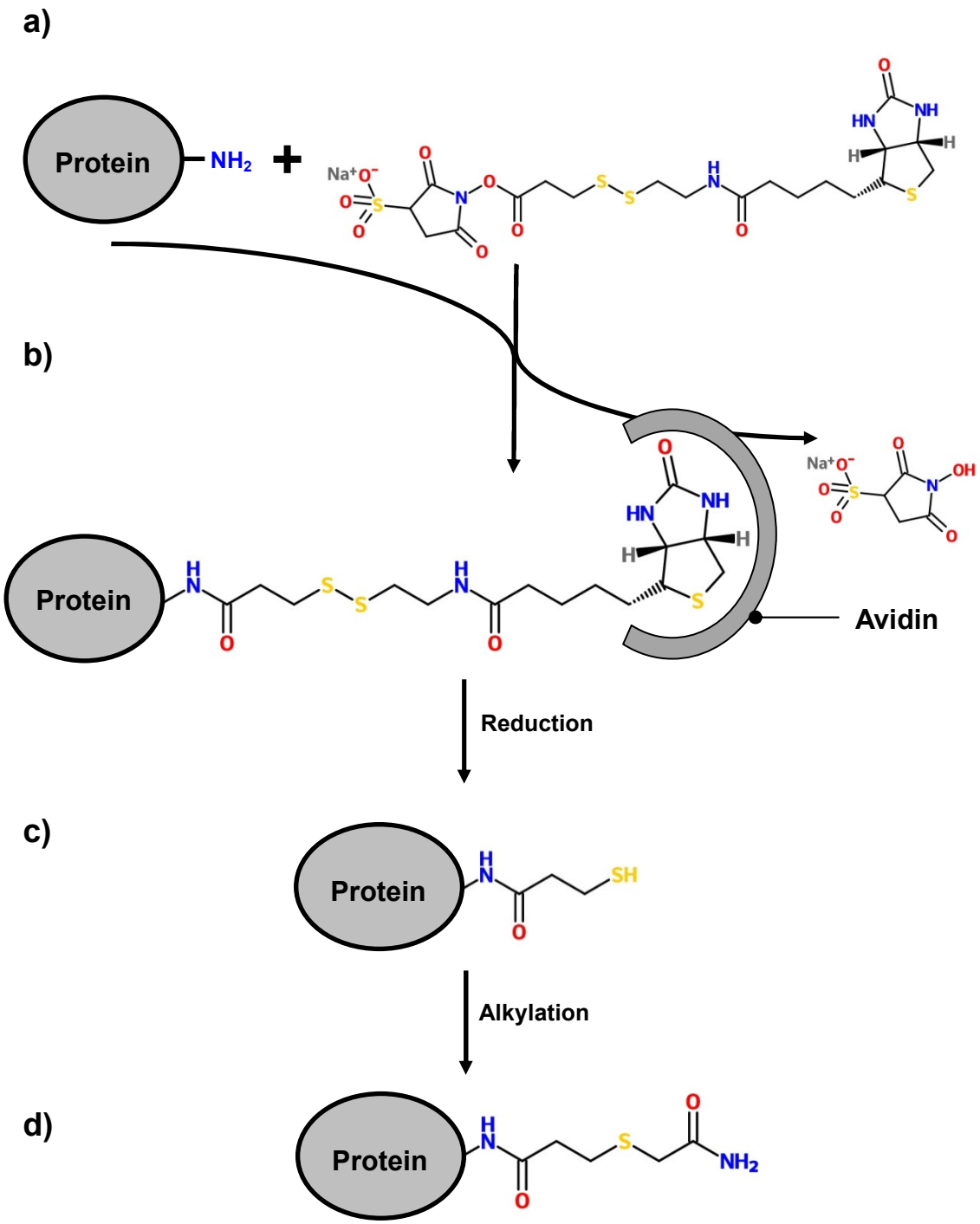

Figure 10: Biotinylation of proteins using EZ-Link™ Sulfo-NHS-SS-Biotin. **a)** The OSu ester reacts covalently with primary amines. **b)** A stable amide bond is formed and an NHS leaving group is released. The biotinylated protein can then be affinity purified using the avidin-biotin interaction. **c)** After affinity purification, the protein can be liberated through reduction of the disulphide bond in the spacer arm of the reagent. This liberates a free thiol **d)** Alkylation converts the thiol to a CAMthiopropanoyl group.

From a mass spectrometry-based proteomics perspective, a major shortcoming of EZ-Link^{TM} Sulfo-NHS-SS-Biotin is the residual CAMthiopropanoyl moiety it leaves on lysine side chains after affinity purification of the biotinylated biomolecules of interest. This chemical group precludes tryptic cleavage at modified lysine residues and would be expected to negatively impact upon the number and size of peptides produced from a tryptic digest of modified proteins.

An 'ideal' amine-directed biotinylation reagent for mass spectrometry-based proteomics would be traceless, that is liberation of biomolecules of interest after affinity purification would be concomitant with regeneration of lysine primary amines. In recent years, a couple of research groups have incorporated such functionality into linkers which are cleaved in response to UV irradiation (Wang *et al.*, 2012) and acidic conditions (Maier and Wagner, 2012).

Our research group has developed RevAmine (Grey *et al*.; unpublished data)**,** an amine-directed biotinylation reagent incorporating a functional group in the spacer arm which exploits the beta elimination behaviour of sulfonyl ethanol derivatives to enable traceless removal upon treatment with mild base **(Fig. 11)**. The reagent has been shown to be soluble in aqueous media and to react with peptides in neutral pH, non-amine buffers. Facile cleavage of tagged peptide had also been demonstrated in concentrations of dilute ammonia as low as 0.01% (v/v) and in ammonium bicarbonate at pH 8. These characteristics suggested that it would be feasible to incorporate this novel reagent into a cell-surface biotinylation and affinity purification-based enrichment strategy with the aim of circumventing the shortcomings of non-traceless reagents, such as the one described above.

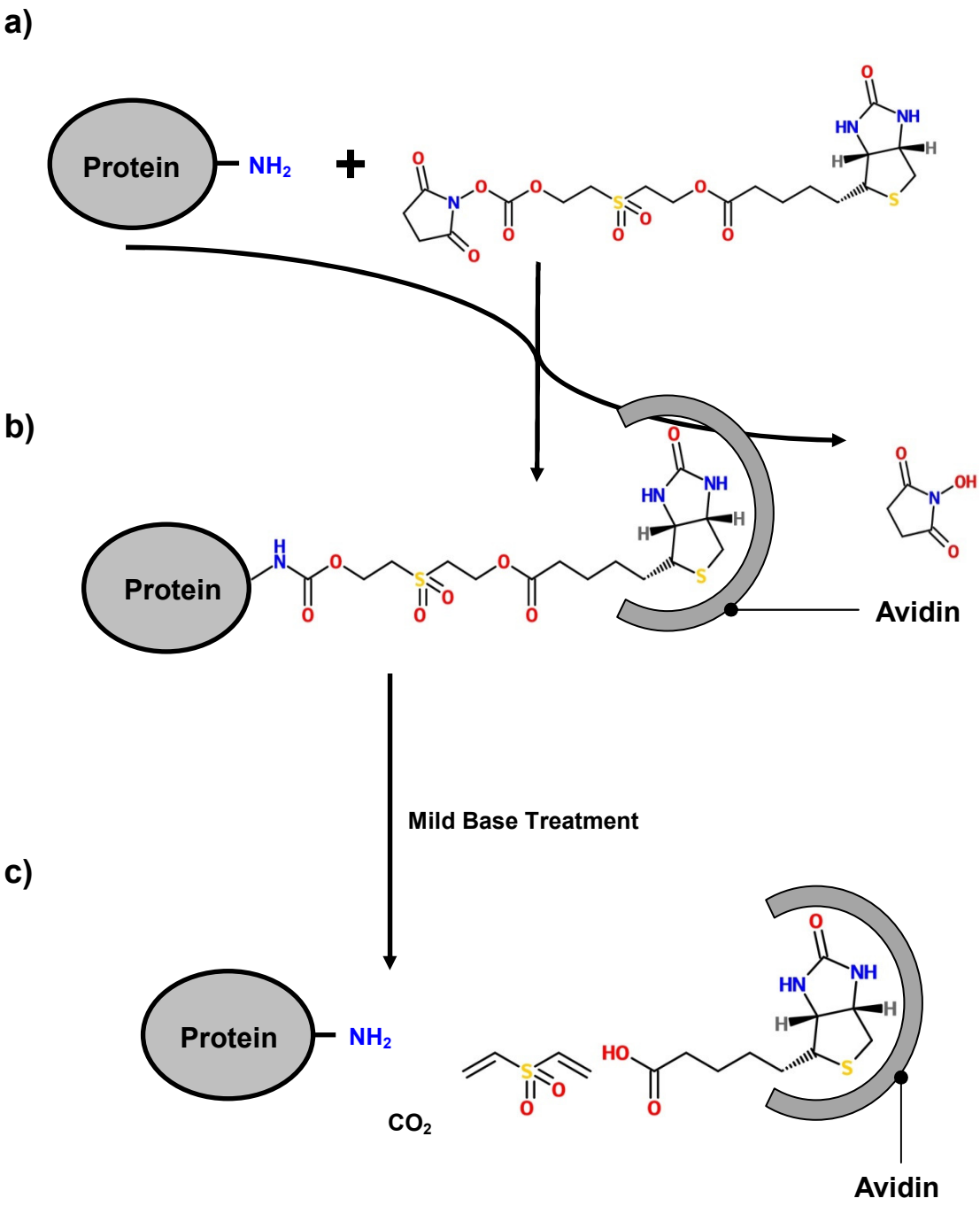

Figure 11: Biotinylation of proteins using RevAmine. **a)** The OSu ester reacts covalently with primary amines. **b)** A carbamate linkage to lysine on the protein is formed and an NHS leaving group is released. The biotinylated protein can then be affinity purified using the avidin-biotin interaction. **c)** After affinity purification, treatment with mild base releases the unmodified protein.

4.2. Results

4.2.1. Characterisation of RevAmine - a novel amine-directed biotinylation reagent

4.2.1.1. MALDI-TOF analysis demonstrates facile conjugation of RevAmine tag to intact BSA

The biochemical properties of RevAmine had previously been elucidated with peptides. Given that it was intended that RevAmine be used in the context of a membrane protein enrichment strategy, the logical progression was to augment the peptide-based studies with some whole protein work. With this in mind, analogous conjugation and removal experiments were performed using BSA.

BSA was reconstituted in PBS and a 20-fold molar excess of either EZ-Link™ Sulfo-NHS-SS-Biotin or RevAmine was added. Biotinylation reactions were allowed to proceed for 1 hour before quenching. A control reaction was also included in which no amine-directed biotinylation reagent was added. All reactions were subsequently column-desalted. Approximately 1 µg protein was spotted onto a MALDI plate using sinapinic acid matrix, allowed to dry and analysed by MALDI-TOF.

The extent of biotinylation in unbiotinylated, EZ-Link™ Sulfo-NHS-SS-Biotin labelled and RevAmine-labelled BSA is shown in **Fig. 12**. These data suggest that both reagents can be used for biotinylation of BSA in isolation. On the basis of the reported average intact mass measurements, it can be inferred that there are approximately 10.46 EZ-Link™ Sulfo-NHS-SS-Biotin molecules per protein and approximately 7.09 RevAmine molecules per protein. These figures are slightly higher than those reported by Pierce for modification of Immunoglobulin G (IgG) with a 20-fold molar excess of EZ-Link™ Sulfo-NHS-SS-Biotin. This may be because there are more accessible surface-exposed reactive groups in BSA than IgG. The higher number of EZ-Link™ Sulfo-NHS-SS-Biotin molecules per protein suggests slightly greater reactivity for this reagent, which may be explained by the improved solubility imparted by the sulfosuccinimide ester.

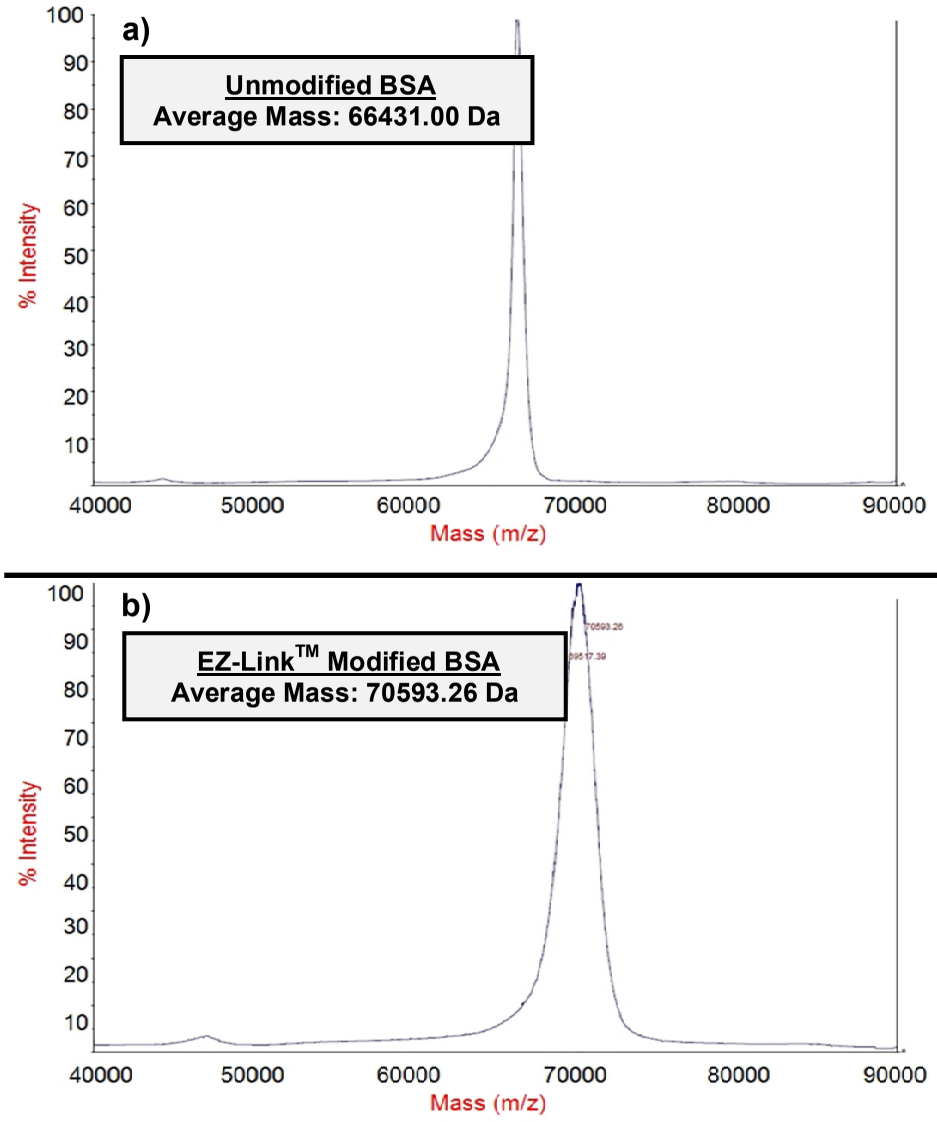

Figure 12: MALDI mass spectra showing intact mass measurements of **a)** unmodified BSA; **b)** BSA modified with EZ-Link™ Sulfo-NHS-SS Biotin; **c)** BSA modified with RevAmine. On the basis of these measurements, there are on average ~10.46 EZ-Link™ modifications per protein and ~7.09 RevAmine modifications per protein. Data are representative of two independent experiments.

4.2.1.2. LC-MS analysis demonstrates facile conjugation and traceless removal of RevAmine tag to and from intact BSA prior to tryptic digestion.

BSA was biotinylated and the reaction quenched as described in section **4.2.1.1.** A control reaction was carried out as before. All biotinylation reactions were subsequently divided into two aliquots. The first of the two aliquots for each condition were immediately buffer exchanged into 50 mM ammonium bicarbonate. The second of the two aliquots for each condition were basified through addition of ammonia solution to a final concentration of 0.1% (v/v) and incubated at room temperature for 1 hour before being buffer exchanged as above. All aliquots were then digested overnight with trypsin, acidified with 1% (v/v) TFA, tip desalted and analysed by LC-MS.

Raw data were processed and searched using Mascot MS/MS search tool with mass shifts resulting from modification of N-terminal and lysine side chain primary amines with EZ-Link™ Sulfo-NHS-SS-Biotin and RevAmine reagents specified as variable modifications. Peptide reports were exported from Mascot MS/MS search as CSV files and imported into Microsoft Excel for further data processing. All peptides detected across all runs were examined for presence of mass shifts indicative of modification with either reagent.

Modified and unmodified peptides derived from the BSA biotinylated with EZ-Link™ Sulfo-NHS-SS-Biotin and not treated with ammonia are shown in **Fig. 13**, whilst modified and unmodified peptides derived from the BSA biotinylated with RevAmine and not treated with ammonia are shown in **Fig. 14**. No mass shifts indicative of modification with either reagent were detected in either replicate for the unbiotinylated BSA not treated with ammonia and these data are not shown. A total of 288 modified peptides were detected across the two replicates for BSA biotinylated with EZ-Link™ Sulfo-NHS-SS-Biotin, with modifications seen at 14 unique residues. In contrast, a total of 54 modified peptides were detected across the two replicates for BSA biotinylated with RevAmine, with modifications seen at 5 unique residues. This disparity may be due in part to the increased reactivity of the commercial reagent owing to the sulfosuccinimide ester and in part to the fact that nearly twice as many peptides were detected in total across the two replicates where it was used.

Modified and unmodified peptides derived from the BSA biotinylated with EZ-Link™ Sulfo-NHS-SS-Biotin and treated with ammonia are shown in **Fig. 15**, whilst modified and unmodified peptides derived from the BSA biotinylated with RevAmine and treated with ammonia are shown in **Fig. 16**. No mass shifts indicative of modification with either reagent were detected in either replicate for the unbiotinylated BSA treated with ammonia and these data are not shown. A total of 82 modified peptides were detected across the two replicates for BSA biotinylated with EZ-Link™ Sulfo-NHS-SS-Biotin and then basified with modifications seen at 8 unique residues. Whilst this figure is less than the number of modified peptides detected in the sample biotinylated with EZ-Link™ Sulfo-NHS-SS-Biotin and not treated with ammonia, the number of total peptides detected across the two replicates is also nearly half that here. Encouragingly, no modified peptides could be detected across the two replicates for BSA biotinylated with RevAmine and then basified. This suggests that the RevAmine reagent behaves in the same manner when incubated under basic conditions, regardless of whether it is reacted with peptides or proteins.

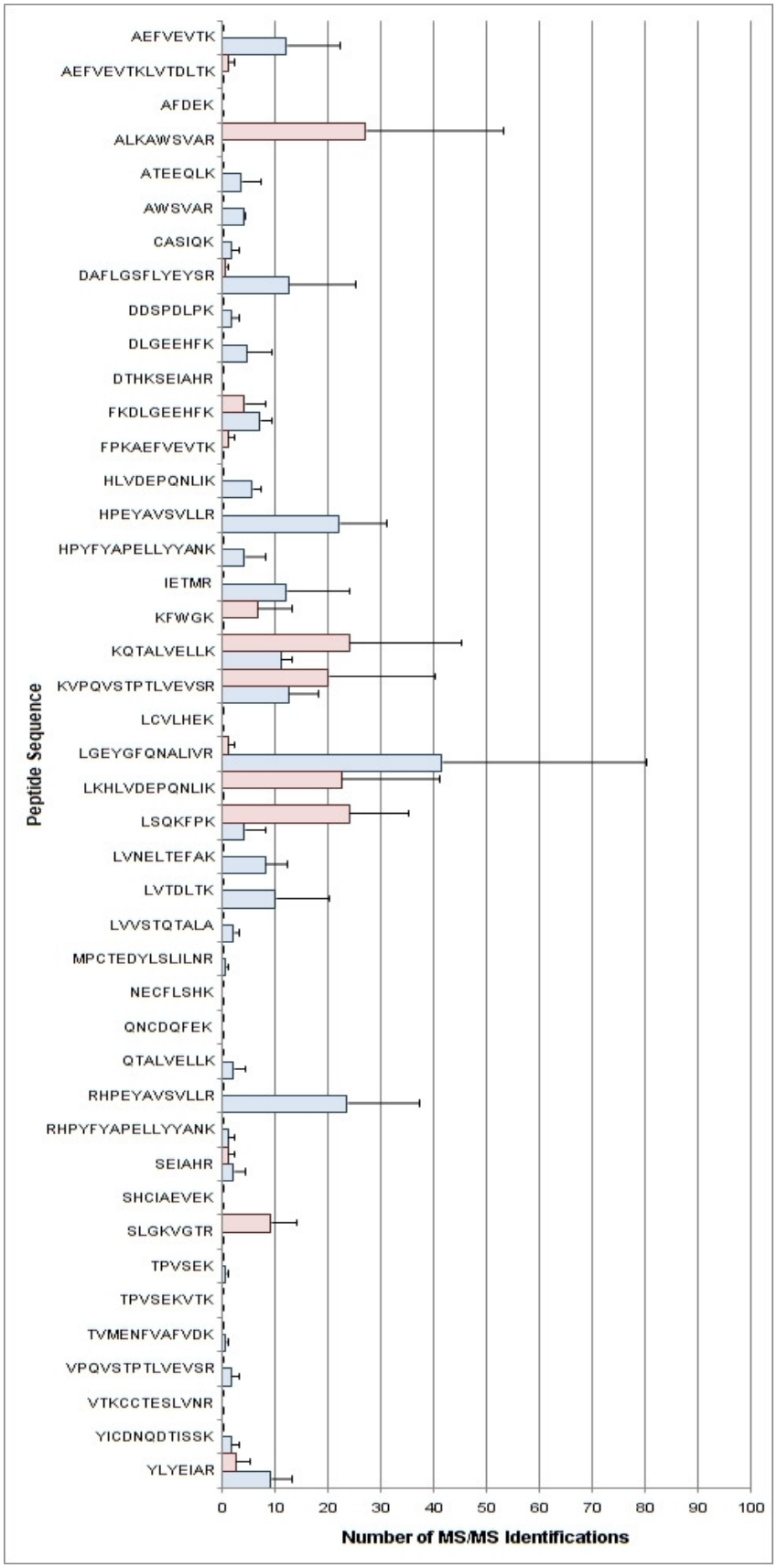

Figure 13: Unmodified and modified BSA peptides detected by LC-MS after tryptic digestion of EZ-Link™-modified BSA. Data are the average of two experimental replicates. 238 MS/MS events corresponded to modified peptides in the first replicate and 50 MS/MS events corresponded to modified peptides in the second replicate. Modifications were detected on 14 unique peptides across the two replicates.

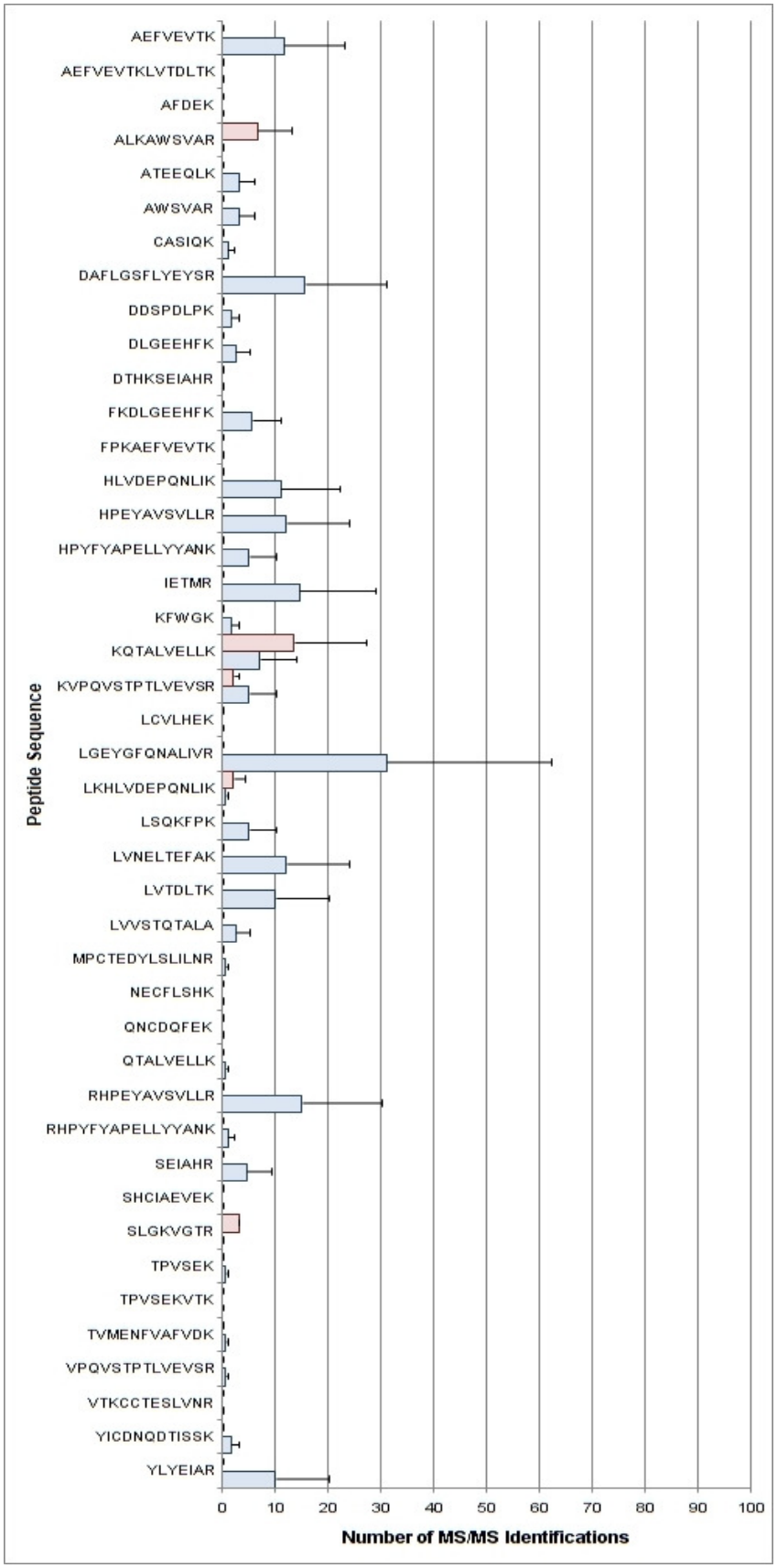

Figure 14: Unmodified and modified BSA peptides detected by LC-MS after tryptic digestion of RevAmine-modified BSA. Data are the average of two experimental replicates. 48 MS/MS events corresponded to modified peptides in the first replicate and 6 MS/MS events corresponded to modified peptides in the second replicate. Modifications were detected on 5 unique peptides across the two replicates.

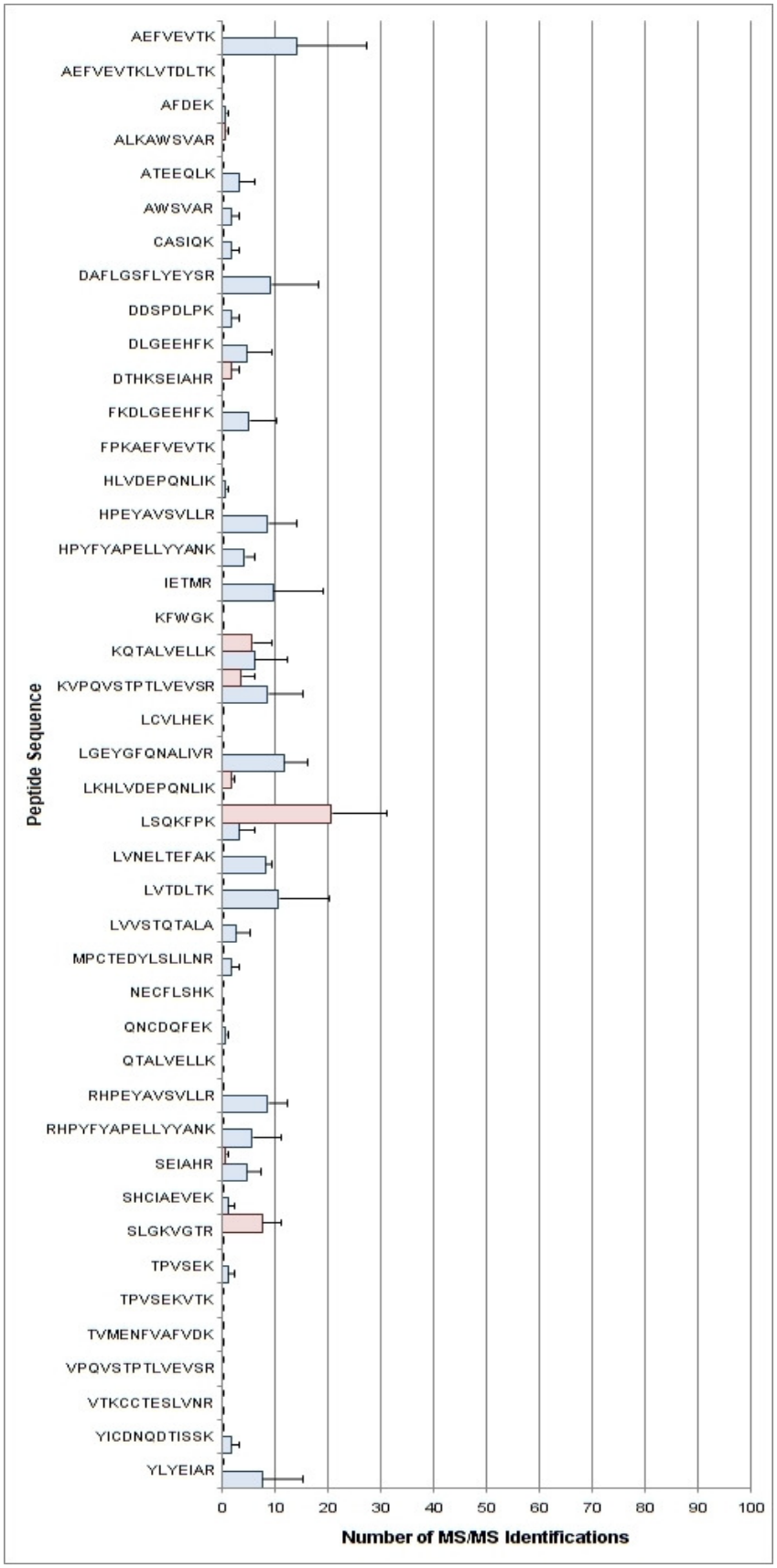

Figure 15: Unmodified and modified BSA peptides detected by LC-MS after tryptic digestion followed by treatment with 0.1% (v/v) NH_3 of EZ-Link^{TM}-modified BSA. Data are the average of two experimental replicates. 32 MS/MS events corresponded to modified peptides in the first replicate and 50 MS/MS events corresponded to modified peptides in the second replicate. Modifications were detected on 8 unique peptides across the two replicates.

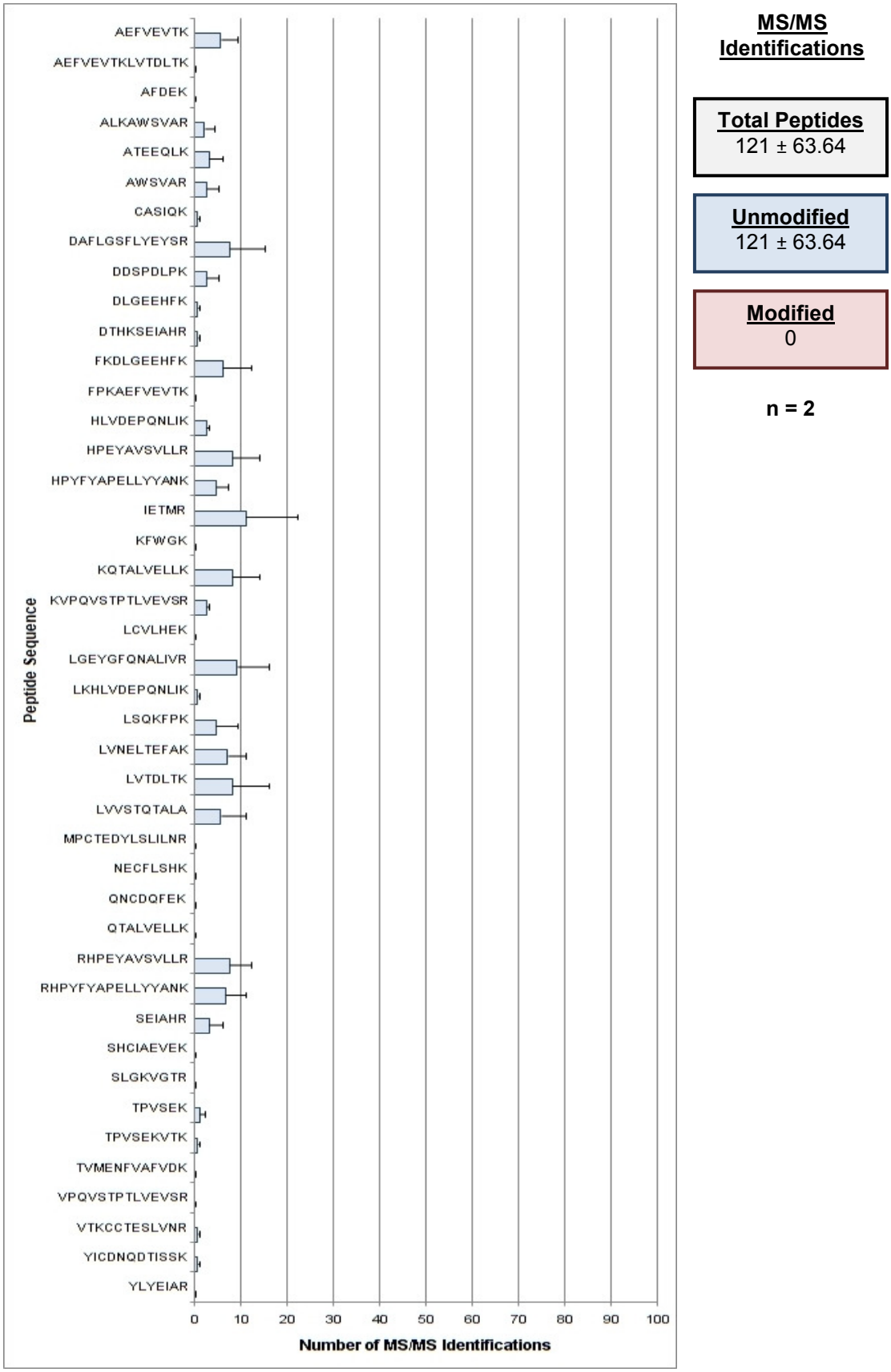

Figure 16: Unmodified and modified BSA peptides detected by LC-MS after tryptic digestion followed by treatment with 0.1% (v/v) NH_3 of RevAmine-modified BSA. Data are the average of two experimental replicates. No MS/MS events corresponding to modified peptides were detected in either replicate, suggesting that base treatment completely removes all traces of the RevAmine tag from intact proteins as desired.

4.2.1.3. Fluorescence confocal microscopy shows RevAmine and EZ-Link™ Sulfo-NHS-SS-Biotin are equally adept at biotinylating cell surface proteins **in situ***.*

Having extended the initial peptide-based studies with RevAmine to an intact protein, the final step was to examine whether it could be used to biotinylate proteins *in situ* on the surface of intact cells.

Jurkat T-cells were incubated in the presence of either EZ-Link™ Sulfo-NHS-SS-Biotin or RevAmine. Excess reagent was quenched using Pierce Cell Surface Isolation Kit 'quenching solution' and removed through extensive washing. The cells were then stained with a Streptavidin – Alexa Fluor 568 conjugate. Stained cells were fixed, cytospun onto microscope slides and mounted using a DAPI mounting medium. Unbiotinylated cells were stained and processed in the same manner. **Fig. 17** suggests that both reagents can be used for cell surface biotinylation, with discernible levels of membrane-localized fluorescence which are not present in the unbiotinylated cells.

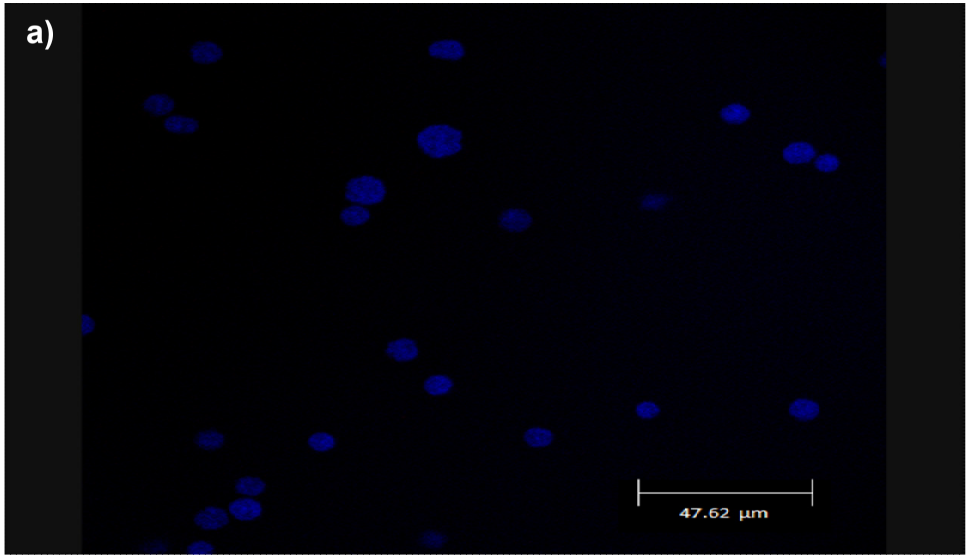

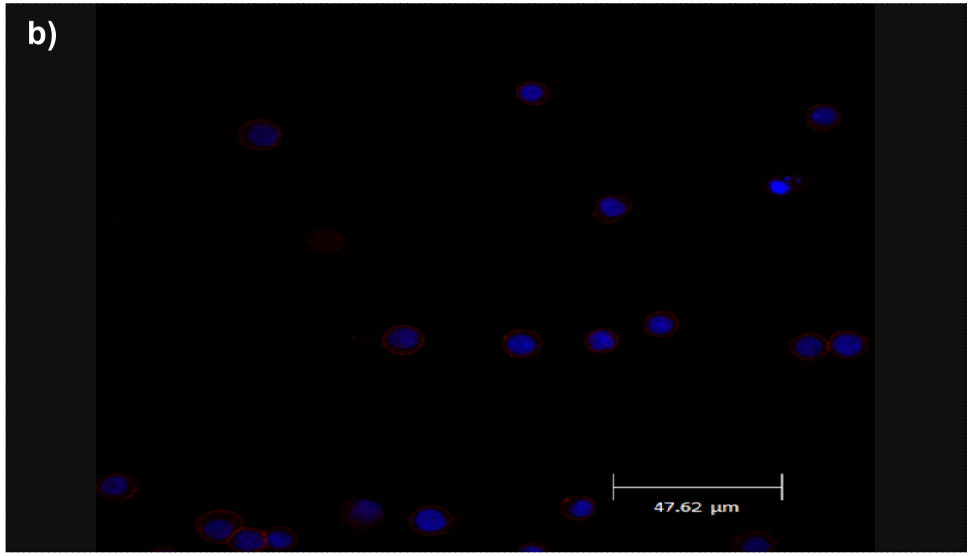

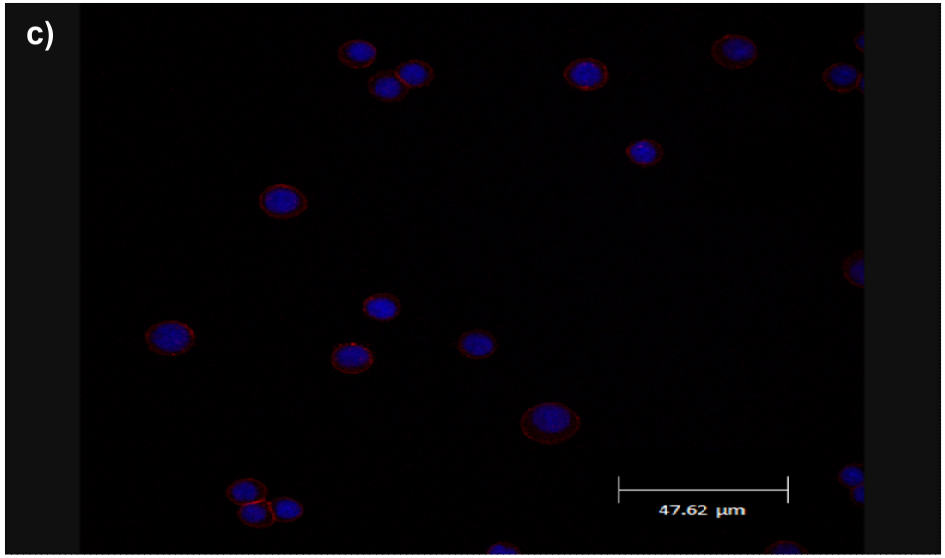

Figure 17: *In situ* biotinylation of cell surface-exposed primary amine residues on Jurkat cells detected through staining with a Streptavidin – Alexa Fluor 568 conjugate followed by fluorescence confocal microscopy. **a)** Unlabelled cells. **b)** EZ-Link™-labelled cells. **c)** RevAmine-labelled cells. All cells were also stained with DAPI prior to imaging. Data is representative of two independent experiments. Detection of Alexa 568 in images **b)** and **c)** and the absence thereof in image **a)** suggests that both EZ-Link™ and RevAmine can be used to label live cells and that labelling is localized to the plasma membrane.

4.2.2. Evaluation of the suitability of amine-directed biotinylation reagents as tools for enrichment of cell surface proteins for analysis by mass spectrometry.

The data shown in section **4.2.1.** suggested that both EZ-Link™ Sulfo-NHS-SS-Biotin and RevAmine could be used to biotinylate surface-exposed primary amine residues on intact cells and that the latter of the two reagents could be completely removed through treatment with dilute base, regenerating the original peptide. It was next investigated whether these biotinylated proteins could be captured and enriched before proceeding with tryptic digestion and LC-MS analysis.

All samples processed using a cell surface biotinylation approach were enriched broadly in accordance with the protocol supplied with the Pierce Cell Surface Isolation Kit, which includes EZ-Link™ Sulfo-NHS-SS-Biotin and all reagents necessary to lyse labelled cells and capture, enrich and elute biotinylated proteins from the lysate. Briefly, after the labelling reaction has been completed, cells are lysed and the lysate is loaded into a spin column containing NeutrAvidin® Agarose Resin. Biotinylated proteins are allowed to bind the resin and non-biotinylated proteins are removed through stringent washing. Biotinylated proteins are then liberated from the column through addition of a buffer containing DTT and collected as the eluate fraction.

4.2.2.1. Filter-Aided Sample Preparation (FASP) performs as effectively as standard in-solution digestion for processing of whole cell lysates for LC-MS analysis.

As touched upon in section **4.1.**, it was desired that FASP be used for digestion of membrane-enriched fractions. The suggested buffer for the elution step in the Pierce Cell Surface Isolation Kit protocol is PAGE sample buffer (containing DTT), which lends itself to a gel-based workflow. For reasons pertaining to the digestion and labelling steps of this particular workflow which will be discussed more fully in **Chapter 6**, we wished to avoid gel-based proteomics. Nevertheless, it was assumed that the elution buffer should be supplemented with a detergent(s) of some description lest the proteins come out of solution in the avidin spin column and not be eluted. The presence of detergent in the elution buffer would necessitate its removal prior to proceeding with the standard in-solution digestion protocol in place in the lab. This could be achieved using a precipitation step or a detergent removal resin (indeed, the latter is how detergent was removed from whole cell lysates prior to digestion for the work presented in **Chapter 5**. However, precipitations will by definition bring all proteins out of solution and even using a detergent removal resin could cause the membrane proteins to come out of solution once more. The first step of the FASP procedure entails solubilization of proteins in SDS / Tris-HCl and reduction with DTT. It was thus reasoned that this solubilization buffer could be employed in place of PAGE Buffer to liberate biotinylated proteins from the avidin spin column. The resultant eluate could then be processed using FASP.

Since FASP had never been used in the lab before, we first wished to examine whether it could be used in place of in-solution digestion for whole cell lysates. This would give an indication as to whether there were any inherent problems with the technique itself. Approximately 100 µg of Jurkat whole cell lysate was digested overnight using either FASP or in-solution digestion. Digests were acidified with 1% (v/v) TFA, desalted using an SPE cartridge and analysed by LC-MS. Raw data were processed and searched using Mascot. Protein summary reports were screen scraped and imported into Microsoft Excel. Uniprot accession code lists were saved as text files. GO annotation was performed using the STRAP software tool (Bhatia *et al.*, 2009). For

transmembrane domain prediction, Uniprot accession code lists were converted to FASTA format and analysed using a TMHMM batch search.

The distribution of cellular component GO annotations for all identified proteins are shown in **Fig. 18a** for in-solution digestion and **Fig. 18b** for FASP. The percentage of total proteins identified with 'plasma membrane', 'cytoplasmic' and 'nuclear' GO annotations is shown to the right of each pie chart. It is worth noting at this point that many proteins have more than one cellular compartment GO annotation and hence the percentages reported do not appear to tally with the corresponding slice of the pie chart and summate to more than 100%. The percentage of proteins predicted to contain transmembrane domains by the TMHMM algorithm is also shown.

The two techniques appear near-equivalent in terms of total protein identifications, distribution of subcellular component ontologies across the identified proteins and percentage of proteins predicted to contain transmembrane helices by TMHMM. This suggested that there were no technical issues with FASP as a digestion technique and it was therefore adopted for digestion of all membrane fractions for optimization of the enrichment aspect of the workflow.

The disparity between plasma membrane annotations and predicted transmembrane proteins also reinforces the need to use multiple methods to infer the extent of membrane protein enrichment in a sample. In the first of the two FASP runs, 51 proteins were assigned a plasma membrane annotation by STRAP. Of these 51 proteins, only 4 were predicted to contain any transmembrane helices by TMHMM. Conversely, of the 6 proteins predicted to contain any transmembrane helices by TMHMM, only 4 were assigned a plasma membrane annotation by STRAP. However, the 2 transmembrane helix-containing proteins which were not assigned a plasma membrane annotation by STRAP were assigned annotations which could be reconciled with some other cellular membrane localization. This suggests that GO annotation overestimates membrane protein enrichment and sounds a note of caution about the automatic annotation of protein lists.

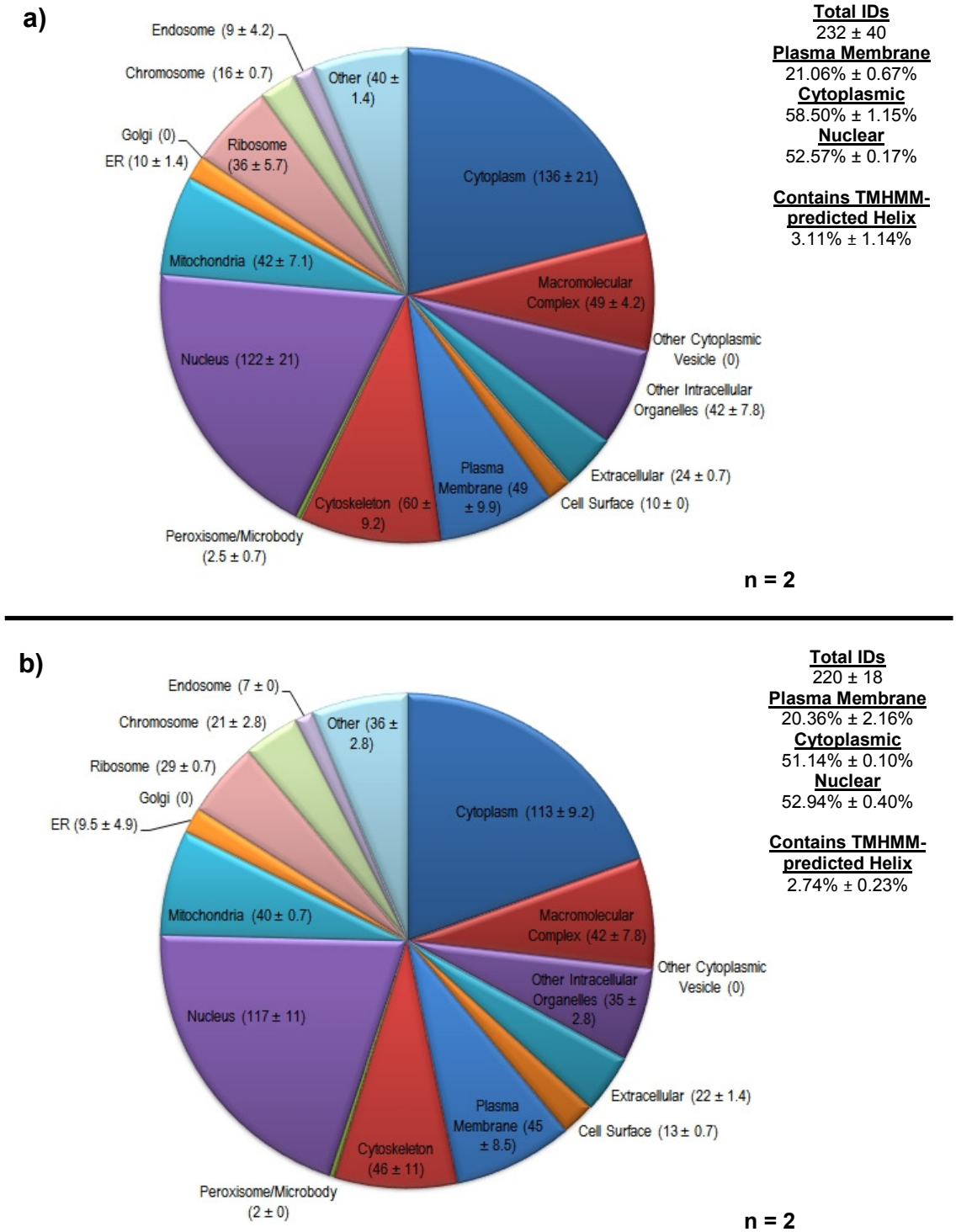

Figure 18: Pie charts illustrating the distribution of cellular component ontologies of proteins identified from LC-MS analysis of a Jurkat whole cell lysate digested using **a)** in-solution digestion; **b)** FASP. The number of total protein identifications; the percentages of total identifications with 'plasma membrane', 'cytoplasmic' and 'nuclear' annotation; and the percentage of proteins predicted to contain transmembrane domains by the TMHMM algorithm are also displayed. The similarities in total identifications and comparable distribution of ontologies suggest that both techniques perform comparably for digestion of whole cell lysates. N.B. many proteins have more than one cellular compartment GO annotation and hence the percentages reported here (and in subsequent pie chart figures) do not appear to tally with the corresponding slice of the pie chart and summate to more than 100%.

4.2.2.2. Use of 'EZ-Link™' Sulfo-NHS-SS-Biotin and RevAmine to enrich for plasma membrane proteins prior to LC-MS analysis produces only a small increase in percentage of plasma membrane protein IDs

FASP was designed to allow initial solubilisation of total lysate protein in high concentrations of detergent and to then permit quantitative depletion of the detergent from the protein solution prior to the introduction of enzyme digestion. For this to occur, it is imperative that the detergent is either diluted well below its CMC prior to digestion such that the majority of detergent passes through the MWCO filter in monomeric form; or that the molecular weight of the micelles is sufficiently small to enable their passage through the filter. Different detergents have different CMCs and monomeric / micellar molecular weights and consequently not all will be quantitatively depleted using the technique.

The Pierce Cell Surface Protein Isolation Kit contains proprietary detergent-based lysis and wash buffers, the constituents of which are commercially sensitive. It was therefore unclear whether any detergent carryover in the eluate fraction from the lysis and wash steps of the procedure would be depleted using FASP. In any event, the lysis and wash buffers are not sold separately and to purchase the entire kit merely to use the buffers was considered impractical. Our initial inclination was thus to substitute these proprietary buffers for SDS-based buffers.

Jurkat cells were incubated in the presence of EZ-Link™ Sulfo-NHS-SS-Biotin. Excess reagent was quenched and removed through extensive washing. Cells were lysed through addition of 0.1 M TRIS-HCl containing 1% (w/v), 2% (w/v) or 4% (w/v) SDS and lysates incubated for 1 hour in a spin column containing Neutravidin® resin. Wash and elution steps were performed using the buffer containing the same concentration of SDS which had been used to lyse the cells. Membrane fractions were digested using FASP and digests cleaned up and analysed as described in section **4.2.2.1.** Data processing, GO annotation and transmembrane domain prediction were also performed as previously described.

The distribution of cellular component GO annotations and percentage of proteins predicted to contain transmembrane domains by TMHMM for all

proteins identified in the membrane fractions processed using 1% (w/v) SDS, 2% (w/v) SDS and 4% (w/v) SDS are shown in **Figs. 19a-c** respectively. The fraction processed using 1% (w/v) SDS appears to exhibit a modest enrichment in membrane proteins, with both plasma membrane GO annotations and proteins predicted to contain transmembrane helices increased relative to the whole cell lysate data shown in section **4.2.2.1.** However, the salient observation from this particular set of experiments is the numbers of total protein identifications across the three samples. The fraction processed using 1% (w/v) SDS yields around half the identifications of either whole cell lysate digest; the fraction processed using 4% (w/v) SDS yields only a tenth the identifications. As detailed in section **4.1.3.**, there are reports that the avidin-biotin interaction can be formed and maintained in harsh conditions (including 1% SDS); though it might be expected that the harsher the conditions, the longer it would take for the initial interaction to form. The decreasing protein identifications observed with increasing concentrations of SDS is most likely due to decreased avidin-biotin binding and suggests increasing incubation times in the higher concentrations to allow for this.

a)

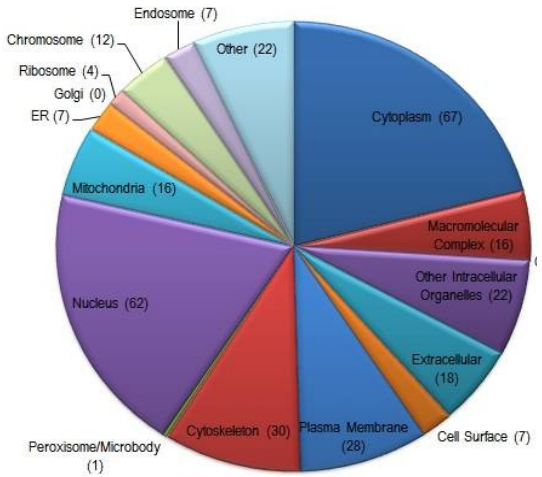

Total IDs
117
Plasma Membrane
23.93%
Cytoplasmic
57.26%
Nuclear
52.99%

Contains TMHMM-predicted Helix
5.98%

n = 1

b)

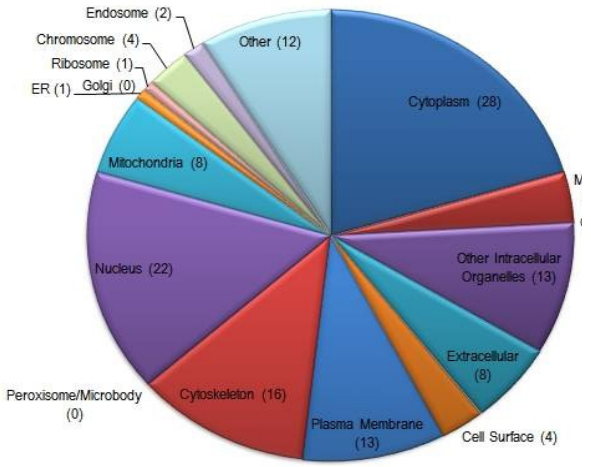

Total IDs
46
Plasma Membrane
28.26%
Cytoplasmic
60.87%
Nuclear
47.83%

Contains TMHMM-predicted Helix
4.35%

n = 1

c)

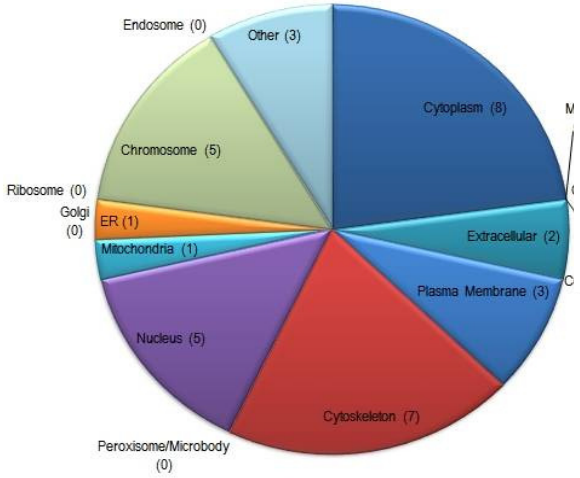

Total IDs
21
Plasma Membrane
14.29%
Cytoplasmic
38.10%
Nuclear
23.81%

Contains TMHMM-predicted Helix
4.76%

n = 1

Figure 19: Pie charts illustrating the distribution of cellular component ontologies of proteins identified from LC-MS analysis of Jurkat membrane fractions prepared using the Pierce Cell Surface Isolation Kit as per supplied protocol but with Pierce Lysis and Wash Buffers substituted for 0.1 M TRIS-HCl (pH 7.4) supplemented with **a)** 1% (w/v) SDS; **b)** 2% (w/v) SDS; **c)** 4% (w/v) SDS. Total protein identifications fall markedly with increasing concentrations of SDS, suggesting that the recommended conditions for avidin-biotin binding in the protocol may be suboptimal when SDS is used instead of the supplied buffers.

Given the observations in section **4.2.2.2.**, the experiment was repeated using different conditions. Cells were incubated in the presence of either EZ-Link^{TM} Sulfo-NHS-SS-Biotin or RevAmine. Unbiotinylated cells were also included as a control to examine the extent of non-specific binding to the NeutrAvidin® resin. Labelled and unlabelled cells were lysed with 0.1 M TRIS-HCl / 4% (w/v) SDS and lysates incubated with the resin overnight rather than for an hour. Wash and elution steps were also performed using this buffer. For comparison and to examine the compatibility of their use with FASP, labelled and unlabelled cells were also processed using the lysis and wash buffers included with the Pierce Kit as per the supplied protocol and eluted using 0.1 M TRIS-HCl / 4% (w/v) SDS. All membrane fractions were digested, cleaned up, analysed and annotated as described previously.

The distributions of cellular component GO annotations and percentage of proteins predicted to contain transmembrane domains by TMHMM for all identified proteins are shown in **Fig. 20** for the samples for which lysis and wash steps were performed using Pierce lysis and wash buffers and **Fig. 21** for the sample for which lysis and wash steps were performed using 4% (w/v) SDS. For each figure, data for unlabelled cells, cells labelled with EZ-Link^{TM} Sulfo-NHS-SS-Biotin and cells labelled with RevAmine are shown in subfigures **(a)**, **(b)** and **(c)** respectively.

The labelled fractions processed using the Pierce lysis and wash buffers both yield around a four-fold increase in total protein identification over the unlabelled control. Plasma membrane GO annotations and proteins predicted to contain transmembrane helices are increased relative to the whole cell lysate data shown in section **4.2.2.1.**, with the latter being increased over four-fold in the cells labelled with both EZ-Link^{TM} Sulfo-NHS-SS-Biotin and RevAmine. However, in both labelled fractions, cytoplasmic and nuclear protein annotations still dominate. The identification of so many non-membrane proteins in these supposedly membrane-enriched fractions was somewhat surprising given the design of the experimental technique.

The fraction labelled using EZ-Link^{TM} Sulfo-NHS-SS-Biotin and processed using 4% (w/v) SDS yields around a three-fold increase in total protein identification over the unlabelled control. Interestingly, plasma membrane GO annotations

here are actually decreased relative to those seen in the whole cell lysates but the proportion of proteins predicted to contain transmembrane helices is increased over three-fold. Of the 29 proteins assigned a plasma membrane annotation here, only 4 are predicted to contain a transmembrane helix; whilst of the 16 proteins predicted to contain a transmembrane helix, only 4 are assigned a plasma membrane GO annotation. This again suggests that there is currently no single method for comprehensive identification of plasma membrane proteins using proteomic datasets and so advocates the use of more than one means of assessing membrane enrichment.

The fraction labelled using RevAmine and processed using 4% (w/v) SDS yields 58 protein identifications, only 8 more than the unlabelled control for this particular set of experiments. This is in stark contrast to the RevAmine-labelled fraction processed with the Pierce lysis and wash buffers and was a little unexpected. The RevAmine tag is cleaved through high pH and presence of primary amines. TRIS contains a hindered primary amine and the TRIS-HCl / SDS buffer used for lysis and wash steps here is at physiological pH (pH 7.4). Nevertheless, it is possible that the longer incubation time with the resin is sufficient to cleave the RevAmine linker, causing biotinylated proteins to elute in the wash steps.

a)

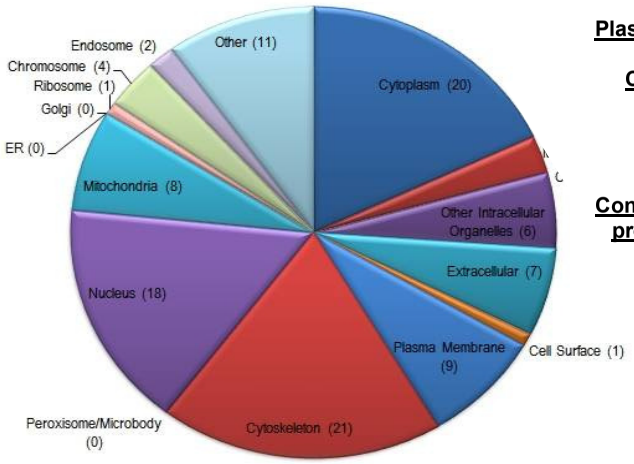

Total IDs
55
Plasma Membrane
16.36%
Cytoplasmic
36.36%
Nuclear
32.73%

Contains TMHMM-predicted Helix
3.64%

n = 1

b)

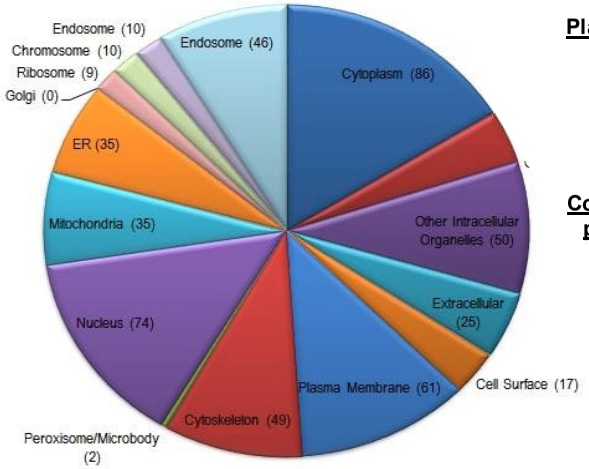

Total IDs
192
Plasma Membrane
31.77%
Cytoplasmic
44.79%
Nuclear
38.54%

Contains TMHMM-predicted Helix
14.06%

n = 1

c)

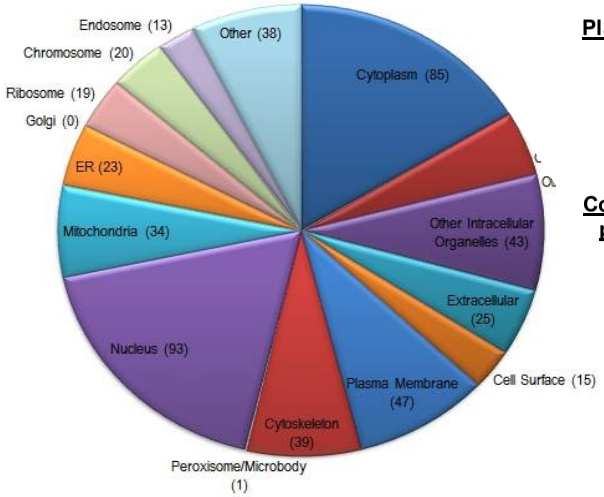

Total IDs
203
Plasma Membrane
23.15%
Cytoplasmic
41.87%
Nuclear
45.81%

Contains TMHMM-predicted Helix
13.30%

n = 1

Figure 20: Pie charts illustrating the distribution of cellular component ontologies of proteins identified from LC-MS analysis of **a)** unlabelled; **b)** EZ-Link^{TM}- labelled; **c)** RevAmine-labelled Jurkat membrane fractions prepared using the Pierce Cell Surface Isolation Kit as per supplied protocol (using Pierce Lysis and Wash Buffers). Increased total protein identifications relative to the unlabelled fraction are observed for both EZ-Link^{TM}- and RevAmine-labelled fractions. A modest enrichment of plasma membrane annotations over that of the whole cell lysates shown in **(Fig.9)** is seen in the RevAmine-labelled fraction; this enrichment is more pronounced in the EZ-Link^{TM}-labelled fraction.

a)

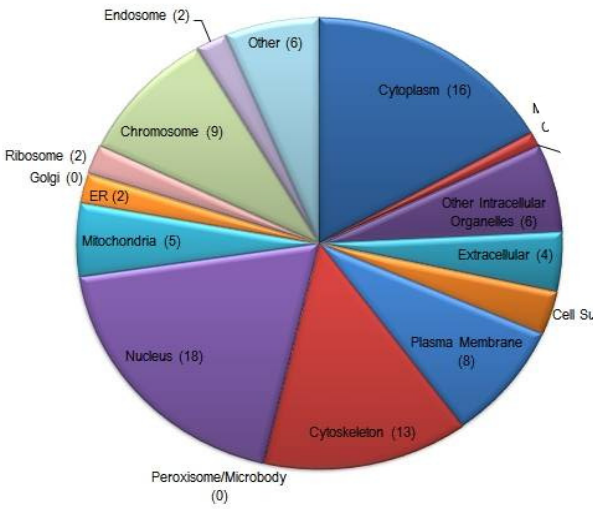

Total IDs
50
Plasma Membrane
16.00%
Cytoplasmic
32.00%
Nuclear
36.00%

Contains TMHMM-predicted Helix
4.00%

n = 1

b)

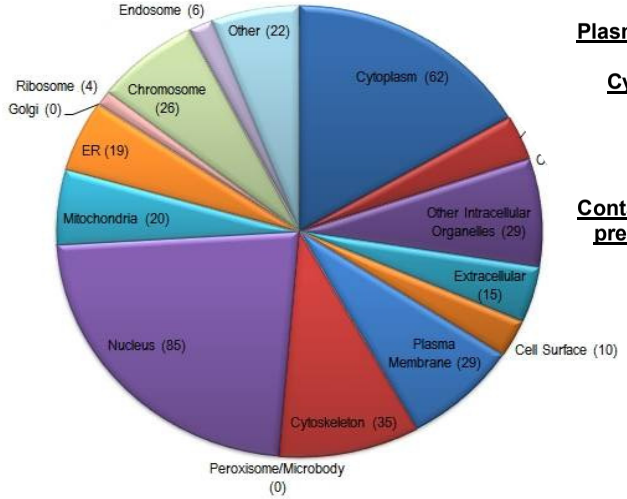

Total IDs
158
Plasma Membrane
18.35%
Cytoplasmic
39.24%
Nuclear
53.80%

Contains TMHMM-predicted Helix
10.13%

n = 1

c)

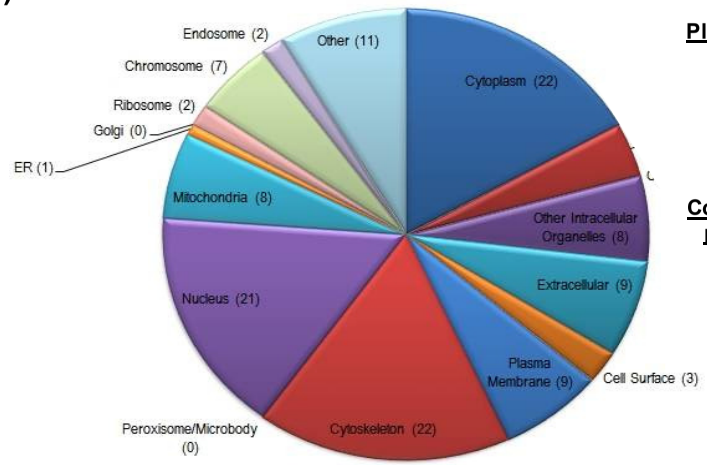

Total IDs
58
Plasma Membrane
15.52%
Cytoplasmic
37.93%
Nuclear
36.21%

Contains TMHMM-predicted Helix
6.90%

n = 1

Figure 21: Pie charts illustrating the distribution of cellular component ontologies of proteins identified from LC-MS analysis of **a)** unlabelled; **b)** EZ-Link™- labelled; **c)** RevAmine-labelled Jurkat membrane fractions prepared using the Pierce Cell Surface Isolation Kit with Pierce Lysis and Wash Buffers substituted for 0.1 M TRIS-HCl (pH 7.4) supplemented with 4% (w/v) SDS and increased incubation time for formation of the avidin-biotin interaction. Increased total protein identifications relative to the unlabelled control and the analogous fraction shown in **(Fig. 10c)** are observed for the EZ-Link™-labelled fraction. The increase in total protein identifications relative to the unlabelled control for the RevAmine-labelled fraction is negligible and no plasma membrane enrichment is observed over that of the whole cell lysates shown in **(Fig.9)**

4.2.2.3. The limited enrichment of plasma membrane proteins in membrane fractions prepared using cell surface biotinylation-based approaches is likely due to biotinylation of intracellular proteins

At this stage it was unclear why the majority of proteins detected in the cell surface biotinylation and affinity purification strategy being pursued were not of membrane origin. Given that biotinylation with EZ-Link™ Sulfo-NHS-SS-Biotin leaves a residual CAMthiopropanoyl moiety even after cleavage of the linker, we first mined the data from the EZ-Link™-modified membrane fractions for peptides detected with this modification and examined the nature of the proteins from which they were derived. These data are shown in **Table 3**.

			GO Annotations (% of Total Identifications)			
	Unique CAMthiopropanoylated Peptides	Unique CAMthiopropanoylated Proteins	Plasma Membrane	Cytoplasmic	Nuclear	TMHMM
Pierce Buffers	37	34	32.35%	50.00%	38.24%	8.82%
4% SDS	41	38	15.79%	23.68%	73.68%	7.89%

Table 3: Number of unique CAMthiopropanoylated peptides and proteins detected from membrane fractions prepared using EZ-Link™ Sulfo-NHS-SS-Biotin and processed with Pierce lysis and wash buffers and 4% (w/v) SDS respectively.

This suggested that only a small fraction of the biotinylated proteins detected in both fractions were of membrane origin and a substantial number of intracellular proteins were also being biotinylated. It is likely that many more proteins were biotinylated but modified peptides derived from these proteins were not detected. Nevertheless, these data are sufficient to call into question the membrane specificity of the labelling.

To investigate this further; fractions were collected from the affinity purification part of the procedure and analysed by SDS-PAGE. Unlabelled and EZ-Link™ Sulfo-NHS-SS-Biotin-labelled cells were processed using Pierce lysis and wash buffers, 1% (w/v) SDS and 4% (w/v) SDS. For each sample a fraction was collected immediately before affinity purification, immediately after affinity purification (the 'flow-through') and at the end of the procedure (the 'eluate'). All fractions were subsequently separated on a gel.

Fractions from the unlabelled cells are shown in **Fig. 22a**, whilst fractions from the EZ-Link™ Sulfo-NHS-SS-Biotin-labelled cells are shown in **Fig. 22b**. Each gel is divided into three segments with three lanes in each segment. The lysates in the first segments were generated and processed using the Pierce lysis and wash buffers supplied with the kit; the lysates in the second and third segments were generated and processed using 1% (w/v) SDS and 4% (w/v) SDS respectively. In each segment, lane **(1)** is unprocessed lysate; lane **(2)** is the 'flow-through' fraction of the affinity purification; and lane **(3)** is the 'eluate fraction' of the affinity purification. The banding patterns in every third lane in **Fig. 22b** bear a striking resemblance to the banding patterns in the corresponding first and second lanes; this is particularly notable for the lysates processed using SDS. In contrast, no bands are seen in the third lanes in **Fig. 22b**. This indicates that the proteins seen in the eluate fractions of the labelled lysates are being specifically enriched and are likely biotinylated. The similar banding patterns in all lanes of **Fig. 22b** suggest that biotinylation in the labelled cells is not restricted to the cell membranes; rather it is disseminated throughout the cell.

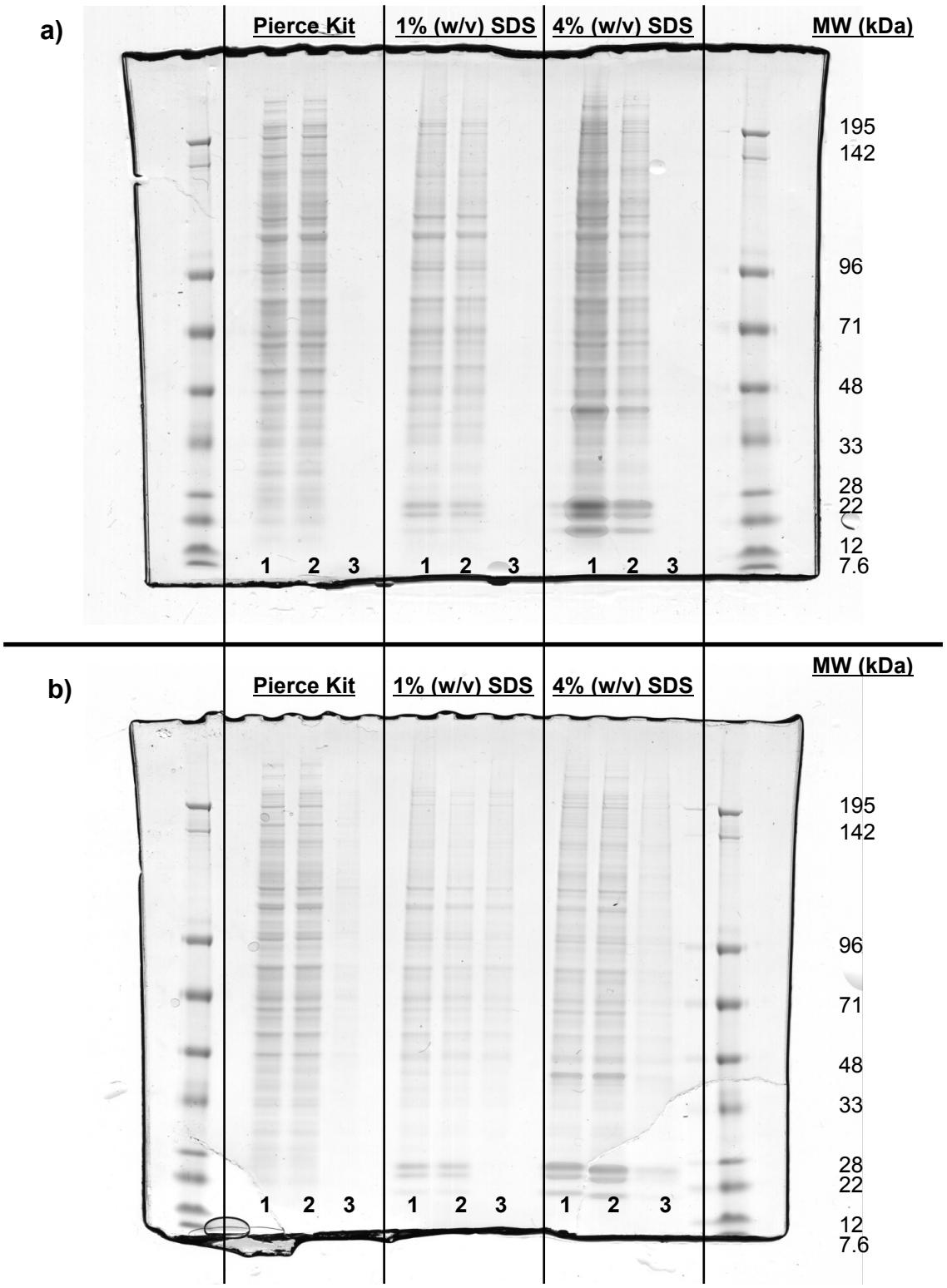

Figure 22: Polyacrylamide gel electrophoresis of unprocessed, flow-through and eluate fractions of **a)** unlabelled Jurkat cell lysate; **b)** EZ-Link™-labelled Jurkat cell lysate processed using the Pierce Cell Surface Isolation Kit as per supplied protocol. Each gel is divided into three segments with three lanes in each segment. The lysates in the first segments were generated and processed using the Pierce buffers supplied with the kit; the lysates in the second and third segments were generated and processed using 1% (w/v) SDS and 4% (w/v) SDS respectively. In each segment, lane **(1)** is unprocessed lysate; lane **(2)** is the affinity purification 'flow-through' fraction; and lane **(3)** is the affinity purification 'eluate fraction'. All gels were stained with colloidal Coomassie.

The fluorescence confocal microscopy experiments described in section **1.2.1.3.** add further weight to the intracellular biotinylation hypothesis. In carrying out these experiments, individual cells labelled with both reagents were occasionally observed for which fluorescence was considerably more intense than that seen in surrounding cells and not restricted to the plasma membrane **(Fig. 23)**. Pierce states that the sulfonate group of EZ-Link^{TM} NHS-SS-Sulfo-Biotin prevents it from permeating cell membranes. However, this does not preclude the possibility of the reagent being able to cross the membranes of cells in which the plasma membrane is already compromised in some way, for instance cells in late stages of apoptosis (Arends and Wyllie, 1991).

As discussed in section **1.1.3.2.**, transmembrane proteins constitute 20 – 30% of all proteins encoded by the genome (Kanapin *et al.*, 2003) but only around 2% of the total cellular protein content by weight (Rahbar and Fenselau, 2004). In contrast, actin alone accounts for 1 – 5% of total cellular protein content (a liver cell typically expresses around 20,000 insulin receptors but around half a billion actin molecules (Lodish *et al.*, 2000)). The most abundant cytoplasmic, cytoskeletal and nuclear proteins are likely present in copy numbers many orders of magnitude greater than plasma membrane proteins. For mass spectrometric purposes, even intracellular biotinylation of a select few cells in a larger population may thus be sufficient to effectively negate any enrichment achieved through membrane-specific biotinylation of the rest of the cells.

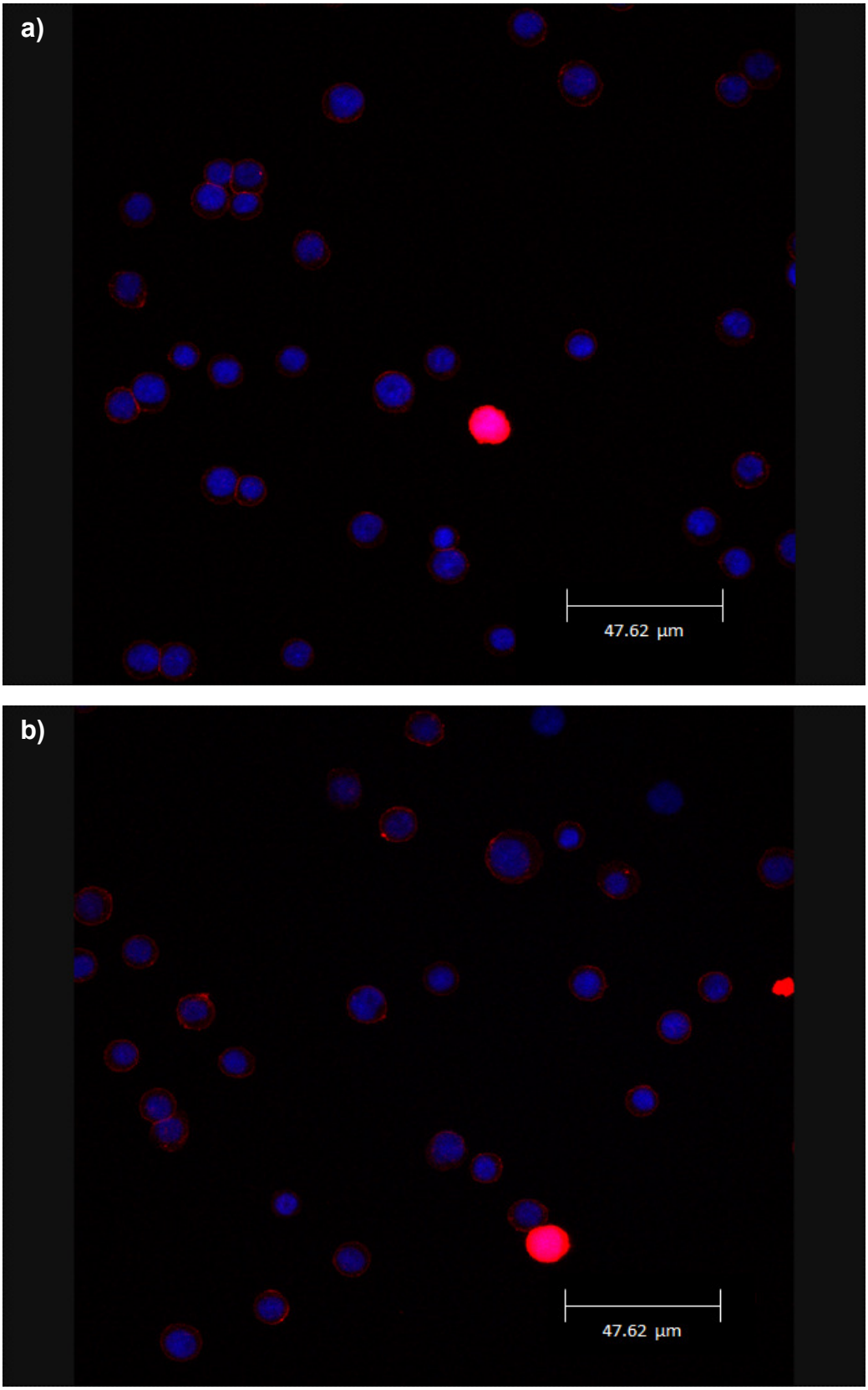

Figure 23: *In situ* biotinylation of cell surface-exposed primary amine residues on Jurkat cells detected through staining with a Streptavidin – Alexa Fluor 568 conjugate followed by fluorescence confocal microscopy. **a)** EZ-Link™-labelled cells. **b)** RevAmine-labelled cells. All cells were also stained with DAPI prior to imaging. The strongly fluorescing cells in both images appear to be biotinylated intracellularly, suggesting that both tags can permeate the plasma membrane in some instances.

4.2.3. Evaluation of the suitability of subcellular fractionation protocols for enrichment of cell surface proteins for analysis by mass spectrometry.

4.2.3.1. Crude membrane preparations processed using sequential extraction in high salt, high pH and urea-containing buffers yield a more significant increase in percentage of membrane protein IDs

In spite of the considerable theoretical promise of the RevAmine reagent, it was decided given the findings above to pursue alternative means of membrane protein enrichment. Intracellular biotinylation appeared to be posing a considerable problem in the Jurkat cell line used for the experiments described in section **4.2.2.** in spite of consistently high viability (> 95%). It was reasoned that this problem would only be exacerbated in primary cultures of mature and tolerogenic DCs, the viability of which is frequently lower simply as a result of the culture conditions. Performing some sort of crude preparation of biotinylated membranes prior to affinity purification was considered, but this had previously been reported to have little effect over and above simply following the protocol supplied with the Pierce kit (Weekes *et al.*, 2010). A further concern in the context of the overall workflow was the considerable amount of parallel processing required were a cell surface biotinylation-based strategy to be used.

Membrane proteins are evidently present in a whole cell lysate solubilised in SDS. They are merely much harder to detect given the relative complexity of the mixture and owing to the presence of more abundant protein species. However, with recent advances in the resolving power of chromatographic separations and in the accuracy, resolution and speed of modern mass spectrometers mean that with state-of-the-art-equipment it is now feasible to identify > 5000 proteins (over half the expressed proteome) from a mammalian whole cell lysate in a single LC-MS run (Thakur *et al.*, 2011).

These technological advances are exemplified by the progression of membrane enrichment procedures employed by Matthias Mann's lab from a protracted 'classical' density gradient centrifugation-based procedure (Olsen *et al.*, 2004) to a simpler 'stepwise depletion of non-membrane molecules' procedure, comprising sequential extraction of crude membrane pellets with high salt, high

pH and urea-containing buffer (Wisniewski *et al.*, 2009a). Using the latter method in conjunction with FASP and peptide fractionation prior to analysis enabled the identification of 4206 unique proteins from a single murine hippocampus, 64% of which had a membrane annotation (though only 25% of which had a plasma membrane annotation). The classical technique enabled identification of 355 unique proteins, around 20% of which had a plasma membrane annotation. The two studies are not directly comparable. The earlier study did not employ any peptide fractionation prior to LC-MS and the peptides were isotopically labelled prior to analysis, but the greater than ten-fold increase in unique proteins identified in the latter study serves to illustrate that membrane preparations need not be extremely pure for identification of appreciable numbers of plasma membrane proteins with modern LC-MS instrumentation.

Using this observation as a starting point, we attempted to recapitulate the 'stepwise depletion' method described by Wisniewski *et al.* The original method was conceived to extract membranous material from whole tissue, and samples are completely homogenized in all extraction steps. The first step comprises initial homogenization of tissue in high salt buffer. This serves to deplete the majority of water-soluble proteins, disrupting even very strong ionic bonds between DNA and histones (Burton *et al.*, 1978). This is followed by three extractions in high pH buffer, the purpose of which is to convert closed membrane vesicles to open membrane sheets and release soluble proteins sequestered within these vesicles (Fujiki *et al.*, 1982). A final extraction in 4 M urea causes the majority of protein domains to unfold whilst preserving the integrity of transmembrane helices, allowing weakly membrane-associated proteins to be removed (Wisniewski, 2009).

Wisniewski *et al.* place much emphasis upon using a high speed blender to facilitate complete sample homogenization at all stages of the procedure, though this is likely due to the fact that the starting material is tissue in all studies in which it has been employed. We did not have access to a high speed blender but intended to apply the method to suspension cell cultures. It was originally recommended that cells be lysed with a Dounce homogenizer and nuclei pelleted before proceeding with the first extraction step (J. R. Wisniewski, personal communication).

Therefore, the first iteration of the 'stepwise depletion' membrane enrichment strategy as applied to Jurkat cells consisted of Dounce homogenisation in hypotonic lysis buffer and centrifugation at 1000*g* to pellet nuclei. The resulting supernatant was subsequently rendered hypertonic and stepwise depletion carried out as described in section **3.2.4.** Cellular component GO annotations and percentage of TMHMM-predicted transmembrane proteins for all proteins identified using this strategy are shown in **Fig. 24a**. The percentage of proteins predicted to contain transmembrane helices here is enriched over three-fold relative to the whole cell lysate data shown in section **4.2.2.1.**, but the percentage of plasma membrane GO annotations does not increase. This is perhaps to be expected given that this particular means of membrane preparation does not specifically enrich for plasma membranes but rather all cellular membranes. Nevertheless, the enrichment figures do not stand up to those seen for cell surface biotinylation with EZ-Link^{TM} Sulfo-NHS-SS-Biotin and processing with Pierce lysis and wash buffers in **Fig. 20b**.

It was noted during the above experiment that the membranes were not pelleting particularly well at the speed suggested by Wisniewski *et al*. and were adhering to the side of the microcentrifuge tubes used, making the high pH and urea extraction steps problematic. The second iteration of this strategy thus substituted standard microcentrifuge tubes for siliconized microcentrifuge tubes and made use of a microcentrifuge with a slightly higher top speed. All other aspects of the strategy remained constant. These adjustments allowed the membranes to be pelleted and extracted more effectively and yielded an increase in percentage of plasma membrane GO annotations from approximately 21% to approximately 28% and a small increase in the percentage of transmembrane helix- containing proteins **(Fig. 24b)**. However, both figures still failed to match those seen in **Fig. 20b**.

A possible explanation for the limited enrichment in the first two iterations of the stepwise depletion method is the means of homogenization. Douncing lyses cells through the shear forces created between the sides of the 'mortar' and 'pestle' as the latter is moved in and out within the former. Cells moving past the pestle are broken apart by these forces. A pestle is normally selected with adequate clearance to lyse cells whilst leaving nuclei intact, ensuring the homogenate is not contaminated with DNA and allowing relatively clean

separation of nuclear material. The vast majority of publications advocate centrifugation for 5 – 10 minutes at 1000*g* to pellet nuclei. However, there are suggestions that spinning at this speed will also pellet plasma membrane material (Wolff *et al.*, 1989), an undesirable outcome in this particular instance. Research in the Lamond lab encompasses nucleolar proteomics and thus they have a vested interest in obtaining pure nuclear pellets. This group uses a considerably slower centrifugation to separate nuclei from the rest of the homogenate (228*g*). It is possible that a 1000*g* nuclear spin may pellet larger membrane fragments in addition to nuclei.

We next explored whether there was any way of replicating the effects of the blender used by Wisniewski *et al.* for sample homogenization without having to incur the considerable expense of the instrument itself. The blender utilizes rotor-stator homogenization to disrupt samples. The QIAshredder column (used principally for clarifying lysates in preparation for RNA extraction) is composed of a biopolymer shredding system housed within a microcentrifuge spin column and applies similar rotor-stator forces to samples as they pass through. We were informed that the columns were not suitable for disruption of intact cell and tissue but could be used to homogenize crude lysate (Qiagen, personal communication). The third iteration of the stepwise depletion strategy therefore substituted Dounce homogenization with a freeze-thaw lysis step followed by passage of this lysate through a QIAshredder column, since this eliminated any differential centrifugation steps in the initial homogenization where membrane material could be lost.

Cellular component GO annotations and percentage of TMHMM-predicted transmembrane proteins for all proteins identified using this third iteration are shown in **Fig. 24c**. Of all the membrane enrichment strategies examined, this yielded the highest percentages of plasma membrane GO annotations (two-fold enrichment over a whole cell lysate) and predicted transmembrane domain-containing proteins (twelve-fold enrichment over a whole cell lysate). Encouragingly, this is also the only strategy examined where plasma membrane GO annotations actually exceed cytoplasmic and nuclear GO annotations. This was thus chosen as the preferred membrane enrichment strategy to use in the context of the wider workflow.

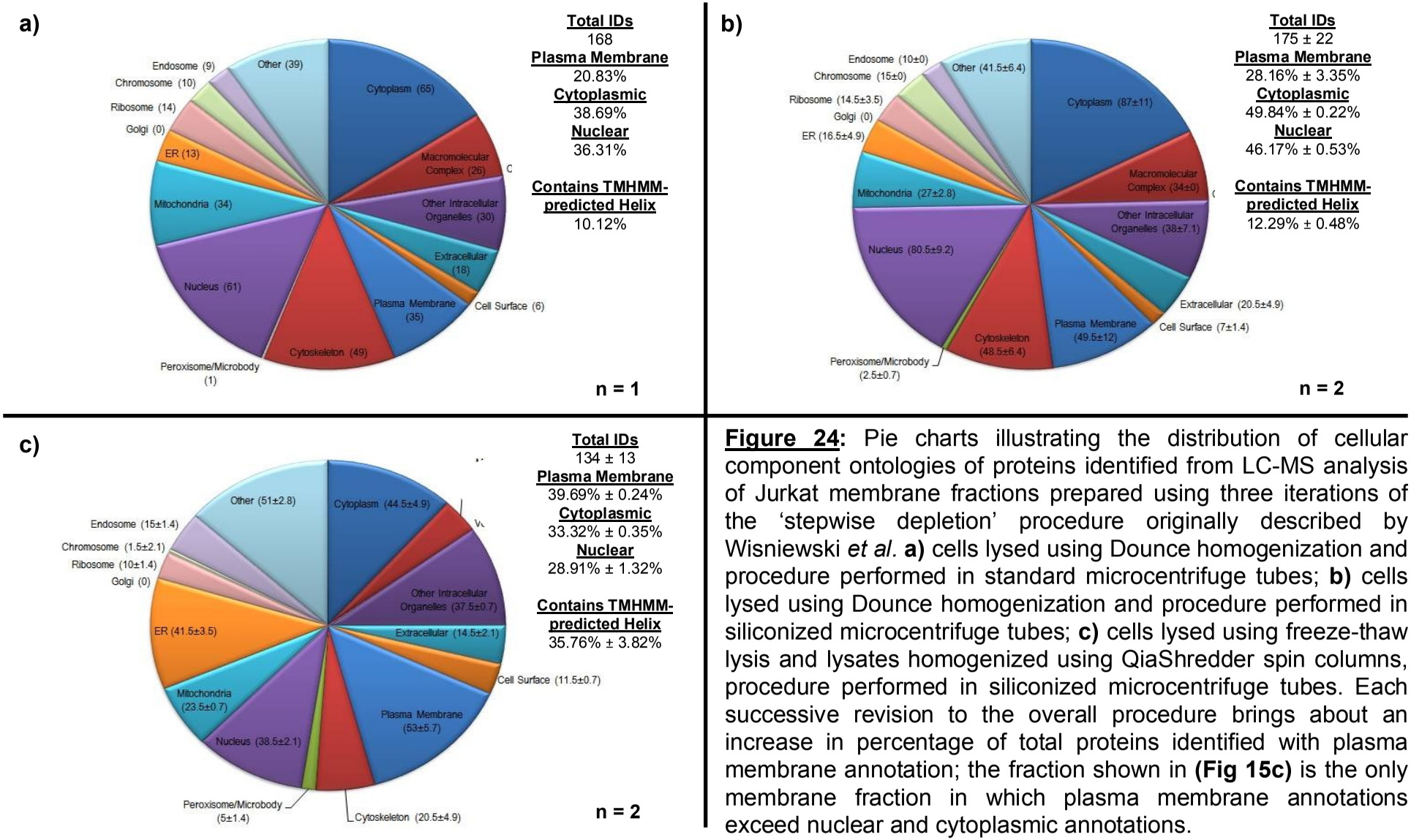

Figure 24: Pie charts illustrating the distribution of cellular component ontologies of proteins identified from LC-MS analysis of Jurkat membrane fractions prepared using three iterations of the 'stepwise depletion' procedure originally described by Wisniewski *et al.* **a)** cells lysed using Dounce homogenization and procedure performed in standard microcentrifuge tubes; **b)** cells lysed using Dounce homogenization and procedure performed in siliconized microcentrifuge tubes; **c)** cells lysed using freeze-thaw lysis and lysates homogenized using QiaShredder spin columns, procedure performed in siliconized microcentrifuge tubes. Each successive revision to the overall procedure brings about an increase in percentage of total proteins identified with plasma membrane annotation; the fraction shown in **(Fig 15c)** is the only membrane fraction in which plasma membrane annotations exceed nuclear and cytoplasmic annotations.

4.2.3.2. Filter-Aided Sample Preparation (FASP) performs more effectively than standard in-solution digestion for processing of crude membrane fractions prepared using 'stepwise depletion' for LC-MS analysis

As detailed in section **4.2.2.1.**, FASP and in-solution digestion perform comparably for digestion of whole cell lysates. With a preferred membrane enrichment strategy now in place, the final question was whether FASP was indeed a superior means of digesting membrane proteins. This question was addressed by digesting membrane fractions prepared via stepwise depletion using the standard lab in-solution digestion protocol. Cellular component GO annotations and percentage of TMHMM-predicted transmembrane proteins for all proteins identified from this in solution digestion are shown in **Fig. 25b**. The in-solution digestion was not carried out concomitantly with the FASP digestion described in section **4.2.3.1**, but both digests were performed on aliquots of the same membrane-enriched fraction. As such, the analogous FASP digestion data shown in **Fig. 24c** is duplicated in **Fig. 25a** for comparison.

Though this in-solution digestion does yield a discernible enrichment in plasma membrane GO annotations and predicted transmembrane proteins above that of a whole cell lysate, it is not as pronounced as that seen for FASP digestion of the same material. This could be due to the acetone precipitation step employed to deplete lipids from the membrane fraction prior to digestion. Such a step is not necessary in FASP as the lipids are quantitatively depleted during the urea washes whilst the proteins are kept in solution. It is also possible that the membrane protein component does not resolubilize as well as the soluble protein complement having been precipitated and is thus less effectively digested.

In conclusion, stepwise depletion (with shredding) followed by FASP was chosen as the preferred membrane protein enrichment and digestion strategy to incorporate into the wider proteomic workflow.

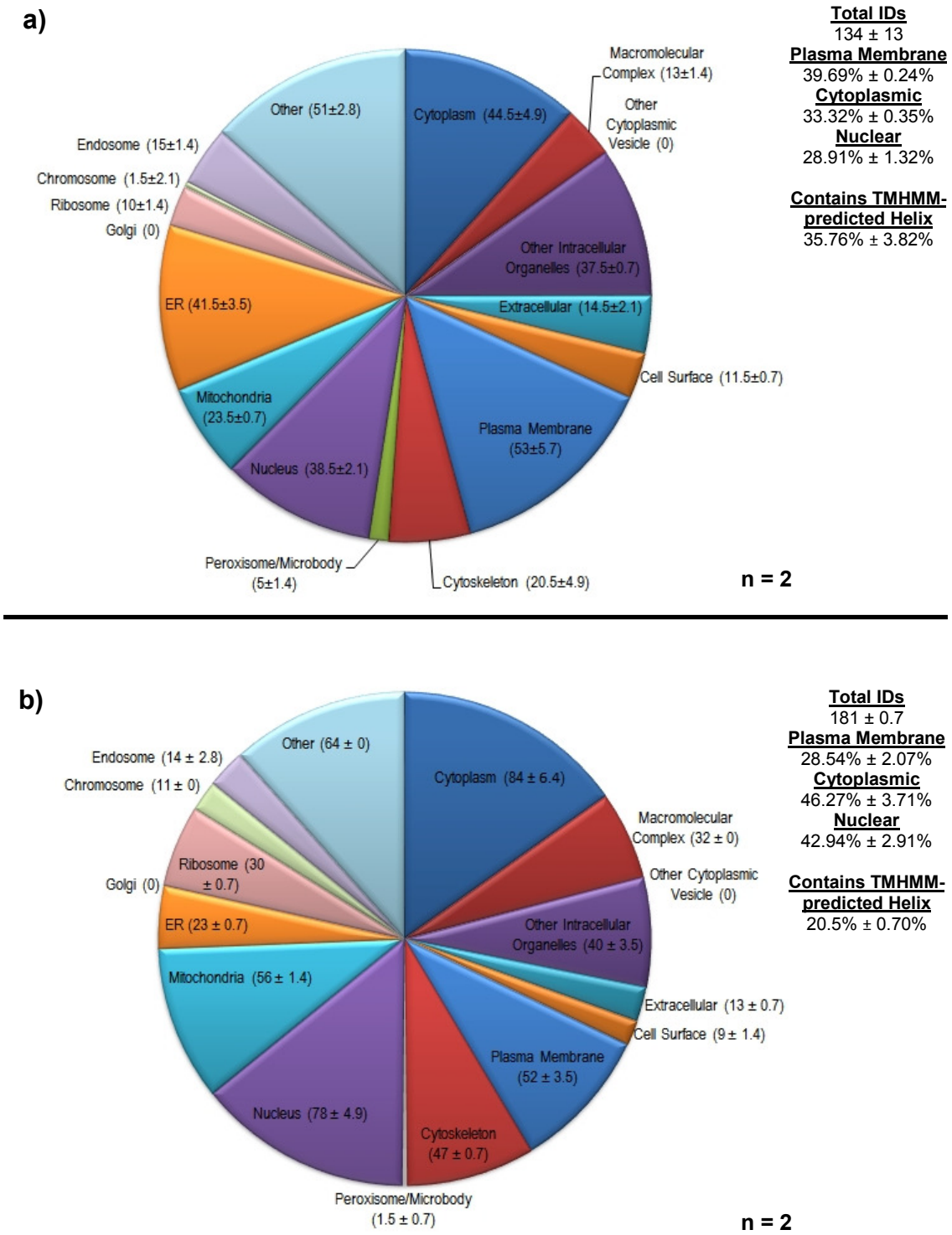

Figure 25: Pie charts illustrating the distribution of cellular component ontologies of proteins identified from LC-MS analysis of Jurkat membrane fractions prepared using the 'stepwise depletion' procedure and digested using **a)** FASP; **b)** In-solution digestion.

4.3. Discussion

The overall aim of the work presented in this chapter was to optimize a membrane enrichment and digestion strategy which could subsequently be used as the first stage of a wider proteomics workflow to enable relative quantitation of significant numbers of membrane proteins between mature and tolerogenic DCs.

The originally intended endpoint was that the enrichment step of this strategy would incorporate RevAmine, a novel and traceless amine-directed biotinylation reagent; validating its suitability for use in large scale proteomic applications whilst concomitantly addressing issues with comparable commercially available reagents which do not exhibit this traceless behaviour. RevAmine has been shown to exhibit all the desirable chemical characteristics that it was originally conceived to: it covalently modifies primary amine residues on peptides and proteins and can be tracelessly removed from both, via treatment with dilute base.

It is less clear whether RevAmine is suitable for enrichment of cell surface proteins for mass spectrometry-based proteomic applications. This uncertainty is not an indictment of the RevAmine reagent in particular, but appears to be symptomatic of a more universal issue affecting amine-directed biotinylation reagents when employed for this purpose. RevAmine and the commercially available EZ-Link^{TM} Sulfo-NHS-SS-Biotin have both been shown to specifically label surface exposed amine residues on viable Jurkat cells. However, limited membrane permeability has also been observed when using both reagents and mass spectrometric identification of biotinylated intracellular proteins was demonstrated using the latter. This has been reported previously. (Luo *et al.*, 2009; Weekes *et al.*, 2010) The negatively charged sulfonate group of EZ-Link^{TM} Sulfo-NHS-SS-Biotin should preclude its passage through an intact plasma membrane, thus the above observations appear to indicate that populations of cells labelled using reagents of this kind must be 100% viable to preclude intracellular protein labelling.

Interestingly, there are relatively few published studies which utilize EZ-Link^{TM} Sulfo-NHS-SS-Biotin and/or the Pierce Cell Surface Isolation Kit in the context of a mass spectrometry-based membrane proteomic workflow. Of those which

do, a couple note comparable contamination of membrane fractions with non-membrane proteins to that seen here (Faca *et al.*, 2008; Garcia *et al.*, 2009). Two of the studies which reported plasma membrane protein IDs as constituting the majority of total protein IDs performed a crude membrane preparation prior to affinity purification (Peirce *et al.*, 2004; Zhao *et al.*, 2004). However, attempts to replicate the enrichment seen in the second of these studies proved unsuccessful; with plasma membrane protein IDs making up less than 20% of total protein IDs (Weekes *et al.*, 2010). One further study uses the reagent to biotinylate cell surface proteins of the protozoan parasite *Trichomonas vaginalis* (de Miguel *et al.*, 2010). Post-labelling, a crude membrane entrapment using avidin is performed and biotinylated proteins are digested on the resin, with the peptides being collected in the eluate. The authors claim that this approach enables the identification of 411 parasite proteins, 35% of which have a putative membrane annotation based on homology of conserved domains with membrane proteins in other organisms and a further 28% of which are unique to *T. vaginalis* and possess predicted transmembrane domains. However, it is not clear why this on-resin digestion strategy was pursued since it somewhat negates the reversible properties of the tag. On-resin digestion would likely result in significant contamination of peptides from enriched proteins with avidin and biotin peptides.

In summary, novel amine-directed biotinylation reagents such as RevAmine theoretically offer considerable promise in facilitating cell surface proteome enrichment for mass spectrometry-based proteomic applications; although their practical use in this regard is still very much in its infancy. Considerable further work is likely necessary to realize this potential and this is presently an area of investigation for our lab.

In order to realize the overall aims of this project, an alternative means of membrane protein enrichment was subsequently explored, entailing stepwise depletion of non-membrane molecules from crude membrane extract prior to digestion. This strategy lacked the novelty of membrane tagging with enrichment; and theoretically would not be expected to provide such a specific enrichment of plasma membrane proteins; nonetheless it has been shown to deliver the enrichment and identification of large numbers of membrane-

annotated proteins. Another of its appeals was its relative simplicity, an important consideration in the context of the wider workflow.

The final optimized stepwise depletion strategy yielded the most significant enrichment of plasma membrane GO annotations and proteins predicted to contain transmembrane helices of any strategy explored in this body of work. Whilst the total numbers of identified proteins (and thus numbers of proteins identified with plasma membrane annotation) do not approach those reported by Wisniewski *et al*., when combined with FASP, the percentage of plasma membrane annotations observed actually exceed those reported in the published study (approx. 40% vs approx. 26% for a single LC-MS run). The disparities in total identifications are likely due to the substantially longer LC gradient used in the published study (240 minutes) and differences in instrumentation (LTQ-Orbitrap capable of scanning twice as quickly).

It is difficult to compare the effectiveness of this particular enrichment and digestion strategy with the effectiveness of those already published, as there are a great many variables at play. In addition to the numerous combinations of enrichment, solubilization and digestion strategies which can be assembled as a single cohesive workflow, additional variability is imparted through different sample types, use of different instrumentation and LC-MS methods and different suites of bioinformatics tools used to assess enrichment. In short, there exists no recognized standard means of evaluating membrane preparation methods for mass spectrometry-based proteomics. It is however not unreasonable to posit on the basis of the work presented here that the initial enrichment step probably has the greatest influence on the percentages of membrane proteins identified by LC-MS. When FASP and in-solution digestion were compared for digestion of whole cell lysate in section **4.2.2.1.**, plasma membrane gene annotations and percentages of proteins predicted to contain transmembrane helices were essentially identical (and low). When the same two techniques were compared for digestion of membrane fractions prepared using stepwise depletion in section **4.2.3.2.**, plasma membrane gene annotations and percentages of proteins predicted to contain transmembrane helices differed between the two digestion techniques, but both techniques allowed for significantly higher membrane protein identification than when either was used for digestion of whole cell lysates.

Bearing this in mind, a selection of publications covering the main methods used for membrane enrichment and reporting high percentages of membrane protein identification inferred using various bioinformatics tools were chosen for comparison (Durr *et al.*, 2004; Zhao *et al.*, 2004; Cao *et al.*, 2006; Zhang *et al.*, 2007; Lee *et al.*, 2009; Wisniewski *et al.*, 2009a; de Miguel *et al.*, 2010). Where supplementary raw protein identification data was provided with these publications, the data were parsed and IDs mapped to Uniprot accession numbers where necessary. GO annotation and transmembrane domain prediction was then performed on these datasets in exactly the same way as before. These comparative data are summarized in **Table 4**.

Ref.	Membrane Enrichment Strategy	Origin of Sample	Reported Total IDs	Reported Enrichment	Inferred By	# IDs Mapped to Uniprot	% Plasma Membrane (STRAP GO)	% TMH (TMHMM)
Durr *et al.* (2004)	1. Cationic Colloical Silica Sedimentation	Rat Lung Microvascular Endothelial Cells	450	81% (60%*) PM	NCBI/Swissprot Annotation, TMHMM	299	36% (34%*)	20%
Zhao *et al.* (2004)	1. Cell surface biotinylation with EZ-Link™ Sulfo-NHS-SS-Biotin 2. Affinity enrichment with magnetic streptavidin beads 3. Depletion of membrane-associated proteins from beads with high salt / high pH washes	Human Lung Cancer Cell Line	898	67% (59%*) IMPs	NCBI Annotation, SOSUI, presence of protein-lipid modification motifs	623	45% (42%*)	38%
Cao *et al.* (2006)	1. Sucrose density gradient centrifugation 2. Aqueous two-phase partitioning	Rat Liver	428	67% (48%*) IMPs	GO Annotation	378	31% (23%*)	30%
Zhang *et al.* (2007)	1. Immunoaffinity purification using secondary antibody superparamagnetic beads	Mouse Liver	248	67% PM & PM-associated	GO Annotation	356**	16% (14%*)	19%

* Reported enrichment if all identified proteins are taken into account rather than those with cellular compartment GO annotation

** Many IPI numbers appear to have mapped to more than one Uniprot identifier in this study.

Table 4: Comparison of reported percentages of membrane protein identifications with percentages of membrane protein identifications computed from STRAP GO annotation and TMHMM transmembrane helix predication of protein lists supplied in supplementary data in publications citing high levels of membrane protein enrichment through various strategies.

Ref.	Membrane Enrichment Strategy	Origin of Sample	Reported Total IDs	Reported Enrichment	Inferred By	# IDs Mapped to Uniprot	% Plasma Membrane (STRAP GO)	% TMH (TMHMM)
Lee *et al.* (2009)	1. Differential centrifugation 2. Sodium carbonate extraction	Rat Liver	195	48% Membrane	GO Annotation, TMHMM	153	20% (17%*)	25%
	1. Differential centrifugation 2. Sodium carbonate extraction 3. Aqueous two-phase partitioning		245 (192**)	77% Membrane		163	22% (17%*)	59%
	1. Differential centrifugation 2. Sodium carbonate extraction 3. Aqueous two-phase partitioning 4. Lectin affinity chromatography		423 (271**)	65% Membrane		205	28% (22%*)	43%
	1. Differential centrifugation 2. Sodium carbonate extraction 3. Aqueous two-phase partitioning 4. Hydrazide chemistry		367 (273**)	81% Membrane		223	18% (13%*)	52%

* Reported enrichment if all identified proteins are taken into account rather than those with cellular compartment GO annotation

** The numbers of protein IDs in the supplementary information supplied with this publication do not tally with reported numbers of protein IDs in the manuscript itself

Table 4 (cont.): Comparison of reported percentages of membrane protein identifications with percentages of membrane protein identifications computed from STRAP GO annotation and TMHMM transmembrane helix predication of protein lists supplied in supplementary data in publications citing high levels of membrane protein enrichment through various strategies.

Ref.	Membrane Enrichment Strategy	Origin of Sample	Reported Total IDs	Reported Enrichment	Inferred By	# IDs Mapped to Uniprot	% Plasma Membrane (STRAP GO)	% TMH (TMHMM)
Wiśnieski *et al*. (2009)	1. Stepwise Depletion	Mouse Hippocampus	4206	64% (55%*) Membrane; 44% (38%*) IMPs; 25% (22%*) PM	GO Annotation (MaxQuant)	4137***	32% (29%*)	39%
de Miguel *et al*. (2010)	1. Cell surface biotinylation with EZ-Link™ Sulfo-NHS-SS-Biotin 2. Affinity enrichment with streptavadin-sepharose resin 3. Extensive washing with buffers containing high concetrations of urea, SDS, NaCl and organic solvent; followed by on-resin digestion	*Trichomonas vaginalis*	411	63% Membrane	*Trichomonas* genome analysis, TMD prediction (algorithm not stated)	386	N/A**	63%

* Reported enrichment if all identified proteins are taken into account rather than those with cellular compartment GO annotation
** No T. vaginalis Uniprot IDs were assigned a plasma membrane GO annotation by STRAP.
*** Of the 4206 proteins identified in this study, only 4137 had a Uniprot identifier

Table 4 (cont.): Comparison of reported percentages of membrane protein identifications with percentages of membrane protein identifications computed from STRAP GO annotation and TMHMM transmembrane helix predication of protein lists supplied in supplementary data in publications citing high levels of membrane protein enrichment through various strategies.

The disparities between percentages of membrane proteins reported in the publications summarised in **Table 4** and the percentages reported when the raw data are reanalysed using STRAP GO annotation and TMHMM transmembrane helix prediction should not be taken at face value. Some discrepancies in the data are likely to be introduced by mapping the protein lists to Uniprot identifiers. For the majority of studies, some data are lost during this mapping but in one of the studies a significant number of additional IDs appear after mapping. This imperfect mapping has previously been reported when converting international protein index (IPI) numbers to Uniprot identifiers (Griss *et al.*, 2011). In addition, different programmes may annotate lists of Uniprot identifiers differently. In the original 'stepwise depletion' publication, GO annotation was performed within MaxQuant and 25% of proteins with a cellular compartment GO annotation are reported to have a plasma membrane GO annotation. When the same dataset is annotated using STRAP, 32% of proteins with a cellular compartment GO annotation are reported to have a plasma membrane GO annotation. This discrepancy cannot be explained away by ID mapping since the Uniprot identifiers from the original study were fed directly into STRAP; though it is possible that more proteins have been assigned plasma membrane GO annotations in the interim.

Nevertheless, this undertaking does reveal some interesting presentation 'quirks'. Firstly, many studies report percentages of membrane protein annotations as a fraction of total proteins which have a cellular component annotation, which often embellishes the final percentage somewhat. One of the studies classifies proteins which have a protein-lipid modification motif as integral membrane proteins despite these motifs being indicative of modifications such as glycosylphosphatidylinositol (GPI)-anchors. However, even taking this into account, the percentages of proteins with a STRAP plasma membrane GO annotation and at least one TMHMM-predicted transmembrane α-helix are frequently lower than the percentages reported in the publications. It is not apparent why this is so, and it is particularly perplexing for those studies where high percentages of integral membrane proteins are reported but analysis of the protein lists with TMHMM generates considerably lower percentages. There is a clear imperative to standardise the way in which

membrane enrichment is reported to enable unbiased comparison between published studies.

Overall, the membrane enrichment and digestion strategy presented here certainly appears to stand up to many previously published strategies when the data from these studies are analysed in the same manner as our own data.

Chapter 5. Development and validation of an isobaric peptide termini labelling-based method to facilitate relative quantitative proteomics between two samples

5.1. Introduction

5.1.1. Requirement for development and validation of alternative stable isotope labelling methods

As detailed in **Chapter 1**, there are a wide variety of approaches available to facilitate quantitative proteomics analyses. Unfortunately, experimental and technical constraints rendered the most widely-used of these approaches redundant for this particular project.

A vital prerequisite for the suitability of any stable isotope labelling-based quantitative strategy is complete or near-complete incorporation of the stable isotope in the labelled sample. In SILAC, this is dependent on extensive turnover of all cellular proteins, a criterion that is generally only met in the rapidly-growing proliferative cell lines originally used to develop the technique (Ong *et al.*, 2002). The fact that monocytes do not proliferate at all as they differentiate into DCs initially suggested that culture in SILAC media would result in incomplete labelling. Spellman *et al*. had previously demonstrated relatively complete SILAC labelling in another non-dividing cell line (primary neurons) (Spellman *et al.*, 2008). However, attempts to replicate this in monocyte-derived DCs proved unsuccessful (Buck, M. unpublished observations). This is likely due to the fact that primary neurons can be kept in culture for significantly longer periods of time, allowing for greater protein turnover.

The operational limitations of the mass spectrometer (ion trap-FT hybrid) used throughout the project also precluded adoption of alternative tagging and label-free strategies. CID in ion trap mass spectrometers is subject to a well-characterized '1/3 mass cut-off rule' which prevents detection of fragment ion masses which are less than one third that of the precursor ion mass, so often excluding the low mass reporter ions of the iTRAQ and TMT reagents. Label-free quantitation is performed through comparison of samples which are analysed independently of one another and thus requires a stable and unfluctuating LC-MS setup. Whilst it is not inconceivable that this could be delivered within the core facility in which this work was undertaken, the requirement for reproducibility and a lack of appropriate software for analysis pose significant obstacles.

Given the aforementioned technical issues, it was thus necessary to develop and optimize an alternative stable isotope labelling method such that the quantitative aspect of the project could be realized.

5.1.2. Strategy for development and validation of alternative stable isotope labelling methods

Two criteria must be met for a stable isotope labelling method to be suitable for use in quantitative proteomic studies. Firstly, as detailed above, label incorporation must be complete in the labelled sample/s. Secondly, the reported ratios of labelled to unlabelled or of differentially labelled peptide must reflect genuine differences in abundance between samples. With this in mind, a two-step strategy was devised for the development and validation of alternative methods. A single model protein (BSA) was used to optimize the labelling reaction to ensure that a method for the complete incorporation of the label in question could be attained. Quantification of labelling was validated by taking a known quantity of complex protein sample (whole cell lysate), dividing it in half, labelling one half and leaving the other half unlabelled and then recombining the two halves in a number of different ratios and examining the extent to which the reported quantitation figures reflected the actual ratios in which the labelled and unlabelled samples were combined.

5.2. ^{18}O Labelling

The labelling method initially evaluated was enzymatic labelling of the carboxyl termini of peptides using trypsin in $H_2{}^{18}O$ water. As mentioned in section **1.1.4.1.2.**, trypsin digestion in $H_2{}^{18}O$ water imparts a mass shift to the peptides produced relative to trypsin digestion in $H_2{}^{16}O$ water (Schnolzer *et al.*, 1996). However, the question of whether the mass shift imparted to a given peptide is 2 Da or 4 Da is slightly more complicated and requires an in-depth look at the two reactions which occur during trypsin-catalyzed digestion of proteins. These reactions are shown in **Fig. 26**.

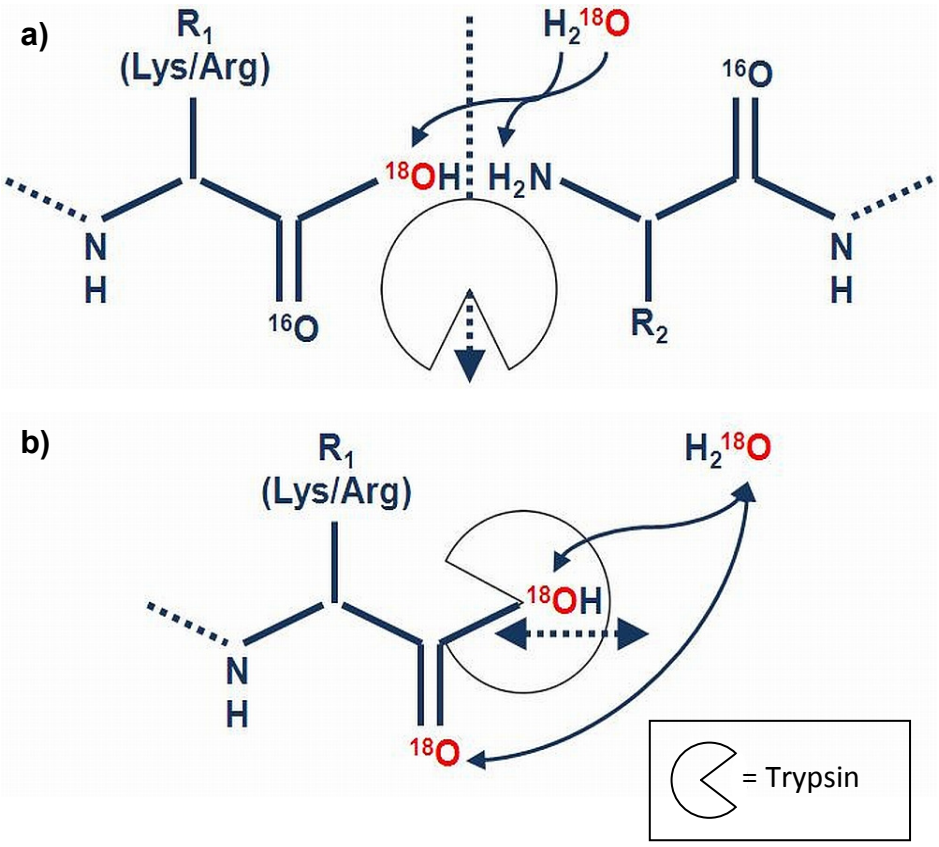

Figure 26: The two reactions which occur during trypsin-catalysed digestion of proteins to peptides in $H_2{}^{18}O$ water. **a)** Hydrolysis (adds a single ^{18}O atom to the carboxyl termini of each peptide produced). **b)** Enzyme-catalysed carboxyl oxygen exchange (exchanges one of the two carboxyl termini oxygen atoms for a free ^{18}O atom). Repeated rounds of carboxyl oxygen exchange in ^{18}O water will result in all peptides incorporating two carboxyl termini ^{18}O atoms.

The first reaction is hydrolysis, whereby a peptide bond is cleaved to release a free carboxylic acid and an amine **(Fig. 26a)**. This reaction occurs only once and if it takes place in $H_2{}^{18}O$ water a single ^{18}O atom will be added to the carboxyl termini of each peptide produced. The second of the two reactions is the carboxyl oxygen exchange reaction, whereby enzyme covalently binds the carboxyl termini of previously cleaved peptides and is then dissociated by water **(Fig. 26b)**. This reaction can occur multiple times for any given peptide and in any single reaction either of the two oxygen atoms at the carboxyl termini can be exchanged. If this reaction takes place in $H_2{}^{18}O$ water, the number of peptides incorporating two ^{18}O atoms will tend towards 100% with repeated rounds of carboxyl oxygen exchange (Miyagi and Rao, 2007). Incorporation of two ^{18}O atoms will never actually reach 100% since isotopically 'pure' $H^2{}_{18}O$ water is typically 95% – 97% ^{18}O.

The nature of the carboxyl oxygen exchange reaction means that variable incorporation is commonly observed in $H_2{}^{18}O$ labelled peptides. Multiple exchanges must take place for complete incorporation of two ^{18}O atoms, but the rate of exchange is very slow under the conditions optimal for hydrolysis and it can also vary with size and sequence of peptides (Stewart *et al.*, 2001). In practice, this leads to the generation of a mixture of peptide species and results in the isotope envelopes of individual peptide species overlapping. This can complicate quantitation and skew reported labelled / unlabelled ratios, as illustrated in **Fig. 27** overleaf. This illustrates the importance of attaining complete double labelling in labelled samples when performing ^{18}O-based quantitative proteomics. If it were assumed that the sample from which spectrum **d)** was derived was completely labelled and this sample was combined in a 1:1 ratio with an unlabelled sample, the reported ratios of unlabelled to labelled peptide would be skewed in favour of the former due to the incomplete labelling of the latter.

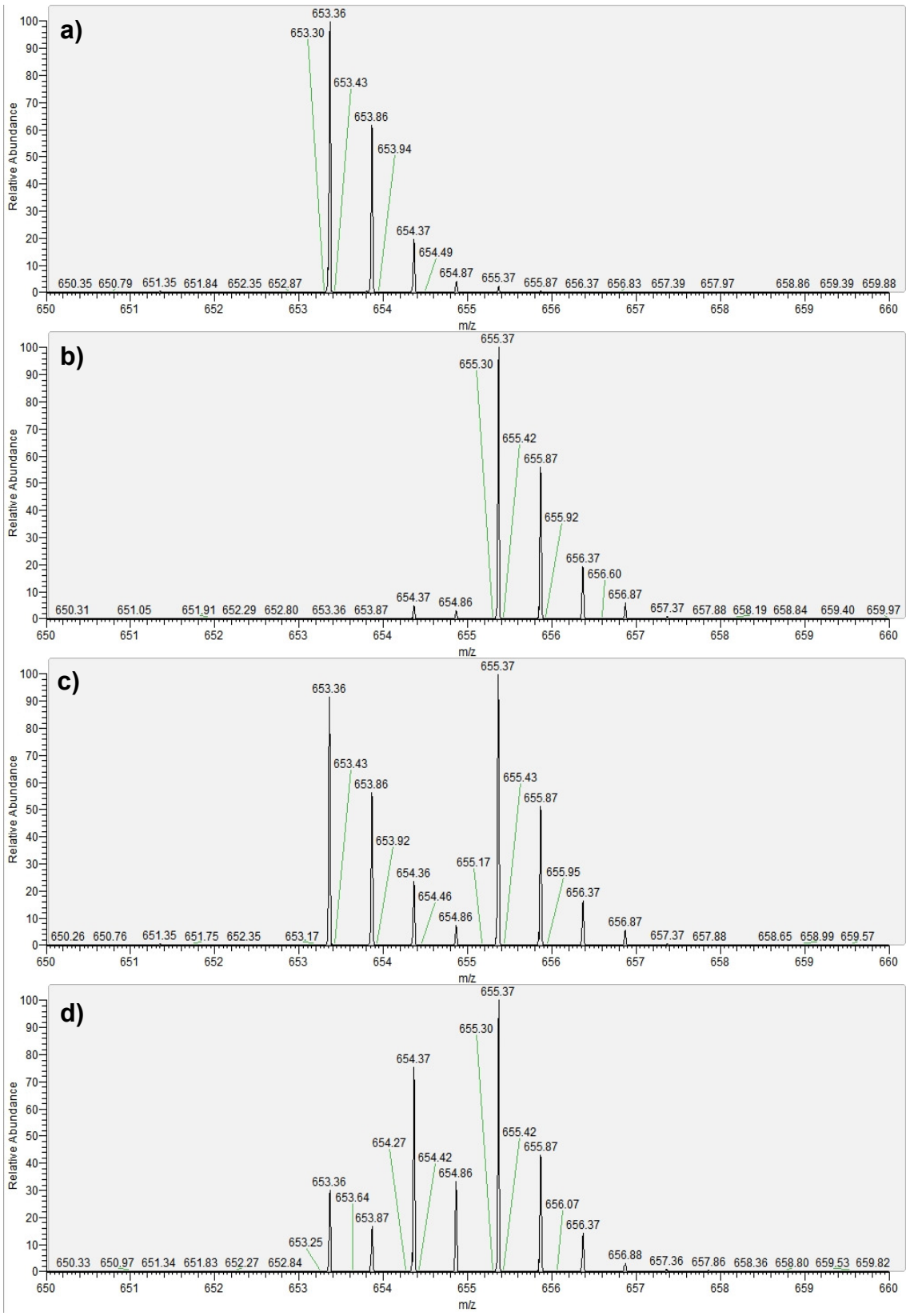

Figure 27: ^{18}O-labelling of a BSA-derived peptide with sequence HLVDEPQNLIK. Spectrum **a)** shows unlabelled peptide. Spectrum **b)** shows peptide completely labelled with two ^{18}O atoms. Spectrum **c)** shows the unlabelled peptide combined in a 1:1 ratio with the completely labelled peptide. Spectrum **d)** shows peptide from a labelling reaction in which the labelling conditions were suboptimal. A mixture of unlabelled, singly ^{18}O-labelled and doubly ^{18}O-labelled species are present.

5.2.1. 'Optimal' ^{18}O Labelling

There are a good number of ^{18}O-based comparative proteomic publications in the literature; however there is a conspicuous lack of agreement on the optimal way to perform the ^{18}O-labelling reaction itself prior to combining labelled and unlabelled samples. The earliest studies simply performed the trypsin digest in ^{18}O water, with both studies noting that the rate of incorporation of ^{18}O atoms varied from peptide to peptide and was not complete for all peptides examined (Stewart *et al.*, 2001; Yao *et al.*, 2001). In 2003, Yao et al. demonstrated the value of 'decoupling' the digestion step from the labelling step as a way of achieving more complete labelling (Yao *et al.*, 2003). There now seems to be a general consensus that this decoupling step is beneficial, though the accord ends here. A summary of the reaction conditions used by groups which have previously published ^{18}O labelling-based proteomic studies is shown overleaf in **Table 5**. (Brown and Fenselau, 2004; Liu *et al.*, 2004b; Staes *et al.*, 2004; Zang *et al.*, 2004; Hood *et al.*, 2005; Smith *et al.*, 2007; Wu *et al.*, 2007; Ang *et al.*, 2008; Kristiansen *et al.*, 2008; Mirza *et al.*, 2008; Lopez-Ferrer *et al.*, 2009; Petritis *et al.*, 2009; Bezstarosti *et al.*, 2010; Wang *et al.*, 2010b; Ye *et al.*, 2010).

Reference	Labelling Decoupled ?	Trypsin Used	E/S Ratio	Labelling Buffer	pH	Incubation Time / Temperature	Method of Trypsin Inactivation
Brown *et al.* (2004)	✓	Immobilized	N/A	50 mM TRIS / 30% CH_3CN	8	5 hours, RT	N/A
Liu *et al.* (2004)	✓	Immobilized	N/A	50 mM ABC / 20% CH_3CN / 10 mM $CaCl_2$	8	24 hours, 30°C	N/A
Staes *et al.* (2004)	✓	In-Solution	1:50	50 mM KH_2PO_4	4.5	Overnight, 37°C	Reduced → Alkylated
Zang *et al.* (2004)	✓	In-Solution	1:20	100 mM AA / 10 mM $CaCl_2$	6.8	20 hours, RT	Acidified → Boiled
Hood *et al.* (2005)	✓	In-Solution	1:50	Not buffered / 20% MeOH	?	16 hours, 37°	Acidified → Boiled
Wu *et al.* (2005)	✓	Immobilized	N/A	50 mM ABC / 20% CH_3CN	8	3 - 5 hours, RT	N/A
Smith *et al.* (2007)	✗	In-Solution	1:50	50 mM ABC	8	18 hours, 37°C	None
Ang *et al.* (2008)	✗	In-Solution	?	25 mM ABC	8	20 hours, 37°C	Boiled
Kristiansen *et al.* (2008)	✓	Immobilized	N/A	50 mM TRIS-HCl / 20% CH_3CN / 50 mM $CaCl_2$	8	4 hours, 25°C	N/A
Mirza *et al.* (2008)	✓	Immobilized	N/A	100 mM ABC	8	15 minutes, RT	N/A
Lopez-Ferrer *et al.* (2009)*	✓	Immobilized	N/A	100 mM AA	6.8	30 seconds	N/A
Petritis *et al.* (2009)	✓	In-Solution	1:50	50 mM ABC / 10 mM $CaCl_2$	7.8	5 hours, 30°C	Boiled → Acidified
Bezstarosti *et al.* (2010)	✓	Immobilized	N/A	50 mM AA	4.5	Overnight, RT	N/A
Wang *et al.* (2010)	✓	In-Solution	1:500	100 mM KH_2PO_4 / 1 M Urea	4.5	20 hours, 37°C	Boiled → Acidified
Ye *et al.* (2010)**	✓	In-Solution	1:20	50 mM ABC / 20% MeOH	8	Overnight, 37°C	Boiled → Acidified

* Labelling performed using high-intensity focussed ultrasound

** Focus of paper is computational means of accounting for incomplete labelling

Table 5: Reaction conditions used in previously published ^{18}O-labelling proteomics papers. CH_3CN: acetonitrile; ABC: ammonium bicarbonate; $CaCl_2$: calcium chloride; KH_2PO_4: potassium phosphate; AA: ammonium acetate; MeOH: methanol.

5.2.2. Results and Discussion

5.2.2.1. Development of a protocol for optimal C-terminal ^{18}O-labelling of peptides

The various methods reported to date for 'optimal' ^{18}O-labelling have been evaluated and three conditions which need to be fulfilled in order to efficiently, stably and reproducibly label peptides with two ^{18}O atoms have been identified.

Use of immobilized trypsin over soluble trypsin is advocated in some of the studies outlined in **Table 5**. It is suggested that the much higher enzyme to substrate ratio increases labelling efficiency (Mirza *et al.*, 2008); and that it is easily removed from the sample via centrifugation or filtration when labelling is complete, preventing trypsin-mediated 'back-exchange' of ^{18}O atoms for ^{16}O atoms when ^{18}O-labelled peptides are resuspended in ^{16}O-based buffers (Sevinsky *et al.*, 2007). On the other hand, immobilized trypsin is considerably more expensive than soluble trypsin and Petritis *et al.* report sample losses when performing ^{18}O-labelling with immobilized trypsin through peptides binding non-specifically to the beads, particularly with small amounts of starting material (Petritis *et al.*, 2009). With this in mind, it was deemed that soluble trypsin would be used to optimize labelling as opposed to immobilized trypsin.

5.2.2.2. Decoupling the carboxyl oxygen exchange reaction from hydrolysis and performing it at pH4.5 with soluble trypsin facilitates labelling of all peptides with two ^{18}O atoms.

The majority of the studies in **Table 5** performed the labelling reaction at pH 8, pH 6.75 or pH 4.5. The two most recent studies in which the reaction was performed at pH 4.5 specifically state that this is the optimal pH for carboxyl oxygen exchange (Bezstarosti *et al.*, 2010; Wang *et al.*, 2010b). One of the studies in which the reaction was performed at pH 6.75 suggests that carboxyl oxygen exchange proceeds faster in slightly more acidic conditions but neglect to investigate pH values lower than 6.75 for fear of significantly reducing trypsin activity (Zang *et al.*, 2004). The studies in which the reaction was performed at pH8 do not consider the pH of the reaction to be a factor in achieving complete labelling.

On the basis of these studies, it was decided that labelling efficiency would be investigated at pH 8 and pH 4.5. 10 µg aliquots of BSA peptides from an in-solution overnight digest were dried *in vacuo* and resuspended in either 50 mM ^{18}O ammonium bicarbonate (pH 8) or 50 mM ^{18}O ammonium acetate (pH 4.5). Labelling reactions were allowed to proceed for either 2 or 24 hours before quenching. A zero time point was also included for each pH value. Here, the peptides were resuspended in either 50 mM ^{16}O ammonium bicarbonate (pH 8) or 50 mM ^{16}O ammonium acetate (pH 4.5) and the reactions were quenched immediately. All reactions were subsequently acidified with 1% TFA, tip desalted and analysed by LC-MS. The extent of label incorporation for the different pH conditions and time points examined was evaluated in 10 BSA peptides.

The extent of label incorporation at 0, 2 and 24 hours when the reaction was performed at pH 8 is shown in **Fig. 28**, whilst the extent of label incorporation at the same time points when the reaction was performed at pH 4.5 is shown in **Fig. 29**. These data indicate that the rate of carboxyl oxygen exchange is peptide-specific, with each peptide examined exhibiting different levels of incorporation of zero, one or two ^{18}O atoms at different time points. However, it is also clear that the exchange reaction proceeds much faster at pH 4.5 than pH 8. The extent of label incorporation observed in all peptides after two hours at pH 4.5 is comparable to that observed in all peptides after 24 hours at pH 8. After 24 hours at pH 4.5, incorporation of two ^{18}O atoms is at least 90% for all peptides examined and considerably more for most of them.

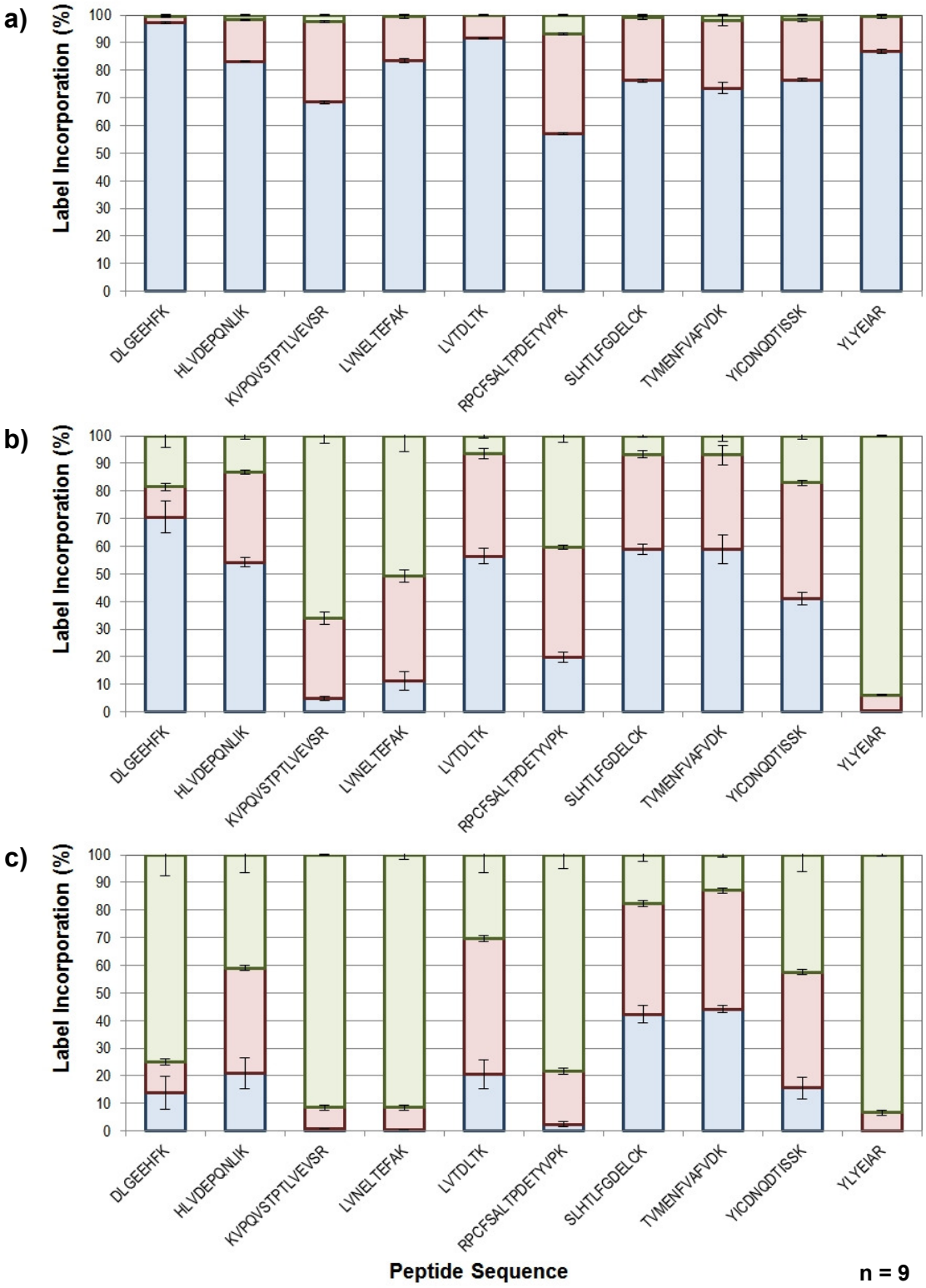

Figure 28: Extent of incorporation of ^{18}O atoms at the carboxyl termini of 10 BSA peptides after **a)** 0 hours; **b)** 2 hours; **c)** 24 hours when the carboxyl oxygen exchange reaction is carried out in 50 mM ammonium bicarbonate (^{18}O, pH 8). The reaction proceeds slowly at pH 8 and a number of peptides remain incompletely labelled after 24 hours. The apparent incorporation of one or two ^{18}O atoms in a small fraction of the peptides at 0 hours is artifactual and is due to the intensity of the third and fifth isotope peaks of each unlabelled peptide. Data are the mean ± mean SD of three experimental replicates, which are in turn the mean ± SD of three technical replicates.

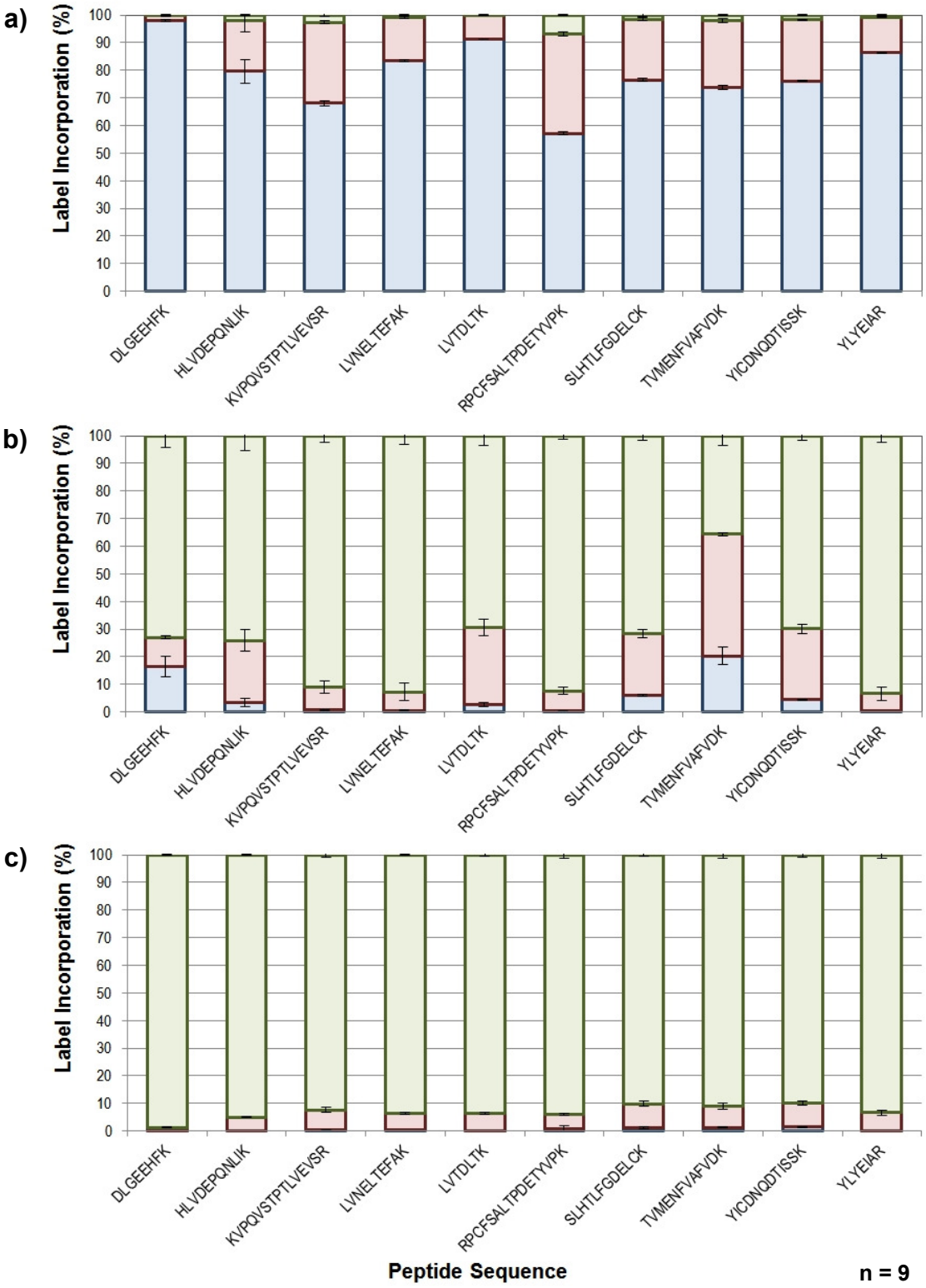

Figure 29: Extent of incorporation of ^{18}O atoms at the carboxyl termini of 10 BSA peptides after **a)** 0 hours; **b)** 2 hours; **c)** 24 hours when the carboxyl oxygen exchange reaction is carried out in 50 mM ammonium bicarbonate (^{18}O, pH 4.5). The reaction proceeds far more rapidly at pH 4.5 and at least 90% of all 10 peptides examined are labelled with two ^{18}O atoms after 24 hours. Data are the mean ± mean SD of three experimental replicates, which are in turn the mean ± SD of three technical replicates.

5.2.2.3. Reducing and alkylating labelled samples with high concentrations of DTT and iodoacetamide prior to resuspension in ^{16}O-based buffers completely abrogates trypsin-catalysed back exchange in labelled peptides.

It would be of little use to have optimised reaction conditions for efficient labelling of peptides with two ^{18}O atoms if the labelling was not stable. In the vast majority of proteomics workflows, ^{18}O labelled peptides have to be resuspended in ^{16}O-based buffers further downstream in the process. With this in mind, trypsin must either be removed from the sample or its activity completely abrogated prior to the addition of this normal water, otherwise it will catalyse the 'back-exchange' of ^{18}O atoms at the carboxyl termini of peptides for ^{16}O atoms present in the buffer.

As aforementioned, one of the purported benefits of labelling with immobilized trypsin is that it can be easily removed from the sample when the reaction is complete. In contrast, if soluble trypsin is used it must be inactivated. Of the studies in **Table 5** which utilize soluble trypsin for labelling, the majority include a 10 minute boiling step at the end of the reaction for trypsin inactivation (Zang *et al.*, 2004; Hood *et al.*, 2005; Petritis *et al.*, 2009; Wang *et al.*, 2010b; Ye *et al.*, 2010). A further study reports that boiling alone does not suffice and some catalytic activity is retained when the sample is returned to room temperature. This study instead recommends reduction / alkylation of the reaction upon completion to prevent the enzyme from reassuming its native conformation (Staes *et al.*, 2004).

The efficacy of both approaches as a means of preventing trypsin-catalysed back-exchange was examined. 10 µg aliquots of BSA peptides from an in-solution overnight digest were labelled for 24 hours at pH 4.5 as described in section **5.2.2.2.** Upon completion, labelling reactions were either left untreated; boiled for 30 minutes and then rapidly cooled to -20ºC; or reduced at 95ºC with 20 mM DTT and then alkylated at 60ºC for 30 minutes with 40 mM iodoacetamide. The reactions were then dried *in vacuo,* resuspended in IEF buffer made up in ^{16}O water and incubated at room temperature for 24 hours. These conditions were chosen to simulate isoelectric focusing, a technique which was originally to be used to sub-fractionate proteomic peptides prior to LC-MS analysis (see **Chapter 6**). A control reaction was left untreated in ^{18}O

ammonium acetate for the same period of time to verify that the labelling reaction itself had gone to completion (data not shown). All reactions were subsequently acidified with 1% TFA, tip desalted and analysed by LC-MS. The extent to which back exchange had occurred was evaluated in the same 10 BSA peptides which had previously been examined for labelling efficiency.

The extent of back exchange in untreated, boiled and reduced / alkylated samples is shown in **Fig. 30**. These data indicate that boiling trypsin alone is insufficient to prevent it catalysing carboxyl oxygen back-exchange when labelled peptides are resuspended in ^{16}O-based buffers. Indeed, there is very little difference in between the boiled sample and the untreated sample in terms of the extent of back exchange. However, reduction and alkylation of trypsin is shown to be highly effective in completely abolishing all residual catalytic activity, with essentially no back exchange observed in this sample even after 24 hours at room temperature in a ^{16}O-based buffer.

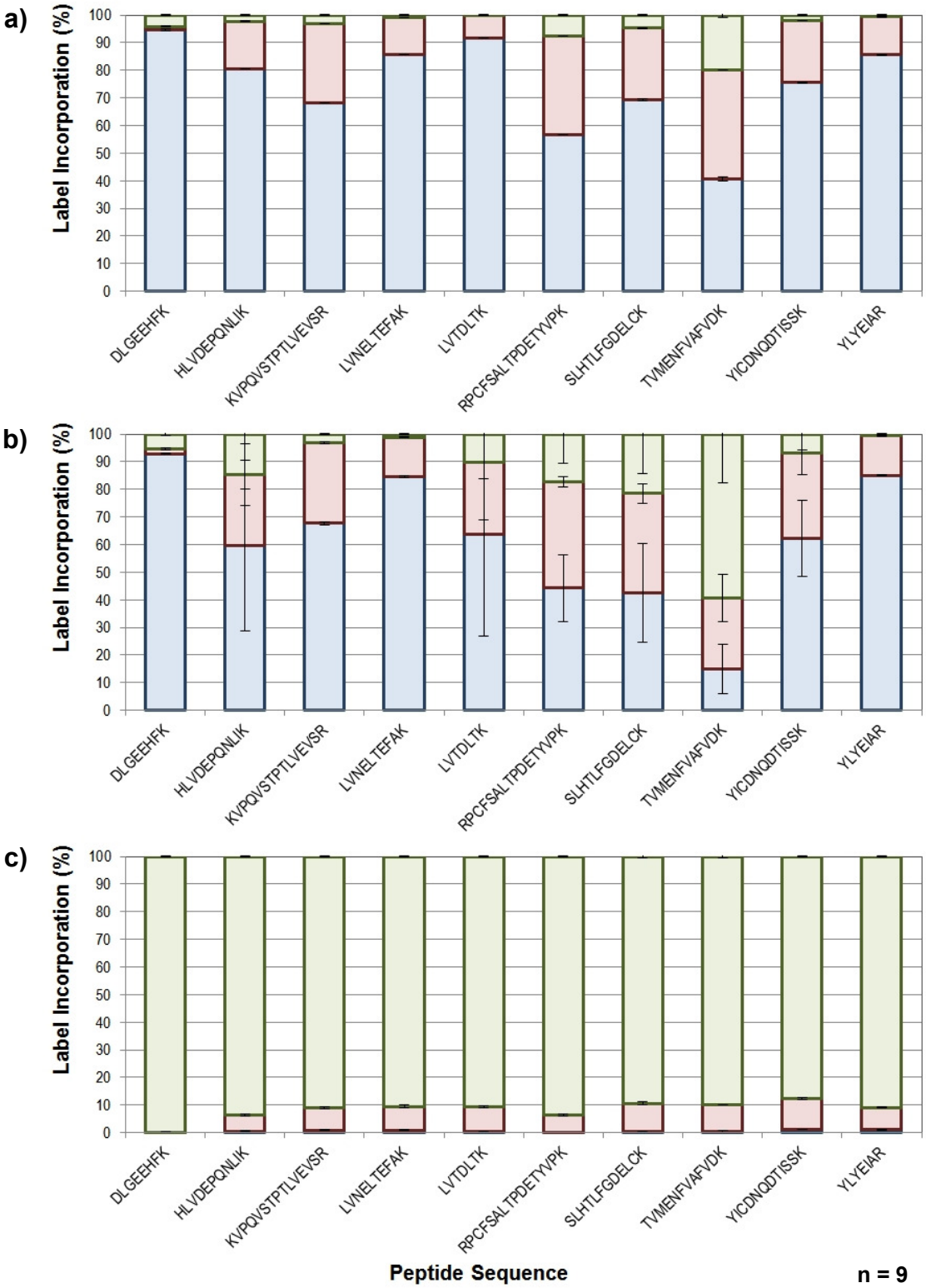

Figure 30: Extent of trypsin-catalysed back exchange of ^{18}O atoms for ^{16}O atoms at the carboxyl termini of 10 fully ^{18}O-labelled BSA peptides when vacuum-dried and resuspended in 50mM ammonium bicarbonate (^{16}O, pH 4.5) and left at room temperature for 24 hours after **a)** no treatment; **b)** incubation at 100ºC for 30 minutes; **c)** reduction with 20 mM DTT at 95ºC for 1 hour followed by alkylation with 40 mM iodoacetamide for 30 minutes. Data are the mean ± mean SD of three experimental replicates, which are in turn the mean ± SD of three technical replicates.

5.2.2.4. Low pH causes small amounts of acid-catalysed back exchange in labelled peptides completely independently of trypsin.

Trypsin activity is not the only mechanism through which carboxyl oxygen exchange can occur. It can also happen completely independently of enzyme provided conditions are sufficiently acidic (Niles *et al.*, 2009). Whilst this acid-catalysed exchange is perhaps not a particularly suitable strategy for labelling peptides in itself (it can also occur on the side chains of aspartic and glutamic acid residues and the reaction kinetics are orders of magnitude slower than trypsin-catalysed exchange) (Niles *et al.*, 2009), it does highlight an important point. Peptides are generally reconstituted in acidic buffers immediately prior to LC-MS analysis. These buffers are ^{16}O-based and it would prove prohibitively costly to make them up using ^{18}O water. The study referenced above suggested that some degree of acid-catalysed back exchange may occur in ^{18}O-labelled samples stored at low pH for long periods of time prior to LC-MS analysis.

To investigate the effects of acid-catalysed back exchange on ^{18}O-labelled peptides, an identical experiment was performed to that described in section **5.2.2.3.** with the exception that labelled peptides were acidified with 1% TFA immediately after being resuspended in IEF buffer. The results are shown in **Fig. 31**.

Whilst acidification with 1% TFA and storage at room temperature represents an ‘extreme’ storage condition, these data suggest that storing labelled peptides in more conventional conditions over prolonged periods of time could potentially cause small but significant amounts of back exchange. Acidification of the untreated and boiled samples resulted in reduced back exchange relative to the analogous samples which were not acidified. This is likely due to inhibition of trypsin activity at the low pH; however in these samples it is not clear what contribution acid-catalysed back exchange makes to the exchange observed overall. In contrast, acidification of the reduced / alkylated sample resulted in an increase in back-exchange relative to the control sample which was not acidified. This increase in exchange can only be explained by an acid-catalysed reaction.

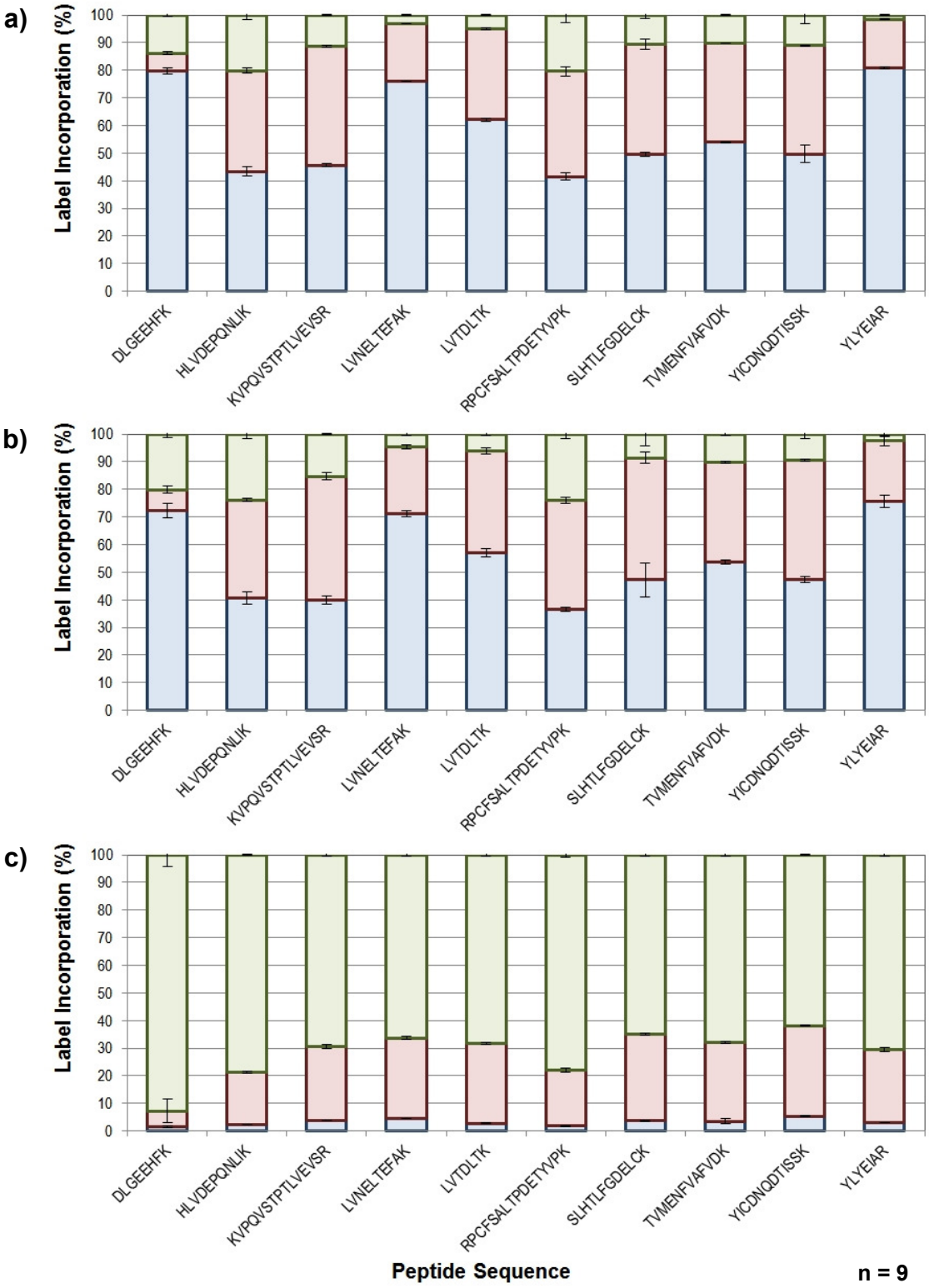

Figure 31: Extent of trypsin-catalysed back exchange of ^{18}O atoms for ^{16}O atoms at the carboxyl termini of 10 fully ^{18}O-labelled BSA peptides when vacuum-dried and resuspended in 50 mM ammonium bicarbonate (^{16}O, pH 4.5), acidified with 1% TFA and left at room temperature for 24 hours after **a)** no treatment; **b)** incubation at 100ºC for 30 minutes; **c)** reduction with 20mM DTT at 95ºC for 1 hour followed by alkylation with 40 mM iodoacetamide for 30 minutes. Data are the mean ± mean SD of three experimental replicates, which are in turn the mean ± SD of three technical replicates.

5.2.2.5. Optimised protocol for C-terminal ^{18}O labelling of peptides

The data presented in sections **5.2.2.2. – 5.2.2.4.** suggest that complete and stable ^{18}O labelling of peptides is dependent on both the pH of the labelling reaction itself and the prevention of trypsin- and acid-catalysed back exchange when the reaction is complete. The optimised protocol is presented in full in section **3.4.2.**

5.2.2.6. Examination of the ability of C-terminal ^{18}O-labelling to quantify differences between labelled and unlabelled proteomic peptides across a wide dynamic range.

As aforementioned, a stable isotope labelling method is only of use for quantitative proteomic applications if the reported ratios of labelled to unlabelled peptide reflect genuine differences in abundance between labelled and unlabelled samples when they are combined. With the ^{18}O-labelling reaction itself optimised, it was next examined whether this second criterion also held true.

10 µg aliquots of proteomic peptides from an in-solution overnight digest of mature DC whole cell lysate were processed using the optimised ^{18}O-labelling procedure detailed in section **3.4.2.** Half of the aliquots were labelled using ammonium acetate and trypsin prepared in ^{18}O water. The other half were subjected to exactly the same procedure but the buffers and enzyme used were prepared in ^{16}O water. This was done in order to preserve consistency between labelled and unlabelled samples. Reduced / alkylated labelling reactions were tip desalted and reconstituted in 100 µl 0.2% FA. Labelled and unlabelled peptides were then combined according to the scheme shown in **Table 6**.

Ratio
^{16}O
(^{16}O) 5:1 (^{18}O)
(^{16}O) 2:1 (^{18}O)
(^{16}O) 1:1 (^{18}O)
(^{16}O) 1:2 (^{18}O)
(^{16}O) 1:5 (^{18}O)
^{18}O

Table 6: Scheme for combining labelled and unlabelled proteomic peptides to examine whether ^{18}O-labelling is suitable for performing quantitative proteomic analyses.

Combined samples were analysed using LC-MS. Raw data were processed, searched and quantified using Mascot Distiller. Protein and peptide quantitation reports were generated and imported into Microsoft Excel for further data processing. Box and whisker plots were generated to visualise the distribution of reported protein and peptide ratios computed by Distiller for each of the combinations. Uncombined samples were not included in the plots but were analysed to verify that the labelling reaction had gone to completion.

The distribution of reported protein ratios computed from the combined proteomic samples is shown in **Fig. 32**. Ideally, these reported ratios would be representative of the actual ratios in which the labelled and unlabelled proteomic peptides are combined. In actuality, the majority of the reported ratios deviate considerably from these expected values. When the peptides are combined 1:1, the reported ratios between the first and third quartiles fall very close to the expected ratio. However, when 95% of the reported ratios surrounding the median ratio are included, the reported ratios span three orders of magnitude. This effect is exacerbated the further the ratio deviates from 1:1. At five parts labelled to one part unlabelled and vice versa, even the reported ratios encompassed within the first and third quartiles span nearly two orders of magnitude.

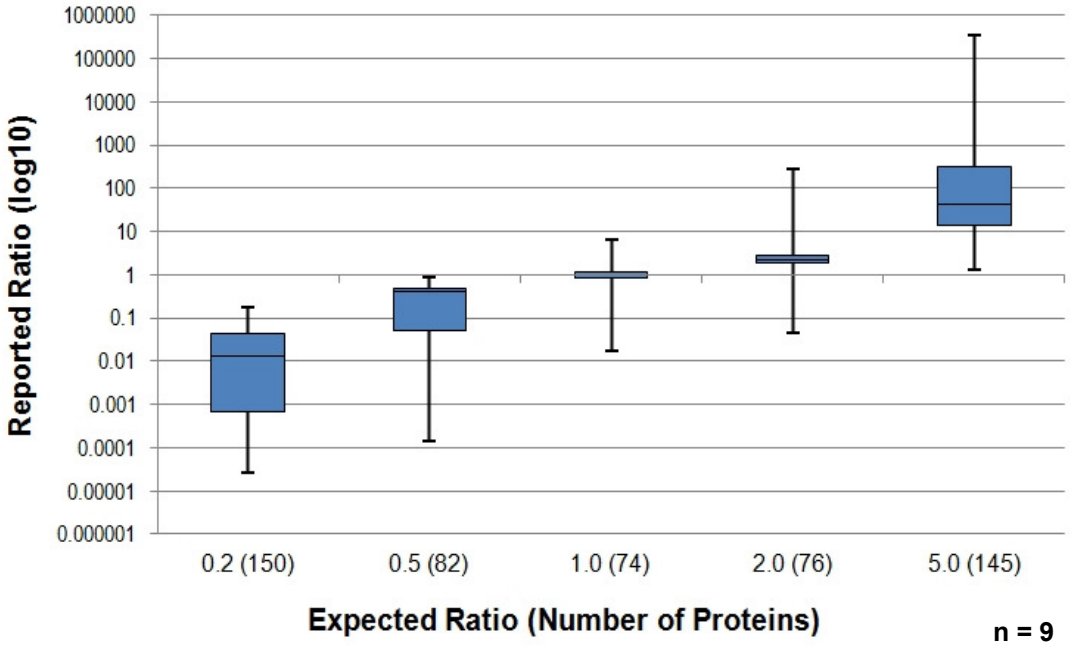

Figure 32: Box and whisker plot showing distribution of protein ratios reported by Mascot Distiller when ^{18}O-labelled and unlabelled proteomic peptides derived from mature DC whole cell lysate are combined in ratios ranging from 5 parts labelled : 1 part unlabelled through to 1 part labelled : 5 parts unlabelled. 50% of reported ratios are contained within the boxes and 95% are contained within the whiskers. The number of unique proteins detected across 9 replicates (3 experimental × 3 technical) is shown in brackets on the X-axis.

To examine the source of the disparity between expected and reported protein ratios, the distribution of reported peptide ratios from the same samples was also examined. Mascot Distiller determines peptide ratios through pairing precursor peaks which are identified in Mascot as being heavy and light isoforms of the same peptide, integrating the areas under the extracted ion chromatograms which correspond to each of the paired precursor peaks and reporting differences in these areas as a ratio of heavy to light peptide **(Fig. 33)**. Finally, the ratios calculated for all peptides derived from a single protein are averaged and reported as a single ratio for that protein. It thus stood to reason that the protein ratios could be being skewed by a few outlying peptide ratios. The distributions of reported peptide ratios are shown in **Figs. 34 and 35**.

The distributions shown in **Fig. 34** are unfiltered; every peptide ratio computed by Mascot Distiller and subsequently assigned to a protein is included. The distributions shown in **Fig. 35** are 'filtered'. Each peptide ratio calculation computed by Mascot Distiller is subject to three statistical tests to filter out 'noisy' data and ensure that only high quality spectra contribute to the final protein ratio reported. Briefly, these are a test on the fraction of peaks versus theoretical isotope profile present in the extracted ion chromatogram which correspond to the peptide being quantitated; a test on the goodness of fit between the predicted and observed isotope envelopes of the peptide being quantitated; and finally a test on the standard error of the reported ratio of the peptide being quantitated across the elution peak. A peptide will be excluded from the protein ratio calculation if it fails one or more of these three tests.

In addition, three distributions **(a, b and c)** are shown in each figure. Distribution **a)** includes all ratios, regardless of the MS1 signal intensity of the most abundant peptide peak in a pair. Distribution **b)** includes only ratios where the most abundant peak in a pair has MS1 signal intensity greater than 10^4; whilst distribution **c)** includes only ratios where the most abundant peak in a pair has MS1 signal intensity greater than 10^5.

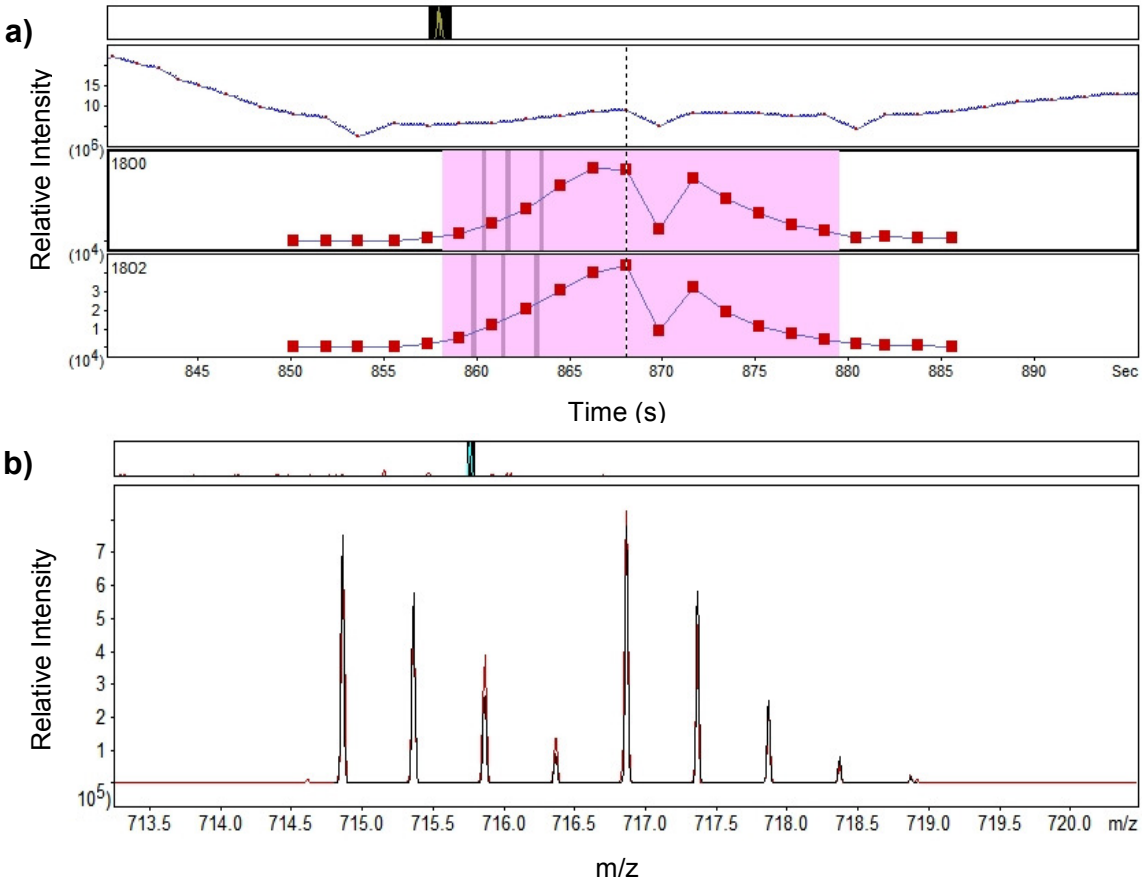

Figure 33: Relative quantitation of a proteomic peptide with sequence SLYASSPGGVYATR derived from unlabelled and ^{18}O-labelled mature DC whole cell lysate combined in a 1:1 ratio. Quantitation is performed by integrating the areas under the extracted ion chromatograms in **a)** which correspond to the unlabelled and ^{18}O-labelled peptide peaks in **b)**. The red profile in **b)** is the actual isotope profile of the peptide, whilst the black profile is the theoretical isotope profile of the peptide. Here, the actual and theoretical profiles are almost identical and the peptide does not fail any of the statistical tests.

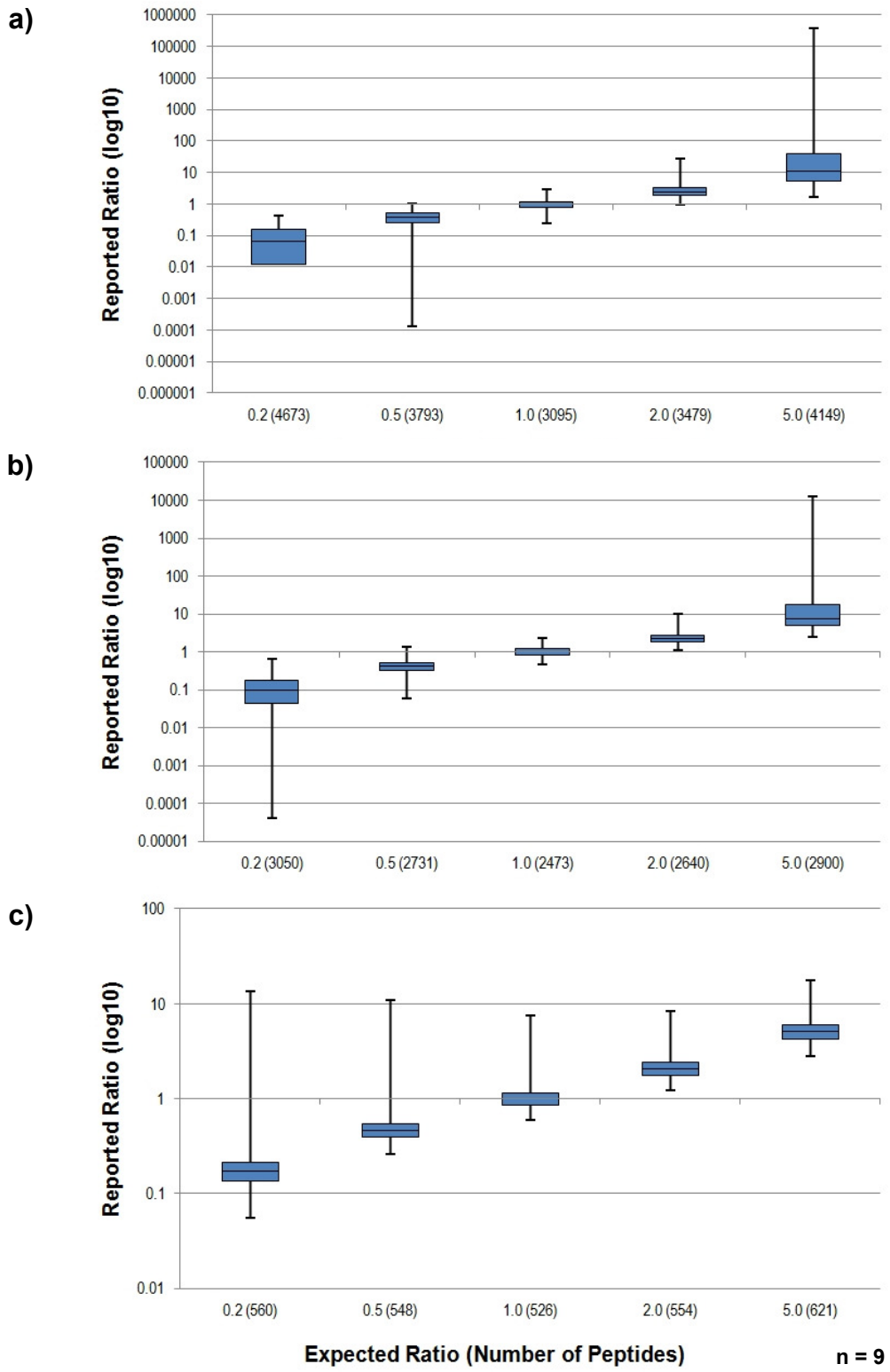

Figure 34: Box and whisker plot showing distribution of unfiltered peptide ratios for **a)** all peptides assigned to proteins; **b)** all peptides with MS1 signal intensity greater than 10^4 assigned to proteins; **c)** all peptides with MS1 signal intensity greater than 10^5 assigned to proteins; reported by Mascot Distiller when ^{18}O-labelled and unlabelled proteomic peptides derived from mature DC whole cell lysate are combined in ratios ranging from 5 parts labelled : 1 part unlabelled through to 1 part labelled : 5 parts unlabelled. 50% of reported ratios are contained within the boxes and 95% are contained within the whiskers. The number of peptides detected across 9 replicates (3 experimental × 3 technical) is shown in brackets on the X-axis.

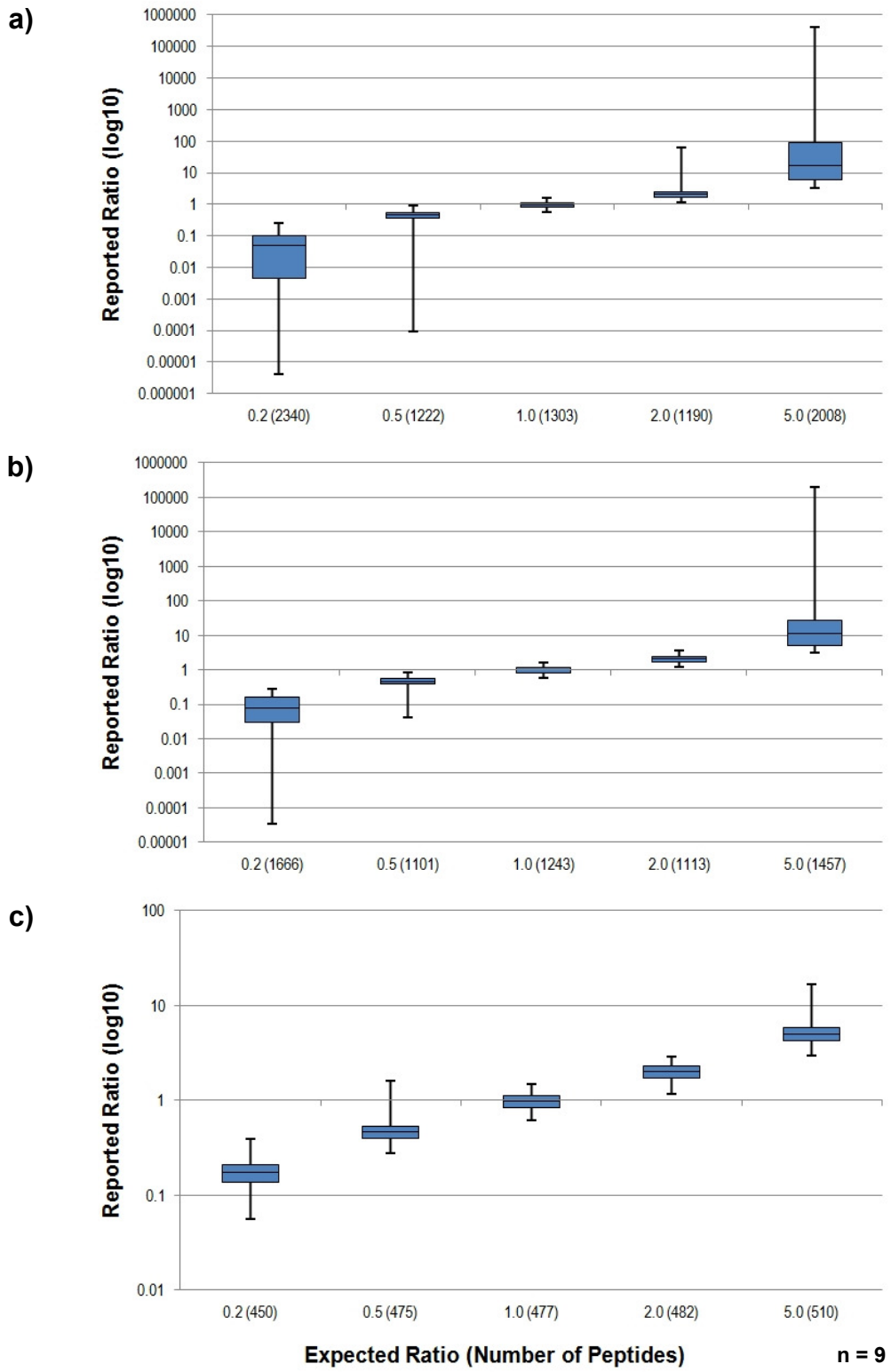

Figure 35: Box and whisker plot showing distribution of filtered peptide ratios for **a)** all peptides assigned to proteins; **b)** all peptides with MS1 signal intensity greater than 10^4 assigned to proteins; **c)** all peptides with MS1 signal intensity greater than 10^5 assigned to proteins; reported by Mascot Distiller when ^{18}O-labelled and unlabelled proteomic peptides derived from mature DC whole cell lysate are combined in ratios ranging from 5 parts labelled : 1 part unlabelled through to 1 part labelled : 5 parts unlabelled. 50% of reported ratios are contained within the boxes and 95% are contained within the whiskers. The number of peptides detected across 9 replicates (3 experimental × 3 technical) is shown in brackets on the X-axis.

The six distributions displayed in **Figs. 34 and 35** collectively suggest that the protein ratios issue is not merely caused by a few outlying peptides but is instead symptomatic of a more extensive disparity between expected and reported peptide ratios. This disparity is somewhat less severe than that seen for the protein ratios plotted in **Fig. 32** (a considerably higher number of peptide ratios are plotted) but it is still appreciable. However, examining the six distributions also sheds light on the factors which contribute to this variability.

It is immediately apparent that MS1 signal intensity has a significant influence on the accuracy of reported ratios. In **Figs. 34c and 35c**, the reported ratios between the first and third quartiles fall very close to the expected ratio for all conditions examined. Outliers within the 95% of reported ratios surrounding the median ratio in **Fig. 35c** are not nearly as severe as those seen in **Figs. 35a-b**. For these two distributions, 95% of reported ratios surrounding the median ratio are reasonably accurate when peptides are combined 1:1. At two parts labelled to one part unlabelled and vice versa, the reported ratios within the first and third quartiles remain reasonably accurate, but inclusion of 95% of reported ratios surrounding the median ratio begins to introduce more extreme outliers. At five parts labelled to one part unlabelled and vice versa, variation around the median becomes more significant for all peptides. The same can be said of **Figs. 34a-b**; however outliers within the 95% of reported ratios surrounding the median ratio in **Fig. 34c** are to an extent more severe than those seen in **Figs. 34a-b**. This is likely due to the fact that the data is unfiltered and the number of peptide ratios plotted in **Fig. 34c** is considerably lower than in **Figs. 34a-b**.

These observations suggest that the accuracy of a reported ratio for a given labelled/unlabelled peptide pair is dependent upon accurate measurement of the MS1 signal intensity of each peak in the pair. The stronger the intensity of a given ion in an MS1 scan, the easier it is to differentiate between signal and noise (Karp *et al.*, 2010). This accounts for the significant improvement in quantitative accuracy seen when ratios computed from peptides with signal intensity lower than 10^5 are excluded from the dataset in **Figs. 34c and 35c**. It also offers an explanation for the poor dynamic range of quantitation. At ratios of five parts labelled to one part unlabelled and vice versa, we would expect the signal intensity of the less abundant isoform of a peptide to be five times weaker than that of the more abundant isoform. It follows that this less abundant

isoform may be difficult to differentiate from noise even if the more abundant isoform is well detected, complicating calculation of the ratio.

Inclusion or exclusion of ratios rejected by Distiller for failing any/all of the three statistical tests seems to have considerably less effect on quantitative accuracy. Comparing the total numbers of reported ratios in **Fig. 34** and **Fig. 35**, it is clear that the majority of ratios rejected by Distiller correspond to peptides with weaker MS1 signal intensity. Indeed, around 60% of all reported ratios are flagged for rejection, but only around 15% of those corresponding to peptides with signal intensity over 10^5 do not make the cut. Disappointingly, even though over half of the raw dataset is excluded in **Figs. 35a and 35b**, a significant number of extreme outliers remain. It is not clear why Distiller fails to reject these aberrant ratios.

With all of the above in mind, one approach to improve the quantitative accuracy of the technique would be to only include ratios derived from peptides detected with high signal intensity. However, this would entail ignoring the majority of the data acquired. Furthermore, the peptides detected with the highest signal intensities are likely to have originated from the most abundant proteins in the initial digest. Depending on the means of sample preparation employed prior to digestion, these proteins may not necessarily be of interest from an experimental perspective. The proteomic material used to generate the data in **Figs. 32, 34 and 35** was whole cell lysate and the peptides with the highest signal intensities consequently come from proteins that are largely cytoplasmic and cytoskeletal.

A further point of note is that a quantitative discovery proteomics study is usually conceived with the intention of detecting differential protein expression in response to differential stimuli applied to an otherwise invariant experimental system. One would expect only a small fraction of all expressed proteins to exhibit differential expression in response to such a stimulus. It could thus be reasonably argued that the majority of proteins identified in such an experiment would be equally abundant across all samples and would hence be quantitated with reasonable accuracy using ^{18}O labelling. Proteins exhibiting differential expression across samples may not necessarily be quantitated accurately but would likely still be flagged as being differentially expressed.

This point raises a further issue distinct to that pertaining to dynamic range. The total number of reported peptide and protein ratios in all six distributions in **Figs. 34 and 35** is rather low considering the data were compiled from three technical repeats of three biological replicates. The lowest numbers of reported peptide and protein ratios are observed when labelled and unlabelled samples are combined in a 1:1 ratio. In an ^{18}O labelling-based quantitative proteomics experiment with optimal ^{18}O labelling, peptides will be present in labelled and unlabelled isoforms, each with distinct masses. This doubles the complexity of every MS1 scan acquired and halves the sensitivity of detection due to the ion current being split between the two isoforms of each peptide (Christoforou and Lilley, 2012). This is an issue common to all stable isotope labelling-based quantitative proteomic methods in which quantitation is performed at the MS1 level. Taken together, these factors considerably limit the numbers of unique peptides which can be identified in a single experiment of this nature.

5.3. Isobaric Peptide Termini Labelling

Though the data in section **5.2.2.6.** appeared to indicate that C-terminal ^{18}O-labelling would prove suboptimal for an in-depth quantitative proteomics study, it was felt that it would be a shame to discard the optimised ^{18}O-labelling method itself. The C-terminal localisation of the modification made it possible for ^{18}O-labelling to be incorporated as the C-terminal labelling step in an isobaric peptide termini labelling-based strategy and this approach was thus explored further.

The concept of isobaric peptide termini labelling (IPTL) was originally conceived by Koehler *et al*. for investigating differential protein expression in two samples (Koehler *et al.*, 2009). In IPTL, each sample is labelled such that an identical mass shift is introduced to both sets of peptides. However, in one of the samples the label is incorporated at the N-terminus whilst in the other sample the label is incorporated at the C-terminus. When two samples are subsequently combined and analysed by LC-MS, differentially labelled peptides of identical sequence have the same mass in the precursor ion scan and are thus simultaneously isolated and fragmented in the same product ion scan. In this regard, the technique is analogous to more widely used isobaric labelling approaches such as iTRAQ and TMT.

The technique differs in the manner in which quantitation is carried out in the product ion scan. Co-fragmentation of differentially labelled IPTL peptides discriminates the mass differences introduced during labelling. Labelled N- and C- terminal fragment ions can thus be distinguished in the product ion scan by merit of the mass differences of the respective peptide termini. Quantitation is performed by comparing the relative signal intensities of the peaks produced by these differentially labelled N- and C-terminal peptide fragment ions. This concept is detailed in **Fig. 36** overleaf.

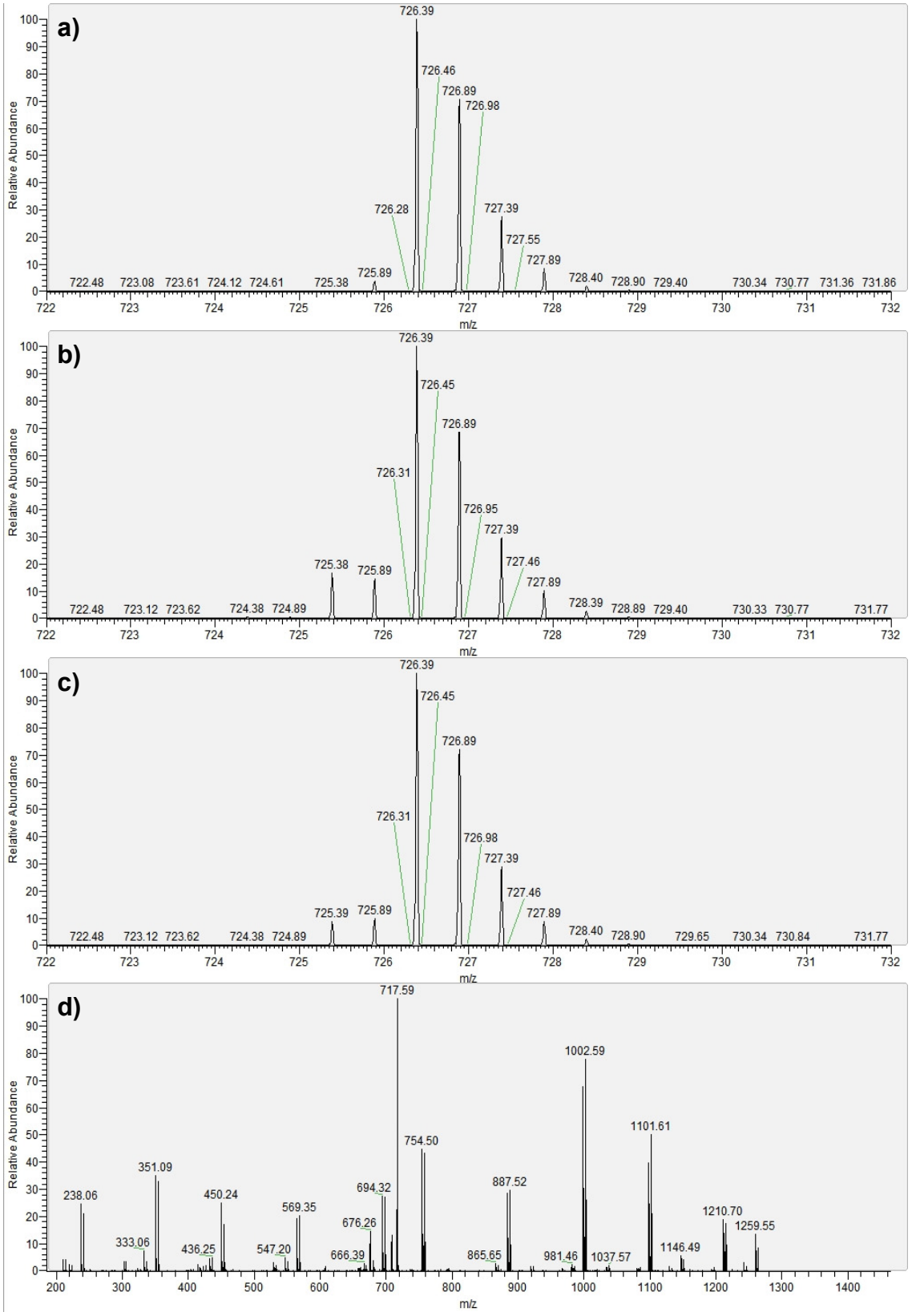

Figure 36: Isobaric peptide termini labelling of a BSA-derived peptide with sequence HLVDEPQNLIK. Spectrum **a)** shows peptide labelled with $^{13}c_4$ succinic anhydride at the N-terminus and unlabelled at the C-terminus. Spectrum **b)** shows peptide labelled with $^{12}c_4$ succinic anhydride at the N-terminus and ^{18}O-labelled at the C-terminus. The peptides in both spectra have also been treated with O-Methylisourea to derivatize the C-terminal lysine residue.

Figure 36 (cont.): Spectrum **c)** is the precursor ion scan of $^{13}c_4{}^{16}O$- and $^{12}c_4{}^{18}O$- labelled peptides combined in a 1:1 ratio. Note that the two peptides are isobaric. Spectrum **d)** is the product ion scan produced after isolation and co-fragmentation of the differentially labelled peptides in spectrum c). This produces many pairs of $^{12}c_4/^{13}c_4$ N-terminal and $^{16}O/^{18}O$ C-terminal peptide fragments. Quantitation is performed on each of these fragment ion pairs.

5.3.1. 'Optimal' N-Terminal Labelling

In ^{18}O-labelling, a 4 Da mass shift is introduced to the C-terminus of labelled peptides relative to unlabelled peptides. To incorporate this into an IPTL-based quantitative strategy, we required a means to introduce a 4 Da mass shift to the N-terminus of the peptides which were not ^{18}O-labelled. There is no reagent available which will add this 4 Da mass shift to one set of peptides whilst leaving the other set unmodified; however there are a number of reagents available for modification of amino termini. Stable isotope variants of some of these reagents allow the requisite mass shift to be introduced to one set of peptides even when both sets are modified. Koehler *et al*. use normal ($C_4H_4O_3$) and tetradeuterated ($C_4D_4O_3$) succinic anhydride.

For an IPTL-based quantitative strategy to be successful, it is vital that the N-terminal labelling step is as highly specific as the C-terminal labelling step. However, reagents which react with N-terminal α-amino groups will also react with ε-amino groups on lysine side chains. The reactivity of each group is dependent on the pH at which the reaction is performed. The pKa of N-terminal α-amino groups (~8.0) is significantly lower than that of lysine (~10.5) side chain ε-amino groups (Greenstein and Winitz, 1961; Means and Feeney, 1971) and thus N-terminal α-amino groups should theoretically be considerably more amenable to modification at pHs of 8 and below. Koehler *et al*. suggest that performing the reaction using 20 mM succinic anhydride in 50 mM sodium acetate (pH 7.6) for 5 minutes at room temperature results in largely complete N-terminal labelling with minimal side-reactivity at lysine residues.

5.3.2. Results and Discussion

5.3.2.1. Development of a protocol for optimal N-terminal succinylation of peptides

Koehler *et al*. currently perform the N-terminal succinylation reaction as part of a two-step, 'one pot' procedure in which the C-terminal modification is introduced to C-terminal lysine residues through dimethylation with formaldehyde or dideuterated formaldehyde immediately after N-terminal modification (Koehler *et al.*, 2011). This reaction scheme requires only a single vacuum drying step. Combining C-terminal ^{18}O labelling and N-terminal succinylation would require both the initial digest to be vacuum dried prior to ^{18}O labelling and the completed ^{18}O labelling reaction to be tip desalted (to remove the high concentrations of DTT and iodoacetamide) prior to N-terminal succinylation. There were concerns with the potential sample losses which may be introduced with repeated rounds of desalting, drying and resuspension prior to LC-MS analysis and so the feasibility of performing the N-terminal reaction whilst the peptides were immobilized on solid phase (having been desalted after ^{18}O-labelling but prior to elution) was explored.

5.3.2.2. Peptides cannot be N-terminally succinylated whilst bound to a solid phase extraction column without significant succinylation of lysine side chains.

Problems were encountered in replicating the buffering conditions specified by Koehler *et al*., in which 20 mM succinic anhydride is prepared in 50 mM sodium acetate (pH 7.6). These conditions would theoretically be optimal for favouring N-terminal modification given the close proximity of the pH to the pKa of α-amino groups. However, Koehler *et al*. do not specify whether the sodium acetate should be at pH 7.6 before or after addition of succinic anhydride. The reagent hydrolyses rapidly in aqueous conditions and addition of 20 mM succinic anhydride to 50 mM sodium acetate (pH 7.6) resulted in a near-immediate and significant drop in the pH of the reaction buffer to ~pH 4.5. It was reasoned that these reaction conditions would be suboptimal for N-terminal succinylation. This could be countered by preparing the reagent in 200 mM sodium acetate (pH 7.6) supplemented with 20 mM sodium hydroxide. The initial addition of sodium hydroxide raises the buffer pH significantly but subsequent addition of 20 mM succinic anhydride results in a reaction buffer which maintains a pH of ~7.6 throughout the reaction.

30 µg aliquots of BSA peptides from an in-solution overnight digest were dried *in vacuo* and resuspended in 1% TFA. The peptides were captured on a C18-bonded silica support contained within a commercially available solid phase extraction cartridge and desalted but not eluted. The immobilized peptides were then reacted with 20 mM succinic anhydride in 200 mM sodium acetate / 20 mM sodium hydroxide at room temperature for 5, 10 or 15 minutes. Upon completion of the reaction, the peptides were washed for a second time and eluted. All reactions were subsequently analysed by LC-MS. The extent of succinylation at the three different time points was evaluated in the same 10 BSA peptides which had been examined during optimization of C-terminal ^{18}O-labelling. This is shown in **Fig. 37**.

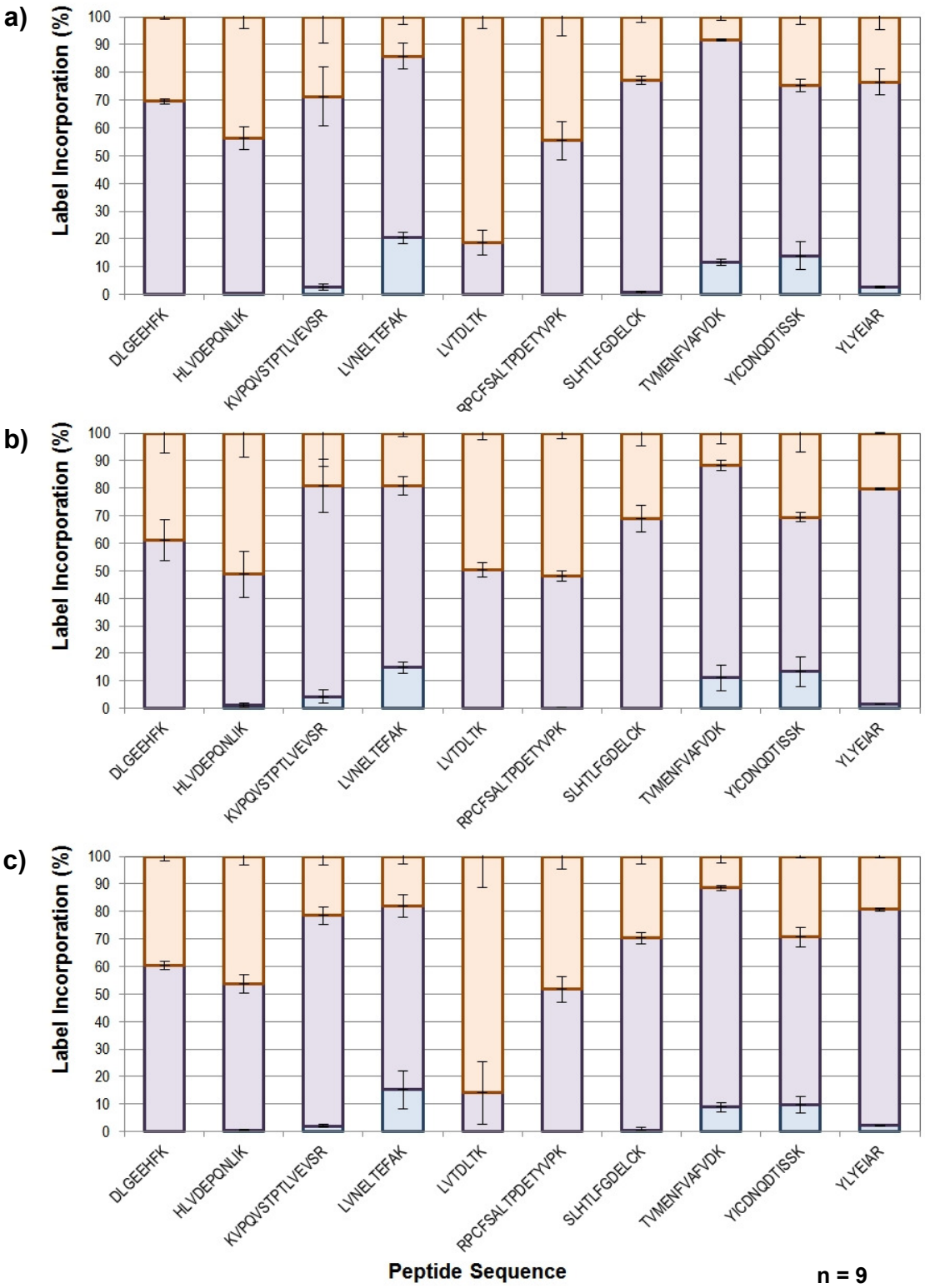

Figure 37: Succinylation of 10 BSA peptides when reacted with 20 mM succinic anhydride in 200 mM sodium acetate / 20 mM sodium hydroxide (pH 7.6) for **a)** 5 minutes; **b)** 10 minutes; **c)** 15 minutes. Given the pKa of N-terminal α-amino groups is significantly lower than the pKa of lysine side chain ε-amino groups, it is assumed that single modifications are N-terminal directed. A mixture of unsuccinylated, singly succinylated and doubly succinylated isoforms are observed for all 10 peptides examined. Data are the mean ± mean SD of three experimental replicates, which are in turn the mean ± SD of three technical replicates.

These data indicate that, as with carboxyl oxygen exchange, the rate of succinylation is peptide-specific. Each peptide examined exhibits varying degrees of single and double succinylation. There is no way to differentiate between N-terminal and side chain succinylation on the basis of precursor ion mass alone. However, given the reaction conditions, a singly succinylated peptide was assumed to have been N-terminally modified whilst a doubly succinylated peptide was assumed to also carry a lysine side chain modification. The validity of this assumption was confirmed by examining MS/MS sequence data using Mascot.

The variable succinylation seen in the 10 peptides across the three time points suggests that exclusive N-terminal modification of peptides whilst they are bound to solid phase is not feasible. The nature of the required modification state here contrasts with that required for C-terminal ^{18}O-labelling. With the latter it is necessary to drive the reaction to completion; here it is necessary to avoid doing so. All 10 peptides examined exhibit some degree of double succinylation even after 5 minutes. On the other hand, an appreciable fraction of 3 of the 10 peptides examined remained unmodified after 15 minutes, in spite of similar fractions of the same peptides also exhibiting double succinylation. Reducing the reaction time below 5 minutes may reduce the incidence of double succinylation but will likely also result in increased incidences of non-modification.

5.3.2.3. Peptides can be specifically guanidinated on lysine side chains whilst bound to a solid phase extraction column

If the ε-amino groups of lysine side chains could be blocked in some way prior to succinylation then N-terminal α-amino labelling could be driven to completion without having to worry about side reactions. One possible means of accomplishing this would be to derivatize lysine residues to homoarginine through guanidination with O-Methylisourea. This modification has previously been reported to be highly specific for the ε-amino group of lysine (Kimmel, 1967). More recently, Beardsley and Reilly have optimised the procedure for the reaction to the extent that it proceeds to completion in a matter of minutes (Beardsley and Reilly, 2002). This optimised procedure now forms the basis of a number of commercially available guanidination kits.

30µg aliquots of BSA peptides from an in-solution overnight digest were captured and desalted without elution on an SPE cartridge as described in section **5.3.2.2.** The immobilized peptides were then reacted with 1 M O-Methylisourea in 6.67% ammonia solution at 65ºC for 10, 20 or 30 minutes. Continuous flow of reagent through the SPE cartridge was facilitated through the vapour pressure generated by the ammonia when the top end of the cartridge was capped. Upon completion of the reaction, excess reaction buffer was aspirated from the cartridge and the peptides were washed for a second time and finally eluted. All reactions were subsequently analysed by LC-MS and the extent of guanidination at the three different time points evaluated as described in section **5.3.3.2.** A summary of the results is shown in **Fig. 38**.

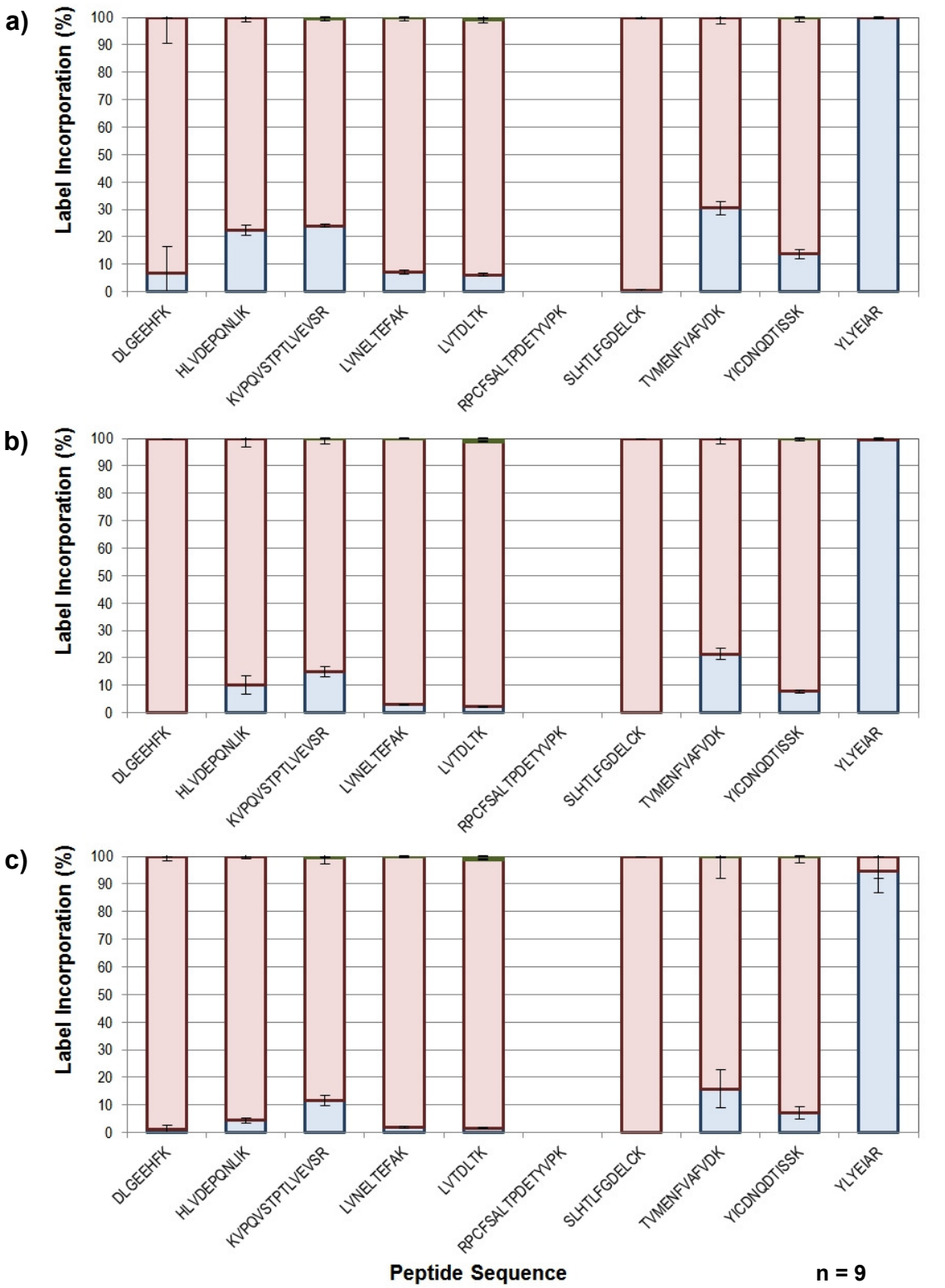

Figure 38: Guanidination of 10 BSA peptides when reacted with ~1 M O-Methylisourea in 6.67% ammonia (pH ~11) at 65ºC for **a)** 10 minutes; **b)** 20 minutes; **c)** 30 minutes. The reaction has previously been reported to be highly specific for the ε-amino group of lysine and thus it is assumed that single modifications are lysine-directed. 8 of the 9 lysine-containing peptides examined are at least 85% derivatized after 30 minutes whilst the non-lysine containing peptide remains largely unmodified. Data are the mean ± mean SD of three experimental replicates, which are in turn the mean ± SD of three technical replicates.

These results support the reported literature that the guanidination reaction catalysed by O-Methylisourea is highly specific for lysine. The potential for N-terminal side-reactivity was taken into account but none of the peptides examined by MS/MS exhibited any double guanidination. After 30 minutes, all 8 lysine-containing peptides are at least 85% guanidinated whilst the non-lysine-containing peptide remains unmodified. Interestingly, the peptide with sequence 'RPCFSALTPDETYVPK' could not be detected at all in any of the biological or technical replicates at any of the time points. It is not clear why this is the case since guanidination is widely accepted to enhance the detection of lysine-containing peptides (Beardsley *et al.*, 2000).

5.3.2.4. Guanidination of lysine side chains renders subsequent succinylation N-terminal specific

The final step in optimising N-terminal succinylation of peptides was to perform the reactions described in sections **5.3.2.3.** and **5.3.2.2.** sequentially. 30µg aliquots of BSA peptides from an in-solution overnight digest were captured and desalted as previously described. Desalted peptides were guanidinated for 30 minutes; desalted a second time; succinylated for 15 minutes; and desalted a final time before elution. All reactions were subsequently analysed by LC-MS. All potential modification states of the 10 BSA peptides examined throughout were taken into account when evaluating the N-terminal specificity of labelling. Results are shown in **Fig. 39**.

These data suggest that guanidination of lysine residues prior to succinylation is an effective means of ensuring that the second of the two reactions remains N-terminal specific. Of the 10 BSA peptides examined, the majority of those which contain lysine are detected with a mass consistent with both lysine derivatization and N-terminal succinylation. The majority of peptides examined which do not contain lysine are detected with a mass consistent with N-terminal succinylation alone.

It is worth noting that a significant fraction of this latter one peptide ('YLYEIAR') was also detected with a mass consistent with two succinyl groups. This was puzzling given the peptide does not contain a lysine residue. Scrutiny of the b-ion series in the product ion scan of this doubly succinylated peptide revealed that both succinylation events were localized to the N-terminus **(Fig. 40)**.

Succinic anhydride side-reactions with tyrosine phenolate side-chains have previously been reported (Hermanson, 2008) and it may be that this particular residue on this particular peptide is more reactive than usual in this regard. Tyrosine is one of the less common amino acids (with an occurrence in proteins of just 3% (http://www.ncbi.nlm.nih.gov/Class/Structure/aa/aa_explorer.cgi)) and the other N-terminal tyrosine peptide examined does not exhibit the same behaviour; thus this is unlikely to present a significant caveat to quantitation.

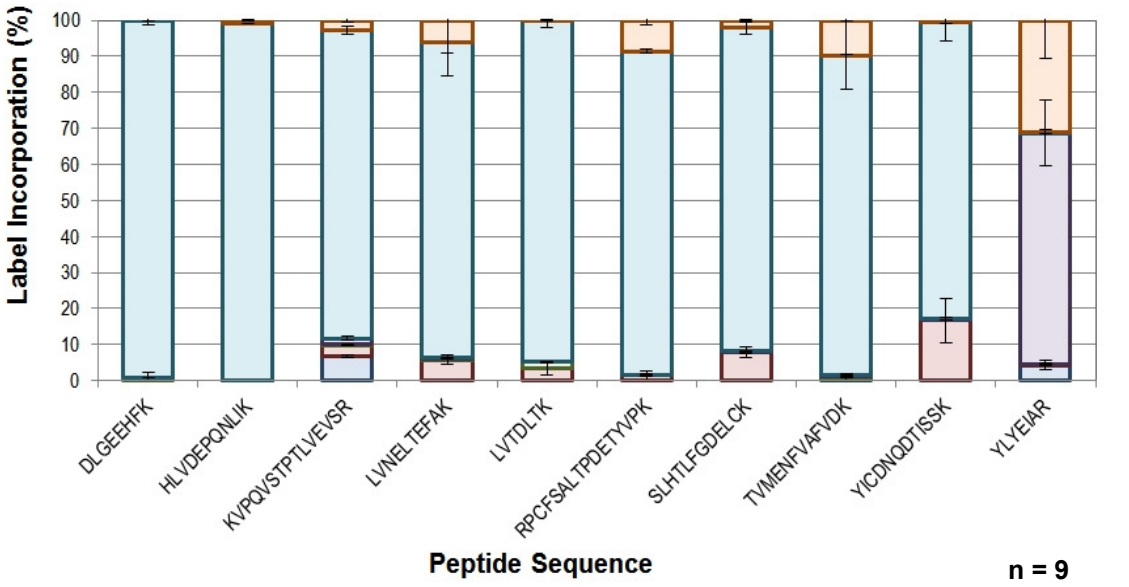

Figure 39: Modification states of 10 BSA peptides when reacted with ~1 M O-Methylisourea in 6.67% ammonia (pH ~11) at 65ºC for 30 minutes and subsequently reacted with 20 mM succinic anhydride in 200 mM sodium acetate / 20 mM sodium hydroxide (pH 7.6) for 15 minutes. At least 82% of all 9 lysine-containing peptides examined exhibit a mass consistent with lysine derivatization and N-terminal succinylation. A significant proportion of the peptide with sequence YLYEIAR exhibits a mass consistent with double succinylation in spite of not having any lysine residues. Data are the mean ± mean SD of three experimental replicates, which are in turn the mean ± SD of three technical replicates.

Figure 40: Mascot fragmentation data of the peptide with sequence YLYEIAR and a mass consistent with **a)** single succinylation; **b)** double succinylation. The b-series ions (highlighted) confirm that both modifications in the doubly succinylated peptide are localized to the N-terminus.

a)

#	a	a^{++}	b	b^{++}	b^{0}	b^{0++}	Seq.
1	236.0917	118.5495	**264.0866**	132.5470			Y
2	349.1758	**175.0915**	**377.1707**	189.0890			L
3	512.2391	256.6232	**540.2340**	270.6207			Y
4	641.2817	321.1446	**669.2766**	335.1420	651.2661	326.1367	E
5	754.3658	**377.6865**	782.3607	391.6840	764.3501	382.6787	I
6	825.4029	413.2051	**853.3978**	427.2025	835.3872	418.1973	A
7							R

b)

#	a	a^{++}	b	b^{++}	b^{0}	b^{0++}	Seq.
1	336.1078	168.5575	***364.1027***	182.5550			Y
2	449.1918	225.0996	***477.1868***	239.0970			L
3	612.2552	306.6312	***640.2501***	320.6287			Y
4	741.2978	371.1525	***769.2927***	385.1500	751.2821	376.1447	E
5	854.3818	427.6946	***882.3767***	441.6920	864.3662	432.6867	I
6	925.4189	463.2131	***953.4139***	477.2106	935.4033	468.2053	A
7							R

5.3.2.5. Optimised protocol for N-terminal succinylation of peptides

The data presented in section **5.3.2.4.** suggest that N-terminal specific modification of peptides with succinic anhydride can be achieved through first derivitizing lysine residues to homoarginine. This prevents concomitant lysine side chain modification during the succinylation reaction itself. The optimised protocol is presented in full in section **3.4.3.**

5.3.2.6. Examination of the ability of isobaric peptide termini labelling employing both N-terminal succinylation and C-terminal ^{18}O labelling to quantify differences between labelled and unlabelled BSA and proteomic peptides across a wide dynamic range

It was next necessary to combine the newly optimised N-terminal succinylation method with the previously optimised C-terminal ^{18}O labelling method and examine whether using the two in tandem addressed the issues with accuracy and dynamic range of quantitation observed when using ^{18}O labelling alone.

30µg aliquots of proteomic peptides from an in-solution overnight digest of Jurkat whole cell lysate were ^{18}O labelled as described in section **3.4.2.** Reduced/alkylated labelling reactions were acidified with 1/10th volume 10% TFA and processed using the optimised N-terminal succinylation procedure detailed in section **3.4.3.** Peptides which had been ^{18}O-labelled were succinylated using normal succinic anhydride whilst peptides which had not been ^{18}O labelled were succinylated using $^{13}C_4$ succinic anhydride. These isobarically labelled peptides were reconstituted in 200 µl 0.2% FA. Labelled and unlabelled peptides were then combined according to the scheme shown in **Table 7**.

Ratio
SA ($^{13}C_4$) - ^{16}O
[SA ($^{13}C_4$) -^{16}O] 20:1 [SA ($^{12}C_4$) - ^{18}O]
[SA ($^{13}C_4$) -^{16}O] 10:1 [SA ($^{12}C_4$) - ^{18}O]
[SA ($^{13}C_4$) -^{16}O] 5:1 [SA ($^{12}C_4$) - ^{18}O]
[SA ($^{13}C_4$) -^{16}O] 2:1 [SA ($^{12}C_4$) - ^{18}O]
[SA ($^{13}C_4$) -^{16}O] 1:1 [SA ($^{12}C_4$) - ^{18}O]
[SA ($^{13}C_4$) -^{16}O] 1:2 [SA ($^{12}C_4$) - ^{18}O]
[SA ($^{13}C_4$) -^{16}O] 1:5 [SA ($^{12}C_4$) - ^{18}O]
[SA ($^{13}C_4$) -^{16}O] 1:10 [SA ($^{12}C_4$) - ^{18}O]
[SA ($^{13}C_4$) -^{16}O] 1:20 [SA ($^{12}C_4$) - ^{18}O]
SA ($^{12}C_4$) - ^{18}O

Table 7: Scheme for combining differentially labelled proteomic peptides to examine whether isobaric peptide termini labelling is suitable for performing quantitative proteomic analyses.

Combined samples were analysed using LC-MS. Raw data were processed, searched and quantified within Mascot itself. Protein quantitation reports were screen scraped directly from Mascot protein summary reports. Peptide quantitation reports were exported from Mascot MS/MS search as CSV files. Both sets of reports were imported into Microsoft Excel for further data processing and Box and whisker plots generated as described in section **5.2.2.6.** Uncombined samples were not included in the plots but were analysed to verify that both labelling reactions had gone to completion.

The distribution of reported protein ratios computed from the combined proteomic samples is shown in **Fig. 41a**, whilst the distribution of reported peptide ratios is shown in **Fig. 41b**. In comparison with the data shown in **Figs. 32, 34 and 35**, these reported protein and peptide ratios approximate much more closely to the actual ratios in which the differentially labelled samples were combined. In both cases, the reported ratios within the first and third quartiles fall very close to the expected ratio when the samples are combined in ratios ranging from 5:1 to 1:5. In contrast to the ^{18}O-labelling data, inclusion of 95% of reported ratios surrounding the median for these combinations does not introduce any extreme outliers. At combination ratios of 10:1 and 1:10, the accuracy of reported ratios begins to diminish slightly and there is a general 'ratio compression' effect where reported ratios tend to underestimate the true combination ratio. This effect becomes more pronounced at combination ratios of 20:1 and 1:20, with neither median reported ratio here being more than 10:1 or 1:10. Nevertheless, this is still a considerable improvement in accuracy and dynamic range of quantitation.

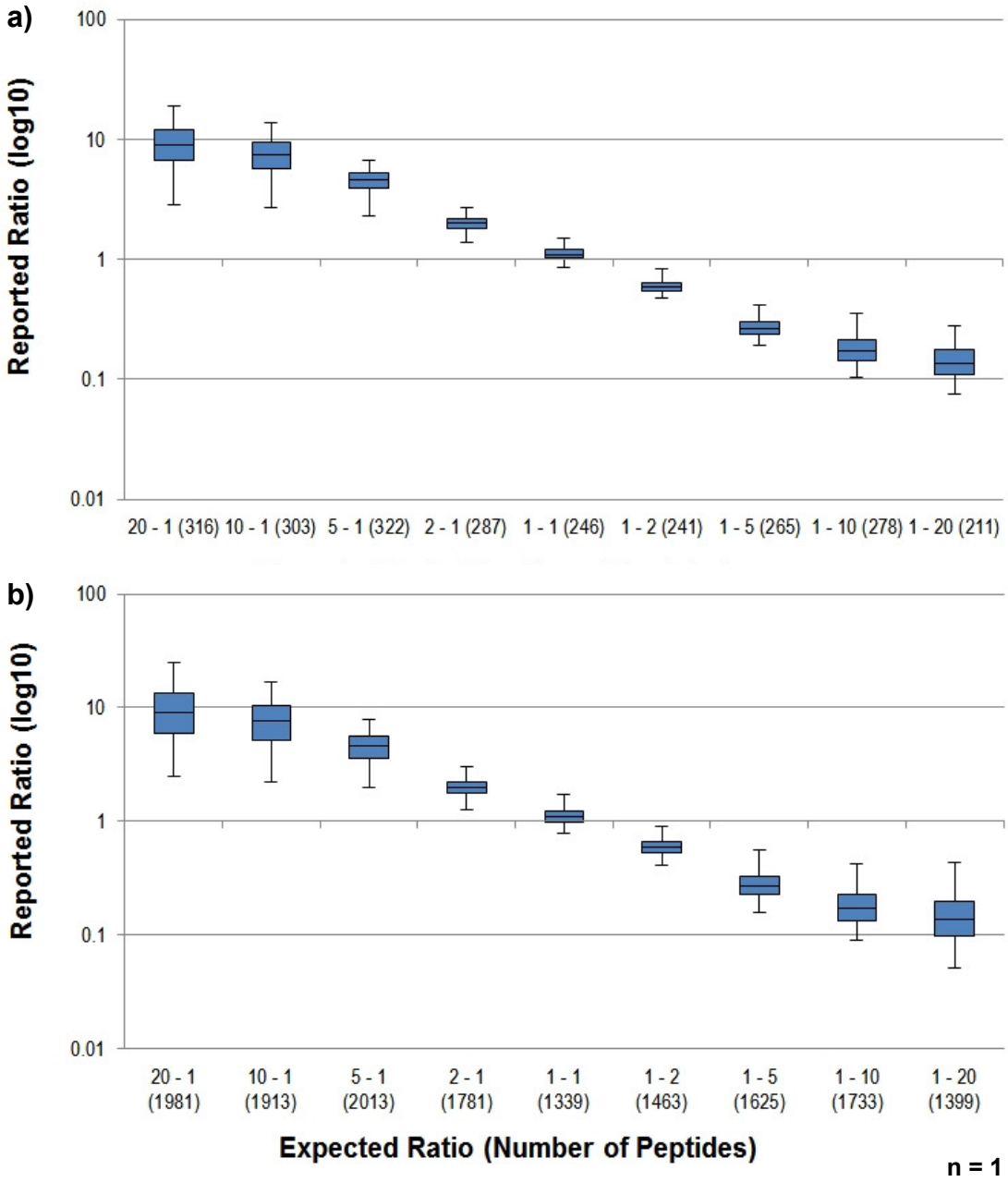

Figure 41: Box and whisker plot showing distribution of **a)** protein ratios; **b)** peptide ratios reported by Mascot when $^{13}C_4$-succinylated and $^{12}C_4$-succinylated / ^{18}O-labelled proteomic peptides derived from Jurkat whole cell lysate are combined in ratios ranging from 20:1 through to 1:20. 50% of reported ratios are contained within the boxes and 95% are contained within the whiskers. The number of peptides detected across 1 replicate is shown in brackets on the X-axis.

In conclusion, the IPTL-based quantitative strategy presented here is well-suited for quantitative proteomics applications. First and foremost, it conforms to the two criteria specified at the beginning of the chapter. Label incorporation has been optimised for both C-terminal ^{18}O labelling and N-terminal-specific succinylation and differences in abundance between differentially labelled samples are accurately reported up to around one order of magnitude in each direction. Labelling is carried out at the peptide level, enabling scrutiny of samples which could not be analysed using metabolic labelling approaches. The collective cost of all labelling reagents is also relatively inexpensive in comparison to commercially available alternatives; the total cost of differentially labelling two 30 µg samples for comparison should not exceed £10.

IPTL is akin to more widely used isobaric peptide labelling methods such as iTRAQ and TMT where quantitation is performed in the product ion scan, circumventing the issues detailed in section **5.2.2.6.** pertaining to precursor scan quantitation. This is seen not only in the increased dynamic range of quantitation relative to ^{18}O-labelling, but also in the considerable increase in protein and peptide identifications. The isobaric nature of the differentially labelled peptides does not result in increased precursor scan complexity and the ion current is not negatively affected because peptides of identical sequence in each sample have (effectively) identical masses.

However, IPTL-based quantitation also possesses novel characteristics which set it apart from iTRAQ and TMT. Quantitation is performed on pairs of differentially labelled N- and C- terminal peptide fragments spanning the entire MS2 spectrum rather than on single reporter ions detected in the low mass region of the spectrum (see **Fig. 36** above). The technique is thus compatible with ion trap mass spectrometers in which the '1/3 parent mass cut-off rule' precludes use of the iTRAQ and TMT reagents and therefore is more generally applicable. In addition, reported peptide ratios are composites of relative quantitation of many pairs of peptide fragments, increasing the confidence in the accuracy of the ratio. Finally, the ratio calculations are by definition peptide-specific and therefore less likely to be skewed by the mixed 'MS/MS' phenomenon seen in iTRAQ and TMT, where isobarically tagged peptides with different sequences but commensurate mass and retention times are fragmented simultaneously (Ow *et al.*, 2009).

This particular IPTL-based method possesses further features which set it apart from the original method. Koehler *et al*. introduce their C-terminal modification through dimethylation after N-terminal succinylation. Consequently, only C-terminal lysine residues are modified and peptides with a C-terminal arginine residue cannot be used for quantitation. The fact that this method utilizes trypsin-catalysed C-terminal ^{18}O labelling enables all tryptic peptides (other than C-terminal peptides) to be labelled and contribute to quantitation. Just recently Yang *et al*. published a further IPTL-based method in which ^{18}O-labelling is used to introduce the C-terminal modification and peptides are subsequently guanidinated prior to N-terminal dimethylation with formaldehyde or dideuterated formaldehyde (Yang *et al.*, 2012). However, this reaction scheme does not allow for the use of a ^{13}C isotope of formaldehyde and (as discussed in section **1.1.4.1.1.**) deuterium is known to affect retention time in RPLC, potentially complicating quantitation (Zhang *et al.*, 2001).

An addition novel feature of this method is that the N-terminal labelling step is performed whilst peptides are immobilized on C18 reversed phase as opposed to in solution. Stable isotope labelling of peptides generally requires the sample to be desalted and dried *in vacuo* prior to the labelling step. This drying step is known to be responsible for substantial sample losses through adsorption of peptides to laboratory plastics (Speicher *et al.*, 2000). If C-terminal ^{18}O labelling, lysine derivatization and N-terminal succinylation were all to be carried out in solution, this would require three separate rounds of desalting and drying. Performing the N-terminal modifications on a single reversed phase 'mini-reactor' reduces this to just one desalting and drying cycle. Peptide modification on C18 had previously been reported for applications outside the field of quantitative proteomics (Conrotto and Hellman, 2005; Cindric *et al.*, 2006; Nika *et al.*, 2012; Nika *et al.*, 2013a; Nika *et al.*, 2013b), however to our knowledge it has not previously been employed in a stable isotope labelling-based relative quantitative proteomics workflow.

Chapter 6. Evaluation of the suitability of OFFGEL fractionation and StageTip-based SAX fractionation as the first dimension of separation for analysis of complex mixtures of proteomic peptides

6.1. Introduction

The rate of development of liquid chromatography and mass spectrometry instrumentation over the past decade has resulted in shotgun-based proteomics far surpassing 2D electrophoresis as the approach of choice for discovery experiments (Lopez, 2007). However, proteomic samples processed using shotgun approaches are frequently too complex to analyse comprehensively in one LC-MS run incorporating a single dimension of reversed phase peptide separation. Reduction in complexity therefore necessitates pre-fractionation of proteomic peptides on the basis of some physicochemical property other than the hydrophobicity relied upon for RP-HPLC.

Pre-fractionation was initially achieved using GeLC-MS (Blagoev *et al.*, 2004), a workflow in which proteins are first separated by size on a 1D-PAGE gel. The gel itself is then sliced into fractions and each fraction subjected to in-gel digestion. Pre-fractionation can also be performed on-line at the peptide level using Multi-Dimensional Protein Identification Technology (MuDPIT) (Wolters *et al.*, 2001) In the wider context of this particular project, using GeLC-MS would necessitate the proteins in each slice being digested then differentially N- and C- terminally labelled individually before being recombined, substantially increasing both the time taken to perform the labelling steps of the workflow and the quantity of labelling reagents required. The LC setup required to perform MuDPIT online was not in routine use in the lab at the time of onset of the project.

Two alternatives which were investigated given the nature of the overall workflow were liquid-phase isoelectric focussing (Horth *et al.*, 2006) and StageTip-based offline anion-exchange chromatography (Wisniewski *et al.*, 2009a). Both techniques have been employed in recent years as the first dimension of multidimensional peptide separation schemes by the highly regarded Mann lab at Max Planck Institute in Martinsried. In evaluating the suitability of each technique for fractionation in practice, it is important to consider three criteria: the number of peptides identified in each fraction, the uniformity of peptide identification frequency across all fractions and the efficiency of the fractionation itself (i.e. the number of fractions in which discrete peptides are identified).

6.2. OFFGEL Fractionation

Liquid-phase isoelectric focussing was first established in 2006 with the introduction of the Agilent OFFGEL Fractionator (Horth *et al.*, 2006). Optimal conditions for peptide focussing using the fractionator have since been comprehensively evaluated by Hubner *et al.* (Hubner *et al.*, 2008). The results from this study were: -

1. OFFGEL fractionation compares favourably to (the *de-facto*) GeLC-MS in terms of numbers of peptides and proteins identified from the same quantity of starting material.

2. Sampling rate and peptide identification decrease with decreased peptide loading, whilst fractionation efficiency decreases with increased peptide loading. A good compromise is to load 50-100 µg of peptide for 12-well separations and 100-250 µg of peptide for 24-well separations.

3. The doubling of starting material and LC-MS analysis time necessitated by 24-well separations is not reflected in a concomitant doubling of peptide and protein IDs, yielding around 40% additional peptide IDs but less than 20% additional protein IDs. 12-well separations are thus recommended over 24-well separations.

At the time of onset of this project, OFFGEL fractionation was routinely used in the lab as the first dimension of separation for proteomic studies and it was initially intended that it be used in this project as well.

6.2.1. Results

6.2.1.1. OFFGEL Fractionation can be used as the first dimension of separation for ^{18}O-based quantitative proteomic experiments.

The first instance in which OFFGEL fractionation was utilised in this project was after optimization of ^{18}O-labelling reaction conditions but before the limitations of ^{18}O-based quantitative proteomics discussed in the previous chapter were fully appreciated. ^{18}O-labelling of a given peptide should not alter its isoelectric point. Thus OFFGEL fractionation was employed as the first dimension of separation in an ^{18}O-based quantitative proteomic comparison of the whole proteomes of mature and tolerogenic DCs. Approximately 50 µg of unlabelled mature DC proteomic peptides were combined with approximately 50 µg of ^{18}O-labelled tolerogenic DC proteomic peptides and fractionated into 12 wells across a pH 3 – 10 IPG strip. Upon completion, individual fractions were recovered from the wells, acidified with 1% (v/v) TFA, tip desalted and analysed by LC-MS. Raw data files were concatenated, processed, searched and quantified using Mascot Distiller. Peptide quantitation reports were generated and imported into Microsoft Excel for further data analysis.

The numbers of total peptides and unique peptides (i.e. total number of peptides of unique sequence) identified per well is shown in **Fig. 42a**, whilst the redundancy of unique peptide identification across all 12 wells is shown in **Fig. 42b & Fig. 42c**. In terms of uniformity and efficiency of fractionation, these data are comparable to those reported by Hubner *et al.* The variability in total number of peptides per well is somewhat similar. The two wells ranked 1st and 2nd in terms of total number of peptides detected in this study (wells 5 and 2) were ranked 2nd and 3rd in the published study, whilst the two wells ranked 11th and 12th (wells 9 and 10) were the same for both studies. However, notably fewer peptides were detected in wells 1, 4 and 7 in this study. This disparity is particularly pronounced for well 1, which ranked 9th here but 1st in the published study. This may be because very little liquid was recovered from well 1 in my experiments. The fractionation efficiency in this study is significantly higher than that reported by Hubner *et al*., with 89% of unique peptides identified detected in a single well in the former and 56% in the latter. The two experiments are not directly comparable in this respect as blanks were run between every fraction in this LC-MS experiment whilst Hubner *et al.* appear to have run all 12 fractions

consecutively. The numbers of peptides identified in each fraction is significantly higher in the published study and the total number of peptides is around five times as high. The column lengths and gradient times are similar (20 cm vs. 15 cm; 85 minutes vs. 105 minutes). However, on the basis of their methods (and assuming equal peptide recovery post-fractionation in both studies), Hubner *et al*. appear to have injected around 4 times as much material per LC-MS run as was injected here; and different LC-MS instrumentation and software was used for data acquisition and analysis. Both of these factors may go some way to explaining this disparity. Nevertheless, overall the data suggests that OFFGEL fractionation is a suitable means of pre-fractionation for ^{18}O-based quantitative proteomic workflows.

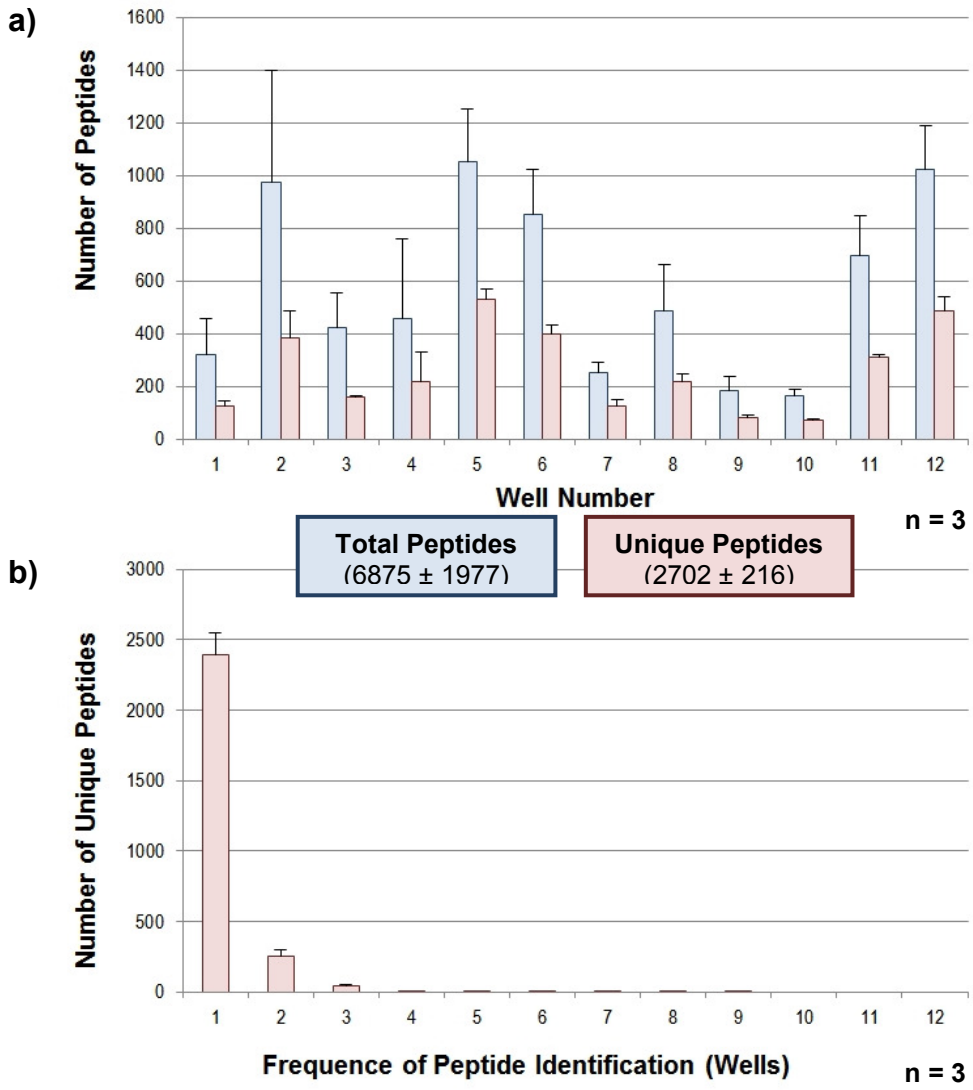

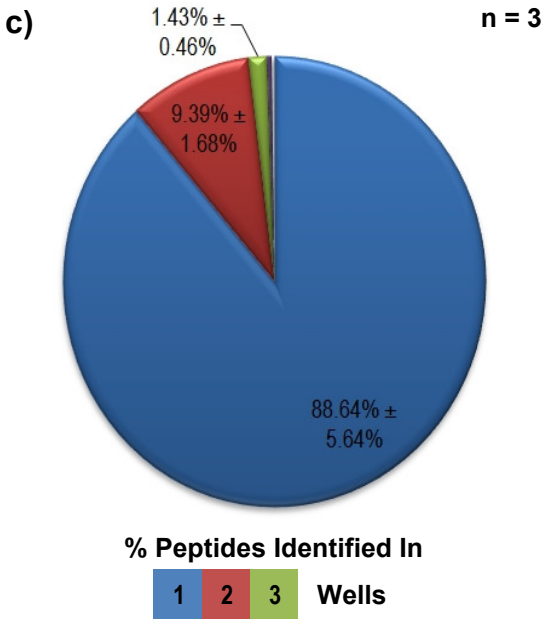

Figure 42: OFFGEL fractionation of ~50 µg peptides derived from an unlabelled mature DC whole cell lysate combined 1:1 with ~50 µg peptides from an ^{18}O-labelled tolerogenic DC whole cell lysate and fractionated on a pH 3-10 IEF strip. **a)** Total and total unique peptides identified in each well; **b) & c)** Redundancy of unique peptide identification across all 12 wells represented as a bar graph and a pie chart respectively. Error bars are calculated from three technical replicates. The peptides fractionate across the entire pH gradient (though some wells contain considerably more peptides than others) and ~89% of all unique peptides are detected in one well only.

6.2.1.2. OFFGEL Fractionation is less effective when used as the first dimension of separation for IPTL-based quantitative proteomic experiments.

As aforementioned, the limitations of ^{18}O-based quantitative proteomics were only fully appreciated after acquisition of the data discussed in the previous chapter. The subsequent addition of the N-terminal labelling step to the stable isotope labelling strategy resulted in the introduction of two further peptide modifications. Lysine derivatization should not change the net charge of a peptide. However, in converting the α-amino group from basic to acidic, N-terminal succinylation will do so (Klapper and Klotz, 1972). This might be expected to affect the uniformity of fractionation across a pH 3 – 10 IPG strip and cause peptides to focus in a more narrow range, migrating towards the acidic end of the strip.

The extent of this effect was revealed when first using OFFGEL fractionation to separate approximately 50 µg of differentially IPTL-labelled and combined mature and tolerogenic DC proteomic peptides. The numbers of total and unique peptides identified per well and the redundancy of unique peptide identification across all 12 wells are shown in **Figs. 43a – 43c**. Uniformity of fractionation is markedly compromised in comparison to the fractionation described in section **6.2.1.1.**, with negligible peptide identifications reported in the wells corresponding to the neutral and basic areas of the strip (wells 5 – 12). In addition, very few peptides are identified in well 3. It is not clear why this is the case given approximately 80% of the peptides identified across all twelve wells are found in the two neighbouring wells The issue may be related to downstream processing and analysis of this particular fraction rather than a peculiarity of the focussing procedure, though there have previously been anecdotal reports of batch-to-batch variation in IPG strips and ampholytes. Fractionation efficiency remains high, with 90% of unique peptides identified detected in a single well. However, given the relative paucity of wells in which significant numbers of peptides are detected at all, this is perhaps a trivial observation.

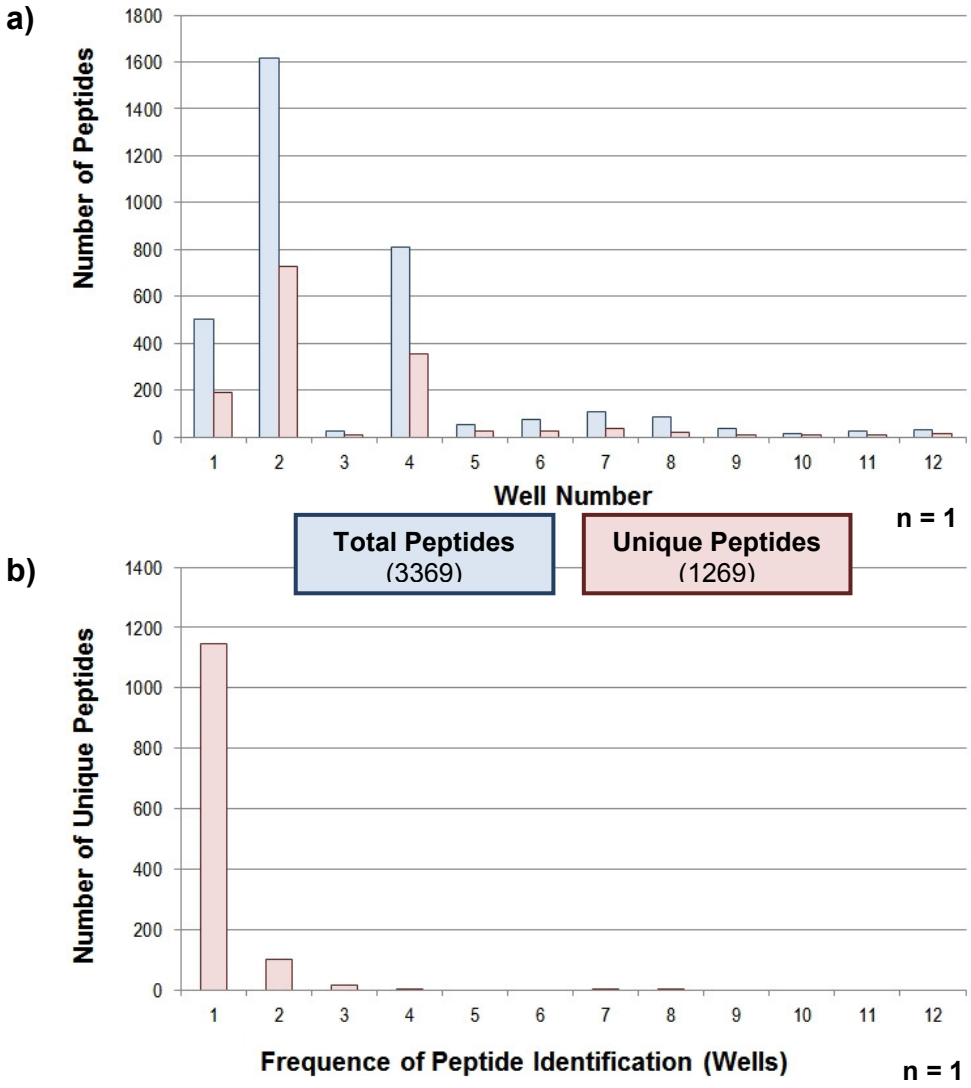

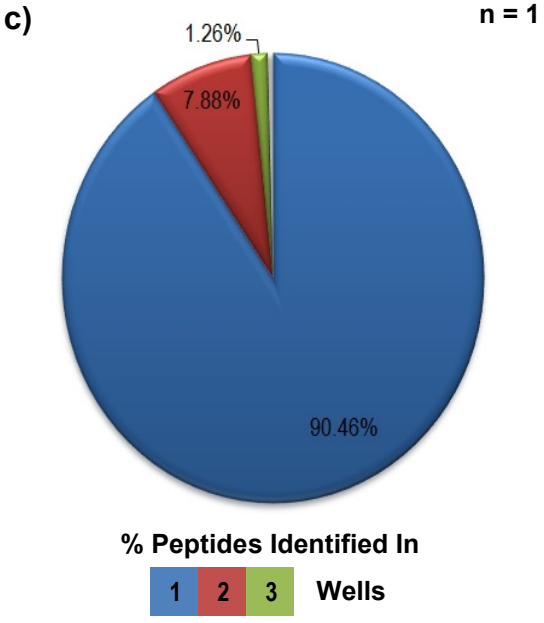

Figure 43: OFFGEL fractionation of peptides derived from a $^{13}C_4$-succinylated mature DC whole cell lysate combined 1:1 with a $^{12}C_4$-succinylated / ^{18}O-labelled tolerogenic DC whole cell lysate and fractionated on a pH 3-10 IEF strip. **a)** Total and total unique peptides identified in each well; **b) & c)** Redundancy of unique peptide identification across all 12 wells represented as a bar graph and a pie chart respectively. Once again, ~90% of all unique peptides are detected in one well only. However, the peptides seem to preferentially fractionate to the acidic end of the IPG strip. This is likely due to the fact that the peptides have been succinylated.

In light of these data, it was clear that OFFGEL fractionation with full range pH 3 – 10 IPG strips would be inadequate for effective pre-fractionation of IPTL-labelled peptides prior to LC-MS analysis. One potential means of counteracting the more acidic focussing range of succinylated peptides would be to use an IPG strip with a narrower pH range. At the time, the principle supplier of IPG strips for use with the OFFGEL instrument (GE Healthcare) did not offer strips with the desired pH range. However, another supplier (Bio-Rad) offered strips with a suitable pH range (pH 3 – 10) together with a published workaround (Berkelman *et al.*, 2011) which consisted of the removal of a single well from the end of an OFFGEL 12 well frame assembly to enable these strips to be used with the OFFGEL device in spite of being slightly too short.

The fractionation described in section **6.2.1.2.** was thus repeated using the Bio-Rad IPG strips and the aforementioned workaround. Numbers of total and unique peptides and redundancy of unique peptide identification across all wells are plotted as previously in **Figs. 44a – 44c**. After fractionation, no liquid was recovered from the 11th well; the data shown are therefore for wells 1 – 10 only. Uniformity of fractionation is only slightly improved relative to the separation described in section **6.2.1.2.** Over 16000 total peptides are identified in wells 1 – 5 (corresponding to the acidic half of the strip). However, very few peptides are identified in wells 6 – 10 (corresponding to the basic half of the strip). IPTL peptides fractionated on a pH 3 – 10 strip **(Fig. 43)** appeared to focus in wells 1 – 4 (save for well 3), which corresponds to a pH range of 3 – 5.33. With this in mind, we might expect IPTL peptides fractionated on a pH 3 – 6 strip to focus in the first eight or nine of the eleven wells rather than just five. One possible explanation for this is that whilst the IPG strip used here had a pH range of 3 – 6, the ampholytes used in the focussing buffer had a broader range of 3 – 10. It has since been suggested that uniformity of fractionation could be further improved through using ampholytes with a narrower and more acidic pH range (Bio-Rad, personal communication). However, an ampholyte solution corresponding precisely to the pH range of the strip itself is not available.

In addition, fractionation efficiency is substantially reduced in comparison to the separations shown in **Fig. 42 & Fig. 43**. Only 60% of unique peptides identified are detected in a single well, with 16%, 8%, 8% and 6% of unique peptides being detected in 2, 3, 4 and 5 wells respectively, Whilst these figures are

comparable to those reported by Hubner *et al*., it is worth noting that the latter study reports identification of significant numbers of peptides in every fraction and (as previously discussed) all twelve LC-MS fractions were run consecutively; neither of which can be said of this particular separation. The reasons for this poorer focussing are unclear, but may be due to incompatibility issues between the OFFGEL instrument and the Bio-Rad IPG strips and ampholytes.

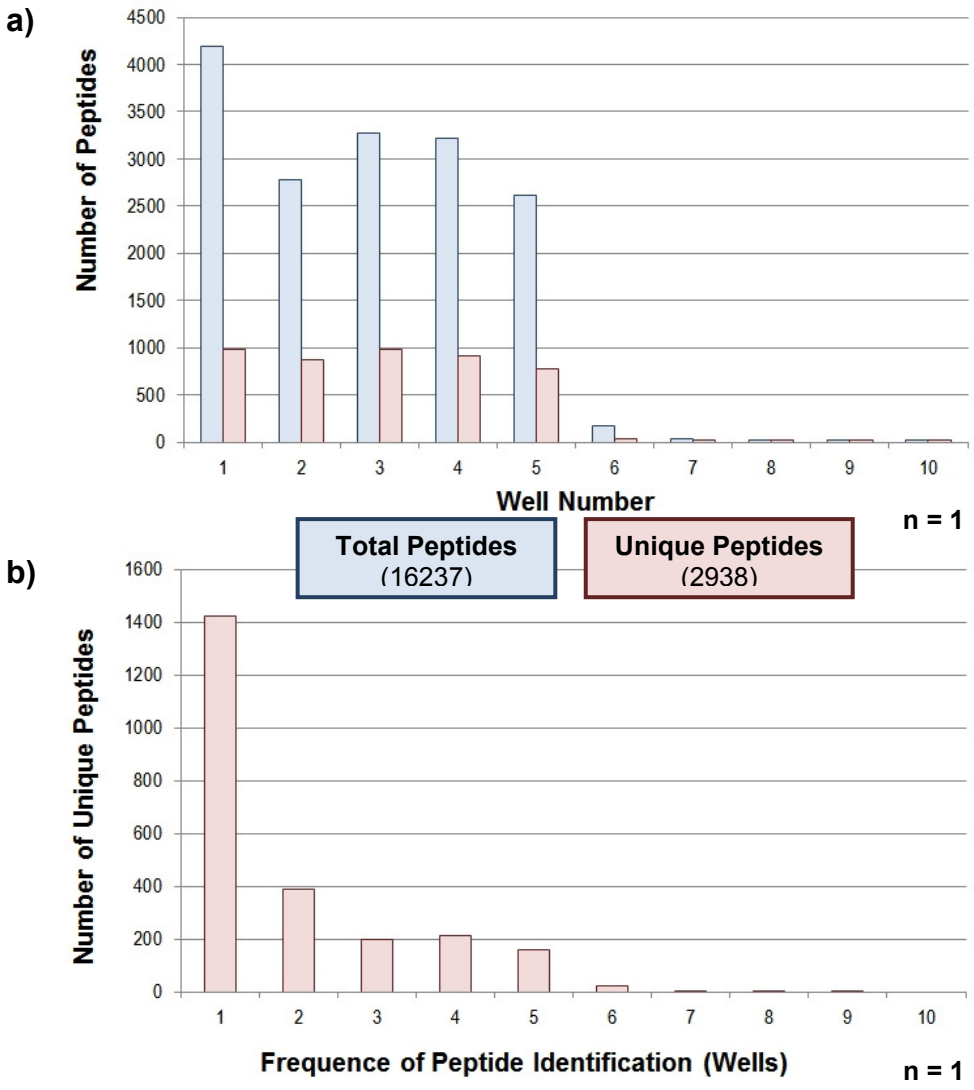

Figure 44: OFFGEL fractionation of peptides derived from a $^{13}C_4$-succinylated mature DC whole cell lysate combined 1:1 with a $^{12}C_4$-succinylated / ^{18}O-labelled tolerogenic DC whole cell lysate and fractionated on a pH 3-6 IEF strip. **a)** Total and total unique peptides identified in each well; **b) & c)** Redundancy of unique peptide identification across all 10 wells represented as a bar graph and a pie chart respectively. The acidic IEF strip slightly improves focussing range of succinylated peptides. However, fractionation efficiency is significantly lower, with ~60% of unique peptides detected in one well only. This may be due to incompatibility of this IEF strip with the OFFGEL fractionator.

6.3. StageTip-based SAX Fractionation

In spite of the recommendation to use ampholytes with a complimentary pH range to that of the pH 3 – 6 IPG strip to focus IPTL peptides, it was decided at this point to explore alternative means of fractionation. An additional impetus for doing so was the lengthy and unpredictable run times observed for each OFFGEL separation (nearly two days in one instance).

A year after the publication of the Hubner *et al.* OFFGEL paper, Wisniewski *et al.* published a further paper (Wisniewski *et al.*, 2009a) in which they described a novel MuDPIT-type offline anion-exchange method for peptide fractionation based on the StageTip method originally conceived for sample desalting prior to LC-MS analysis (Rappsilber *et al.*, 2003). In this method, peptides are resuspended in pH 11 Britton-Robinson (BR) buffer, bound to anion exchange resin housed within a pipette tip and eluted stepwise with BR buffers of decreasing pH values. Wisniewski *et al.* report that whilst this separation scheme is slightly inferior to OFFGEL fractionation in terms of redundancy across fractions; its speed, simplicity and reproducibility make it a desirable alternative.

6.3.1. Results

6.3.1.1. Evaluation of StageTip-based SAX fractionation as an alternative to OFFGEL Fractionation for first-dimensional separation of succinylated peptides

Though isoelectric focussing and ion exchange chromatography are distinct separation strategies, both share a common mode in separating molecules on the basis of charge state. With this in mind, it was not clear whether the same difficulties experienced with OFFGEL fractionation of IPTL-labelled peptides would also be seen when using StageTip-based SAX fractionation, particularly since peptides are loaded at high pH and the first couple of elutions are at neutral pH or above. The technique was thus evaluated using unlabelled and succinylated proteomic peptides from a Jurkat whole cell lysate as opposed to material derived from mature and tolerogenic dendritic cells.

6.3.1.2. StageTip-based SAX fractionation is an effective alternative to OFFGEL Fractionation for the first dimension of separation of unmodified and succinylated peptides

Approximately 25 µg of unmodified Jurkat proteomic peptides and a similar quantity of succinylated Jurkat proteomic peptides were fractionated as described by Wisniewski *et al.* with a couple of notable exceptions. In the published study, the first elution is performed at pH 8 whereas we performed our first elution at pH 7, based on our experiences with IPG strips. Additionally, the last elution in the published study is performed at pH 3 whereas we included an addition elution step at pH2. All fractions and the pH 11 flow-through were acidified with 1% (v/v) TFA, tip desalted and analysed by LC-MS. Raw data were processed and searched within Mascot itself. Peptide reports were exported from Mascot as CSV files and imported into Microsoft Excel for further data processing.

The numbers of total and unique unmodified peptides identified per fraction is shown in **Fig. 45a**; whilst the redundancy of unique unmodified peptide identification across all seven fractions is shown in **Figs. 45b & 45c**. Corresponding data for succinylated peptides is shown in **Figs. 46a – 46c**.

The data for unmodified peptides are comparable to those reported by Wisniewski *et al.* and also compare favourably with the data shown in section **6.2.1.1.** for OFFGEL fractionation of a combination of unlabelled and ^{18}O-labelled peptides. The separation is considerably more uniform than the corresponding OFFGEL fractionation, with approximately 11000 peptides identified in the highest yielding fraction (pH 6) and approximately 6000 peptides identified in the lowest yielding fraction (pH 3). This uniformity and peptide identification frequency is also seen in the published study. As previously acknowledged, Wisniewski *et al*. suggest that fractionation efficiency may be slightly compromised in comparison to OFFGEL fractionation. However, approximately 77% of unique peptides identified here are only detected in a single fraction in spite of blanks not being run between the LC-MS fractions. This value is higher than that reported in the published study, where less than 50% of unique peptides identified were detected in a single fraction.

The data for succinylated peptides also compares favourably to those shown in section **6.2.1.2.** for OFFGEL fractionation of IPTL-labelled peptides. The separation is not as uniform as that seen for unmodified peptides, with notably fewer total peptide identifications from the pH4 and pH3 fractions. However, appreciable numbers of peptides are identified in every fraction and there are no fractions for which analysis would be deemed counterproductive on the basis of wasted instrument time. Total peptide identifications are markedly reduced in every fraction in comparison with the analogous unmodified fractions. This may be because peptides carrying an additional ~100 Da succinyl group (potentially two succinyl groups for many peptides since lysine residues were not derivatized in this particular experiment) are less likely to fly well than their unmodified counterparts. As with unmodified peptides, fractionation efficiency remains favourably high (approximately 81% of unique peptides detected in a single fraction).

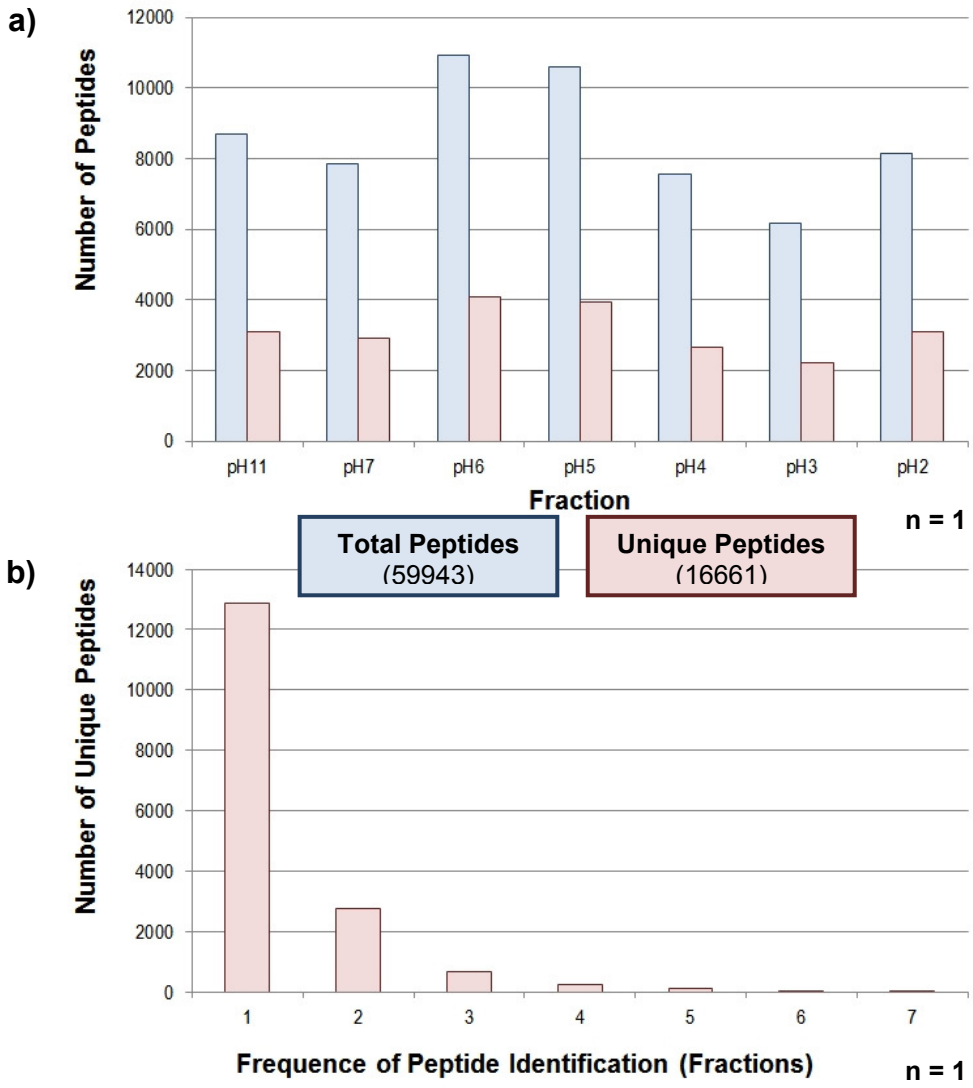

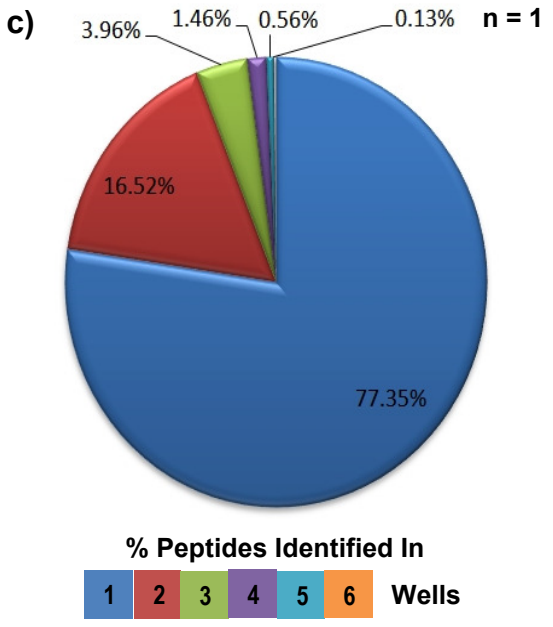

Figure 45: First StageTip-based SAX fractionation of 25 µg unlabelled peptides derived from a Jurkat whole-cell lysate. **a)** Total and total unique peptides identified in each fraction; **b) & c)** Redundancy of unique peptide identification across all 7 fractions represented as a bar graph and a pie chart respectively. The data suggest that StageTip-based SAX fractionation is an effective alternative to OFFGEL fractionation for unlabelled peptides. High numbers of peptides are identified in each fraction and ~77% of all unique peptides are detected in one well only in spite of blanks not being run between SAX fractions.

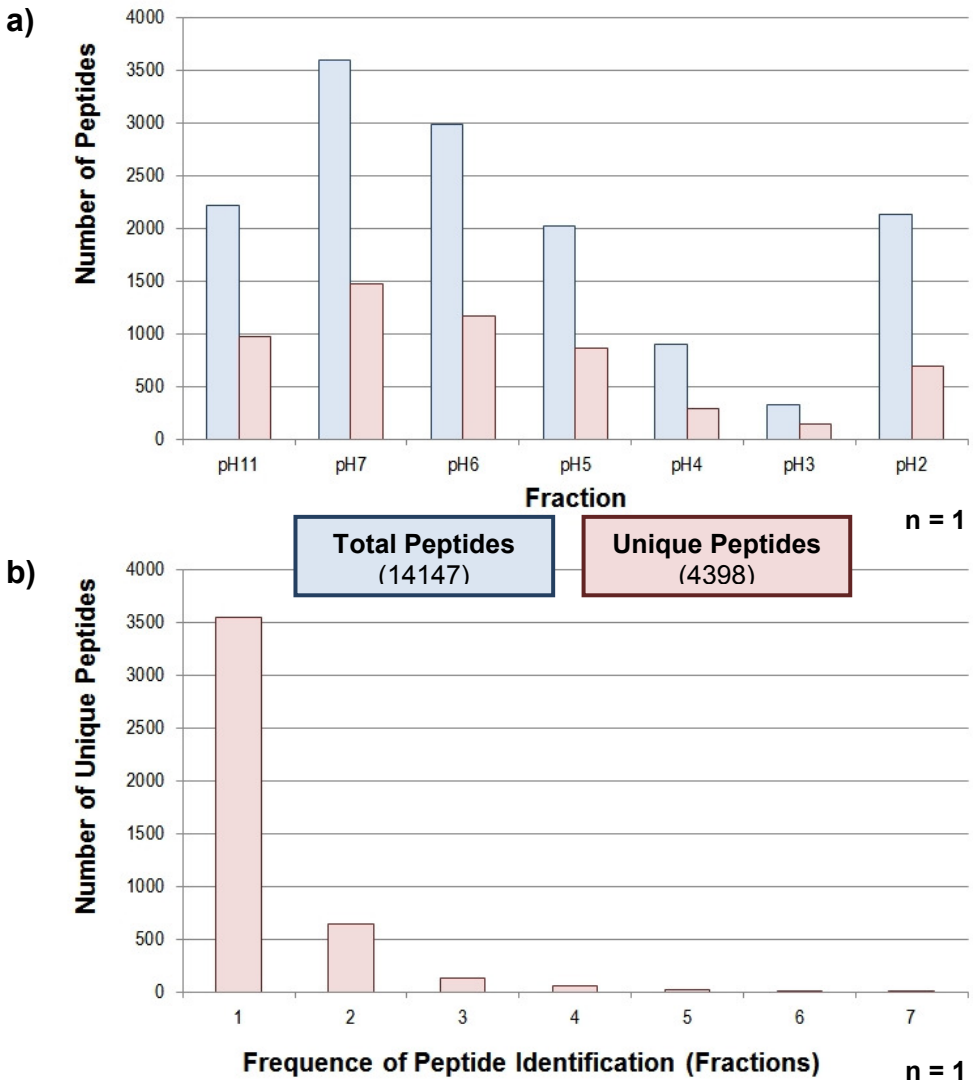

Figure 46: First StageTip-based SAX fractionation of 25 µg succinylated peptides derived from a Jurkat whole-cell lysate. **a)** Total and total unique peptides identified in each fraction; **b) & c)** Redundancy of unique peptide identification across all 7 fractions represented as a bar graph and a pie chart respectively. The data suggest that StageTip-based SAX fractionation can alleviate the pitfalls observed with OFFGEL fractionation for succinylated peptides. Appreciable numbers of peptides are identified in each fraction and ~81% of all unique peptides are detected in one well only in spite of blanks not being run between SAX fractions.

6.3.1.3. Peptides bound to anion exchange resin in StageTip-based SAX fractionation appear to interact with the polystyrene sorbent of the resin in addition to the quaternary ammonium functional groups

One of the two alterations made to the published StageTip-based SAX fractionation procedure adhered to in section **6.3.1.2.** was the inclusion of an additional elution step at pH 2. The data in **Figs. 45 and 46** suggest that substantial amounts of peptide remain bound to the anion exchange resin after the pH 3 elution step (the final elution step in the published study). This residual material is particularly marked when separating succinylated peptides, with more total peptide identifications in the pH 2 fraction than in the pH 3 and pH 4 fraction combined. Taking the possibility of non-specific binding into consideration, the fractionation described in section **6.3.1.2.** was repeated with the inclusion of a further elution step with a buffer composed of 50% (v/v) BR buffer (pH 2) and 50% (v/v) acetonitrile. A corresponding amount of unfractionated peptide (assuming fractionation resulted in identical amounts of material in each fraction, therefore 1/9th of total material) was also analysed for both unmodified and succinylated samples to assess the increase in peptide identifications attained through performing the procedure.

Fractions and flow-through were processed as described previously. The number of total and unique unmodified peptides identified per fraction is shown in **Fig. 47a**, whilst the redundancy of unique peptide identification across all eight fractions is shown in **Figs. 47b & 47c**. Corresponding data for succinylated peptides is shown in **Figs. 48a – 48c**.

These data clearly demonstrate the advantages of performing an additional dimension of peptide separation upstream of LC-MS analysis. Separation into eight fractions allows for 82559 total (20713 unique) unmodified peptides and 39269 total (8619 unique) succinylated peptides to be identified across all eight runs. In contrast 13718 total (5366 unique) unmodified peptides and 6407 total (2523 unique) succinylated peptides are identified when the material is not fractionated and analysed in a single run. Fractionation will thus result in the identification of more proteins (detection of more unique peptides) with greater confidence (unique peptides detected more frequently).

Interestingly, the elution step incorporating 50% acetonitrile liberates significant amounts of unmodified and succinylated peptide material even after the elution step at pH 2. This is particularly notable for the succinylated separation, where the highest number of total protein identifications was observed in this fraction. Furthermore, the total amount of peptide material released with this final elution step is around four times that released in the preceding step as inferred through signal intensity across the total ion chromatograms (data not shown). The majority of peptides identified in the final elution are unique to this fraction for both unmodified and succinylated samples (approx. 84% and approx. 78% respectively, data not shown). This suggests that there are non-specific hydrophobic interactions occurring between the peptides and the polystyrene sorbent in addition to the ionic interactions taking place between the peptides and the quaternary ammonium functional groups of the resin. The unique peptides identified in the final elution probably interact more strongly with the polystyrene than the quaternary ammonium.

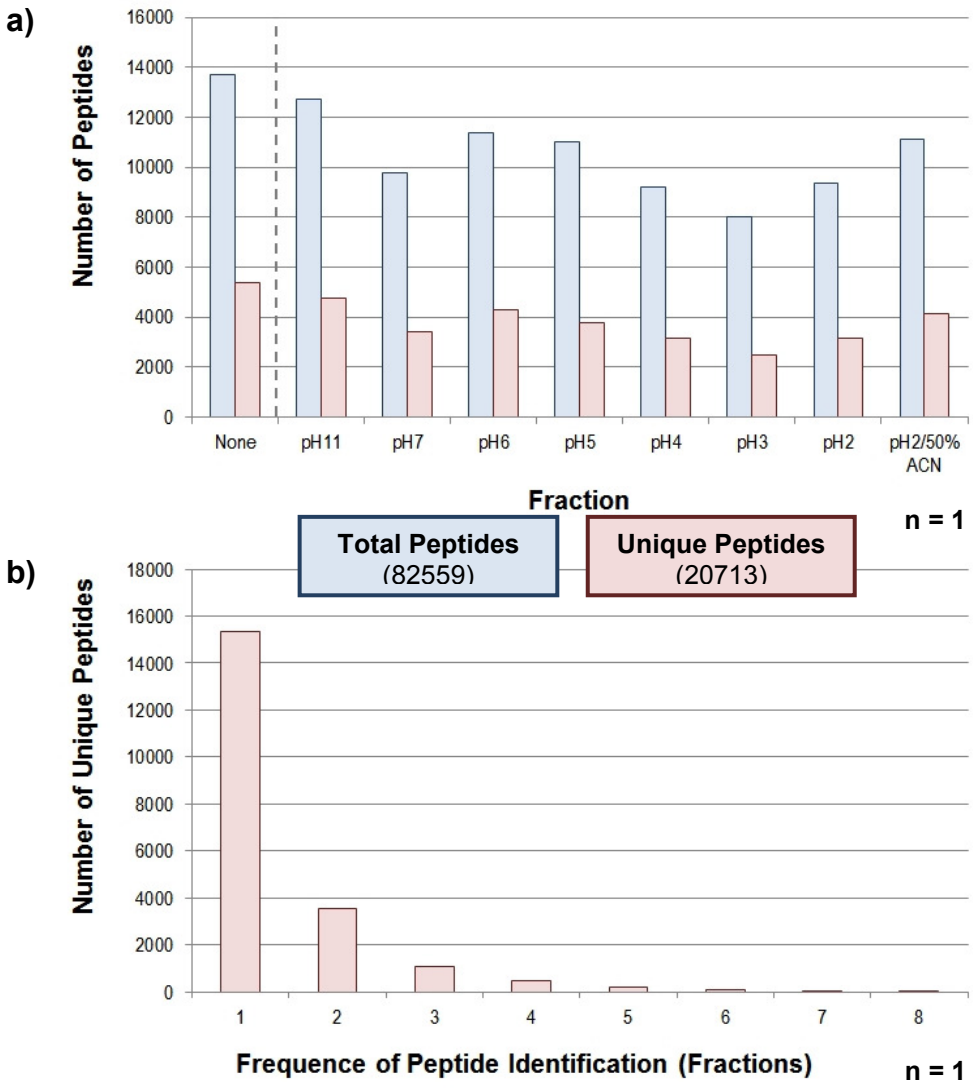

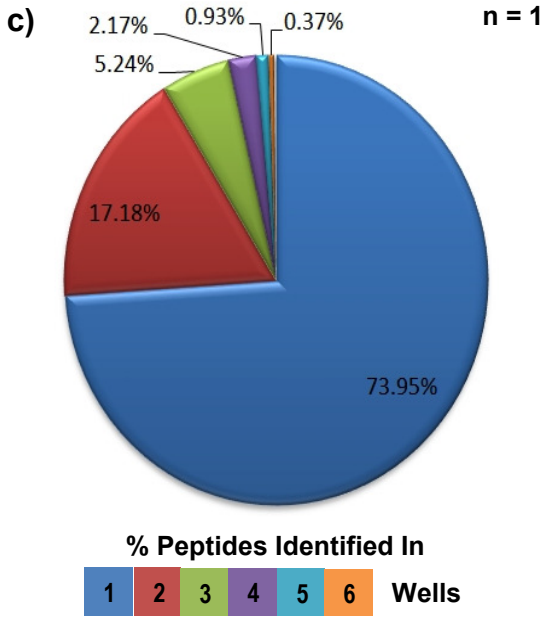

Figure 47: Second StageTip-based SAX fractionation of 25 µg unlabelled peptides derived from a Jurkat whole-cell lysate. **a)** Total and total unique peptides identified in each fraction and in an equivalent amount of unfractionated material; **b) & c)** Redundancy of unique peptide identification across all 8 fractions represented as a bar graph and a pie chart respectively. The number of unique peptides detected exclusively in the final elution step implies that some peptides may interact more strongly with the polystyrene sorbent of the resin than the quaternary ammonium groups. ~74% of all unique peptides are detected in one well only in spite of blanks not being run between SAX fractions.

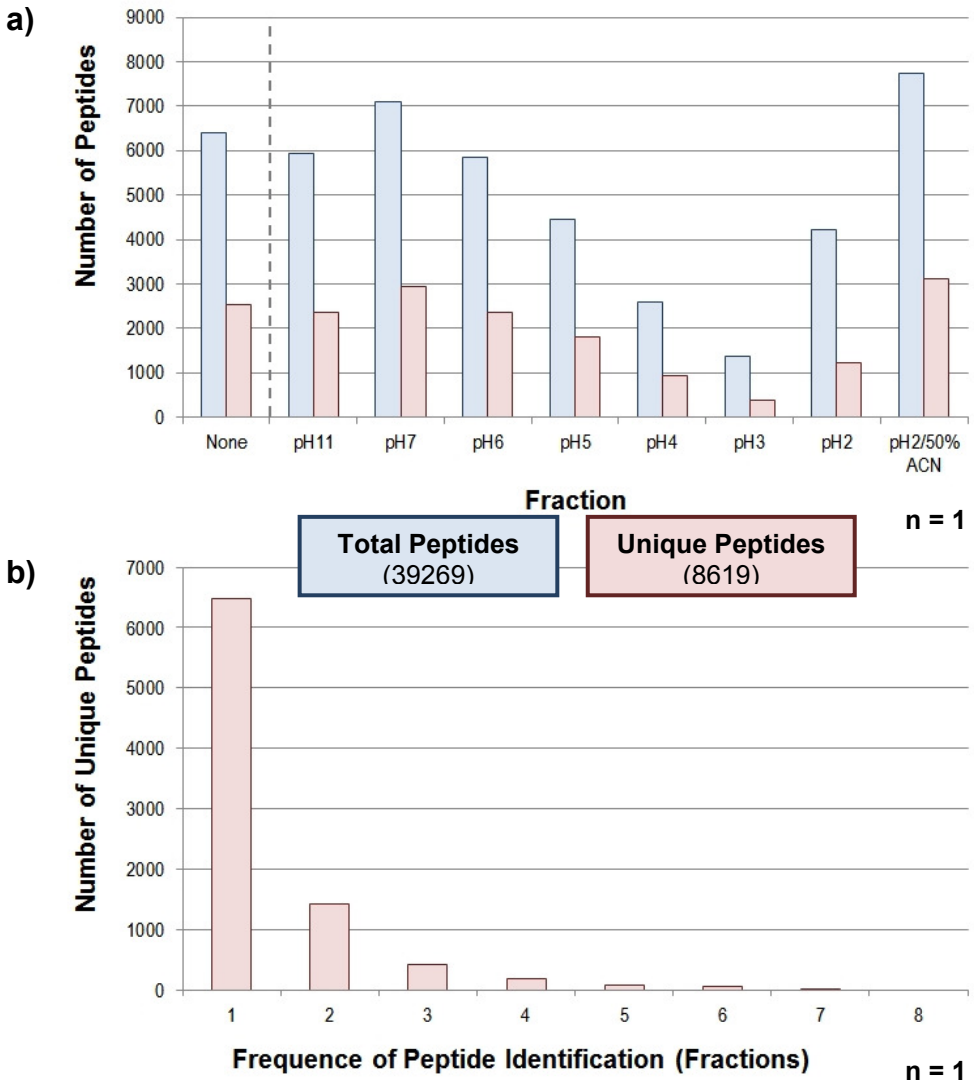

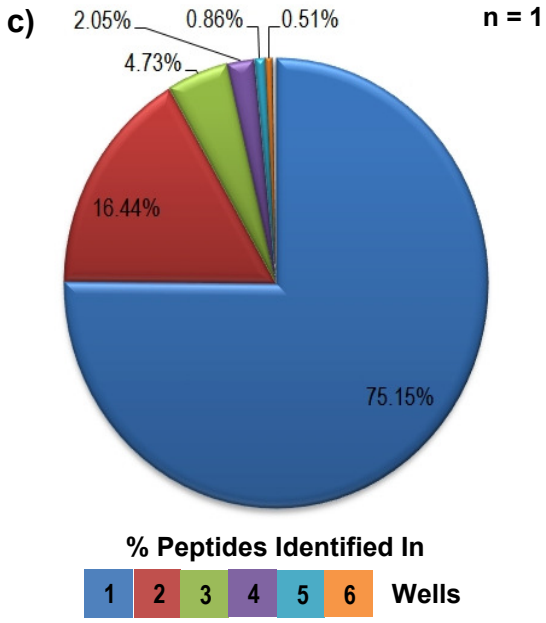

Figure 48: Second StageTip-based SAX fractionation of 25 µg succinylated peptides derived from a Jurkat whole-cell lysate. **a)** Total and total unique peptides identified in each fraction and in an equivalent amount of unfractionated material; **b) & c)** Redundancy of unique peptide identification across all 8 fractions represented as a bar graph and a pie chart respectively. As with the unmodified peptide data shown in **(Fig. 6)**, a large number of unique peptides are detected exclusively in the final fraction and fractionation efficiency remains high (~75% of all unique peptides detected in one well only).

6.3.1.4. The ionic interactions of peptides with the resin in StageTip-based SAX fractionation that appears to vary with successive decreases in pH is strongly affected by the presence of acetonitrile in the buffer

Given the substantial amount of material present in the final fraction in the experiment described in section **1.3.1.3.**, a further fractionation was performed in which elutions with BR buffer at every pH step were followed by an elution with a buffer composed of 50% (v/v) BR buffer and 50% (v/v) acetonitrile before moving down to the next pH step. It was reasoned that if both ionic and hydrophobic interactions were playing a role in determining whether peptides were retained or released from the resin in any given elution step, this alteration to the procedure might aid in distributing the peptide material more evenly across the fractions. Fractions and flow-through were processed as described previously and data for unmodified and succinylated peptides are plotted as in previous figures in **Fig. 49** and **Fig. 50** respectively.

For both unmodified and succinylated separations, these additional elution steps do not impart the desired effect. Instead, a large amount of peptide material is liberated in the pH 7 acetonitrile elution in comparison to the preceding pH 7 or subsequent pH 6 elutions (around five times as much for the succinylated sample and around ten times as much for the unmodified sample as inferred through signal intensity across the total ion chromatograms, data not shown). All subsequent elutions for both sets of samples contain considerably less peptide material and yield considerably less total peptide identifications than in the corresponding fractionations described in sections **6.3.1.2.** and **6.3.1.3.**, where acetonitrile was either not used at all or only introduced at the final elution step.

Interestingly, peptide yield and identifications recover somewhat at the lowest pH elutions. This is only really seen in the pH 2 BR and pH 2 acetonitrile elution with the unmodified peptides, but is also seen in the pH 3 and pH 4 acetonitrile elutions with the succinylated peptides. This observation may offer some insight into what is happening. Acetonitrile has a powerful elutrophic effect on peptides bound to this solid-phase support, disrupting hydrophobic interactions which may still endure in the absence of ionic interactions. Thus many basic peptides (pH 7 – pH 11) which are retained at pH 7 owing to hydrophobic interactions are

released in the pH 7 acetonitrile elution. Acidic peptides retained on the basis of ionic interactions rather than or in addition to hydrophobic interactions are retained until the pH of the elution buffer is sufficiently low to disrupt these ionic interactions. Addition of acetonitrile to low pH buffers enhances release of these acidic peptides in the same manner. Succinylated peptides are more acidic, which would explain why we see peptide yield and identifications begin to recover in the pH 4 acetonitrile elution in the succinylated separation. The equivalent unmodified (less acidic) peptides would likely have already been eluted in an earlier fraction.

In conclusion, the cons of this particular elution scheme probably outweigh the pros. It does not seem to be of detriment to fractionation efficiency with succinylated peptides (approx. 77% of unique peptides detected in a single fraction), though unmodified peptide fractions do appear to be slightly more diffuse (approx. 68% of unique peptides detected in a single fraction). However, the abundance of peptide material liberated in the pH 7 acetonitrile elution results in a number of subsequent weakly acidic elutions containing comparatively little material and yielding relatively few peptide identifications. It may be that there is an optimal concentration of acetonitrile to add to each elution buffer in order to obtain a more homogeneous distribution of peptide material across the thirteen fractions; however this would likely require considerable further experimental work. However, it is now obvious that binding and elution to and from this SAX material involves a ‘mixed-mode’ of action. This phenomenon has previously been reported for MuDPIT separations, where application of a 10% - 30% acetonitrile gradient at the end of the conventional salt step gradient resulted in an increase in peptide identifications of around 23% (Liu *et al.*, 2006).

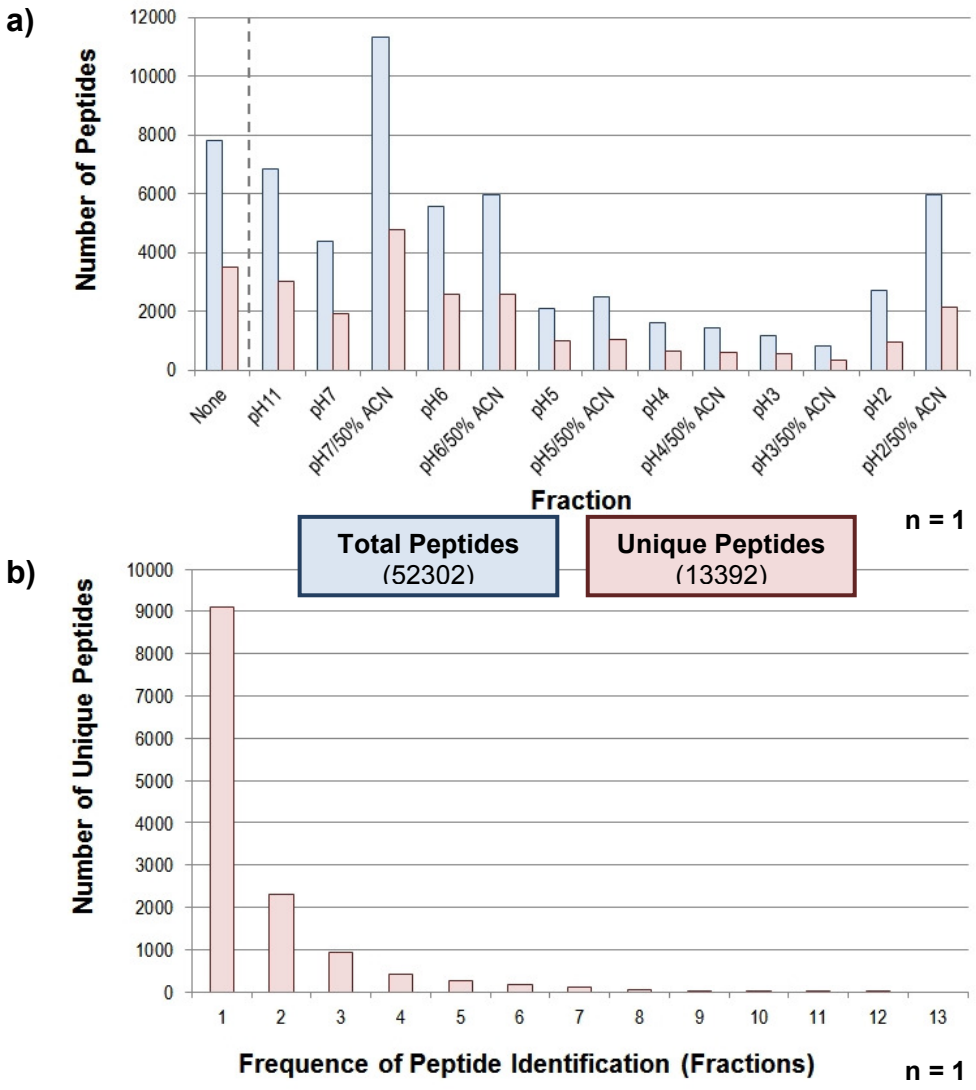

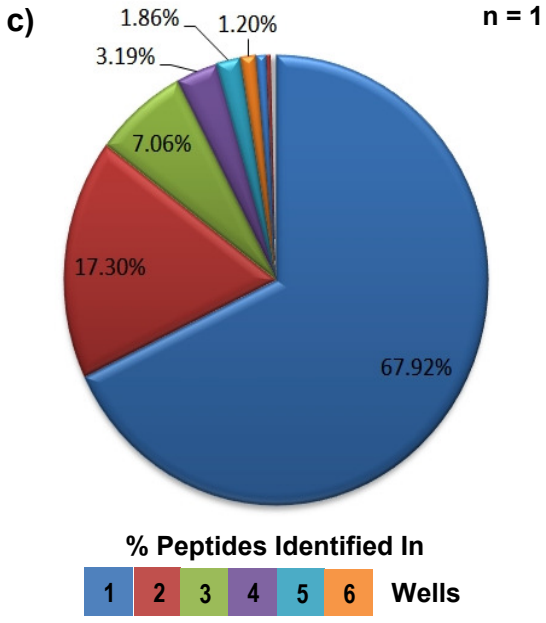

Figure 49: Third StageTip-based SAX fractionation of 25 µg unlabelled peptides derived from a Jurkat whole-cell lysate. **a)** Total and total unique peptides identified in each fraction and in an equivalent amount of unfractionated material; **b) & c)** Redundancy of unique peptide identification across all 13 fractions represented as a bar graph and a pie chart respectively. The inclusion of elution steps incorporating 50% acetonitrile across the entire pH range of the procedure releases a disproportionately large amount of peptide material from the resin in the pH 7 acetonitrile fraction. Later fractions contain considerably less material and yield fewer IDs than the corresponding fractions shown in **(Figs. 4 and 6)**.

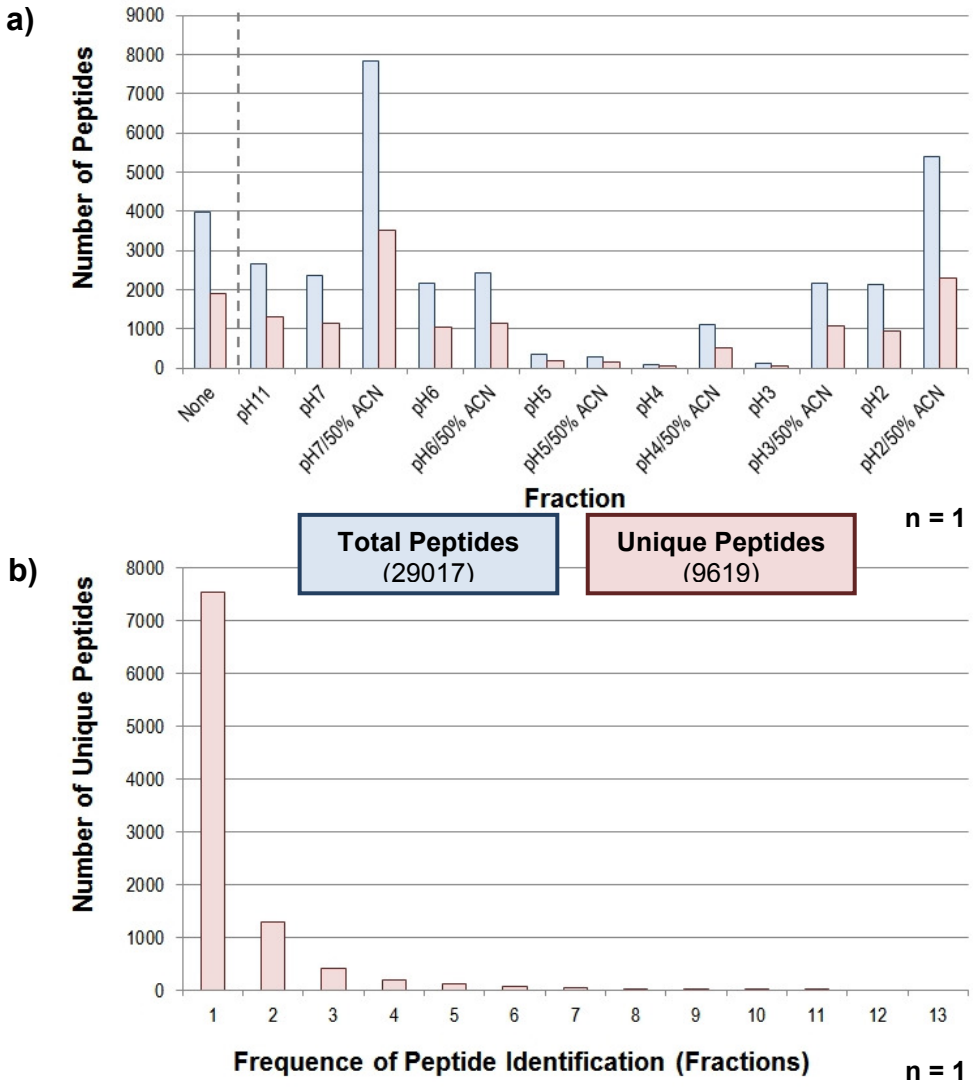

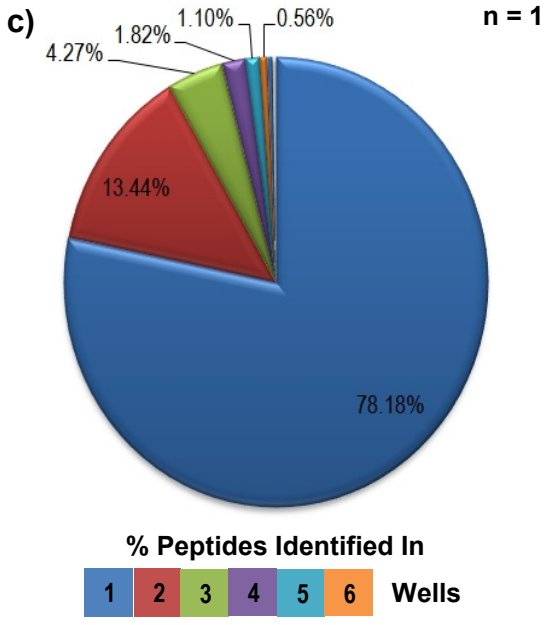

Figure 50: Third StageTip-based SAX fractionation of 25 µg succinylated peptides derived from a Jurkat whole-cell lysate. **a)** Total and total unique peptides identified in each fraction and in an equivalent amount of unfractionated material; **b) & c)** Redundancy of unique peptide identification across all 13 fractions represented as a bar graph and a pie chart respectively. As with the unmodified peptide data shown in **(Fig. 8)**, there is a spike in peptide material released from the resin in the pH 7 acetonitrile fraction, with less material contained in later fractions in comparison to the corresponding fractions shown in **(Figs. 5 & 7)**.

6.4. Discussion

As previously touched upon, the OFFGEL and SAX fractionation data presented in this chapter are not directly comparable: the latter was explored as an alternative when it became clear that the former might not be well-suited to separating IPTL-labelled peptides as opposed to all experiments being performed as a cohesive body of work. The fractionation efficiency figures reported for OFFGEL fractionation appear superior to those reported to SAX fractionation because OFFGEL fractionation is a more effective technique in this regard, but also because blanks were run between all OFFGEL fractions whilst all SAX fractions were analysed consecutively. The majority of residual peptide material retained on the LC column after a given sample fraction will therefore be liberated in the blank fraction as opposed to the following sample fraction. On the other hand, the numbers of total and unique peptide identifications reported for SAX fractionation were consistently higher than those reported for OFFGEL fractionation because SAX fractionation enables greater recovery of starting material, but also because the SAX fractions were analysed using a considerably longer LC column, affording greater peptide loading capacity and enhanced peak resolving power. In much the same way, neither dataset is directly comparable to the data published by Hubner *et al.* and Wisniewski *et al.* as these studies employed entirely different experimental systems from which to derive their starting material and performed all analysis using different instruments and set-ups. The primary objective here is thus not to draw any absolute parallels between the techniques but merely to weigh the relative merits of the two.

Taking the above into account, these data strongly advocate employing StageTip-based anion exchange chromatography as the first dimension of separation in the context of this particular proteomics workflow. Firstly, the StageTip-based format of the SAX procedure renders it considerably quicker and simpler to perform than OFFGEL electrophoresis. Secondly, the separations described in section **6.2.1.2.** would suggest that there are inherent issues in using liquid phase isoelectric focussing to fractionate peptides with modifications which alter charge state. These issues may not necessarily be insurmountable, but also appear to be largely circumvented when using SAX fractionation.

Of the three elution schemes explored for StageTip-based SAX fractionation, the second of the three (incorporating a final elution step with 50% (v/v) BR buffer (pH 2) and 50% (v/v) acetonitrile) appears to be the most favourable compromise in terms of the trade-off between the numbers of total and unique peptides identified across all of the fractions and the instrument time required to analyse all of these fractions. As previously discussed, it is likely that this second scheme is not completely optimised and more peptide identifications could be gleaned if the material released from the anion exchange resin with the addition of acetonitrile could be separated more uniformly across all of the preceding elutions. However, of all peptide fractionation experiments performed over the course of this project, this particular methodology proved most successful in terms of meeting the criteria set out at the beginning of the chapter. The next logical step would be to apply this methodology to fractionate a mixture of differentially labelled, membrane enriched dendritic cell proteomic peptides.

Chapter 7. Application of optimized quantitative and membrane proteomics methods to mature and tolerogenic dendritic cells

7.1. Introduction

At various intervals throughout the course of this body of work, the methods developed and heretofore described were applied to perform proteomic analyses on mature and tolerogenic dendritic cells. More specifically, development of the IPTL-based quantitation strategy described in **Chapter 5** and the StageTip-based SAX fractionation procedure described in **Chapter 6** were in part informed by quantitative proteomic comparisons of the whole cell proteomes of mature and tolerogenic DCs using both ^{18}O labelling and IPTL in combination with OFFGEL fractionation. Whilst these latter two workflows were subsequently found to be suboptimal from a technical viewpoint, this did not preclude the possibility that the experiments themselves yielded information that was of biological interest. The optimized membrane enrichment and digestion strategy described in **Chapter 4** was also latterly applied successfully for qualitative profiling of the membrane proteomes of mature and tolerogenic DC. The results of these quantitative and qualitative experiments are described herein.

7.2. ^{18}O-based quantitative profiling of the whole cell proteomes of mature and tolerogenic DC

Mature and tolerogenic DC whole cell lysates were prepared using the whole cell lysate preparation for the in-solution digestion procedure described in section **3.2.1.** Detergent removal was performed as described in section **3.3.1.** and digestion as described in section **3.3.2.** Mature DC peptides were ^{18}O labelled, whilst tolerogenic DC peptides remained unlabelled. A small quantity of mature DC peptides were analysed to verify that labelling had run to completion. Approximately 50 µg each of labelled and unlabelled peptides were then combined in a 1:1 ratio and focused into 12 fractions by OFFGEL electrophoresis. Focused fractions were recovered, cleaned-up and analysed as described in section **3.5.1.** Two biological replicates were performed and three technical replicates carried out for each fraction, giving a total of 36 raw data files for each biological replicate.

The 36 files were concatenated, searched and quantitated using Mascot Distiller (Matrix Science). 10678 peptides corresponding to 1008 proteins were identified in the first biological replicate (false discovery rate: 4.31%) and 7060 peptides corresponding to 779 proteins were identified in the second biological replicate (false discovery rate: 4.09%). Protein quantitation ratios were reported if a minimum of two peptides were detected that passed all three of the statistical tests described in section **5.2.2.6.** Refining using these criteria, 416 proteins were quantitated in the first biological replicate and 296 proteins were quantitated in the second biological replicate. Quantitation ratios were normalized on the median reported ratio and a labelled to unlabelled ratio of ≥ 2 or ≤ 0.5 (twofold change) was taken as the minimum criteria for differential expression. It was noted that Distiller frequently reports ratios for C-terminal peptides (which do not ^{18}O label and should thus be exempt from ratio calculations) and occasionally calls the fifth isotope peak of particularly intense unlabelled peptides as the first isotope peak of equivalent labelled peptides, skewing the resultant protein ratios. With this in mind, the spectra of the individual peptides identified in differentially expressed proteins were manually examined in order to remove spurious results. This left 15 proteins of twofold or greater abundance in mature DCs than in tolerogenic DCs and 9 proteins of twofold or greater abundance in tolerogenic DCs than in mature DCs for the first

biological replicate; and 17 proteins of twofold or greater abundance in mature DCs than in tolerogenic DCs and 13 proteins of twofold or greater abundance in tolerogenic DCs than in mature DCs for the second biological replicate.

Proteins detected in either or both biological replicates with twofold or greater expression in mature DCs than in tolerogenic DCs are shown in **Table 8**. Proteins detected in either or both biological replicates with twofold or greater expression in tolerogenic DCs than in mature DCs are shown in **Table 9**. Ratios are reported as the product of abundance of labelled peptide divided by abundance of unlabelled peptide. Identification of a protein as having twofold or greater expression in one cell type relative to the other does not permit inference of whether the protein is upregulated in the first cell type or downregulated in the second, merely that the protein is differentially expressed.

To further increase confidence in results, the quantitation ratios of differentially expressed proteins in the first biological replicate were examined in the second biological replicate and vice versa. In instances where a protein had been quantitated in both biological replicates and the ratios conflicted, the spectra of individual peptides of that protein were manually examined in both replicates and the replicate with the best quality data (in terms of number and / or intensity of peptides quantitated) was assumed to be more representative of the true ratio. These ratios are shaded in grey in the tables. For both tables, proteins detected with twofold or greater expression in both biological replicates, proteins detected in both biological replicates with twofold or greater expression in the replicate with the best quality data and proteins detected with twofold or greater expression in one biological replicate but not detected in the other are listed in the top section of the table. Proteins detected in both biological replicates with less than twofold expression in the replicate with the best quality data are listed separately in the bottom section of table.

	Proteins with ≥2× expression in Mature DC					
		Replicate 1		Replicate 2		
	Accession	Ratio	# Matches	Ratio	# Matches	Protein
1	Q16658	9.548	19	24.84	7	Fascin
2	Q6ZS81	–	–	7.445	6	WD repeat- and FYVE domain-containing protein 4
3	Q13077	3.24	6	6.97	3	TNF receptor-associated factor 1
4	P04233	3.448	5	3.192	5	HLA class II histocompatibility antigen gamma chain
5	P10599	0.746	1	3.253	4	Thioredoxin
6	P12277	–	–	3.249	2	Creatine kinase B-type
7	P05161	1.471	13	2.98	10	Ubiquitin-like protein ISG15
8	Q15019	2.569	4	–	–	Septin-2
9	Q16555	2.172	10	2.533	4	Dihydropyrimidinase-related protein 2
10	P01903	1.542	1	2.452	12	HLA class II histocompatibility antigen, DR alpha chain
11	P29016	–	–	2.42	2	T-cell surface glycoprotein CD1b
12	Q5K4L6	2.397	3			Long-chain fatty acid transport protein 3
13	P11215	1.137	3	2.357	3	Integrin alpha-M
14	Q14204	2.24	3	–	–	Cytoplasmic dynein 1 heavy chain 1
15	P20036	2.212	2	–	–	HLA class II histocompatibility antigen, DP alpha 1 chain
16	P08133	2.205	5	–	–	Annexin A6
17	P61769	2.177	13	2.112	11	Beta-2-microglobulin
18	Q9Y5A7	2.039	2	–	–	NEDD8 ultimate buster 1
19	P02786	2.031	15	1.662	2	Transferrin receptor protein 1
20	Q8NHP1	–	–	2.014	2	Aflatoxin B1 aldehyde reductase member 4
21	P16050	1.622	17	2.008	31	Arachidonate 15-lipoxygenase
22	O43707	1.669	12	2.659	11	Alpha-actinin-4
23	Q562R1	2.113	34	1.673	96	Beta-actin-like protein 2
24	P12814	1.51	19	2.519	14	Alpha-actinin-1
25	P09382	1.413	22	2.041	17	Galectin-1
26	O75369	3.302	2	1.302	6	Filamin-B

Table 8: Proteins identified in ^{18}O-based quantitative profiling of whole cell proteomes of mature and tolerogenic DCs with twofold or greater expression in mature DCs. In instances where a protein had been quantitated in both biological replicates and the ratios conflicted, the spectra of individual peptides of that protein were manually examined in both replicates and the replicate with the best quality data (in terms of number and / or intensity of peptides quantitated) was assumed to be more representative of the true ratio. These ratios are shaded in grey in the tables.

	Proteins with ≥2× expression in Tolerogenic DC					
		Replicate 1		Replicate 2		
	Accession	Ratio	# Matches	Ratio	# Matches	Protein
1	P05981	–	–	0.0742	2	Serine protease hepsin
2	Q16851	0.5588	4	0.1864	6	UTP--glucose-1-phosphate uridylyltransferase
3	P07858	0.3216	10	–	–	Cathepsin B
4	P05455	0.3586	2	–	–	Lupus La protein
5	P12236	1.296	4	0.36	7	ADP/ATP translocase 3
6	P05141	1.218	6	0.3818	8	ADP/ATP translocase 2
7	O75368	0.3997	3	–	–	SH3 domain-binding glutamic acid-rich-like protein
8	P09651	0.6477	2	0.4423	2	Heterogeneous nuclear ribonucleoprotein A1
9	O75874	0.6547	15	0.4442	14	Isocitrate dehydrogenase [NADP] cytoplasmic
10	P20292	0.4472	3	–	–	Arachidonate 5-lipoxygenase-activating protein
11	Q5QNW6	–	–	0.4474	9	Histone H2B type 2-F
12	P15090	0.4475	3	–	–	Fatty acid-binding protein, adipocyte
13	P61916	0.4489	4	0.56	4	Epididymal secretory protein E1
14	Q96M42	–	–	0.4521	6	Putative uncharacterized protein encoded by LINC00479
15	P55060	–	–	0.4548	6	Exportin-2
16	P11940	0.4667	8	–	–	Polyadenylate-binding protein 1
17	P53004	0.4801	4	1.148	3	Biliverdin reductase A
18	P15586	0.4934	2	–	–	N-acetylglucosamine-6-sulfatase
19	P17931	0.5931	23	0.4822	9	Galectin-3
20	P13073	0.6344	2	0.4927	3	Cytochrome c oxidase subunit 4 isoform 1, mitochondria
21	P25774	0.8358	3	0.4551	2	Cathepsin S

Table 9: Proteins identified in ^{18}O-based quantitative profiling of whole cell proteomes of mature and tolerogenic DCs with twofold or greater expression in tolerogenic DCs. In instances where a protein had been quantitated in both biological replicates and the ratios conflicted, the spectra of individual peptides of that protein were manually examined in both replicates and the replicate with the best quality data (in terms of number and / or intensity of peptides quantitated) was assumed to be more representative of the true ratio. These ratios are shaded in grey in the tables.

7.3. IPTL-based quantitative profiling of the whole cell proteomes of mature and tolerogenic DC

Mature and tolerogenic DC whole cell lysates were prepared and digested as described in section **7.2.** Mature DC peptides were labelled with $^{13}C_4$-succinic anhydride only and tolerogenic DC peptides were labelled with ^{18}O water and $^{12}C_4$-succinic anhydride. A small quantity of mature and tolerogenic DC peptides were individually analysed to verify that labelling had run to completion. Approximately 50 µg of differentially labelled peptides were then combined in a 1:1 ratio and focused into 10 fractions by modified OFFGEL electrophoresis using a Bio-Rad pH 3 – 6 IPG strip. Focused fractions were recovered, cleaned-up and analysed as described in section **7.2.**

The 10 files were concatenated using Mascot Daemon and then searched and quantitated within Mascot. A total of 5765 peptides corresponding to 478 proteins were identified (false discovery rate: 3.73%). Whilst this is less than either of the two ^{18}O-labelling experiments, it is worth noting that the majority of peptides fractionated into the first five wells (see section **6.2.1.2.**) and no technical replicates were performed for this reason. Protein quantitation ratios were reported if a minimum of two peptides were detected and quantified. Applying these criteria, 351 of the 478 proteins were quantitated. Quantitation ratios were normalized on the median reported ratio and a labelled to unlabelled ratio of ≥ 2 or ≤ 0.5 (twofold change) was taken as the minimum criteria for differential expression. Just 7 proteins were identified with twofold or greater abundance in mature DCs than in tolerogenic DCs, while only 2 proteins were identified with twofold or greater abundance in tolerogenic DCs than in mature DCs. Manual examination of the spectra of the individual peptides identified in differentially expressed proteins confirmed that all results appeared genuine. The identities of these proteins are shown in **Table 10**.

Whilst treatment of tolerogenic DCs with dexamethasone and vitamin D3 would be expected to result in differential expression in a small subset of proteins relative to mature DCs, the cells differentiate from a common precursor ($CD14^+$ monocytes) and the culture protocol is broadly similar, thus global protein expression should by and large remain equivalent across the two cell types. The distribution of all reported protein ratios computed from the combined mature and tolerogenic DC samples is shown in **Fig. 51**. These data suggest

that this is indeed the case and reinforce the quantitative accuracy of the IPTL method in lieu of a biological replicate for the experiment described in section **5.3.2.6.**

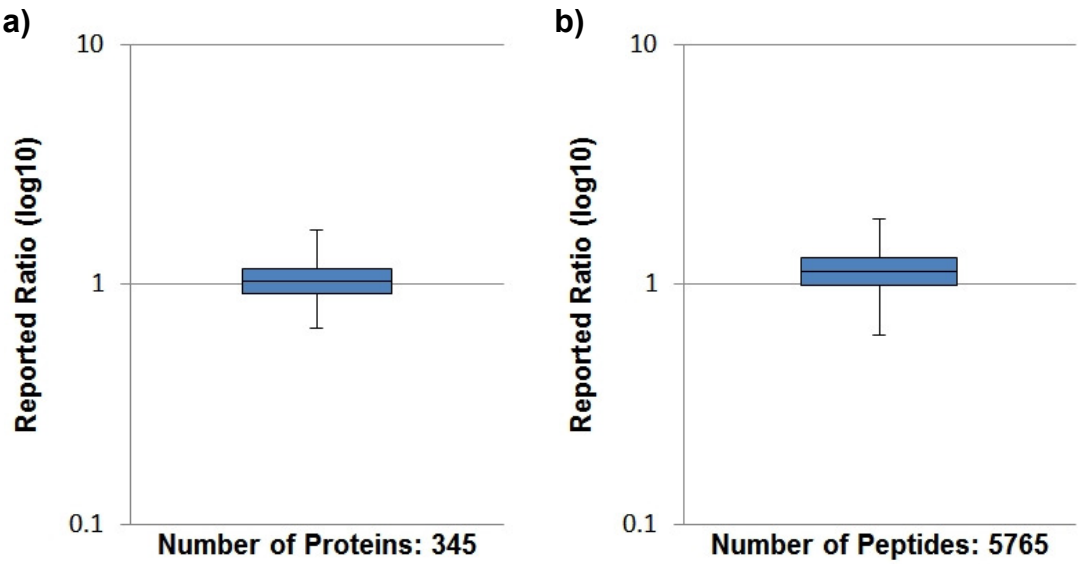

Figure 51: Box and whisker plot showing distribution of **a)** protein ratios; **b)** peptide ratios reported by Mascot when $^{13}C_4$-succinylated mature DC proteomic peptides and $^{12}C_4$-succinylated / ^{18}O-labelled tolerogenic DC proteomic peptides are combined in a 1:1 ratio. 50% of reported ratios are contained within the boxes and 95% are contained within the whiskers.

	Proteins with ≥2× expression in Mature DC			
	Accession	**Ratio**	**# Matches**	**Protein**
1	P13760	5.044	2	HLA class II histocompatibility antigen, DRB1-4 beta cha
2	P12277	3.047	15	Creatine kinase B-type
3	P36956	2.733	2	Sterol regulatory element binding protein 1
4	P50453	2.535	2	Serpin B9
5	P40123	2.35	4	Adenylyl cyclase-associated protein 2
6	P52566	2.23	6	Rho GDP-dissociation inhibitor 2
7	P21980	2.1	14	Protein-glutamine gamma-glutamyltransferase 2

	Proteins with ≥2× expression in Tolerogenic DC			
	Accession	**Ratio**	**# Matches**	**Protein**
8	P36957	0.32	3	Dihydrolipolysine-residue succinyltransferase component of 2-oxoglutarate dehydrogenase complex, mitochondrial
9	P79483	0.321	4	HLA class II histocompatibility antigen, DR beta 3 chain

Table 10: Proteins identified in IPTL-based quantitative profiling of whole cell proteomes of mature and tolerogenic DCs with twofold or greater expression in one cell type relative to the other.

7.4. Discussion (whole cell proteomes)

Many of the proteins identified as being of two-fold or greater abundance in mature DCs over tolerogenic DCs in these whole proteome quantitative comparisons have previously been reported to be induced upon and/or have functions reconcilable with DC maturation and immune activation.

Fascin (Table 8, protein 1) is an actin-bundling protein which has been shown to be essential in mature DC dendrite formation (Ross *et al.*, 2000), and there is evidence that increased expression of Fascin is linked with concomitantly increased expression of MHC class II and co-stimulatory molecules (Al-Alwan *et al.*, 2001). It has been suggested that HLA class II histocompatibility antigen gamma chain (CD74) (Table 8, protein 4) is transiently induced in the early stages of LPS-induced DC maturation, temporarily inhibiting migration and facilitating maximal antigen uptake (Faure-Andre *et al.*, 2008); though it is not clear whether this increased expression would persist a full 24 hours after LPS stimulation (the time-point at which our mature and tolerogenic DCs are harvested). Thioredoxin (Table 8, protein 5) is important in generating the reducing extracellular microenvironment necessary for T cell activation (Angelini *et al.*, 2002) and has been shown to be highly upregulated in LPS-matured monocyte-derived DCs relative to immature DCs in a previous proteomics study (Pereira *et al.*, 2005). Levels of rho GDP-dissociation inhibitor 2 (Table 10, protein 6) were similarly increased in the same study. Ubiquitin-like protein ISG15 (Table 8, protein 7) mRNA and protein levels have been shown to be induced during LPS-induced DC maturation using microarray analysis, RT-PCR and immunoblotting (Ebstein *et al.*, 2009). β_2-microglobulin (Table 8, protein 17) is a subunit of MHC Class I molecules, which are highly upregulated on the surface of mature DCs to enable cross presentation (Ackerman and Cresswell, 2003). Transferrin receptor protein 1 (Table 8, protein 19) mediates iron uptake in mature DCs (Brinkmann *et al.*, 2007), and iron depletion has been shown to inhibit DC maturation (Kramer *et al.*, 2002). Serpin B9 (Table 10, protein 4) inhibits granzyme B and enables mature DC to cross present to $CD8^+$ T cells without succumbing to contact-mediated cytotoxicity themselves (Lovo *et al.*, 2012). Finally, protein-glutamine gamma glutamyltransferase 2 (Table 10, protein 7) has been postulated to play an important role in the maturation

process itself, with DCs from knockout mice exhibiting impaired maturation and reduced response to LPS stimulation (Matic *et al.*, 2010).

In contrast, it is less easy to ascribe roles from the literature in immune tolerance to many of the proteins identified as being of twofold or greater abundance in tolerogenic DCs than in mature DCs. This is not to say that the proteins do not play a role in the process: DC-mediated T cell tolerance is a less well characterized phenomenon than DC-mediated T cell activation and some of the proteins are not characterised at all. Nevertheless, a few proteins do stand out.

The cathepsins are a family of lysosomal proteases known to be important in antigen processing and MHC class II loading (Honey and Rudensky, 2003). The precise roles of individual members of the family in this process is yet to be completely delineated but evidence suggests that they are not redundant (Honey and Rudensky, 2003). Treatment of DCs with ZLRL (a highly-specific inhibitor of Cathepsin B) enhanced their ability to present tetanus toxin C-fragment peptides and induce a pro-inflammatory response (Reich *et al.*, 2009). In contrast, treatment of DCs with CLIK-60 (an inhibitor of Cathepsin S) impairs their ability to present alpha-fodrin peptides in Sjogren's syndrome and suppresses the pro-inflammatory response (Katunuma *et al.*, 2003). These data suggest that Cathepsin B (Table 9, protein 3) is significantly more abundant in tolerogenic DCs whilst Cathepsin S (Table 9, protein, 21) expression is more equivocal, with the more compelling of the two biological replicates suggesting little difference in abundance between the two cell types.

Additionally, adipocyte fatty acid-binding protein (Table 9, protein 12) is a target gene of the transcription factor PPARγ (Szanto *et al.*, 2010), which our group has previously shown is upregulated in tolerogenic DCs relative to mature DCs (unpublished observations). The conversion of biliverdin to bilirubin by surface expressed biliverdin reductase (BVR) (Table 9, protein 17) induces BVR phosphorylation and downstream activation of protein kinase B signalling, leading to enhanced IL-10 production in macrophages (Wegiel *et al.*, 2009). Finally, whilst these data suggest that expression levels of Galectin-3 (Table 9, protein 19) in tolerogenic DCs fall just below the threshold for differential expression, it merits consideration as there is evidence that siRNA knockdown

of the protein in immature and mature DCs results in enhanced T cell activation (Mobergslien and Sioud, 2012).

7.5. Qualitative profiling of the membrane proteomes of mature and tolerogenic DC

Enriched mature and tolerogenic DC membrane fractions were prepared and digested using the optimized stepwise depletion and FASP procedure described in section **4.2.3.1.** Digests were cleaned up and analysed as described in section **3.6. – 3.7.** Data processing, GO annotation and transmembrane domain prediction were also performed as previously described. A total of 1134 peptides corresponding to 351 proteins were identified in the mature DC membrane fraction (false discovery rate: 8.99%) and a total of 1232 peptides corresponding to 429 proteins were identified in the tolerogenic DC membrane fraction (false discovery rate: 9.50%).

The distribution of cellular component GO annotations and percentage of proteins predicted to contain transmembrane domains by TMHMM for all proteins identified in the mature and tolerogenic DC membrane fractions are shown in **Fig. 52a** and **Fig. 52b** respectively. Both fractions exhibit comparable membrane protein enrichment to the Jurkat membrane fraction shown in **Fig. 24c**, with plasma membrane GO annotations once again exceeding cytoplasmic and nuclear GO annotations in both instances. Interestingly, whilst similar total numbers of plasma membrane-annotated proteins and proteins predicted to possess transmembrane domains are identified in both mature and tolerogenic DC membrane fractions, the percentages are notably higher for the mature DC fraction by merit of the larger number of total proteins identified in the tolerogenic DC fraction. The aim was to inject identical amounts of peptide from both fractions and the total ion chromatograms (TICs) from the LC-MS runs seem to suggest that this was the case **Fig. 53**, with marginally more material in the mature DC fraction if anything.

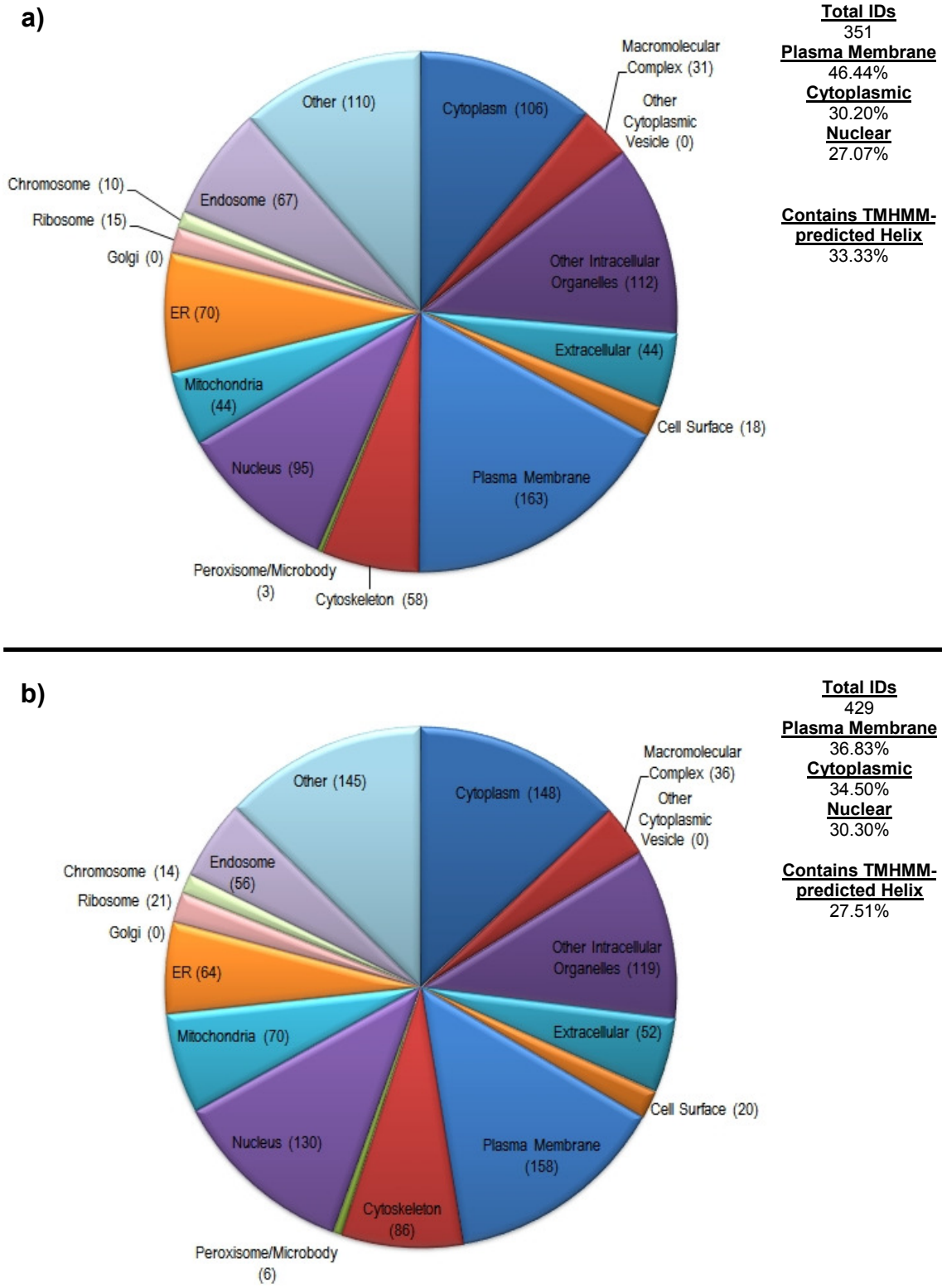

Figure 52: Pie charts illustrating the distribution of cellular component ontologies of proteins identified from LC-MS analysis of **a)** mature DC membranes and **b)** tolerogenic DC membranes prepared using the optimized stepwise depletion enrichment method described in Chapter 4 and digested using FASP. The number of total protein identifications; the percentages of total identifications with 'plasma membrane', 'cytoplasmic' and 'nuclear' annotation; and the percentage of proteins predicted to contain transmembrane domains by the TMHMM algorithm are also displayed.

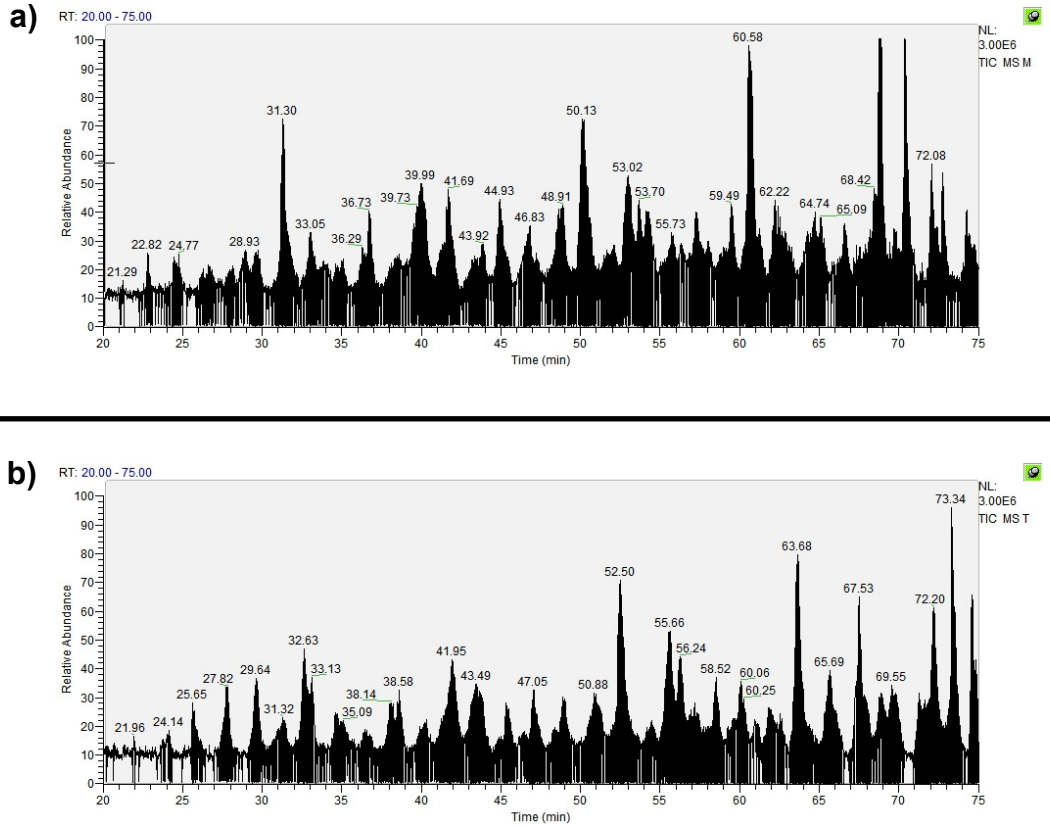

Figure 53: Total ion chromatograms from LC-MS analysis of **a)** mature DC membranes and **b)** tolerogenic DC membranes.

Given the similar amounts of material contained in each fraction, it was reasoned that it would not be entirely unwarranted to make some very basic quantitative inferences in the absence of stable isotope labelling through comparison of the protein content of the two fractions. The identities of plasma membrane proteins identified exclusively in the mature fraction are shown in **Table 11** and the identities of plasma membrane proteins identified exclusively in the tolerogenic fraction are shown in **Table 12**. Where a plasma membrane protein was detected in both fractions, emPAI scores were used to infer whether it appeared to be differentially expressed in one fraction relative to the other. The emPAI score of a protein is calculated by taking the exponent of the number of observed peptides over the number of theoretically observable peptides and subtracting one (Ishishama *et al.*, 2005). It is proportional to protein content in a sample over around two orders of magnitude but it is worth noting that this relationship does not hold for emPAI values less than 0.1 (Kim *et al.*, 2012). Plasma membrane proteins potentially exhibiting differential

expression are shown in **Table 13**, whilst plasma membrane proteins appearing to be equally abundant in both fractions are shown in **Table 14**. For the sake of stringency, a protein was only taken as being a plasma membrane protein if it was assigned a plasma membrane GO annotation and had at least one TMHMM-predicted transmembrane helix.

Mature DC Only										
			Mature DC				Tolerogenic DC			
	Accession	Protein	Score	# Peptides	Unique	emPAI	Score	# Peptides	Unique	emPAI
1	P04222	HLA class I histocompatibility antigen, Cw-3 alpha chain	467	12	3	0.36	–	–	–	–
2	P18462	HLA class I histocompatibility antigen, A-25 alpha chain	292	8	2	0.17	–	–	–	–
3	P01893	Putative HLA class I histocompatibility antigen, alpha chain H	241	6	3	0.26	–	–	–	–
4	P01889	HLA class I histocompatibility antigen, B-7 alpha chain	238	8	4	0.26	–	–	–	–
5	Q04826	HLA class I histocompatibility antigen, B-40 alpha chain	235	8	3	0.26	–	–	–	–
6	P30443	HLA class I histocompatibility antigen, A-1 alpha chain	195	8	4	0.17	–	–	–	–
7	P05534	HLA class I histocompatibility antigen, A-24 alpha chain	195	8	4	0.17	–	–	–	–
8	P13746	HLA class I histocompatibility antigen, A-11 alpha chain	195	8	4	0.17	–	–	–	–
9	P50993	Sodium/potassium-transporting ATPase subunit alpha-2	186	6	5	0.09	–	–	–	–
10	P30447	HLA class I histocompatibility antigen, A-23 alpha chain	185	9	4	0.17	–	–	–	–
11	Q31610	HLA class I histocompatibility antigen, B-81 alpha chain	160	7	4	0.26	–	–	–	–
12	P78324	Tyrosine-protein phosphatase non-receptor type substrate 1	120	3	3	0.19	–	–	–	–
13	P10321	HLA class I histocompatibility antigen, Cw-7 alpha chain	119	3	3	0.26	–	–	–	–
14	P29017	T-cell surface glycoprotein CD1c	119	4	1	0.09	–	–	–	–
15	Q31612	HLA class I histocompatibility antigen, B-73 alpha chain	116	5	3	0.26	–	–	–	–
16	Q9NQ25	SLAM family member 7	97	4	3	0.09	–	–	–	–
17	P05556	Integrin beta-1	83	3	2	0.04	–	–	–	–
18	Q9NZQ7	Programmed cell death 1 ligand 1	75	3	2	0.21	–	–	–	–
19	Q95604	HLA class I histocompatibility antigen, Cw-17 alpha chain	72	2	2	0.17	–	–	–	–
20	Q9Y336	Sialic acid-binding Ig-like lectin 9	60	2	2	0.06	–	–	–	–
21	Q9UMR7	C-type lectin domain family 4 member A	58	1	1	0.12	–	–	–	–
22	P79483	HLA class II histocompatibility antigen, DR beta 3 chain	57	13	3	0.23	–	–	–	–
23	Q10589	Bone marrow stromal antigen 2	52	1	1	0.17	–	–	–	–
24	P32942	Intercellular adhesion molecule 3	52	4	2	0.11	–	–	–	–
25	O15427	Monocarboxylate transporter 4	52	2	1	0.07	–	–	–	–
26	Q9H3Z4	DnaJ homolog subfamily C member 5	39	1	1	0.15	–	–	–	–
27	P04114	Apolipoprotein B-100	31	3	2	0.01	–	–	–	–
28	P08648	Integrin alpha-5	30	1	1	0.03	–	–	–	–
29	Q6NV75	Probable G-protein coupled receptor 153	28	1	1	0.05	–	–	–	–
30	Q9Y5S1	Transient receptor potential cation channel subfamily V member 2	28	2	2	0.08	–	–	–	–
31	Q08828	Adenylate cyclase type 1	27	8	2	0.03	–	–	–	–
32	P13762	HLA class II histocompatibility antigen, DR beta 4 chain	26	11	3	0.11	–	–	–	–
33	P20036	HLA class II histocompatibility antigen, DP alpha 1 chain	25	4	2	0.11	–	–	–	–
34	Q8J025	Protein APCDD1	23	1	1	0.06	–	–	–	–
35	Q9Y2Q0	Probable phospholipid-transporting ATPase IA	22	3	1	0.03	–	–	–	–
36	Q8NGS9	Olfactory receptor 13C2	21	3	1	0.09	–	–	–	–
37	Q13308	Inactive tyrosine-protein kinase 7	20	3	1	0.09	–	–	–	–
38	O15245	Solute carrier family 22 member 1	17	6	1	0.05	–	–	–	–

Table 11: Proteins identified exclusively in mature DC membrane-enriched fraction.

Tolerogenic DC Only										
			Mature DC				Tolerogenic DC			
	Accession	Protein	Score	# Peptides	Unique	emPAI	Score	# Peptides	Unique	emPAI
1	P30453	HLA class I histocompatibility antigen, A-34 alpha chain	–	–	–	–	115	3	2	0.08
2	P30273	High affinity immunoglobulin epsilon receptor subunit gamma	–	–	–	–	90	3	2	0.84
3	Q13291	Signaling lymphocytic activation molecule	–	–	–	–	89	3	2	0.18
4	P21964	Catechol O-methyltransferase	–	–	–	–	87	3	2	0.23
5	P12235	ADP/ATP translocase 1	–	–	–	–	71	13	4	0.21
6	Q9H2X3	C-type lectin domain family 4 member M	–	–	–	–	58	2	1	0.07
7	Q86VB7	Scavenger receptor cysteine-rich type 1 protein M130	–	–	–	–	57	2	2	0.05
8	P33121	Long-chain-fatty-acid--CoA ligase 1	–	–	–	–	43	4	4	0.04
9	P54707	Potassium-transporting ATPase alpha chain 2	–	–	–	–	43	6	3	0.06
10	P28068	HLA class II histocompatibility antigen, DM beta chain	–	–	–	–	39	1	1	0.11
11	P13473	Lysosome-associated membrane glycoprotein 2	–	–	–	–	39	1	1	0.07
12	P09601	Heme oxygenase 1	–	–	–	–	38	1	1	0.07
13	P20648	Potassium-transporting ATPase alpha chain 1	–	–	–	–	33	2	2	0.03
14	A0AVI2	Fer-1-like protein 5	–	–	–	–	29	3	1	0.01
15	Q13740	CD166 antigen	–	–	–	–	25	1	1	0.05
16	O60603	Toll-like receptor 2	–	–	–	–	24	4	2	0.04
17	Q92629	Delta-sarcoglycan	–	–	–	–	24	2	1	0.10
18	Q86UP2	Kinectin	–	–	–	–	24	7	4	0.02
19	Q7RTY1	Monocarboxylate transporter 9	–	–	–	–	21	1	1	0.06
20	P12318	Low affinity immunoglobulin gamma Fc region receptor II-a	–	–	–	–	20	1	1	0.09
21	P21817	Ryanodine receptor 1	–	–	–	–	20	8	4	0.01
22	Q92736	Ryanodine receptor 2	–	–	–	–	20	8	5	0.01
23	Q9Y5E6	Protocadherin beta-3	–	–	–	–	18	4	3	0.04
24	Q9Y5E9	Protocadherin beta-14	–	–	–	–	18	3	2	0.04
25	Q8NGL1	Olfactory receptor 5D18	–	–	–	–	18	2	1	0.10

Table 12: Proteins identified exclusively in tolerogenic DC membrane-enriched fraction.

Mature DC ≥ Tolerogenic DC

		Accession	Protein	Mature DC				Tolerogenic DC			
				Score	# Peptides	Unique	emPAI	Score	# Peptides	Unique	emPAI
≥2×	1	P05107	Integrin beta-2	1246	53	19	0.86	384	21	12	0.39
	2	P06126	T-cell surface glycoprotein CD1a	1031	21	4	0.40	186	4	1	0.09
	3	P20702	Integrin alpha-X	630	28	13	0.28	90	4	3	0.05
	4	P08575	Receptor-type tyrosine-protein phosphatase C	573	26	10	0.16	201	9	4	0.07
	5	P11215	Integrin alpha-M	545	18	9	0.19	160	4	2	0.05
	6	P04233	HLA class II histocompatibility antigen gamma chain	291	8	4	0.32	249	4	1	0.10
	7	P16150	Leukosialin	169	6	3	0.27	149	4	1	0.08
	8	P20020	Plasma membrane calcium-transporting ATPase 1	142	5	3	0.07	64	4	2	0.02
	9	Q01814	Plasma membrane calcium-transporting ATPase 2	133	6	3	0.05	64	4	2	0.02
≥1.5×	10	Q29836	HLA class I histocompatibility antigen, B-67 alpha chain	506	17	5	0.48	202	10	3	0.26
	11	P16070	CD44 antigen	295	16	6	0.27	188	11	5	0.17
	12	P25942	Tumor necrosis factor receptor superfamily member 5	256	19	5	0.81	92	8	4	0.49
≥1×	13	P01911	HLA class II histocompatibility antigen, DRB1-15 beta chain	685	37	9	1.07	506	28	6	0.87
	14	Q29974	HLA class II histocompatibility antigen, DRB1-16 beta chain	434	28	8	0.87	286	18	5	0.68
	15	P01912	HLA class II histocompatibility antigen, DRB1-3 chain	334	29	6	0.86	252	27	5	0.68

Tolerogenic DC ≥ Mature DC

		Accession	Protein	Mature DC				Tolerogenic DC			
				Score	# Peptides	Unique	emPAI	Score	# Peptides	Unique	emPAI
≥2×	16	Q9NZM1	Myoferlin	93	6	5	0.03	158	4	4	0.06
	17	P08962	CD63 antigen	21	1	1	0.13	42	4	2	0.27
≥1.5×	18	P16615	Sarcoplasmic/endoplasmic reticulum calcium ATPase 2	231	5	3	0.06	271	7	4	0.09
	19	P27105	Erythrocyte band 7 integral membrane protein	140	4	3	0.49	451	12	6	0.81
	20	Q00325	Phosphate carrier protein, mitochondrial	31	2	2	0.17	91	8	4	0.27

Table 13: Proteins identified in both mature and tolerogenic DC membrane-enriched fractions with emPAI scores suggesting differential expression.

Mature DC = Tolerogenic DC										
			Mature DC				Tolerogenic DC			
	Accession	Protein	Score	# Peptides	Unique	emPAI	Score	# Peptides	Unique	emPAI
1	P01903	HLA class II histocompatibility antigen, DR alpha chain	2106	55	5	0.73	1874	48	5	0.73
2	Q30167	HLA class II histocompatibility antigen, DRB1-10 beta chain	906	22	4	0.37	273	19	4	0.37
3	P20039	HLA class II histocompatibility antigen, DRB1-11 beta chain	527	22	5	0.68	333	18	5	0.68
4	Q30154	HLA class II histocompatibility antigen, DR beta 5 chain	458	23	7	0.87	316	17	6	0.87
5	P13760	HLA class II histocompatibility antigen, DRB1-4 beta chain	428	24	4	0.37	322	21	3	0.37
6	P29016	T-cell surface glycoprotein CD1b	327	5	1	0.09	195	3	1	0.09
7	P15144	Aminopeptidase N	301	22	7	0.26	419	19	8	0.26
8	P05023	Sodium/potassium-transporting ATPase subunit alpha-1	284	12	7	0.18	265	10	8	0.18
9	P04440	HLA class II histocompatibility antigen, DP beta 1 chain	271	12	4	0.38	175	8	4	0.38
10	P30485	HLA class I histocompatibility antigen, B-47 alpha chain	254	10	3	0.26	182	10	3	0.26
11	P05141	ADP/ATP translocase 2	152	12	6	0.61	523	24	6	0.61
12	P02786	Transferrin receptor protein 1	117	4	3	0.12	110	4	3	0.12
13	Q04941	Proteolipid protein 2	87	3	1	0.20	26	3	2	0.20
14	P12821	Angiotensin-converting enzyme	86	5	3	0.02	47	4	3	0.02
15	Q9BV40	Vesicle-associated membrane protein 8	73	4	2	0.69	74	3	2	0.69
16	Q9P0L0	Vesicle-associated membrane protein-associated protein A	71	1	1	0.12	137	2	1	0.12
17	P04839	Cytochrome b-245 heavy chain	70	2	2	0.05	63	1	1	0.05
18	Q5HYA8	Meckelin	51	4	2	0.03	53	4	1	0.03
19	P11279	Lysosome-associated membrane glycoprotein 1	48	1	1	0.07	129	4	1	0.07
20	Q9GIY3	HLA class II histocompatibility antigen, DRB1-14 beta chain	43	11	3	0.23	30	12	3	0.23
21	P18084	Integrin beta-5	37	2	1	0.04	23	1	1	0.04
22	P26010	Integrin beta-7	37	4	3	0.04	23	2	2	0.04
23	P60033	CD81 antigen	36	1	1	0.13	59	2	2	0.13
24	Q12791	Calcium-activated potassium channel subunit alpha-1	36	5	1	0.02	42	2	1	0.02
25	P20645	Cation-dependent mannose-6-phosphate receptor	34	3	2	0.11	55	3	2	0.11
26	Q03518	Antigen peptide transporter 1	29	2	2	0.04	27	2	2	0.04
27	Q86UE4	Protein LYRIC	29	1	1	0.05	23	2	2	0.05
28	Q8NBS3	Sodium bicarbonate transporter-like protein 11	28	10	1	0.03	28	9	2	0.03
29	Q9UKU0	Long-chain-fatty-acid--CoA ligase 6	28	1	1	0.04	42	1	1	0.04
30	Q8TAV4	Stomatin-like protein 3	27	2	2	0.10	43	1	1	0.10
31	P51841	Retinal guanylyl cyclase 2	25	5	2	0.03	32	5	2	0.03
32	Q13061	Triadin	22	2	1	0.04	19	3	1	0.04
33	Q6ZRP7	Sulfhydryl oxidase 2	22	2	1	0.04	31	3	1	0.04

Table 14: Proteins identified in both mature and tolerogenic DC membrane-enriched fractions with emPAI scores suggesting commensurate expression.

7.6. Discussion (membrane proteomes)

The case for making quantitative inferences in the absence of stable isotope labelling is strengthened somewhat by the fact that the majority of HLA Class II antigens have emPAI values which suggest that they are equally abundant in both mature and tolerogenic DCs, which is supported by cell surface profiling data from our group obtained using a pan-HLA-DR stain (Anderson *et al.*, 2008). In addition, the majority of HLA Class I antigens are detected exclusively in the mature DC fraction, which tallies with the observations of Ackerman *et al.* described above (Ackerman and Cresswell, 2003).

Of the other proteins detected exclusively in the mature DC fraction or detected in both fractions with emPAI values suggesting greater abundance in the mature DC fraction, many can once again be reconciled with roles in DC maturation and immune activation. Interactions between Integrin beta-1 (CD29) (Table 11, protein 17) and fibronectin present in the extracellular matrix have been shown to be important in dendrite formation (Swetman Andersen *et al.*, 2006) and CD29 had been shown to be upregulated in murine DCs upon LPS stimulation in a previous proteomics study (Ferret-Bernard *et al.*, 2012). Bone marrow stromal antigen 2 (CD317) (Table 11, protein 23) expression is induced in LPS-stimulated myeloid and monocyte-derived DCs and is thought to play a role in sequestration of viruses such as HIV-1 at the cell surface to prevent their dissemination to T cells (Blanchet *et al.*, 2013). Intercellular adhesion molecule 3 (CD50) (Table 11, protein 24) is the most abundantly expressed co-stimulatory ligand for T cell lymphocyte function-associated antigen 1 on blood DCs (Starling *et al.*, 1995) and integrin alpha-5 (CD49e) (Table 11, protein 28) expression is increased in lung DCs relative to peripheral blood monocytes (Nicod and el Habre, 1992). LPS-stimulated DCs from receptor-type tyrosine protein phosphatase C (CD45) (Table 13, protein 4) knockout mice exhibit a decreased capacity to elicit T_h1 responses (Cross *et al.*, 2008). Finally, CD44 (Table 13, protein 11) expression appears to be important in conferring migratory properties to mature DCs (Weiss *et al.*, 1997).

Encouragingly, a number of the proteins detected exclusively in the tolerogenic DC fraction or detected in both fractions with emPAI values suggesting greater abundance in the tolerogenic DC fraction have been reported as having established or putative roles in tolerance induction. shRNA-mediated

knockdown of CD63 (Table 13, protein 17) in Epstein-Barr virus-transformed B lymphoblastoid cells has been shown to lead to increased $CD4^+$ T cell activation through increased formation of MHC Class II-containing exosomes (Petersen *et al.*, 2011). It has been suggested that high affinity immunoglobulin epsilon receptor subunit gamma (FcεRIγ) (Table 12, protein 2) forms a signalling complex with C-type lectin domain family 4 member C (CD303) which suppresses inflammatory cytokine production in plasmacytoid dendritic cells (Cao *et al.*, 2007). Signalling lymphocyte activation molecule (CD150) (Table 12, protein 3) is upregulated on monocyte-derived DCs treated with IL-10 (McBride *et al.*, 2002) and *Taenia solium* cysticerci (Adalid-Peralta *et al.*, 2013), the latter being proposed as a parasite immune evasion strategy. Scavenger receptor cysteine-rich type protein M130 (CD163) (Table 12, protein 7) is known to be highly expressed and play a role in the anti-inflammatory properties of alternatively-activated macrophages (Moestrup and Moller, 2004); and has also previously been reported to be upregulated on dexamethasone-treated blood DCs (Maniecki *et al.*, 2006). The haemoglobin-scavenging properties of CD163 may provide more heme for degradation by heme oxygenase 1 (Table 12, protein 12), another protein detected exclusively in the tolerogenic DC membrane fraction. Heme oxygenase 1 expression by murine DCs has been shown to be essential for the suppression of effector T cell function by $CD4^+$ $CD25^+$ T_{regs} (George *et al.*, 2008). Increased expression of these two proteins in tolerogenic DCs also ties in with the increased expression of biliverdin reductase observed in the quantitative profiling of the whole cell proteomes of mature and tolerogenic DCs, as biliverdin is a degradation product of heme.

In murine XS106 cells (a DC cell line), co-stimulation of C-type lectin domain family 4 member M (CD299) (Table 12, protein 6) and TLR-2 with lipoarabinomannan and FSL-1 respectively suppresses NF-κB activation and pro-inflammatory cytokine production compared with FSL-1 stimulation alone (Ohtani *et al.*, 2012). TLR-2 (Table 12, protein 16) itself has previously been shown to be upregulated on monocyte-derived tolerogenic DCs generated using dexamethasone and vitamin D3, both alone and in synergy, by our group (Harry *et al.*, 2010) and others (Chamorro *et al.*, 2009). A recent study also demonstrated that TLR-2 signalling in murine macrophages upregulates cell surface expression of the inhibitory Fc receptor FcγRIIB (CD32b) (Abdollahi-

Roodsaz *et al.*, 2013) (Table 12, protein 20). CD32 has previously been reported to be upregulated on monocyte-derived dendritic cells in response to treatment with both dexamethasone (Piemonti *et al.*, 1999) and vitamin D3 (Piemonti *et al.*, 2000), though the antibody used in the studies did not differentiate between CD32a (activating Fc receptor FcγRIIA) and CD32b. CD32a is reported as being detected exclusively in the tolerogenic DC membrane fraction, although the peptide detected is shared with CD32b. Manual inspection of the total ion chromatograms for the peptide in question across the two fractions suggest it is relatively strongly detected in the tolerogenic DC fraction (approx. 1.5×10^4 counts) but completely absent in the mature DC fraction **(Fig. 54)**. CD32b has previously been identified by our group as highly expressed on tolerogenic DCs but absent on mature DCs in a low density array (data not shown). This raises the exciting prospect that CD32b could be used as the much sought-after quality control marker of tolerogenic phenotype discussed in section **1.2.7.**

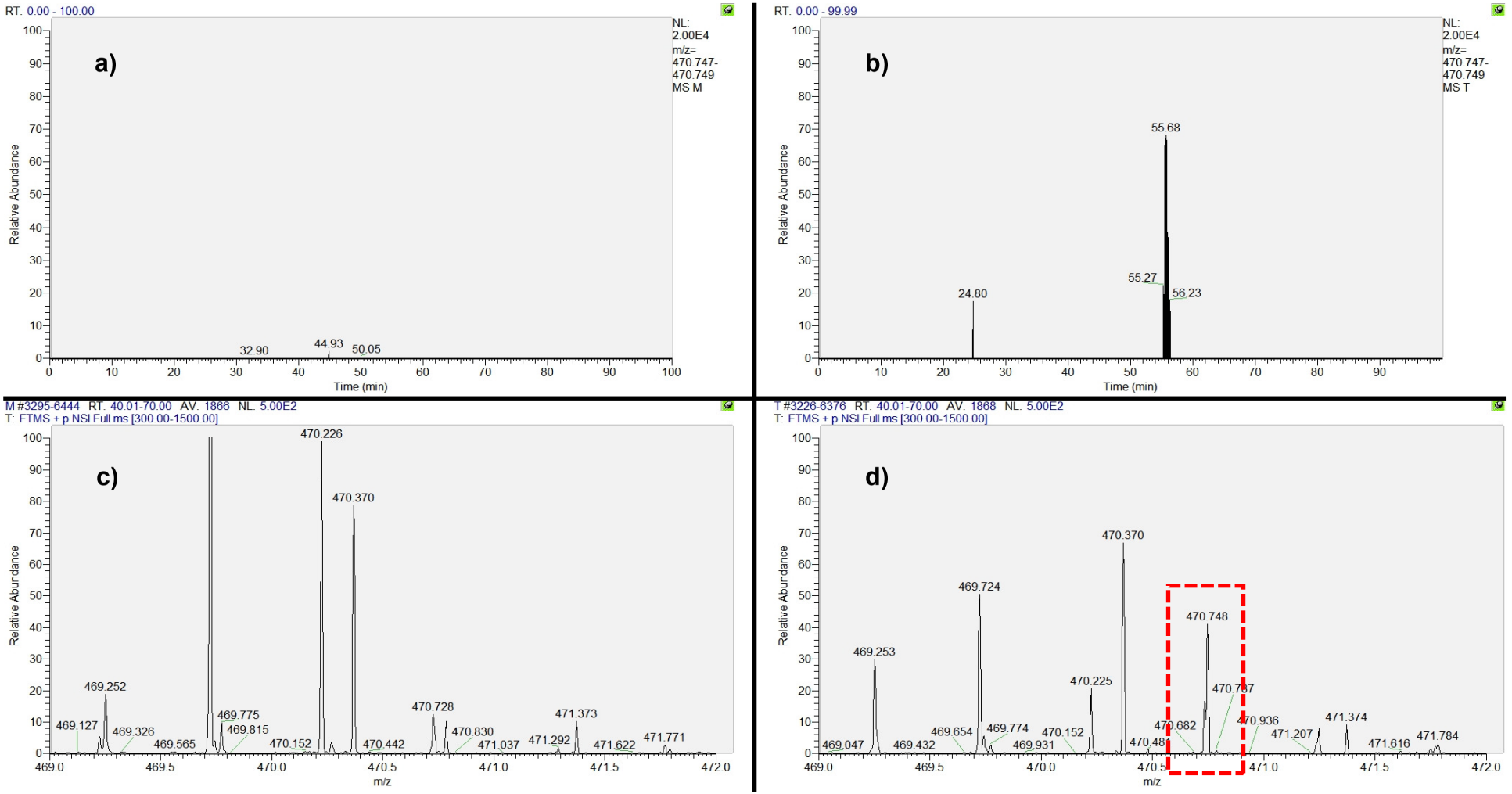

Figure 54: Extracted ion chromatograms (XICs) and MS/MS spectra for the CD32-derived peptide of interest with sequence VTFFQNGK. **a)** Mature DC XIC, **b)** tolerogenic DC XIC; **c)** mature DC MS/MS spectrum; **d)** tolerogenic DC MS/MS spectrum.

Chapter 8. General Discussion

There is little doubt that tolerogenic dendritic cells represent a promising and innovative avenue for amelioration of autoimmune pathologies. They offer the prospect of specific and enduring suppression of autoreactive T cells whilst circumventing the side effects frequently observed when using global immunosuppressive agents. Tolerogenic DC therapy for rheumatoid arthritis at Newcastle University has shown promise in preclinical studies and has just recently entered the clinic. Further progression would be both facilitated and expedited through a more thorough understanding of the mechanisms through which the cells exert their effects and the establishment of a means to positively distinguish cells as being tolerogenic (thus safeguarding against undesirable immune reactivity upon reinoculation into patients).

The overall aim of this body of work was to develop a mass spectrometry-based quantitative proteomics workflow in order to compare and contrast the plasma membrane proteomes of mature and tolerogenic DCs. Plasma membrane proteins are of paramount importance in determining the way in which a given cell responds to and interacts with its extracellular environment and other cells within it. It was envisaged that examining differential expression of plasma membrane proteins present on mature and tolerogenic DCs would enable the identification of cell surface markers of the tolerogenic phenotype and also identify proteins with a role in the induction and propagation of tolerance, thereby shedding light on some of the ambiguities in our understanding of the nature of tolerogenic DCs.

The comprehensive realization of this aim required optimization and validation of various aspects of the bottom-up proteomic workflow described in section **1.1.2.** Specifically, it was necessary to develop methods to enable extraction and isolation of plasma membrane proteins prior to proteolytic digestion, thereby favouring their detection over the more abundant cytoplasmic and nuclear proteins also present in cell lysates without any enrichment. It was also important to provide a robust means of performing relative quantitation of proteins derived from two distinct biological samples (in this case mature and tolerogenic DCs). The non-replicative nature of monocyte-derived DCs and the LC-MS instrumentation employed throughout (ion trap) precluded the use of both metabolic labelling (SILAC) and reporter ion-based MS2 quantitation (iTRAQ / TMT) respectively and consequently necessitated the development

and optimization of a different method of stable isotope labelling distinct from these more commonly employed techniques.

Herein we report that these two requirements have both been successfully met. Initial efforts to specifically isolate plasma membrane proteins using cell surface biotinylation and affinity purification did not turn out to be nearly as effective in practice as might have been anticipated. However, adaptation of a previously reported crude membrane extraction procedure (Wisniewski *et al.*, 2009a) in which non-membrane molecules are sequentially depleted prior to proteome solubilization proved considerably more fruitful; outperforming the affinity purification strategy examined here and also yielding comparable plasma membrane proteome enrichment to that reported in a wide variety of previously published strategies, in spite of its relative technical simplicity and not exclusively enriching for plasma membrane proteins. The need to employ an alternative means of stable isotope labelling to SILAC and iTRAQ / TMT was initially explored through optimization of ^{18}O-labelling such that all labelled peptides incorporated two ^{18}O atoms at their C-termini. When limitations were subsequently identified pertaining to the quantitative accuracy and dynamic range of ^{18}O-based quantitation (as detailed in **Chapter 5**), the optimized ^{18}O-labelling procedure was then further developed by coupling it with an N-terminal labelling procedure. This then enabled differential stable isotope labelling of peptide N- and C- termini and established what was, at the time, a novel means of MS2-level quantitation. This 'isobaric peptide termini labelling'-based strategy (Koehler *et al*., 2009) exhibits a dynamic range of quantitation of around an order of magnitude in either direction; is compatible with both samples from any biological origin and a wide range of mass spectrometers; and is not subject to ratio compression effects owing to mixed MS/MS (Ow *et al*., 2009).

In order to attain maximum proteome coverage, it was always our intention to perform peptide fractionation immediately prior to LC-MS analysis, although it was not anticipated that this stage of the bottom-up workflow would require optimization to the same extent. However, our experiments showed that peptide fractionation performed using OFFGEL electrophoresis (IEF) was negatively affected by the presence of N-terminal succinylation inherent to the IPTL methodology. This led to the exploration of alternative means of fractionation, culminating in the adoption and adaptation of a previously reported offline SAX

fractionation procedure (Wisniewski *et al.*, 2009a). We incorporated two additional productive elution steps, the first at pH 2 and the second at pH 2 in combination with 50% acetonitrile. This procedure both fractionates unmodified peptides as effectively as that described in the published study and additionally fractionates succinylated peptides in a considerably more uniform manner than OFFGEL electrophoresis. In addition, use of the final two elution steps have not previously been reported in a mass spectrometry-based proteomics context.

Whilst development and optimisation of the steps of the overall workflow described above were carried out using both BSA (as a model protein) and a Jurkat cell line (as model cells); efforts were made throughout to apply aspects of this workflow to mature and tolerogenic DCs themselves. Quantitative analyses of the mature and tolerogenic DC whole cell proteomes were performed using both ^{18}O-labelling and IPTL in combination with OFFGEL electrophoresis and qualitative profiling of the mature and tolerogenic DC membrane proteomes was performed with the aid of the optimized membrane extraction procedure. A number of the proteins identified as being differentially expressed in the quantitative analyses and inferred as being differentially expressed in the qualitative profiling have previously been reported as having roles in both immune activation and immune tolerance (see **Chapter 7**). Many others are less easily explained in the above context and it is also difficult to delineate those which may play roles in previously unreported aspects of the tolerogenic phenotype, especially in the absence of significant numbers of biological replicates. Nevertheless, as discussed in section **1.2.7.**, there is not a great deal known of the mechanisms by which our tolerogenic DCs induce tolerance and this profiling and comparison of the mature and tolerogenic DC membrane proteomes has putatively identified both a number of proteins which may potentially stimulate further inquiry and also a candidate quality control marker for tolerogenic cells in the form of CD32b.

Much is made of the matchup between mass spectrometry-based proteomics and the more mature technology of transcriptomics, with some suggesting that the former is well placed to usurp the latter as the go-to means of scrutinizing biological systems from a panoptic perspective (Cox and Mann, 2007). There is little doubt that proteome analysis possesses a number of conceptual and material advantages over transcriptome analysis. Proteins are the principle

executors of biological function and proteomics provides a direct readout of their presence or abundance in a sample as opposed to the mRNA-based proxy readout produced by transcriptomics. mRNA abundance measurements cannot account for the effects of protein synthesis and decay rates on the protein complement of a cell and the most comprehensive study carried out to date to address the correlation between the two sets of biological macromolecules by Schwanhäusser *et al.* suggests that only around 40% of variation in protein abundance can be attributed to variation in mRNA abundance (Schwanhausser *et al.*, 2011). Proteomics also allows for the identification and quantitation of post-translational modification isoforms, a further dimension of regulation imperceptible at the transcriptome level. On the other hand, transcriptomics continues to advance at a comparable pace to proteomics such that it is commonplace today for transcriptome data to document all transcribed gene products (Lundberg *et al.*, 2010). Powerful technologies such as RNA-Seq and RT-PCR-Seq can provide an encyclopaedic snapshot of mRNA presence and abundance at any given point in time (Howald *et al.*, 2012). Whilst it was determined at the outset that we would attempt to address the questions posed with regard to differential expression of mature and tolerogenic DC plasma membrane proteins using proteomics, they could equally have been tackled using transcriptomics. A transcriptomics approach may have given a faster readout of differential expression between the two cell types, enabling more time to be dedicated to functional follow-up studies of candidate proteins of interest for putative roles in tolerance induction. However, given the limitations described above, a proteomics approach was chosen on the basis that it was expected to deliver a more representative cell surface profile. In truth, transcriptomics and proteomics should not be seen as at odds with one another but rather as two complementary techniques which, when performed in tandem, have the potential to provide a more comprehensive picture of global protein expression than either is able to do in isolation.

Given more time and with a little further work to bring all elements of this particular proteomics workflow together would have enabled a more expansive and comprehensive quantitative comparison of the membrane proteomes of mature and tolerogenic DCs to be undertaken. This is no mean feat in itself; indeed the vast majority of in-depth membrane proteome studies published to

date have been qualitative in nature (Vuckovic *et al.*, 2013). One notable study utilized SILAC labelling, an ultracentrifugation / carbonate extraction membrane preparation method and GeLC-MS for relative quantitation of the membrane proteomes of self-renewing and differentiating human embryonic stem cells (hESCs) (Prokhorova *et al.*, 2009). 1556 proteins were identified in total, of which 811 had a membrane GO annotation (although only 438 of these 811 proteins also possessed at least one predicted transmembrane domain). Of the 811 proteins, 702 were relatively quantified using at least two peptides and a number of candidate biomarkers of the hESC differentiation state were identified.

It is not unreasonable to posit that a crucial consideration for the overall success of a membrane-directed quantitative proteomics study is the amount of peptide material that one has for LC-MS analysis having proceeded through the bottom-up workflow. Constraints can present in the form of limiting amounts of starting material and be compounded through sample losses as the workflow progresses. Such losses may be concurrent with specific steps of the workflow (for instance, around 50% of loaded material is typically recovered from the FASP procedure (Wisniewski *et al.*, 2011)) or losses may simply occur through non-specific adsorption of proteins and peptides to laboratory plastics (Bark and Hook, 2007) and glassware (Stejskal *et al.*, 2013). In the study by Prokhorova *et al.* outlined above, starting material was not limiting as replicative cell lines were used and SILAC labelling precluded the potential for sample losses during peptide-level stable isotope labelling. In our workflow, starting material is necessarily limited to the number of monocytes which can be isolated from a single component donation cone. In addition the proteomics workflow is somewhat more protracted when membrane isolation, digestion, C- and N-terminal labelling and peptide fractionation steps are considered collectively. It is unclear at present whether sufficient peptide material from our isolates can carry through the entire procedure to permit the thorough proteome coverage desired. This may represent a notable limitation of the workflow as a whole. On the other hand, if peptide material does not prove limiting, there is ample evidence in advocacy of the methods presented herein to suggest that a detailed and accurate quantitative comparison of the mature and tolerogenic DC membrane proteomes is certainly within reach.

As discussed at the very beginning of this thesis, mass spectrometry-based proteomics has come a long way since the turn of the century and has continued to develop at an unprecedented rate even within the period in which the work presented here was undertaken. Today, with the aid of long chromatography columns and gradients, 'ultra' performance LC instruments, and the latest mass spectrometers endowed with increased scanning speed, attomole sensitivity and ≥ 100 K resolving power; it is now feasible to identify thousands more distinct proteins in a single LC-MS run than was possible only 5 years ago (Thakur *et al.*, 2011). The performance of the instrumentation used throughout this body of work cannot match this latest high-end equipment in terms of scan speed and sensitivity but it can still be considered adequate in comparison to the present installed user base at most UK universities. For example, the second replicate of the SAX fractionation experiment for unmodified peptides shown in section **6.3.1.3.** yielded 82559 total and 20713 unique peptide identifications, equating to 4407 unique protein identifications; the largest number of identifications from a set of fractionated proteomic peptides during the course of this work by some distance and an impressive figure even by today's standards. Notably, these LC-MS runs were carried out with a 50 cm column, suggesting that our current LC-MS setup is adequately equipped to benefit from the movement towards long columns currently taking place. Any future attempts to consolidate the findings herein into a finalised quantitative membrane proteomics workflow would undoubtedly benefit from the use of these longer columns. Although less immediately practicable, it would also be very interesting to see how the optimised workflow and its individual components would perform were analysis carried out using cutting-edge instrumentation.

Of course, the identification of any potential biomarker is only the first phase in the protracted process which culminates in it becoming valuable from a clinical perspective, and differential expression of CD32b (and any future biomarkers) will have to be further validated using distinct approaches. Clinical biomarkers are commonly sought in biofluids (most frequently blood), in which case validation can be carried out through serum immunoassay (e.g. enzyme-linked immunosorbent assay (ELISA)). However, the nature of what is desired in this particular instance (quality control markers which conclusively define cells as

being tolerogenic *ex vivo* prior to intra-articular injection) means that the validation phase could be accomplished equally effectively using flow cytometry.

Application of either of the above techniques requires the existence of good quality antibodies against the candidate biomarker of interest. Monoclonal antibodies are already available which differentiate between the various isoforms of CD32 (Veri *et al.*, 2007) but it is possible that good quality antibodies against further biomarkers of the tolerogenic phenotype will not be available, particularly if they are less well characterized. If this proves to be the case, antibodies may be raised against molecules of interest using a technique such as selected lymphocyte antibody method (SLAM), which entails immunization of animals and subsequent isolation of B-cells specific to said molecules through haemolytic plaque assays (Babcook *et al.*, 1996) or high-throughput ELISA-based antigen binding assays. (Tickle *et al.*, 2009). Alternatively, targeted mass spectrometry-based strategies using selected reaction monitoring coupled with stable isotope dilution of labelled standards (e.g. AQUA / QconCAT peptides) allows simultaneous monitoring of 30 – 100 candidate biomarkers at detection thresholds up to 100 times lower than would be possible in an untargeted experiment (Keshishian *et al*., 2007). Sensitivity may be further increased using stable isotope standards and capture by anti-peptide antibodies (SISCAPA), in which the peptides to be monitored are first enriched using anti-peptide antibodies (Anderson *et al*., 2004). These targeted strategies have the potential to circumvent the often protracted process of raising and validating novel protein antibodies entirely.

In conclusion, the proteomic methods developed and described herein are now well poised both to facilitate the potential identification and validation of further putative markers of the tolerogenic dendritic cell phenotype and beyond that, for possible future applications in the wider field of general proteomics.

References

Abdollahi-Roodsaz, S., Koenders, M.I., Walgreen, B., Bolscher, J., Helsen, M.M., van den Bersselaar, L.A., van Lent, P.L., van de Loo, F.A. and van den Berg, W.B. (2013) 'Toll-like receptor 2 controls acute immune complex-driven arthritis in mice by regulating the inhibitory Fcgamma receptor IIB', *Arthritis Rheum*, 65(10), pp. 2583-93.

Ackerman, A.L. and Cresswell, P. (2003) 'Regulation of MHC class I transport in human dendritic cells and the dendritic-like cell line KG-1', *J Immunol*, 170(8), pp. 4178-88.

Adalid-Peralta, L., Arce-Sillas, A., Fragoso, G., Cardenas, G., Rosetti, M., Casanova-Hernandez, D., Rangel-Escareno, C., Uribe-Figueroa, L., Fleury, A. and Sciutto, E. (2013) 'Cysticerci drive dendritic cells to promote in vitro and in vivo Tregs differentiation', *Clin Dev Immunol*, 2013, p. 981468.

Agrawal, S., Agrawal, A., Doughty, B., Gerwitz, A., Blenis, J., Van Dyke, T. and Pulendran, B. (2003) 'Cutting edge: different Toll-like receptor agonists instruct dendritic cells to induce distinct Th responses via differential modulation of extracellular signal-regulated kinase-mitogen-activated protein kinase and c-Fos', *J Immunol*, 171(10), pp. 4984-9.

Al-Alwan, M.M., Rowden, G., Lee, T.D. and West, K.A. (2001) 'Fascin is involved in the antigen presentation activity of mature dendritic cells', *J Immunol*, 166(1), pp. 338-45.

Alban, A., David, S.O., Bjorkesten, L., Andersson, C., Sloge, E., Lewis, S. and Currie, I. (2003) 'A novel experimental design for comparative two-dimensional gel analysis: two-dimensional difference gel electrophoresis incorporating a pooled internal standard', *Proteomics*, 3(1), pp. 36-44.

Almen, M.S., Nordstrom, K.J., Fredriksson, R. and Schioth, H.B. (2009) 'Mapping the human membrane proteome: a majority of the human membrane proteins can be classified according to function and evolutionary origin', *BMC Biol*, 7, p. 50.

Alpert, A.J. (1990) 'Hydrophilic-interaction chromatography for the separation of peptides, nucleic acids and other polar compounds', *J Chromatogr*, 499, pp. 177-96.

Altin, J.G. and Pagler, E.B. (1995) 'A one-step procedure for biotinylation and chemical cross-linking of lymphocyte surface and intracellular membrane-associated molecules', *Anal Biochem*, 224(1), pp. 382-9.

Amster, I.J. (1996) 'Fourier Transform Mass Spectrometry', *Journal of Mass Spectrometry*, 31(12), pp. 1325-1337.

Anderson, A.E., Sayers, B.L., Haniffa, M.A., Swan, D.J., Diboll, J., Wang, X.N., Isaacs, J.D. and Hilkens, C.M. (2008) 'Differential regulation of naive and memory CD4+ T cells by alternatively activated dendritic cells', *J Leukoc Biol*, 84(1), pp. 124-33.

Anderson, A.E., Swan, D.J., Sayers, B.L., Harry, R.A., Patterson, A.M., von Delwig, A., Robinson, J.H., Isaacs, J.D. and Hilkens, C.M. (2009) 'LPS activation is required for migratory activity and antigen presentation by tolerogenic dendritic cells', *J Leukoc Biol*, 85(2), pp. 243-50.

Ang, C.S., Veith, P.D., Dashper, S.G. and Reynolds, E.C. (2008) 'Application of $^{16}O/^{18}O$ reverse proteolytic labeling to determine the effect of biofilm culture on the cell envelope proteome of *Porphyromonas gingivalis W50*', *Proteomics*, 8(8), pp. 1645-60.

Angelini, G., Gardella, S., Ardy, M., Ciriolo, M.R., Filomeni, G., Di Trapani, G., Clarke, F., Sitia, R. and Rubartelli, A. (2002) 'Antigen-presenting dendritic cells provide the reducing extracellular microenvironment required for T lymphocyte activation', *Proc Natl Acad Sci U S A*, 99(3), pp. 1491-6.

Angenieux, C., Fricker, D., Strub, J.M., Luche, S., Bausinger, H., Cazenave, J.P., Van Dorsselaer, A., Hanau, D., de la Salle, H. and Rabilloud, T. (2001) 'Gene induction during differentiation of human monocytes into dendritic cells: an integrated study at the RNA and protein levels', *Funct Integr Genomics*, 1(5), pp. 323-9.

Antharavally, B.S., Mallia, K.A., Rosenblatt, M.M., Salunkhe, A.M., Rogers, J.C., Haney, P. and Haghdoost, N. (2011) 'Efficient removal of detergents from proteins and peptides in a spin column format', *Anal Biochem*, 416(1), pp. 39-44.

Arends, M.J. and Wyllie, A.H. (1991) 'Apoptosis: mechanisms and roles in pathology', *Int Rev Exp Pathol*, 32, pp. 223-54.

Arstila, T.P., Casrouge, A., Baron, V., Even, J., Kanellopoulos, J. and Kourilsky, P. (1999) 'A direct estimate of the human alphabeta T cell receptor diversity', *Science*, 286(5441), pp. 958-61.

Ashburner, M., Ball, C.A., Blake, J.A., Botstein, D., Butler, H., Cherry, J.M., Davis, A.P., Dolinski, K., Dwight, S.S., Eppig, J.T., Harris, M.A., Hill, D.P., Issel-Tarver, L., Kasarskis, A., Lewis, S., Matese, J.C., Richardson, J.E., Ringwald, M., Rubin, G.M. and Sherlock, G. (2000) 'Gene ontology: tool for the unification of biology. The Gene Ontology Consortium', *Nat Genet*, 25(1), pp. 25-9.

Babcook, J.S., Leslie, K.B., Olsen, O.A., Salmon, R.A. and Schrader, J.W. (1996) 'A novel strategy for generating monoclonal antibodies from single, isolated lymphocytes producing antibodies of defined specificities', *Proc Natl Acad Sci U S A*, 93(15), pp. 7843-8.

Bachem, A., Guttler, S., Hartung, E., Ebstein, F., Schaefer, M., Tannert, A., Salama, A., Movassaghi, K., Opitz, C., Mages, H.W., Henn, V., Kloetzel, P.M., Gurka, S. and Kroczek, R.A. (2010) 'Superior antigen cross-presentation and XCR1 expression define human CD11c+CD141+ cells as homologues of mouse CD8+ dendritic cells', *J Exp Med*, 207(6), pp. 1273-81.

Bantscheff, M., Lemeer, S., Savitski, M.M. and Kuster, B. (2012) 'Quantitative mass spectrometry in proteomics: critical review update from 2007 to the present', *Anal Bioanal Chem*, 404(4), pp. 939-65.
Bark, S.J. and Hook, V. (2007) 'Differential recovery of peptides from sample tubes and the reproducibility of quantitative proteomic data', *J Proteome Res*, 6(11), pp. 4511-6.

Beardsley, R.L., Karty, J.A. and Reilly, J.P. (2000) 'Enhancing the intensities of lysine-terminated tryptic peptide ions in matrix-assisted laser desorption/ionization mass spectrometry', *Rapid Commun Mass Spectrom*, 14(23), pp. 2147-53.

Beardsley, R.L. and Reilly, J.P. (2002) 'Optimization of guanidination procedures for MALDI mass mapping', *Anal Chem*, 74(8), pp. 1884-90.

Bergman, M.P., Engering, A., Smits, H.H., van Vliet, S.J., van Bodegraven, A.A., Wirth, H.P., Kapsenberg, M.L., Vandenbroucke-Grauls, C.M., van Kooyk, Y. and Appelmelk, B.J. (2004) '*Helicobacter pylori* modulates the T helper cell 1/T helper cell 2 balance through phase-variable interaction between lipopolysaccharide and DC-SIGN', *J Exp Med*, 200(8), pp. 979-90.

Berkelman, T., Bandhakavi, S., Stone, M.D., Hahn-Windgassen, A. and Paulus, A. (2011) *'Use of the PROTEAN® i12TM IEF System for In-Gel Peptide Fractionation Prior to LC-MS and Comparison with Off-Gel Fractionation'.* Available: http://www.bio-rad.com/webroot/web/pdf/lsr/literature/Bulletin_6140A.pdf. Last accessed 12th Feb 2014.

Beynon, R.J., Doherty, M.K., Pratt, J.M. and Gaskell, S.J. (2005) 'Multiplexed absolute quantification in proteomics using artificial QCAT proteins of concatenated signature peptides', *Nat Methods*, 2(8), pp. 587-9.

Bezstarosti, K., Ghamari, A., Grosveld, F.G. and Demmers, J.A. (2010) 'Differential proteomics based on ^{18}O labeling to determine the cyclin dependent kinase 9 interactome', *J Proteome Res*, 9(9), pp. 4464-75.

Bhatia, V.N., Perlman, D.H., Costello, C.E. and McComb, M.E. (2009) 'Software tool for researching annotations of proteins: open-source protein annotation software with data visualization', *Anal Chem*, 81(23), pp. 9819-23.
Blagoev, B., Ong, S.E., Kratchmarova, I. and Mann, M. (2004) 'Temporal analysis of phosphotyrosine-dependent signaling networks by quantitative proteomics', *Nat Biotechnol*, 22(9), pp. 1139-45.

Blanchet, F.P., Stalder, R., Czubala, M., Lehmann, M., Rio, L., Mangeat, B. and Piguet, V. (2013) 'TLR-4 engagement of dendritic cells confers a BST-2/tetherin-mediated restriction of HIV-1 infection to CD4+ T cells across the virological synapse', *Retrovirology*, 10, p. 6.

Bodanszky, A. and Bodanszky, M. (1970) 'Sepharose-avidin column for the binding of biotin or biotin-containing peptides', *Experientia*, 26(3), p. 327.

Bondarenko, P.V., Chelius, D. and Shaler, T.A. (2002) 'Identification and relative quantitation of protein mixtures by enzymatic digestion followed by capillary reversed-phase liquid chromatography-tandem mass spectrometry', *Anal Chem*, 74(18), pp. 4741-9.

Bosserhoff, A., Wallach, J. and Frank, R.W. (1989) 'Micropreparative separation of peptides derived from sodium dodecyl sulphate-solubilized proteins', *J Chromatogr*, 473(1), pp. 71-7.

Braun, P. and von Heijne, G. (1999) 'The aromatic residues Trp and Phe have different effects on the positioning of a transmembrane helix in the microsomal membrane', *Biochemistry*, 38(30), pp. 9778-82.

Brenk, M., Scheler, M., Koch, S., Neumann, J., Takikawa, O., Hacker, G., Bieber, T. and von Bubnoff, D. (2009) 'Tryptophan deprivation induces inhibitory receptors ILT3 and ILT4 on dendritic cells favoring the induction of human CD4+CD25+ Foxp3+ T regulatory cells', *J Immunol*, 183(1), pp. 145-54.

Brinkmann, M., Teuffel, R., Laham, N., Ehrlich, R., Decker, P., Lemonnier, F.A. and Pascolo, S. (2007) 'Expression of iron transport proteins divalent metal

transporter-1, Ferroportin-1, HFE and transferrin receptor-1 in human monocyte-derived dendritic cells', *Cell Biochem Funct*, 25(3), pp. 287-96.
Brocker, T., Riedinger, M. and Karjalainen, K. (1997) 'Targeted expression of major histocompatibility complex (MHC) class II molecules demonstrates that dendritic cells can induce negative but not positive selection of thymocytes in vivo', *J Exp Med*, 185(3), pp. 541-50.

Brown, K.J. and Fenselau, C. (2004) 'Investigation of doxorubicin resistance in MCF-7 breast cancer cells using shot-gun comparative proteomics with proteolytic ^{18}O labeling', *J Proteome Res*, 3(3), pp. 455-62.

Bruder, D., Westendorf, A.M., Hansen, W., Prettin, S., Gruber, A.D., Qian, Y., von Boehmer, H., Mahnke, K. and Buer, J. (2005) 'On the edge of autoimmunity: T-cell stimulation by steady-state dendritic cells prevents autoimmune diabetes', *Diabetes*, 54(12), pp. 3395-401.

Brun, V., Dupuis, A., Adrait, A., Marcellin, M., Thomas, D., Court, M., Vandenesch, F. and Garin, J. (2007) 'Isotope-labeled protein standards: toward absolute quantitative proteomics', *Mol Cell Proteomics*, 6(12), pp. 2139-49.

Burton, D.R., Butler, M.J., Hyde, J.E., Phillips, D., Skidmore, C.J. and Walker, I.O. (1978) 'The interaction of core histones with DNA: equilibrium binding studies', *Nucleic Acids Res*, 5(10), pp. 3643-63.

Buschow, S.I., Lasonder, E., van Deutekom, H.W., Oud, M.M., Beltrame, L., Huynen, M.A., de Vries, I.J., Figdor, C.G. and Cavalieri, D. (2010) 'Dominant processes during human dendritic cell maturation revealed by integration of proteome and transcriptome at the pathway level', *J Proteome Res*, 9(4), pp. 1727-37.

Cao, R., Li, X., Liu, Z., Peng, X., Hu, W., Wang, X., Chen, P., Xie, J. and Liang, S. (2006) 'Integration of a two-phase partition method into proteomics research on rat liver plasma membrane proteins', *J Proteome Res*, 5(3), pp. 634-42.

Cao, W., Zhang, L., Rosen, D.B., Bover, L., Watanabe, G., Bao, M., Lanier, L.L. and Liu, Y.J. (2007) 'BDCA2/Fc epsilon RI gamma complex signals through a novel BCR-like pathway in human plasmacytoid dendritic cells', *PLoS Biol*, 5(10), p. e248.

Caux, C., Vanbervliet, B., Massacrier, C., Azuma, M., Okumura, K., Lanier, L.L. and Banchereau, J. (1994) 'B70/B7-2 is identical to CD86 and is the major functional ligand for CD28 expressed on human dendritic cells', *J Exp Med*, 180(5), pp. 1841-7.

Cella, M., Engering, A., Pinet, V., Pieters, J. and Lanzavecchia, A. (1997) 'Inflammatory stimuli induce accumulation of MHC class II complexes on dendritic cells', *Nature*, 388(6644), pp. 782-7.

Chamorro, S., Garcia-Vallejo, J.J., Unger, W.W., Fernandes, R.J., Bruijns, S.C., Laban, S., Roep, B.O., t Hart, B.A. and van Kooyk, Y. (2009) 'TLR triggering on tolerogenic dendritic cells results in TLR2 up-regulation and a reduced proinflammatory immune program', *J Immunol*, 183(5), pp. 2984-94.

Chaney, L.K. and Jacobson, B.S. (1983) 'Coating cells with colloidal silica for high yield isolation of plasma membrane sheets and identification of transmembrane proteins', *J Biol Chem*, 258(16), pp. 10062-72.

Chelius, D. and Bondarenko, P.V. (2002) 'Quantitative profiling of proteins in complex mixtures using liquid chromatography and mass spectrometry', *J Proteome Res*, 1(4), pp. 317-23.

Chen, W., Jin, W., Hardegen, N., Lei, K.J., Li, L., Marinos, N., McGrady, G. and Wahl, S.M. (2003) 'Conversion of peripheral CD4+CD25- naive T cells to CD4+CD25+ regulatory T cells by TGF-beta induction of transcription factor Foxp3', *J Exp Med*, 198(12), pp. 1875-86.

Christoforou, A.L. and Lilley, K.S. (2012) 'Isobaric tagging approaches in quantitative proteomics: the ups and downs', *Anal Bioanal Chem*, 404(4), pp. 1029-37.

Cindric, M., Cepo, T., Skrlin, A., Vuletic, M. and Bindila, L. (2006) 'Accelerated on-column lysine derivatization and cysteine methylation by imidazole reaction in a deuterated environment for enhanced product ion analysis', *Rapid Commun Mass Spectrom*, 20(4), pp. 694-702.

Coates, P.T., Krishnan, R., Kireta, S., Johnston, J. and Russ, G.R. (2001) 'Human myeloid dendritic cells transduced with an adenoviral interleukin-10 gene construct inhibit human skin graft rejection in humanized NOD-scid chimeric mice', *Gene Ther*, 8(16), pp. 1224-33.

Cole, S.R., Ashman, L.K. and Ey, P.L. (1987) 'Biotinylation: an alternative to radioiodination for the identification of cell surface antigens in immunoprecipitates', *Mol Immunol*, 24(7), pp. 699-705.

Collin, M., McGovern, N. and Haniffa, M. (2013) 'Human dendritic cell subsets', *Immunology*, 140(1), pp. 22-30.

Conrotto, P. and Hellman, U. (2005) 'Sulfonation chemistry as a powerful tool for MALDI TOF/TOF de novo sequencing and post-translational modification analysis', *J Biomol Tech*, 16(4), pp. 441-52.

Coombes, J.L., Siddiqui, K.R., Arancibia-Carcamo, C.V., Hall, J., Sun, C.M., Belkaid, Y. and Powrie, F. (2007) 'A functionally specialized population of mucosal CD103+ DCs induces Foxp3+ regulatory T cells via a TGF-beta and retinoic acid-dependent mechanism', *J Exp Med*, 204(8), pp. 1757-64.

Cox, J. and Mann, M. (2007) 'Is proteomics the new genomics?', *Cell*, 130(3), pp. 395-8.

Cox, J. and Mann, M. (2008) 'MaxQuant enables high peptide identification rates, individualized p.p.b.-range mass accuracies and proteome-wide protein quantification', *Nat Biotechnol*, 26(12), pp. 1367-72.

Cross, J.L., Kott, K., Miletic, T. and Johnson, P. (2008) 'CD45 regulates TLR-induced proinflammatory cytokine and IFN-beta secretion in dendritic cells', *J Immunol*, 180(12), pp. 8020-9.

Crozat, K., Guiton, R., Contreras, V., Feuillet, V., Dutertre, C.A., Ventre, E., Vu Manh, T.P., Baranek, T., Storset, A.K., Marvel, J., Boudinot, P., Hosmalin, A., Schwartz-Cornil, I. and Dalod, M. (2010) 'The XC chemokine receptor 1 is a conserved selective marker of mammalian cells homologous to mouse CD8alpha+ dendritic cells', *J Exp Med*, 207(6), pp. 1283-92.

Cuatrecasas, P. and Wilchek, M. (1968) 'Single-step purification of avidin from egg white by affinity chromatography on biocytin-Sepharose columns', *Biochemical and Biophysical Research Communications*, 33(2), pp. 235-239.

Dai, J., Wang, L.S., Wu, Y.B., Sheng, Q.H., Wu, J.R., Shieh, C.H. and Zeng, R. (2009) 'Fully automatic separation and identification of phosphopeptides by continuous pH-gradient anion exchange online coupled with reversed-phase liquid chromatography mass spectrometry', *J Proteome Res*, 8(1), pp. 133-41.

Dayon, L., Hainard, A., Licker, V., Turck, N., Kuhn, K., Hochstrasser, D.F., Burkhard, P.R. and Sanchez, J.C. (2008) 'Relative quantification of proteins in human cerebrospinal fluids by MS/MS using 6-plex isobaric tags', *Anal Chem*, 80(8), pp. 2921-31.

de Jong, E.C., Vieira, P.L., Kalinski, P. and Kapsenberg, M.L. (1999) 'Corticosteroids inhibit the production of inflammatory mediators in immature monocyte-derived DC and induce the development of tolerogenic DC3', *J Leukoc Biol*, 66(2), pp. 201-4.

de Miguel, N., Lustig, G., Twu, O., Chattopadhyay, A., Wohlschlegel, J.A. and Johnson, P.J. (2010) 'Proteome analysis of the surface of *Trichomonas vaginalis* reveals novel proteins and strain-dependent differential expression', *Mol Cell Proteomics*, 9(7), pp. 1554-66.

De Palma, A., Roveri, A., Zaccarin, M., Benazzi, L., Daminelli, S., Pantano, G., Buttarello, M., Ursini, F., Gion, M. and Mauri, P.L. (2010) 'Extraction methods of red blood cell membrane proteins for Multidimensional Protein Identification Technology (MudPIT) analysis', *J Chromatogr A*, 1217(33), pp. 5328-36.

Dhodapkar, M.V. and Steinman, R.M. (2002) 'Antigen-bearing immature dendritic cells induce peptide-specific CD8(+) regulatory T cells in vivo in humans', *Blood*, 100(1), pp. 174-7.

Dhodapkar, M.V., Steinman, R.M., Krasovsky, J., Munz, C. and Bhardwaj, N. (2001) 'Antigen-specific inhibition of effector T cell function in humans after injection of immature dendritic cells', *J Exp Med*, 193(2), pp. 233-8.

Dillon, S., Agrawal, A., Van Dyke, T., Landreth, G., McCauley, L., Koh, A., Maliszewski, C., Akira, S. and Pulendran, B. (2004) 'A Toll-like receptor 2 ligand stimulates Th2 responses in vivo, via induction of extracellular signal-regulated kinase mitogen-activated protein kinase and c-Fos in dendritic cells', *J Immunol*, 172(8), pp. 4733-43.

Durr, E., Yu, J., Krasinska, K.M., Carver, L.A., Yates, J.R., Testa, J.E., Oh, P. and Schnitzer, J.E. (2004) 'Direct proteomic mapping of the lung microvascular endothelial cell surface in vivo and in cell culture', *Nat Biotechnol*, 22(8), pp. 985-92.

Ebstein, F., Lange, N., Urban, S., Seifert, U., Kruger, E. and Kloetzel, P.M. (2009) 'Maturation of human dendritic cells is accompanied by functional remodelling of the ubiquitin-proteasome system', *Int J Biochem Cell Biol*, 41(5), pp. 1205-15.

Elias, J.E. and Gygi, S.P. (2007) 'Target-decoy search strategy for increased confidence in large-scale protein identifications by mass spectrometry', *Nat Methods*, 4(3), pp. 207-14.

Eng, J.K., McCormack, A.L. and Yates, J.R. (1994) 'An approach to correlate tandem mass spectral data of peptides with amino acid sequences in a protein database', *J Am Soc Mass Spectrom*, 5(11), pp. 976-89.

Essader, A.S., Cargile, B.J., Bundy, J.L. and Stephenson, J.L., Jr. (2005) 'A comparison of immobilized pH gradient isoelectric focusing and strong-cation-exchange chromatography as a first dimension in shotgun proteomics', *Proteomics*, 5(1), pp. 24-34.

Faca, V.M., Ventura, A.P., Fitzgibbon, M.P., Pereira-Faca, S.R., Pitteri, S.J., Green, A.E., Ireton, R.C., Zhang, Q., Wang, H., O'Briant, K.C., Drescher, C.W., Schummer, M., McIntosh, M.W., Knudsen, B.S. and Hanash, S.M. (2008) 'Proteomic analysis of ovarian cancer cells reveals dynamic processes of protein secretion and shedding of extra-cellular domains', *PLoS One*, 3(6), p. e2425.

Faure-Andre, G., Vargas, P., Yuseff, M.I., Heuze, M., Diaz, J., Lankar, D., Steri, V., Manry, J., Hugues, S., Vascotto, F., Boulanger, J., Raposo, G., Bono, M.R., Rosemblatt, M., Piel, M. and Lennon-Dumenil, A.M. (2008) 'Regulation of dendritic cell migration by CD74, the MHC class II-associated invariant chain', *Science*, 322(5908), pp. 1705-10.

Fenn, J.B., Mann, M., Meng, C.K., Wong, S.F. and Whitehouse, C.M. (1989) 'Electrospray ionization for mass spectrometry of large biomolecules', *Science*, 246(4926), pp. 64-71.

Ferreira, G.B., Kleijwegt, F.S., Waelkens, E., Lage, K., Nikolic, T., Hansen, D.A., Workman, C.T., Roep, B.O., Overbergh, L. and Mathieu, C. (2012) 'Differential protein pathways in 1,25-dihydroxyvitamin d(3) and dexamethasone modulated tolerogenic human dendritic cells', *J Proteome Res*, 11(2), pp. 941-71.

Ferreira, G.B., Mathieu, C. and Overbergh, L. (2010) 'Understanding dendritic cell biology and its role in immunological disorders through proteomic profiling', *Proteomics Clin Appl*, 4(2), pp. 190-203.

Ferreira, G.B., Overbergh, L., van Etten, E., Lage, K., D'Hertog, W., Hansen, D.A., Maris, M., Moreau, Y., Workman, C.T., Waelkens, E. and Mathieu, C. (2008) 'Protein-induced changes during the maturation process of human dendritic cells: A 2-D DIGE approach', *Proteomics Clin Appl*, 2(9), pp. 1349-60.

Ferreira, G.B., van Etten, E., Lage, K., Hansen, D.A., Moreau, Y., Workman, C.T., Waer, M., Verstuyf, A., Waelkens, E., Overbergh, L. and Mathieu, C. (2009) 'Proteome analysis demonstrates profound alterations in human dendritic cell nature by TX527, an analogue of vitamin D', *Proteomics*, 9(14), pp. 3752-64.

Ferret-Bernard, S., Castro-Borges, W., Dowle, A.A., Sanin, D.E., Cook, P.C., Turner, J.D., MacDonald, A.S., Thomas, J.R. and Mountford, A.P. (2012) 'Plasma membrane proteomes of differentially matured dendritic cells identified by LC-MS/MS combined with iTRAQ labelling', *J Proteomics*, 75(3), pp. 938-48.

Fink, A.L. and Painter, B. (1987) 'Characterization of the unfolding of ribonuclease A in aqueous methanol solvents', *Biochemistry*, 26(6), pp. 1665-71.

Fujiki, Y., Hubbard, A.L., Fowler, S. and Lazarow, P.B. (1982) 'Isolation of intracellular membranes by means of sodium carbonate treatment: application to endoplasmic reticulum', *J Cell Biol*, 93(1), pp. 97-102.

Gallien, S., Duriez, E. and Domon, B. (2011) 'Selected reaction monitoring applied to proteomics', *J Mass Spectrom*, 46(3), pp. 298-312.

Gallucci, S. and Matzinger, P. (2001) 'Danger signals: SOS to the immune system', *Curr Opin Immunol*, 13(1), pp. 114-9.

Garavito, R.M. and Ferguson-Miller, S. (2001) 'Detergents as tools in membrane biochemistry', *J Biol Chem*, 276(35), pp. 32403-6.

Garcia, J., Faca, V., Jarzembowski, J., Zhang, Q., Park, J. and Hanash, S. (2009) 'Comprehensive profiling of the cell surface proteome of Sy5Y

neuroblastoma cells yields a subset of proteins associated with tumor differentiation', *J Proteome Res*, 8(8), pp. 3791-6.

Garin, M.I., Chu, C.C., Golshayan, D., Cernuda-Morollon, E., Wait, R. and Lechler, R.I. (2007) 'Galectin-1: a key effector of regulation mediated by CD4+CD25+ T cells', *Blood*, 109(5), pp. 2058-65.

Garrett, W.S., Chen, L.M., Kroschewski, R., Ebersold, M., Turley, S., Trombetta, S., Galan, J.E. and Mellman, I. (2000) 'Developmental control of endocytosis in dendritic cells by Cdc42', *Cell*, 102(3), pp. 325-34.

Ge, Y., Lawhorn, B.G., ElNaggar, M., Strauss, E., Park, J.H., Begley, T.P. and McLafferty, F.W. (2002) 'Top down characterization of larger proteins (45 kDa) by electron capture dissociation mass spectrometry', *J Am Chem Soc*, 124(4), pp. 672-8.

Geiger, T., Cox, J., Ostasiewicz, P., Wisniewski, J.R. and Mann, M. (2010) 'Super-SILAC mix for quantitative proteomics of human tumor tissue', *Nat Methods*, 7(5), pp. 383-5.

Geijtenbeek, T.B., Van Vliet, S.J., Koppel, E.A., Sanchez-Hernandez, M., Vandenbroucke-Grauls, C.M., Appelmelk, B. and Van Kooyk, Y. (2003) 'Mycobacteria target DC-SIGN to suppress dendritic cell function', *J Exp Med*, 197(1), pp. 7-17.

Geissmann, F., Jung, S. and Littman, D.R. (2003) 'Blood monocytes consist of two principal subsets with distinct migratory properties', *Immunity*, 19(1), pp. 71-82.

George, J.F., Braun, A., Brusko, T.M., Joseph, R., Bolisetty, S., Wasserfall, C.H., Atkinson, M.A., Agarwal, A. and Kapturczak, M.H. (2008) 'Suppression by CD4+CD25+ regulatory T cells is dependent on expression of heme oxygenase-1 in antigen-presenting cells', *Am J Pathol*, 173(1), pp. 154-60.

Gerber, S.A., Rush, J., Stemman, O., Kirschner, M.W. and Gygi, S.P. (2003) 'Absolute quantification of proteins and phosphoproteins from cell lysates by tandem MS', *Proc Natl Acad Sci U S A*, 100(12), pp. 6940-5.

Ghosh, D., Krokhin, O., Antonovici, M., Ens, W., Standing, K.G., Beavis, R.C. and Wilkins, J.A. (2004) 'Lectin affinity as an approach to the proteomic analysis of membrane glycoproteins', *J Proteome Res*, 3(4), pp. 841-50.

Goo, Y.A., Yi, E.C., Baliga, N.S., Tao, W.A., Pan, M., Aebersold, R., Goodlett, D.R., Hood, L. and Ng, W.V. (2003) 'Proteomic analysis of an extreme halophilic archaeon, *Halobacterium sp. NRC-1*', *Mol Cell Proteomics*, 2(8), pp. 506-24.

Green, N.M. (1963) 'Avidin. 4. Stability at extremes of pH and dissociation into sub-units by guanidine hydrochloride', *Biochem J*, 89, pp. 609-20.

Green, N.M. (1975) 'Avidin', *Adv Protein Chem*, 29, pp. 85-133.

Greenstein, J. P. and Winitz, M. (1961) *'Chemistry of the Amino Acids'*, New York: Wiley, pp. 486 - 488.

Griss, J., Martin, M., O'Donovan, C., Apweiler, R., Hermjakob, H. and Vizcaino, J.A. (2011) 'Consequences of the discontinuation of the International Protein Index (IPI) database and its substitution by the UniProtKB "complete proteome" sets', *Proteomics*, 11(22), pp. 4434-8.

Gstaiger, M. and Aebersold, R. (2009) 'Applying mass spectrometry-based proteomics to genetics, genomics and network biology', *Nat Rev Genet*, 10(9), pp. 617-27.

Guilhaus, M. (1995) 'Principles and instrumentation in time-of-flight mass spectrometry', *Journal of Mass Spectrometry*, 30(11), pp. 1519-1532.

Gundacker, N.C., Haudek, V.J., Wimmer, H., Slany, A., Griss, J., Bochkov, V., Zielinski, C., Wagner, O., Stockl, J. and Gerner, C. (2009) 'Cytoplasmic

proteome and secretome profiles of differently stimulated human dendritic cells', *J Proteome Res*, 8(6), pp. 2799-811.

Gygi, S.P., Rist, B., Gerber, S.A., Turecek, F., Gelb, M.H. and Aebersold, R. (1999) 'Quantitative analysis of complex protein mixtures using isotope-coded affinity tags', *Nat Biotechnol*, 17(10), pp. 994-9.

Han, X., Jin, M., Breuker, K. and McLafferty, F.W. (2006) 'Extending top-down mass spectrometry to proteins with masses greater than 200 kilodaltons', *Science*, 314(5796), pp. 109-12.

Hansen, K.C., Schmitt-Ulms, G., Chalkley, R.J., Hirsch, J., Baldwin, M.A. and Burlingame, A.L. (2003) 'Mass spectrometric analysis of protein mixtures at low levels using cleavable 13C-isotope-coded affinity tag and multidimensional chromatography', *Mol Cell Proteomics*, 2(5), pp. 299-314.

Harry, R.A., Anderson, A.E., Isaacs, J.D. and Hilkens, C.M. (2010) 'Generation and characterisation of therapeutic tolerogenic dendritic cells for rheumatoid arthritis', *Ann Rheum Dis*, 69(11), pp. 2042-50.

Hartinger, J., Stenius, K., Hogemann, D. and Jahn, R. (1996) '16-BAC/SDS-PAGE: a two-dimensional gel electrophoresis system suitable for the separation of integral membrane proteins', *Anal Biochem*, 240(1), pp. 126-33.

Havlis, J. and Shevchenko, A. (2004) 'Absolute quantification of proteins in solutions and in polyacrylamide gels by mass spectrometry', *Anal Chem*, 76(11), pp. 3029-36.

Hawiger, D., Inaba, K., Dorsett, Y., Guo, M., Mahnke, K., Rivera, M., Ravetch, J.V., Steinman, R.M. and Nussenzweig, M.C. (2001) 'Dendritic cells induce peripheral T cell unresponsiveness under steady state conditions in vivo', *J Exp Med*, 194(6), pp. 769-79.

Helbig, A.O., Heck, A.J. and Slijper, M. (2010) 'Exploring the membrane proteome--challenges and analytical strategies', *J Proteomics*, 73(5), pp. 868-78.

Heller, M., Michel, P.E., Morier, P., Crettaz, D., Wenz, C., Tissot, J.D., Reymond, F. and Rossier, J.S. (2005) 'Two-stage Off-Gel isoelectric focusing: protein followed by peptide fractionation and application to proteome analysis of human plasma', *Electrophoresis*, 26(6), pp. 1174-88.

Henzel, W.J., Billeci, T.M., Stults, J.T., Wong, S.C., Grimley, C. and Watanabe, C. (1993) 'Identifying proteins from two-dimensional gels by molecular mass searching of peptide fragments in protein sequence databases', *Proc Natl Acad Sci U S A*, 90(11), pp. 5011-5.

Hermanson, G (2008) *'Bioconjugate Techniques'* 2nd ed. Academic Press, pp. 103 & 508.

Hilkens, C.M. and Isaacs, J.D. (2013) 'Tolerogenic dendritic cell therapy for rheumatoid arthritis: where are we now?', *Clin Exp Immunol*, 172(2), pp. 148-57.

Hilkens, C.M., Isaacs, J.D. and Thomson, A.W. (2010) 'Development of dendritic cell-based immunotherapy for autoimmunity', *Int Rev Immunol*, 29(2), pp. 156-83.

Hodge, K., Have, S.T., Hutton, L. and Lamond, A.I. (2013) 'Cleaning up the masses: exclusion lists to reduce contamination with HPLC-MS/MS', *J Proteomics*, 88, pp. 92-103.

Honey, K. and Rudensky, A.Y. (2003) 'Lysosomal cysteine proteases regulate antigen presentation', *Nat Rev Immunol*, 3(6), pp. 472-82.

Hood, B.L., Lucas, D.A., Kim, G., Chan, K.C., Blonder, J., Issaq, H.J., Veenstra, T.D., Conrads, T.P., Pollet, I. and Karsan, A. (2005) 'Quantitative analysis of the low molecular weight serum proteome using ^{18}O stable isotope labeling in a

lung tumor xenograft mouse model', *J Am Soc Mass Spectrom*, 16(8), pp. 1221-30.

Horth, P., Miller, C.A., Preckel, T. and Wenz, C. (2006) 'Efficient fractionation and improved protein identification by peptide OFFGEL electrophoresis', *Mol Cell Proteomics*, 5(10), pp. 1968-74.

Hortin, G.L. and Sviridov, D. (2010) 'The dynamic range problem in the analysis of the plasma proteome', *J Proteomics*, 73(3), pp. 629-36.

Howald, C., Tanzer, A., Chrast, J., Kokocinski, F., Derrien, T., Walters, N., Gonzalez, J.M., Frankish, A., Aken, B.L., Hourlier, T., Vogel, J.H., White, S., Searle, S., Harrow, J., Hubbard, T.J., Guigo, R. and Reymond, A. (2012) 'Combining RT-PCR-seq and RNA-seq to catalog all genic elements encoded in the human genome', *Genome Res*, 22(9), pp. 1698-710.

Hsu, F.J., Benike, C., Fagnoni, F., Liles, T.M., Czerwinski, D., Taidi, B., Engleman, E.G. and Levy, R. (1996) 'Vaccination of patients with B-cell lymphoma using autologous antigen-pulsed dendritic cells', *Nat Med*, 2(1), pp. 52-8.

Hsu, J.L., Huang, S.Y., Chow, N.H. and Chen, S.H. (2003) 'Stable-isotope dimethyl labeling for quantitative proteomics', *Anal Chem*, 75(24), pp. 6843-52.

Hu, Q., Noll, R.J., Li, H., Makarov, A., Hardman, M. and Graham Cooks, R. (2005) 'The Orbitrap: a new mass spectrometer', *Journal of Mass Spectrometry*, 40(4), pp. 430-443.

Hubner, N.C., Ren, S. and Mann, M. (2008) 'Peptide separation with immobilized pI strips is an attractive alternative to in-gel protein digestion for proteome analysis', *Proteomics*, 8(23-24), pp. 4862-72.

Hurley, W.L., Finkelstein, E. and Holst, B.D. (1985) 'Identification of surface proteins on bovine leukocytes by a biotin-avidin protein blotting technique', *J Immunol Methods*, 85(1), pp. 195-202.

Hurwitz, N., Pellegrini-Calace, M. and Jones, D.T. (2006) 'Towards genome-scale structure prediction for transmembrane proteins', *Philos Trans R Soc Lond B Biol Sci*, 361(1467), pp. 465-75.

Hwu, P., Du, M.X., Lapointe, R., Do, M., Taylor, M.W. and Young, H.A. (2000) 'Indoleamine 2,3-dioxygenase production by human dendritic cells results in the inhibition of T cell proliferation', *J Immunol*, 164(7), pp. 3596-9.

Ilarregui, J.M., Croci, D.O., Bianco, G.A., Toscano, M.A., Salatino, M., Vermeulen, M.E., Geffner, J.R. and Rabinovich, G.A. (2009) 'Tolerogenic signals delivered by dendritic cells to T cells through a galectin-1-driven immunoregulatory circuit involving interleukin 27 and interleukin 10', *Nat Immunol*, 10(9), pp. 981-91.

Ishihama, Y., Oda, Y., Tabata, T., Sato, T., Nagasu, T., Rappsilber, J. and Mann, M. (2005) 'Exponentially modified protein abundance index (emPAI) for estimation of absolute protein amount in proteomics by the number of sequenced peptides per protein', *Mol Cell Proteomics*, 4(9), pp. 1265-72.

Itoh, M., Takahashi, T., Sakaguchi, N., Kuniyasu, Y., Shimizu, J., Otsuka, F. and Sakaguchi, S. (1999) 'Thymus and autoimmunity: production of CD25+CD4+ naturally anergic and suppressive T cells as a key function of the thymus in maintaining immunologic self-tolerance', *J Immunol*, 162(9), pp. 5317-26.

James, P. (1997) 'Protein identification in the post-genome era: the rapid rise of proteomics', *Q Rev Biophys*, 30(4), pp. 279-331.

James, P., Quadroni, M., Carafoli, E. and Gonnet, G. (1993) 'Protein identification by mass profile fingerprinting', *Biochem Biophys Res Commun*, 195(1), pp. 58-64.

Jenkins, M.K. and Schwartz, R.H. (1987) 'Antigen presentation by chemically modified splenocytes induces antigen-specific T cell unresponsiveness in vitro and in vivo', *J Exp Med*, 165(2), pp. 302-19.

Jennings, K.R. (1968) 'Collision-induced decompositions of aromatic molecular ions', *International Journal of Mass Spectrometry and Ion Physics*, 1(3), pp. 227-235.

Jensen, O.N. (2004) 'Modification-specific proteomics: characterization of post-translational modifications by mass spectrometry', *Curr Opin Chem Biol*, 8(1), pp. 33-41.

Jongbloed, S.L., Kassianos, A.J., McDonald, K.J., Clark, G.J., Ju, X., Angel, C.E., Chen, C.J., Dunbar, P.R., Wadley, R.B., Jeet, V., Vulink, A.J., Hart, D.N. and Radford, K.J. (2010) 'Human CD141+ (BDCA-3)+ dendritic cells (DCs) represent a unique myeloid DC subset that cross-presents necrotic cell antigens', *J Exp Med*, 207(6), pp. 1247-60.

Kadowaki, N., Ho, S., Antonenko, S., Malefyt, R.W., Kastelein, R.A., Bazan, F. and Liu, Y.J. (2001) 'Subsets of human dendritic cell precursors express different toll-like receptors and respond to different microbial antigens', *J Exp Med*, 194(6), pp. 863-9.

Kalinski, P., Hilkens, C.M., Wierenga, E.A. and Kapsenberg, M.L. (1999) 'T-cell priming by type-1 and type-2 polarized dendritic cells: the concept of a third signal', *Immunol Today*, 20(12), pp. 561-7.

Kanapin, A., Batalov, S., Davis, M.J., Gough, J., Grimmond, S., Kawaji, H., Magrane, M., Matsuda, H., Schonbach, C., Teasdale, R.D. and Yuan, Z. (2003) 'Mouse proteome analysis', *Genome Res*, 13(6b), pp. 1335-44.

Karas, M. and Hillenkamp, F. (1988) 'Laser desorption ionization of proteins with molecular masses exceeding 10,000 daltons', *Anal Chem*, 60(20), pp. 2299-301.

Karp, N.A., Huber, W., Sadowski, P.G., Charles, P.D., Hester, S.V. and Lilley, K.S. (2010) 'Addressing accuracy and precision issues in iTRAQ quantitation', *Mol Cell Proteomics*, 9(9), pp. 1885-97.

Katunuma, N., Matsunaga, Y., Himeno, K. and Hayashi, Y. (2003) 'Insights into the roles of cathepsins in antigen processing and presentation revealed by specific inhibitors', *Biol Chem*, 384(6), pp. 883-90.

Kim, S.H., Kim, S., Evans, C.H., Ghivizzani, S.C., Oligino, T. and Robbins, P.D. (2001) 'Effective treatment of established murine collagen-induced arthritis by systemic administration of dendritic cells genetically modified to express IL-4', *J Immunol*, 166(5), pp. 3499-505.

Kimmel J. R. (1967) '[70] Guanidination of proteins'. In: Hirs, C. H. W. (ed) *Methods in Enzymology 11,* Academic Press, pp. 584 - 9.

Klapper, M. H. and Klotz, I. M. (1972) '[46] Acylation with dicarboxylic acid anhydrides'. In: Hirs, C. H. W. and Timasheff, S. N. (eds) *Methods in Enzymology 25,* Academic Press, pp. 531-6

Klechevsky, E., Morita, R., Liu, M., Cao, Y., Coquery, S., Thompson-Snipes, L., Briere, F., Chaussabel, D., Zurawski, G., Palucka, A.K., Reiter, Y., Banchereau, J. and Ueno, H. (2008) 'Functional specializations of human epidermal Langerhans cells and CD14+ dermal dendritic cells', *Immunity*, 29(3), pp. 497-510.

Klein, C., Garcia-Rizo, C., Bisle, B., Scheffer, B., Zischka, H., Pfeiffer, F., Siedler, F. and Oesterhelt, D. (2005) 'The membrane proteome of *Halobacterium salinarum*', *Proteomics*, 5(1), pp. 180-97.

Koehler, C.J., Arntzen, M.O., Strozynski, M., Treumann, A. and Thiede, B. (2011) 'Isobaric peptide termini labeling utilizing site-specific N-terminal succinylation', *Anal Chem*, 83(12), pp. 4775-81.

Koehler, C.J., Strozynski, M., Kozielski, F., Treumann, A. and Thiede, B. (2009) 'Isobaric peptide termini labeling for MS/MS-based quantitative proteomics', *J Proteome Res*, 8(9), pp. 4333-41.

Konstantinov, S.R., Smidt, H., de Vos, W.M., Bruijns, S.C., Singh, S.K., Valence, F., Molle, D., Lortal, S., Altermann, E., Klaenhammer, T.R. and van Kooyk, Y. (2008) 'S layer protein A of *Lactobacillus acidophilus NCFM* regulates immature dendritic cell and T cell functions', *Proc Natl Acad Sci U S A*, 105(49), pp. 19474-9.

Kraj, A. and Silberring, J. (2008) *'Proteomics: introduction to methods and applications',* New York: Wiley, p. 1

Kramer, J.L., Baltathakis, I., Alcantara, O.S. and Boldt, D.H. (2002) 'Differentiation of functional dendritic cells and macrophages from human peripheral blood monocyte precursors is dependent on expression of p21 (WAF1/CIP1) and requires iron', *Br J Haematol*, 117(3), pp. 727-34.

Kristiansen, T.Z., Harsha, H.C., Gronborg, M., Maitra, A. and Pandey, A. (2008) 'Differential membrane proteomics using ^{18}O-labeling to identify biomarkers for cholangiocarcinoma', *J Proteome Res*, 7(11), pp. 4670-7.

Krogh, A., Larsson, B., von Heijne, G. and Sonnhammer, E.L. (2001) 'Predicting transmembrane protein topology with a hidden Markov model: application to complete genomes', *J Mol Biol*, 305(3), pp. 567-80.

Kruger, M., Moser, M., Ussar, S., Thievessen, I., Luber, C.A., Forner, F., Schmidt, S., Zanivan, S., Fassler, R. and Mann, M. (2008) 'SILAC mouse for quantitative proteomics uncovers kindlin-3 as an essential factor for red blood cell function', *Cell*, 134(2), pp. 353-64.

Laemmli, U.K. (1970) 'Cleavage of structural proteins during the assembly of the head of *bacteriophage T4*', *Nature*, 227(5259), pp. 680-5.

Lan, Y.Y., Wang, Z., Raimondi, G., Wu, W., Colvin, B.L., de Creus, A. and Thomson, A.W. (2006) '"Alternatively activated" dendritic cells preferentially secrete IL-10, expand Foxp3+CD4+ T cells, and induce long-term organ allograft survival in combination with CTLA4-Ig', *J Immunol*, 177(9), pp. 5868-77.

le Maire, M., Champeil, P. and Moller, J.V. (2000) 'Interaction of membrane proteins and lipids with solubilizing detergents', *Biochim Biophys Acta*, 1508(1-2), pp. 86-111.

Le Naour, F., Hohenkirk, L., Grolleau, A., Misek, D.E., Lescure, P., Geiger, J.D., Hanash, S. and Beretta, L. (2001) 'Profiling changes in gene expression during differentiation and maturation of monocyte-derived dendritic cells using both oligonucleotide microarrays and proteomics', *J Biol Chem*, 276(21), pp. 17920-31.

Lee, A., Kolarich, D., Haynes, P.A., Jensen, P.H., Baker, M.S. and Packer, N.H. (2009) 'Rat liver membrane glycoproteome: enrichment by phase partitioning and glycoprotein capture', *J Proteome Res*, 8(2), pp. 770-81.

Li, J., Steen, H. and Gygi, S.P. (2003) 'Protein profiling with cleavable isotope-coded affinity tag (cICAT) reagents: the yeast salinity stress response', *Mol Cell Proteomics*, 2(11), pp. 1198-204.

Li, Y., Chu, N., Rostami, A. and Zhang, G.X. (2006) 'Dendritic cells transduced with SOCS-3 exhibit a tolerogenic/DC2 phenotype that directs type 2 Th cell differentiation in vitro and in vivo', *J Immunol*, 177(3), pp. 1679-88.

Liang, X., Lu, L., Chen, Z., Vickers, T., Zhang, H., Fung, J.J. and Qian, S. (2003) 'Administration of dendritic cells transduced with antisense oligodeoxyribonucleotides targeting CD80 or CD86 prolongs allograft survival', *Transplantation*, 76(4), pp. 721-9.

Liao, L., Sando, R.C., Farnum, J.B., Vanderklish, P.W., Maximov, A. and Yates, J.R. (2012) '15N-labeled brain enables quantification of proteome and phosphoproteome in cultured primary neurons', *J Proteome Res*, 11(2), pp. 1341-53.

Lim, D.S., Kang, M.S., Jeong, J.A. and Bae, Y.S. (2009) 'Semi-mature DC are immunogenic and not tolerogenic when inoculated at a high dose in collagen-induced arthritis mice', *Eur J Immunol*, 39(5), pp. 1334-43.

Lin, Y., Zhou, J., Bi, D., Chen, P., Wang, X. and Liang, S. (2008) 'Sodium-deoxycholate-assisted tryptic digestion and identification of proteolytically resistant proteins', *Anal Biochem*, 377(2), pp. 259-66.

Lipton, M.S., Pasa-Tolic, L., Anderson, G.A., Anderson, D.J., Auberry, D.L., Battista, J.R., Daly, M.J., Fredrickson, J., Hixson, K.K., Kostandarithes, H., Masselon, C., Markillie, L.M., Moore, R.J., Romine, M.F., Shen, Y., Stritmatter, E., Tolic, N., Udseth, H.R., Venkateswaran, A., Wong, K.K., Zhao, R. and Smith, R.D. (2002) 'Global analysis of the *Deinococcus radiodurans* proteome by using accurate mass tags', *Proc Natl Acad Sci U S A*, 99(17), pp. 11049-54.

Liu, H., Finch, J.W., Luongo, J.A., Li, G.Z. and Gebler, J.C. (2006) 'Development of an online two-dimensional nano-scale liquid chromatography/mass spectrometry method for improved chromatographic performance and hydrophobic peptide recovery', *J Chromatogr A*, 1135(1), pp. 43-51.

Liu, H., Sadygov, R.G. and Yates, J.R., 3rd (2004a) 'A model for random sampling and estimation of relative protein abundance in shotgun proteomics', *Anal Chem*, 76(14), pp. 4193-201.

Liu, T., Qian, W.J., Strittmatter, E.F., Camp, D.G., 2nd, Anderson, G.A., Thrall, B.D. and Smith, R.D. (2004b) 'High-throughput comparative proteome analysis using a quantitative cysteinyl-peptide enrichment technology', *Anal Chem*, 76(18), pp. 5345-53.

Liu, Z., Xu, X., Hsu, H.C., Tousson, A., Yang, P.A., Wu, Q., Liu, C., Yu, S., Zhang, H.G. and Mountz, J.D. (2003) 'CII-DC-AdTRAIL cell gene therapy inhibits infiltration of CII-reactive T cells and CII-induced arthritis', *J Clin Invest*, 112(9), pp. 1332-41.

Lodish, H., Berk, A., Zipursky, S.L., Matsuidara, P., Baltimore, D. and Darnell, J. (2000) The Actin Cytoskeleton. *Molecular Cell Biology*, Section 18.1. New York: W. H. Freeman.

Loo, R.R., Dales, N. and Andrews, P.C. (1994) 'Surfactant effects on protein structure examined by electrospray ionization mass spectrometry', *Protein Sci*, 3(11), pp. 1975-83.

Lopez-Ferrer, D., Hixson, K.K., Smallwood, H., Squier, T.C., Petritis, K. and Smith, R.D. (2009) 'Evaluation of a high-intensity focused ultrasound-immobilized trypsin digestion and ^{18}O-labeling method for quantitative proteomics', *Anal Chem*, 81(15), pp. 6272-7.

Lopez, J.L. (2007) 'Two-dimensional electrophoresis in proteome expression analysis', *J Chromatogr B Analyt Technol Biomed Life Sci*, 849(1-2), pp. 190-202.

Lorber, B., Bishop, J.B. and DeLucas, L.J. (1990) 'Purification of octyl beta-D-glucopyranoside and re-estimation of its micellar size', *Biochim Biophys Acta*, 1023(2), pp. 254-65.

Lovo, E., Zhang, M., Wang, L. and Ashton-Rickardt, P.G. (2012) 'Serine protease inhibitor 6 is required to protect dendritic cells from the kiss of death', *J Immunol*, 188(3), pp. 1057-63.

Lu, L., Gambotto, A., Lee, W.C., Qian, S., Bonham, C.A., Robbins, P.D. and Thomson, A.W. (1999) 'Adenoviral delivery of CTLA4Ig into myeloid dendritic cells promotes their in vitro tolerogenicity and survival in allogeneic recipients', *Gene Ther*, 6(4), pp. 554-63.

Lundberg, E., Fagerberg, L., Klevebring, D., Matic, I., Geiger, T., Cox, J., Algenas, C., Lundeberg, J., Mann, M. and Uhlen, M. (2010) 'Defining the transcriptome and proteome in three functionally different human cell lines', *Mol Syst Biol*, 6, p. 450.

Lundby, A. and Olsen, J.V. (2011) 'GeLCMS for in-depth protein characterization and advanced analysis of proteomes', *Methods Mol Biol*, 753, pp. 143-55.

Luo, Y., McDonald, K. and Hanrahan, J.W. (2009) 'Trafficking of immature DeltaF508-CFTR to the plasma membrane and its detection by biotinylation', *Biochem J*, 419(1), pp. 211-9, 2 p following 219.

Macagno, A., Napolitani, G., Lanzavecchia, A. and Sallusto, F. (2007) 'Duration, combination and timing: the signal integration model of dendritic cell activation', *Trends Immunol*, 28(5), pp. 227-33.

Macatonia, S.E., Hosken, N.A., Litton, M., Vieira, P., Hsieh, C.S., Culpepper, J.A., Wysocka, M., Trinchieri, G., Murphy, K.M. and O'Garra, A. (1995) 'Dendritic cells produce IL-12 and direct the development of Th1 cells from naive CD4+ T cells', *J Immunol*, 154(10), pp. 5071-9.

Macher, B.A. and Yen, T.Y. (2007) 'Proteins at membrane surfaces-a review of approaches', *Mol Biosyst*, 3(10), pp. 705-13.

Maier, K. and Wagner, E. (2012) 'Acid-labile traceless click linker for protein transduction', *J Am Chem Soc*, 134(24), pp. 10169-73.

Makkouk, A. and Abdelnoor, A.M. (2009) 'The potential use of Toll-like receptor (TLR) agonists and antagonists as prophylactic and/or therapeutic agents', *Immunopharmacol Immunotoxicol*, 31(3), pp. 331-8.

Mallick, P. and Kuster, B. (2010) 'Proteomics: a pragmatic perspective', *Nat Biotechnol*, 28(7), pp. 695-709.

Malmstrom, J., Lee, H., Nesvizhskii, A.I., Shteynberg, D., Mohanty, S., Brunner, E., Ye, M., Weber, G., Eckerskorn, C. and Aebersold, R. (2006) 'Optimized peptide separation and identification for mass spectrometry based proteomics via free-flow electrophoresis', *J Proteome Res*, 5(9), pp. 2241-9.

Manicassamy, S., Reizis, B., Ravindran, R., Nakaya, H., Salazar-Gonzalez, R.M., Wang, Y.C. and Pulendran, B. (2010) 'Activation of beta-catenin in dendritic cells regulates immunity versus tolerance in the intestine', *Science*, 329(5993), pp. 849-53.

Maniecki, M.B., Moller, H.J., Moestrup, S.K. and Moller, B.K. (2006) 'CD163 positive subsets of blood dendritic cells: the scavenging macrophage receptors CD163 and CD91 are coexpressed on human dendritic cells and monocytes', *Immunobiology*, 211(6-8), pp. 407-17.

Mann, M. (2008) 'Can proteomics retire the western blot?', *J Proteome Res*, 7(8), p. 3065.

Mann, M., Hojrup, P. and Roepstorff, P. (1993) 'Use of mass spectrometric molecular weight information to identify proteins in sequence databases', *Biol Mass Spectrom*, 22(6), pp. 338-45.

Mann, M. and Wilm, M. (1994) 'Error-tolerant identification of peptides in sequence databases by peptide sequence tags', *Anal Chem*, 66(24), pp. 4390-9.

March, R.E. (1997) 'An Introduction to Quadrupole Ion Trap Mass Spectrometry', *Journal of Mass Spectrometry*, 32(4), pp. 351-369.

Martin, E., Capini, C., Duggan, E., Lutzky, V.P., Stumbles, P., Pettit, A.R., O'Sullivan, B. and Thomas, R. (2007) 'Antigen-specific suppression of established arthritis in mice by dendritic cells deficient in NF-kappaB', *Arthritis Rheum*, 56(7), pp. 2255-66.

Matasic, R., Dietz, A.B. and Vuk-Pavlovic, S. (1999) 'Dexamethasone inhibits dendritic cell maturation by redirecting differentiation of a subset of cells', *J Leukoc Biol*, 66(6), pp. 909-14.

Matic, I., Sacchi, A., Rinaldi, A., Melino, G., Khosla, C., Falasca, L. and Piacentini, M. (2010) 'Characterization of transglutaminase type II role in dendritic cell differentiation and function', *J Leukoc Biol*, 88(1), pp. 181-8.

McBride, J.M., Jung, T., de Vries, J.E. and Aversa, G. (2002) 'IL-10 alters DC function via modulation of cell surface molecules resulting in impaired T-cell responses', *Cell Immunol*, 215(2), pp. 162-72.

McClatchy, D.B., Dong, M.Q., Wu, C.C., Venable, J.D. and Yates, J.R., 3rd (2007) '15N metabolic labeling of mammalian tissue with slow protein turnover', *J Proteome Res*, 6(5), pp. 2005-10.

McGuirk, P., McCann, C. and Mills, K.H. (2002) 'Pathogen-specific T regulatory 1 cells induced in the respiratory tract by a bacterial molecule that stimulates interleukin 10 production by dendritic cells: a novel strategy for evasion of protective T helper type 1 responses by *Bordetella pertussis*', *J Exp Med*, 195(2), pp. 221-31.

McLafferty, F.W. and Bryce, T.A. (1967) 'Metastable-ion characteristics: characterization of isomeric molecules', *Chemical Communications (London)*, (23), pp. 1215-1217.

Medawar, P. B. '*Nobel Lecture, December 12, 1960',* Available: http://www.nobelprize.org/nobel_prizes/medicine/laureates/1960/medawar-lecture.html. Last accessed 12th Feb 2014.

Means, G. E. & Feeney, R. E. (1971) *'Chemical Modification of Proteins'*. San Francisco: Holden-Day, pp. 14-15 & 68-71.

Meier, T., Arni, S., Malarkannan, S., Poincelet, M. and Hoessli, D. (1992) 'Immunodetection of biotinylated lymphocyte-surface proteins by enhanced chemiluminescence: a nonradioactive method for cell-surface protein analysis', *Anal Biochem*, 204(1), pp. 220-6.

Mellor, A.L., Baban, B., Chandler, P., Marshall, B., Jhaver, K., Hansen, A., Koni, P.A., Iwashima, M. and Munn, D.H. (2003) 'Cutting edge: induced indoleamine 2,3 dioxygenase expression in dendritic cell subsets suppresses T cell clonal expansion', *J Immunol*, 171(4), pp. 1652-5.

Michalski, A., Damoc, E., Hauschild, J.P., Lange, O., Wieghaus, A., Makarov, A., Nagaraj, N., Cox, J., Mann, M. and Horning, S. (2011) 'Mass spectrometry-based proteomics using Q Exactive, a high-performance benchtop quadrupole Orbitrap mass spectrometer', *Mol Cell Proteomics*, 10(9), p. M111.011015.

Miliotis, T., Kjellstrom, S., Nilsson, J., Laurell, T., Edholm, L.E. and Marko-Varga, G. (2000) 'Capillary liquid chromatography interfaced to matrix-assisted laser desorption/ionization time-of-flight mass spectrometry using an on-line coupled piezoelectric flow-through microdispenser', *J Mass Spectrom*, 35(3), pp. 369-77.

Min, W.P., Gorczynski, R., Huang, X.Y., Kushida, M., Kim, P., Obataki, M., Lei, J., Suri, R.M. and Cattral, M.S. (2000) 'Dendritic cells genetically engineered to express Fas ligand induce donor-specific hyporesponsiveness and prolong allograft survival', *J Immunol*, 164(1), pp. 161-7.

Mirza, S.P., Greene, A.S. and Olivier, M. (2008) '^{18}O labeling over a coffee break: a rapid strategy for quantitative proteomics', *J Proteome Res*, 7(7), pp. 3042-8.

Miyagi, M. and Rao, K.C. (2007) 'Proteolytic ^{18}O-labeling strategies for quantitative proteomics', *Mass Spectrom Rev*, 26(1), pp. 121-36.

Mobergslien, A. and Sioud, M. (2012) 'Galectin-1 and -3 gene silencing in immature and mature dendritic cells enhances T cell activation and interferon-gamma production', *J Leukoc Biol*, 91(3), pp. 461-7.

Moestrup, S.K. and Moller, H.J. (2004) 'CD163: a regulated hemoglobin scavenger receptor with a role in the anti-inflammatory response', *Ann Med*, 36(5), pp. 347-54.

Moglich, A., Krieger, F. and Kiefhaber, T. (2005) 'Molecular basis for the effect of urea and guanidinium chloride on the dynamics of unfolded polypeptide chains', *J Mol Biol*, 345(1), pp. 153-62.

Mucida, D., Park, Y., Kim, G., Turovskaya, O., Scott, I., Kronenberg, M. and Cheroutre, H. (2007) 'Reciprocal TH17 and regulatory T cell differentiation mediated by retinoic acid', *Science*, 317(5835), pp. 256-60.

Nagaraj, N., Kulak, N.A., Cox, J., Neuhauser, N., Mayr, K., Hoerning, O., Vorm, O. and Mann, M. (2012) 'System-wide perturbation analysis with nearly complete coverage of the yeast proteome by single-shot ultra HPLC runs on a bench top Orbitrap', *Mol Cell Proteomics*, 11(3), p. M111.013722.

Nagaraj, N., Lu, A., Mann, M. and Wisniewski, J.R. (2008) 'Detergent-based but gel-free method allows identification of several hundred membrane proteins in single LC-MS runs', *J Proteome Res*, 7(11), pp. 5028-32.

Napoletano, C., Pinto, D., Bellati, F., Taurino, F., Rahimi, H., Tomao, F., Panici, P.B., Rughetti, A., Frati, L. and Nuti, M. (2007) 'A comparative analysis of serum and serum-free media for generation of clinical grade DCs', *J Immunother*, 30(5), pp. 567-76.

Nesvizhskii, A.I. and Aebersold, R. (2005) 'Interpretation of shotgun proteomic data: the protein inference problem', *Mol Cell Proteomics*, 4(10), pp. 1419-40.

Nesvizhskii, A.I., Keller, A., Kolker, E. and Aebersold, R. (2003) 'A statistical model for identifying proteins by tandem mass spectrometry', *Anal Chem*, 75(17), pp. 4646-58.

Nicod, L.P. and el Habre, F. (1992) 'Adhesion molecules on human lung dendritic cells and their role for T-cell activation', *Am J Respir Cell Mol Biol*, 7(2), pp. 207-13.

Nika, H., Lee, J., Willis, I.M., Angeletti, R.H. and Hawke, D.H. (2012) 'Phosphopeptide characterization by mass spectrometry using reversed-phase supports for solid-phase beta-elimination/Michael addition', *J Biomol Tech*, 23(2), pp. 51-68.

Nika, H., Nieves, E., Hawke, D.H. and Angeletti, R.H. (2013a) 'Optimization of the beta-Elimination/Michael Addition Chemistry on Reversed-Phase Supports for Mass Spectrometry Analysis of O-Linked Protein Modifications', *J Biomol Tech*, 24(3), pp. 132-53.

Nika, H., Nieves, E., Hawke, D.H. and Angeletti, R.H. (2013b) 'Phosphopeptide enrichment by covalent chromatography after derivatization of protein digests immobilized on reversed-phase supports', *J Biomol Tech*, 24(3), pp. 154-77.

Niles, R., Witkowska, H.E., Allen, S., Hall, S.C., Fisher, S.J. and Hardt, M. (2009) 'Acid-catalyzed oxygen-18 labeling of peptides', *Anal Chem*, 81(7), pp. 2804-9.

Nilsson, J., Persson, B. and von Heijne, G. (2005) 'Comparative analysis of amino acid distributions in integral membrane proteins from 107 genomes', *Proteins*, 60(4), pp. 606-16.

Norris, J.L., Porter, N.A. and Caprioli, R.M. (2003) 'Mass spectrometry of intracellular and membrane proteins using cleavable detergents', *Anal Chem*, 75(23), pp. 6642-7.

O'Farrell, P.H. (1975) 'High resolution two-dimensional electrophoresis of proteins', *J Biol Chem*, 250(10), pp. 4007-21.

Oda, Y., Huang, K., Cross, F.R., Cowburn, D. and Chait, B.T. (1999) 'Accurate quantitation of protein expression and site-specific phosphorylation', *Proc Natl Acad Sci U S A*, 96(12), pp. 6591-6.

Oda, Y., Owa, T., Sato, T., Boucher, B., Daniels, S., Yamanaka, H., Shinohara, Y., Yokoi, A., Kuromitsu, J. and Nagasu, T. (2003) 'Quantitative chemical proteomics for identifying candidate drug targets', *Anal Chem*, 75(9), pp. 2159-65.

Ohtani, M., Iyori, M., Saeki, A., Tanizume, N., Into, T., Hasebe, A., Totsuka, Y. and Shibata, K. (2012) 'Involvement of suppressor of cytokine signalling-1-mediated degradation of MyD88-adaptor-like protein in the suppression of Toll-like receptor 2-mediated signalling by the murine C-type lectin SIGNR1-mediated signalling', *Cell Microbiol*, 14(1), pp. 40-57.

Olsen, J.V., Andersen, J.R., Nielsen, P.A., Nielsen, M.L., Figeys, D., Mann, M. and Wisniewski, J.R. (2004) 'HysTag--a novel proteomic quantification tool applied to differential display analysis of membrane proteins from distinct areas of mouse brain', *Mol Cell Proteomics*, 3(1), pp. 82-92.

Ong, S.E., Blagoev, B., Kratchmarova, I., Kristensen, D.B., Steen, H., Pandey, A. and Mann, M. (2002) 'Stable isotope labeling by amino acids in cell culture, SILAC, as a simple and accurate approach to expression proteomics', *Mol Cell Proteomics*, 1(5), pp. 376-86.

Overington, J.P., Al-Lazikani, B. and Hopkins, A.L. (2006) 'How many drug targets are there?', *Nat Rev Drug Discov*, 5(12), pp. 993-6.

Ow, S.Y., Cardona, T., Taton, A., Magnuson, A., Lindblad, P., Stensjo, K. and Wright, P.C. (2008) 'Quantitative shotgun proteomics of enriched heterocysts from *Nostoc sp. PCC 7120* using 8-plex isobaric peptide tags', *J Proteome Res*, 7(4), pp. 1615-28.

Ow, S.Y., Salim, M., Noirel, J., Evans, C., Rehman, I. and Wright, P.C. (2009) 'iTRAQ underestimation in simple and complex mixtures: "the good, the bad and the ugly"', *J Proteome Res*, 8(11), pp. 5347-55.

Palmer, E. (2003) 'Negative selection--clearing out the bad apples from the T-cell repertoire', *Nat Rev Immunol*, 3(5), pp. 383-91.

Pappin, D.J., Hojrup, P. and Bleasby, A.J. (1993) 'Rapid identification of proteins by peptide-mass fingerprinting', *Curr Biol*, 3(6), pp. 327-32.

Patra, M., Salonen, E., Terama, E., Vattulainen, I., Faller, R., Lee, B.W., Holopainen, J. and Karttunen, M. (2006) 'Under the influence of alcohol: the effect of ethanol and methanol on lipid bilayers', *Biophys J*, 90(4), pp. 1121-35.

Peirce, M.J., Wait, R., Begum, S., Saklatvala, J. and Cope, A.P. (2004) 'Expression profiling of lymphocyte plasma membrane proteins', *Mol Cell Proteomics*, 3(1), pp. 56-65.

Penna, G. and Adorini, L. (2000) '1 Alpha,25-dihydroxyvitamin D3 inhibits differentiation, maturation, activation, and survival of dendritic cells leading to impaired alloreactive T cell activation', *J Immunol*, 164(5), pp. 2405-11.

Pereira, S.R., Faca, V.M., Gomes, G.G., Chammas, R., Fontes, A.M., Covas, D.T. and Greene, L.J. (2005) 'Changes in the proteomic profile during differentiation and maturation of human monocyte-derived dendritic cells stimulated with granulocyte macrophage colony stimulating factor/interleukin-4 and lipopolysaccharide', *Proteomics*, 5(5), pp. 1186-98.

Perkins, D.N., Pappin, D.J., Creasy, D.M. and Cottrell, J.S. (1999) 'Probability-based protein identification by searching sequence databases using mass spectrometry data', *Electrophoresis*, 20(18), pp. 3551-67.

Petersen, S.H., Odintsova, E., Haigh, T.A., Rickinson, A.B., Taylor, G.S. and Berditchevski, F. (2011) 'The role of tetraspanin CD63 in antigen presentation via MHC class II', *Eur J Immunol*, 41(9), pp. 2556-61.

Petritis, B.O., Qian, W.J., Camp, D.G., 2nd and Smith, R.D. (2009) 'A simple procedure for effective quenching of trypsin activity and prevention of ^{18}O-labeling back-exchange', *J Proteome Res*, 8(5), pp. 2157-63.

Piemonti, L., Monti, P., Allavena, P., Sironi, M., Soldini, L., Leone, B.E., Socci, C. and Di Carlo, V. (1999) 'Glucocorticoids affect human dendritic cell differentiation and maturation', *J Immunol*, 162(11), pp. 6473-81.

Piemonti, L., Monti, P., Sironi, M., Fraticelli, P., Leone, B.E., Dal Cin, E., Allavena, P. and Di Carlo, V. (2000) 'Vitamin D3 affects differentiation, maturation, and function of human monocyte-derived dendritic cells', *J Immunol*, 164(9), pp. 4443-51.

Poulin, L.F., Salio, M., Griessinger, E., Anjos-Afonso, F., Craciun, L., Chen, J.L., Keller, A.M., Joffre, O., Zelenay, S., Nye, E., Le Moine, A., Faure, F., Donckier, V., Sancho, D., Cerundolo, V., Bonnet, D. and Reis e Sousa, C. (2010) 'Characterization of human DNGR-1+ BDCA3+ leukocytes as putative

equivalents of mouse CD8alpha+ dendritic cells', *J Exp Med*, 207(6), pp. 1261-71.

Probst, H.C., Lagnel, J., Kollias, G. and van den Broek, M. (2003) 'Inducible transgenic mice reveal resting dendritic cells as potent inducers of CD8+ T cell tolerance', *Immunity*, 18(5), pp. 713-20.

Prokhorova, T.A., Rigbolt, K.T., Johansen, P.T., Henningsen, J., Kratchmarova, I., Kassem, M. and Blagoev, B. (2009) 'Stable isotope labeling by amino acids in cell culture (SILAC) and quantitative comparison of the membrane proteomes of self-renewing and differentiating human embryonic stem cells', *Mol Cell Proteomics*, 8(5), pp. 959-70.

Punta, M., Forrest, L.R., Bigelow, H., Kernytsky, A., Liu, J. and Rost, B. (2007) 'Membrane protein prediction methods', *Methods*, 41(4), pp. 460-74.

Rahbar, A.M. and Fenselau, C. (2004) 'Integration of Jacobson's pellicle method into proteomic strategies for plasma membrane proteins', *J Proteome Res*, 3(6), pp. 1267-77.

Rappsilber, J., Ishihama, Y. and Mann, M. (2003) 'Stop and go extraction tips for matrix-assisted laser desorption/ionization, nanoelectrospray, and LC/MS sample pretreatment in proteomics', *Anal Chem*, 75(3), pp. 663-70.

Reich, M., Wieczerzak, E., Jankowska, E., Palesch, D., Boehm, B.O. and Burster, T. (2009) 'Specific cathepsin B inhibitor is cell-permeable and activates presentation of TTC in primary human dendritic cells', *Immunol Lett*, 123(2), pp. 155-9.

Reis e Sousa, C. (2001) 'Dendritic cells as sensors of infection', *Immunity*, 14(5), pp. 495-8.

Reithmeier, R.A. (1995) 'Characterization and modeling of membrane proteins using sequence analysis', *Curr Opin Struct Biol*, 5(4), pp. 491-500.

Rejtar, T., Hu, P., Juhasz, P., Campbell, J.M., Vestal, M.L., Preisler, J. and Karger, B.L. (2002) 'Off-line coupling of high-resolution capillary electrophoresis to MALDI-TOF and TOF/TOF MS', *J Proteome Res*, 1(2), pp. 171-9.

Ridder, A.N., Morein, S., Stam, J.G., Kuhn, A., de Kruijff, B. and Killian, J.A. (2000) 'Analysis of the role of interfacial tryptophan residues in controlling the topology of membrane proteins', *Biochemistry*, 39(21), pp. 6521-8.

Rodriguez-Ortega, M.J., Norais, N., Bensi, G., Liberatori, S., Capo, S., Mora, M., Scarselli, M., Doro, F., Ferrari, G., Garaguso, I., Maggi, T., Neumann, A., Covre, A., Telford, J.L. and Grandi, G. (2006) 'Characterization and identification of vaccine candidate proteins through analysis of the group A *Streptococcus* surface proteome', *Nat Biotechnol*, 24(2), pp. 191-7.

Roepstorff, P. and Fohlman, J. (1984) 'Proposal for a common nomenclature for sequence ions in mass spectra of peptides', *Biomed Mass Spectrom*, 11(11), p. 601.

Ross, P.L., Huang, Y.N., Marchese, J.N., Williamson, B., Parker, K., Hattan, S., Khainovski, N., Pillai, S., Dey, S., Daniels, S., Purkayastha, S., Juhasz, P., Martin, S., Bartlet-Jones, M., He, F., Jacobson, A. and Pappin, D.J. (2004) 'Multiplexed protein quantitation in *Saccharomyces cerevisiae* using amine-reactive isobaric tagging reagents', *Mol Cell Proteomics*, 3(12), pp. 1154-69.

Ross, R., Jonuleit, H., Bros, M., Ross, X.L., Yamashiro, S., Matsumura, F., Enk, A.H., Knop, J. and Reske-Kunz, A.B. (2000) 'Expression of the actin-bundling protein fascin in cultured human dendritic cells correlates with dendritic morphology and cell differentiation', *J Invest Dermatol*, 115(4), pp. 658-63.

Russell, W.K., Park, Z.Y. and Russell, D.H. (2001) 'Proteolysis in mixed organic-aqueous solvent systems: applications for peptide mass mapping using mass spectrometry', *Anal Chem*, 73(11), pp. 2682-5.

Salazar, L., Aravena, O., Abello, P., Escobar, A., Contreras-Levicoy, J., Rojas-Colonelli, N., Catalan, D., Aguirre, A., Zuniga, R., Pesce, B., Gonzalez, C.,

Cepeda, R., Cuchacovich, M., Molina, M.C., Salazar-Onfray, F., Delgado, M., Toes, R.E. and Aguillon, J.C. (2008) 'Modulation of established murine collagen-induced arthritis by a single inoculation of short-term lipopolysaccharide-stimulated dendritic cells', *Ann Rheum Dis*, 67(9), pp. 1235-41.

Sallusto, F., Cella, M., Danieli, C. and Lanzavecchia, A. (1995) 'Dendritic cells use macropinocytosis and the mannose receptor to concentrate macromolecules in the major histocompatibility complex class II compartment: downregulation by cytokines and bacterial products', *J Exp Med*, 182(2), pp. 389-400.

Sallusto, F. and Lanzavecchia, A. (1994) 'Efficient presentation of soluble antigen by cultured human dendritic cells is maintained by granulocyte/macrophage colony-stimulating factor plus interleukin 4 and downregulated by tumor necrosis factor alpha', *J Exp Med*, 179(4), pp. 1109-18.

Sallusto, F., Schaerli, P., Loetscher, P., Schaniel, C., Lenig, D., Mackay, C.R., Qin, S. and Lanzavecchia, A. (1998) 'Rapid and coordinated switch in chemokine receptor expression during dendritic cell maturation', *Eur J Immunol*, 28(9), pp. 2760-9.

Samsom, J.N., van Berkel, L.A., van Helvoort, J.M., Unger, W.W., Jansen, W., Thepen, T., Mebius, R.E., Verbeek, S.S. and Kraal, G. (2005) 'Fc gamma RIIB regulates nasal and oral tolerance: a role for dendritic cells', *J Immunol*, 174(9), pp. 5279-87.

Schagger, H. and von Jagow, G. (1991) 'Blue native electrophoresis for isolation of membrane protein complexes in enzymatically active form', *Anal Biochem*, 199(2), pp. 223-31.

Schiffer, M., Chang, C.H. and Stevens, F.J. (1992) 'The functions of tryptophan residues in membrane proteins', *Protein Eng*, 5(3), pp. 213-4.

Schindler, J., Lewandrowski, U., Sickmann, A., Friauf, E. and Nothwang, H.G. (2006) 'Proteomic analysis of brain plasma membranes isolated by affinity two-phase partitioning', *Mol Cell Proteomics*, 5(2), pp. 390-400.

Schmidt, A., Kellermann, J. and Lottspeich, F. (2005) 'A novel strategy for quantitative proteomics using isotope-coded protein labels', *Proteomics*, 5(1), pp. 4-15.

Schnolzer, M., Jedrzejewski, P. and Lehmann, W.D. (1996) 'Protease-catalyzed incorporation of ^{18}O into peptide fragments and its application for protein sequencing by electrospray and matrix-assisted laser desorption/ionization mass spectrometry', *Electrophoresis*, 17(5), pp. 945-53.

Schwanhausser, B., Busse, D., Li, N., Dittmar, G., Schuchhardt, J., Wolf, J., Chen, W. and Selbach, M. (2011) 'Global quantification of mammalian gene expression control', *Nature*, 473(7347), pp. 337-42.

Schwanhausser, B., Gossen, M., Dittmar, G. and Selbach, M. (2009) 'Global analysis of cellular protein translation by pulsed SILAC', *Proteomics*, 9(1), pp. 205-9.

Seddon, A.M., Curnow, P. and Booth, P.J. (2004) 'Membrane proteins, lipids and detergents: not just a soap opera', *Biochim Biophys Acta*, 1666(1-2), pp. 105-17.

Serbina, N.V., Salazar-Mather, T.P., Biron, C.A., Kuziel, W.A. and Pamer, E.G. (2003) 'TNF/iNOS-producing dendritic cells mediate innate immune defense against bacterial infection', *Immunity*, 19(1), pp. 59-70.

Sevinsky, J.R., Brown, K.J., Cargile, B.J., Bundy, J.L. and Stephenson, J.L., Jr. (2007) 'Minimizing back exchange in $^{18}O/^{16}O$ quantitative proteomics experiments by incorporation of immobilized trypsin into the initial digestion step', *Anal Chem*, 79(5), pp. 2158-62.

Shen, Y. and Smith, R.D. (2002) 'Proteomics based on high-efficiency capillary separations', *Electrophoresis*, 23(18), pp. 3106-24.

Shevchenko, A., Wilm, M., Vorm, O. and Mann, M. (1996) 'Mass spectrometric sequencing of proteins silver-stained polyacrylamide gels', *Anal Chem*, 68(5), pp. 850-8.

Shortman, K. and Naik, S.H. (2007) 'Steady-state and inflammatory dendritic-cell development', *Nat Rev Immunol*, 7(1), pp. 19-30.

Siegal, F.P., Kadowaki, N., Shodell, M., Fitzgerald-Bocarsly, P.A., Shah, K., Ho, S., Antonenko, S. and Liu, Y.J. (1999) 'The nature of the principal type 1 interferon-producing cells in human blood', *Science*, 284(5421), pp. 1835-7.

Smith, J.R., Olivier, M. and Greene, A.S. (2007) 'Relative quantification of peptide phosphorylation in a complex mixture using ^{18}O labeling', *Physiol Genomics*, 31(2), pp. 357-63.

Speers, A.E. and Wu, C.C. (2007) 'Proteomics of integral membrane proteins--theory and application', *Chem Rev*, 107(8), pp. 3687-714.

Speicher, K.D., Kolbas, O., Harper, S. and Speicher, D.W. (2000) 'Systematic analysis of peptide recoveries from in-gel digestions for protein identifications in proteome studies', *J Biomol Tech*, 11(2), pp. 74-86.

Spellman, D.S., Deinhardt, K., Darie, C.C., Chao, M.V. and Neubert, T.A. (2008) 'Stable isotopic labeling by amino acids in cultured primary neurons: application to brain-derived neurotrophic factor-dependent phosphotyrosine-associated signaling', *Mol Cell Proteomics*, 7(6), pp. 1067-76.

Staden, R. (1979) 'A strategy of DNA sequencing employing computer programs', *Nucleic Acids Res*, 6(7), pp. 2601-10.

Staes, A., Demol, H., Van Damme, J., Martens, L., Vandekerckhove, J. and Gevaert, K. (2004) 'Global differential non-gel proteomics by quantitative and

stable labeling of tryptic peptides with oxygen-18', *J Proteome Res*, 3(4), pp. 786-91.

Starling, G.C., McLellan, A.D., Egner, W., Sorg, R.V., Fawcett, J., Simmons, D.L. and Hart, D.N. (1995) 'Intercellular adhesion molecule-3 is the predominant co-stimulatory ligand for leukocyte function antigen-1 on human blood dendritic cells', *Eur J Immunol*, 25(9), pp. 2528-32.

Steen, H., Kuster, B. and Mann, M. (2001) 'Quadrupole time-of-flight versus triple-quadrupole mass spectrometry for the determination of phosphopeptides by precursor ion scanning', *J Mass Spectrom*, 36(7), pp. 782-90.

Steinbrink, K., Wolfl, M., Jonuleit, H., Knop, J. and Enk, A.H. (1997) 'Induction of tolerance by IL-10-treated dendritic cells', *J Immunol*, 159(10), pp. 4772-80.

Steinman, R.M. and Banchereau, J. (2007) 'Taking dendritic cells into medicine', *Nature*, 449(7161), pp. 419-26.

Steinman, R.M. and Cohn, Z.A. (1973) 'Identification of a novel cell type in peripheral lymphoid organs of mice. I. Morphology, quantitation, tissue distribution', *J Exp Med*, 137(5), pp. 1142-62.

Stejskal, K., Potesil, D. and Zdrahal, Z. (2013) 'Suppression of peptide sample losses in autosampler vials', *J Proteome Res*, 12(6), pp. 3057-62.

Stewart, II, Thomson, T. and Figeys, D. (2001) '^{18}O labeling: a tool for proteomics', *Rapid Commun Mass Spectrom*, 15(24), pp. 2456-65.

Stoop, J.N., Harry, R.A., von Delwig, A., Isaacs, J.D., Robinson, J.H. and Hilkens, C.M. (2010) 'Therapeutic effect of tolerogenic dendritic cells in established collagen-induced arthritis is associated with a reduction in Th17 responses', *Arthritis Rheum*, 62(12), pp. 3656-65.

Strom, T.B., Roy-Chaudhury, P., Manfro, R., Zheng, X.X., Nickerson, P.W., Wood, K. and Bushell, A. (1996) 'The Th1/Th2 paradigm and the allograft response', *Curr Opin Immunol*, 8(5), pp. 688-93.

Sun, C.M., Hall, J.A., Blank, R.B., Bouladoux, N., Oukka, M., Mora, J.R. and Belkaid, Y. (2007) 'Small intestine lamina propria dendritic cells promote de novo generation of Foxp3 T reg cells via retinoic acid', *J Exp Med*, 204(8), pp. 1775-85.

Sun, D., Wang, N. and Li, L. (2012) 'Integrated SDS removal and peptide separation by strong-cation exchange liquid chromatography for SDS-assisted shotgun proteome analysis', *J Proteome Res*, 11(2), pp. 818-28.

Swetman Andersen, C.A., Handley, M., Pollara, G., Ridley, A.J., Katz, D.R. and Chain, B.M. (2006) 'beta1-Integrins determine the dendritic morphology which enhances DC-SIGN-mediated particle capture by dendritic cells', *Int Immunol*, 18(8), pp. 1295-303.

Syka, J.E., Coon, J.J., Schroeder, M.J., Shabanowitz, J. and Hunt, D.F. (2004a) 'Peptide and protein sequence analysis by electron transfer dissociation mass spectrometry', *Proc Natl Acad Sci U S A*, 101(26), pp. 9528-33.

Syka, J.E., Marto, J.A., Bai, D.L., Horning, S., Senko, M.W., Schwartz, J.C., Ueberheide, B., Garcia, B., Busby, S., Muratore, T., Shabanowitz, J. and Hunt, D.F. (2004b) 'Novel linear quadrupole ion trap/FT mass spectrometer: performance characterization and use in the comparative analysis of histone H3 post-translational modifications', *J Proteome Res*, 3(3), pp. 621-6.

Szanto, A., Balint, B.L., Nagy, Z.S., Barta, E., Dezso, B., Pap, A., Szeles, L., Poliska, S., Oros, M., Evans, R.M., Barak, Y., Schwabe, J. and Nagy, L. (2010) 'STAT6 transcription factor is a facilitator of the nuclear receptor PPARgamma-regulated gene expression in macrophages and dendritic cells', *Immunity*, 33(5), pp. 699-712.

Takeuchi, O. and Akira, S. (2010) 'Pattern recognition receptors and inflammation', *Cell*, 140(6), pp. 805-20.

Tan, S., Tan, H.T. and Chung, M.C. (2008) 'Membrane proteins and membrane proteomics', *Proteomics*, 8(19), pp. 3924-32.

Thakur, S.S., Geiger, T., Chatterjee, B., Bandilla, P., Frohlich, F., Cox, J. and Mann, M. (2011) 'Deep and highly sensitive proteome coverage by LC-MS/MS without prefractionation', *Mol Cell Proteomics*, 10(8), p. M110.003699.

Thimiri Govinda Raj, D.B., Ghesquiere, B., Tharkeshwar, A.K., Coen, K., Derua, R., Vanderschaeghe, D., Rysman, E., Bagadi, M., Baatsen, P., De Strooper, B., Waelkens, E., Borghs, G., Callewaert, N., Swinnen, J., Gevaert, K. and Annaert, W. (2011) 'A novel strategy for the comprehensive analysis of the biomolecular composition of isolated plasma membranes', *Mol Syst Biol*, 7, p. 541.

Thingholm, T.E., Larsen, M.R., Ingrell, C.R., Kassem, M. and Jensen, O.N. (2008) 'TiO(2)-based phosphoproteomic analysis of the plasma membrane and the effects of phosphatase inhibitor treatment', *J Proteome Res*, 7(8), pp. 3304-13.

Thompson, A., Schafer, J., Kuhn, K., Kienle, S., Schwarz, J., Schmidt, G., Neumann, T., Johnstone, R., Mohammed, A.K. and Hamon, C. (2003) 'Tandem mass tags: a novel quantification strategy for comparative analysis of complex protein mixtures by MS/MS', *Anal Chem*, 75(8), pp. 1895-904.

Tickle, S., Adams, R., Brown, D., Griffiths, M., Lightwood, D. and Lawson, A. (2009) 'High-Throughput Screening for High Affinity Antibodies', *Journal of the Association for Laboratory Automation*, 14(5), pp. 303-307.

Tran, J.C., Zamdborg, L., Ahlf, D.R., Lee, J.E., Catherman, A.D., Durbin, K.R., Tipton, J.D., Vellaichamy, A., Kellie, J.F., Li, M., Wu, C., Sweet, S.M., Early, B.P., Siuti, N., LeDuc, R.D., Compton, P.D., Thomas, P.M. and Kelleher, N.L. (2011) 'Mapping intact protein isoforms in discovery mode using top-down proteomics', *Nature*, 480(7376), pp. 254-8.

Trinchieri, G. (2007) 'Pillars of immunology: The birth of a cell type', *J Immunol*, 178(1), pp. 3-4.

Turnquist, H.R., Raimondi, G., Zahorchak, A.F., Fischer, R.T., Wang, Z. and Thomson, A.W. (2007) 'Rapamycin-conditioned dendritic cells are poor stimulators of allogeneic CD4+ T cells, but enrich for antigen-specific Foxp3+ T regulatory cells and promote organ transplant tolerance', *J Immunol*, 178(11), pp. 7018-31.

Valencia, J., Hernandez-Lopez, C., Martinez, V.G., Hidalgo, L., Zapata, A.G., Vicente, A., Varas, A. and Sacedon, R. (2011) 'Wnt5a skews dendritic cell differentiation to an unconventional phenotype with tolerogenic features', *J Immunol*, 187(8), pp. 4129-39.

van der Kleij, D., Latz, E., Brouwers, J.F., Kruize, Y.C., Schmitz, M., Kurt-Jones, E.A., Espevik, T., de Jong, E.C., Kapsenberg, M.L., Golenbock, D.T., Tielens, A.G. and Yazdanbakhsh, M. (2002) 'A novel host-parasite lipid cross-talk. *Schistosomal* lyso-phosphatidylserine activates toll-like receptor 2 and affects immune polarization', *J Biol Chem*, 277(50), pp. 48122-9.

van Meerwijk, J.P., Marguerat, S., Lees, R.K., Germain, R.N., Fowlkes, B.J. and MacDonald, H.R. (1997) 'Quantitative impact of thymic clonal deletion on the T cell repertoire', *J Exp Med*, 185(3), pp. 377-83.

Venable, J.D., Dong, M.Q., Wohlschlegel, J., Dillin, A. and Yates, J.R. (2004) 'Automated approach for quantitative analysis of complex peptide mixtures from tandem mass spectra', *Nat Methods*, 1(1), pp. 39-45.

Veri, M.C., Gorlatov, S., Li, H., Burke, S., Johnson, S., Stavenhagen, J., Stein, K.E., Bonvini, E. and Koenig, S. (2007) 'Monoclonal antibodies capable of discriminating the human inhibitory Fcgamma-receptor IIB (CD32B) from the activating Fcgamma-receptor IIA (CD32A): biochemical, biological and functional characterization', *Immunology*, 121(3), pp. 392-404.

Voigtlander, C., Rossner, S., Cierpka, E., Theiner, G., Wiethe, C., Menges, M., Schuler, G. and Lutz, M.B. (2006) 'Dendritic cells matured with TNF can be further activated in vitro and after subcutaneous injection in vivo which converts their tolerogenicity into immunogenicity', *J Immunother*, 29(4), pp. 407-15.

von Heijne, G. and Gavel, Y. (1988) 'Topogenic signals in integral membrane proteins', *Eur J Biochem*, 174(4), pp. 671-8.

Vuckovic, D., Dagley, L.F., Purcell, A.W. and Emili, A. (2013) 'Membrane proteomics by high performance liquid chromatography-tandem mass spectrometry: Analytical approaches and challenges', *Proteomics*, 13(3-4), pp. 404-23.

Waithman, J., Allan, R.S., Kosaka, H., Azukizawa, H., Shortman, K., Lutz, M.B., Heath, W.R., Carbone, F.R. and Belz, G.T. (2007) 'Skin-derived dendritic cells can mediate deletional tolerance of class I-restricted self-reactive T cells', *J Immunol*, 179(7), pp. 4535-41.

Walker, L.S. and Abbas, A.K. (2002) 'The enemy within: keeping self-reactive T cells at bay in the periphery', *Nat Rev Immunol*, 2(1), pp. 11-9.

Wall, D.B., Berger, S.J., Finch, J.W., Cohen, S.A., Richardson, K., Chapman, R., Drabble, D., Brown, J. and Gostick, D. (2002) 'Continuous sample deposition from reversed-phase liquid chromatography to tracks on a matrix-assisted laser desorption/ionization precoated target for the analysis of protein digests', *Electrophoresis*, 23(18), pp. 3193-204.

Waner, M.J., Navrotskaya, I., Bain, A., Oldham, E.D. and Mascotti, D.P. (2004) 'Thermal and sodium dodecylsulfate induced transitions of streptavidin', *Biophys J*, 87(4), pp. 2701-13.

Wang, H., Chang-Wong, T., Tang, H.Y. and Speicher, D.W. (2010a) 'Comparison of extensive protein fractionation and repetitive LC-MS/MS analyses on depth of analysis for complex proteomes', *J Proteome Res*, 9(2), pp. 1032-40.

Wang, H., Hu, G., Zhang, Y., Yuan, Z., Zhao, X., Zhu, Y., Cai, D., Li, Y., Xiao, S. and Deng, Y. (2010b) 'Optimization and quality assessment of the post-digestion ^{18}O labeling based on urea for protein denaturation by HPLC/ESI-TOF mass spectrometry', *J Chromatogr B Analyt Technol Biomed Life Sci*, 878(22), pp. 1946-52.

Wang, R., Yan, F., Qiu, D., Jeong, J.S., Jin, Q., Kim, T.Y. and Chen, L. (2012) 'Traceless cross-linker for photocleavable bioconjugation', *Bioconjug Chem*, 23(4), pp. 705-13.

Washburn, M.P., Wolters, D. and Yates, J.R., 3rd (2001) 'Large-scale analysis of the yeast proteome by multidimensional protein identification technology', *Nat Biotechnol*, 19(3), pp. 242-7.

Weekes, M.P., Antrobus, R., Lill, J.R., Duncan, L.M., Hor, S. and Lehner, P.J. (2010) 'Comparative analysis of techniques to purify plasma membrane proteins', *J Biomol Tech*, 21(3), pp. 108-15.

Wegiel, B., Baty, C.J., Gallo, D., Csizmadia, E., Scott, J.R., Akhavan, A., Chin, B.Y., Kaczmarek, E., Alam, J., Bach, F.H., Zuckerbraun, B.S. and Otterbein, L.E. (2009) 'Cell surface biliverdin reductase mediates biliverdin-induced anti-inflammatory effects via phosphatidylinositol 3-kinase and Akt', *J Biol Chem*, 284(32), pp. 21369-78.

Wei, J., Sun, J., Yu, W., Jones, A., Oeller, P., Keller, M., Woodnutt, G. and Short, J.M. (2005) 'Global proteome discovery using an online three-dimensional LC-MS/MS', *J Proteome Res*, 4(3), pp. 801-8.

Weiss, J.M., Sleeman, J., Renkl, A.C., Dittmar, H., Termeer, C.C., Taxis, S., Howells, N., Hofmann, M., Kohler, G., Schopf, E., Ponta, H., Herrlich, P. and Simon, J.C. (1997) 'An essential role for CD44 variant isoforms in epidermal Langerhans cell and blood dendritic cell function', *J Cell Biol*, 137(5), pp. 1137-47.

Welinder, K.G. (1988) 'Generation of peptides suitable for sequence analysis by proteolytic cleavage in reversed-phase high-performance liquid chromatography solvents', *Anal Biochem*, 174(1), pp. 54-64.

Wessel, D. and Flugge, U.I. (1984) 'A method for the quantitative recovery of protein in dilute solution in the presence of detergents and lipids', *Anal Biochem*, 138(1), pp. 141-3.

Wilkins, M.R., Pasquali, C., Appel, R.D., Ou, K., Golaz, O., Sanchez, J.C., Yan, J.X., Gooley, A.A., Hughes, G., Humphery-Smith, I., Williams, K.L. and Hochstrasser, D.F. (1996) 'From proteins to proteomes: large scale protein identification by two-dimensional electrophoresis and amino acid analysis', *Biotechnology (N Y)*, 14(1), pp. 61-5.

Wisniewski, J.R., Zielinska, D.F. and Mann, M. (2011) 'Comparison of ultrafiltration units for proteomic and N-glycoproteomic analysis by the filter-aided sample preparation method', *Anal Biochem*, 410(2), pp. 307-9.

Wisniewski, J.R., Zougman, A. and Mann, M. (2009a) 'Combination of FASP and StageTip-based fractionation allows in-depth analysis of the hippocampal membrane proteome', *J Proteome Res*, 8(12), pp. 5674-8.

Wisniewski, J.R., Zougman, A., Nagaraj, N. and Mann, M. (2009b) 'Universal sample preparation method for proteome analysis', *Nat Methods*, 6(5), pp. 359-62.

Wisniewski, R.J. (2009) 'Protocol to enrich and analyze plasma membrane proteins', *Methods Mol Biol*, 528, pp. 127-34.

Wolff, A.A., Hines, D.K. and Karliner, J.S. (1989) 'Refined membrane preparations mask ischemic fall in myocardial beta-receptor density', *Am J Physiol*, 257(3 Pt 2), pp. H1032-6.

Wolters, D.A., Washburn, M.P. and Yates, J.R., 3rd (2001) 'An automated multidimensional protein identification technology for shotgun proteomics', *Anal Chem*, 73(23), pp. 5683-90.

Wood, K.J., Bushell, A.R. and Jones, N.D. (2010) 'The discovery of immunological tolerance: now more than just a laboratory solution', *J Immunol*, 184(1), pp. 3-4.

Wu, S.L., Kim, J., Hancock, W.S. and Karger, B. (2005) 'Extended Range Proteomic Analysis (ERPA): a new and sensitive LC-MS platform for high sequence coverage of complex proteins with extensive post-translational modifications-comprehensive analysis of beta-casein and epidermal growth factor receptor (EGFR)', *J Proteome Res*, 4(4), pp. 1155-70.

Wu, W.W., Wang, G., Yu, M.J., Knepper, M.A. and Shen, R.F. (2007) 'Identification and quantification of basic and acidic proteins using solution-based two-dimensional protein fractionation and label-free or ^{18}O-labeling mass spectrometry', *J Proteome Res*, 6(7), pp. 2447-59.

Xu, H., Chen, T., Wang, H.Q., Ji, M.J., Zhu, X. and Wu, W.X. (2006) 'Prolongation of rat intestinal allograft survival by administration of donor interleukin-12 *p35*-silenced bone marrow-derived dendritic cells', *Transplant Proc*, 38(5), pp. 1561-3.

Yamazaki, S., Inaba, K., Tarbell, K.V. and Steinman, R.M. (2006) 'Dendritic cells expand antigen-specific Foxp3+ CD25+ CD4+ regulatory T cells including suppressors of alloreactivity', *Immunol Rev*, 212, pp. 314-29.

Yang, S.J., Nie, A.Y., Zhang, L., Yan, G.Q., Yao, J., Xie, L.Q., Lu, H.J. and Yang, P.Y. (2012) 'A novel quantitative proteomics workflow by isobaric terminal labeling', *J Proteomics*, 75(18), pp. 5797-806.

Yao, X., Afonso, C. and Fenselau, C. (2003) 'Dissection of proteolytic ^{18}O labeling: endoprotease-catalyzed ^{16}O-to-^{18}O exchange of truncated peptide substrates', *J Proteome Res*, 2(2), pp. 147-52.

Yao, X., Freas, A., Ramirez, J., Demirev, P.A. and Fenselau, C. (2001) 'Proteolytic ^{18}O labeling for comparative proteomics: model studies with two serotypes of adenovirus', *Anal Chem*, 73(13), pp. 2836-42.

Yarilin, D., Duan, R., Huang, Y.M. and Xiao, B.G. (2002) 'Dendritic cells exposed in vitro to TGF-beta1 ameliorate experimental autoimmune myasthenia gravis', *Clin Exp Immunol*, 127(2), pp. 214-9.

Yates, J.R., 3rd (1998) 'Mass spectrometry and the age of the proteome', *J Mass Spectrom*, 33(1), pp. 1-19.

Yates, J.R., 3rd, Speicher, S., Griffin, P.R. and Hunkapiller, T. (1993) 'Peptide mass maps: a highly informative approach to protein identification', *Anal Biochem*, 214(2), pp. 397-408.

Yates, J.R., Cociorva, D., Liao, L. and Zabrouskov, V. (2006) 'Performance of a linear ion trap-Orbitrap hybrid for peptide analysis', *Anal Chem*, 78(2), pp. 493-500.

Yates, J.R., Ruse, C.I. and Nakorchevsky, A. (2009) 'Proteomics by mass spectrometry: approaches, advances, and applications', *Annu Rev Biomed Eng*, 11, pp. 49-79.

Ye, X., Luke, B.T., Johann, D.J., Jr., Ono, A., Prieto, D.A., Chan, K.C., Issaq, H.J., Veenstra, T.D. and Blonder, J. (2010) 'Optimized method for computing (18)O/(16)O ratios of differentially stable-isotope labeled peptides in the context of postdigestion (18)O exchange/labeling', *Anal Chem*, 82(13), pp. 5878-86.

Yu, Y.Q., Gilar, M., Lee, P.J., Bouvier, E.S. and Gebler, J.C. (2003) 'Enzyme-friendly, mass spectrometry-compatible surfactant for in-solution enzymatic digestion of proteins', *Anal Chem*, 75(21), pp. 6023-8.

Zang, L., Palmer Toy, D., Hancock, W.S., Sgroi, D.C. and Karger, B.L. (2004) 'Proteomic analysis of ductal carcinoma of the breast using laser capture

microdissection, LC-MS, and $^{16}O/^{18}O$ isotopic labeling', *J Proteome Res*, 3(3), pp. 604-12.

Zhang, H., Li, X.J., Martin, D.B. and Aebersold, R. (2003) 'Identification and quantification of N-linked glycoproteins using hydrazide chemistry, stable isotope labeling and mass spectrometry', *Nat Biotechnol*, 21(6), pp. 660-6.

Zhang, L., Wang, X., Peng, X., Wei, Y., Cao, R., Liu, Z., Xiong, J., Ying, X., Chen, P. and Liang, S. (2007) 'Immunoaffinity purification of plasma membrane with secondary antibody superparamagnetic beads for proteomic analysis', *J Proteome Res*, 6(1), pp. 34-43.

Zhang, L., Xie, J., Wang, X., Liu, X., Tang, X., Cao, R., Hu, W., Nie, S., Fan, C. and Liang, S. (2005) 'Proteomic analysis of mouse liver plasma membrane: use of differential extraction to enrich hydrophobic membrane proteins', *Proteomics*, 5(17), pp. 4510-24.

Zhang, N. and Li, L. (2004) 'Effects of common surfactants on protein digestion and matrix-assisted laser desorption/ionization mass spectrometric analysis of the digested peptides using two-layer sample preparation', *Rapid Commun Mass Spectrom*, 18(8), pp. 889-96.

Zhang, R., Sioma, C.S., Wang, S. and Regnier, F.E. (2001) 'Fractionation of isotopically labeled peptides in quantitative proteomics', *Anal Chem*, 73(21), pp. 5142-9.

Zhang, Y., Fonslow, B.R., Shan, B., Baek, M.C. and Yates, J.R., 3rd (2013) 'Protein analysis by shotgun/bottom-up proteomics', *Chem Rev*, 113(4), pp. 2343-94.

Zhang, Z. (2012) 'Automated precursor ion exclusion during LC-MS/MS data acquisition for optimal ion identification', *J Am Soc Mass Spectrom*, 23(8), pp. 1400-7.

Zhao, Y., Zhang, W., Kho, Y. and Zhao, Y. (2004) 'Proteomic analysis of integral plasma membrane proteins', *Anal Chem*, 76(7), pp. 1817-23.

Zheng, J., Jiang, H.Y., Li, J., Tang, H.C., Zhang, X.M., Wang, X.R., Du, J.T., Li, H.B. and Xu, G. (2012) 'MicroRNA-23b promotes tolerogenic properties of dendritic cells in vitro through inhibiting Notch1/NF-kappaB signalling pathways', *Allergy*, 67(3), pp. 362-70.

Zhong, H., Marcus, S.L. and Li, L. (2005) 'Microwave-assisted acid hydrolysis of proteins combined with liquid chromatography MALDI MS/MS for protein identification', *J Am Soc Mass Spectrom*, 16(4), pp. 471-81.

Zhou, H., Ning, Z., Starr, A.E., Abu-Farha, M. and Figeys, D. (2012a) 'Advancements in top-down proteomics', *Anal Chem*, 84(2), pp. 720-34.

Zhou, J., Zhou, T., Cao, R., Liu, Z., Shen, J., Chen, P., Wang, X. and Liang, S. (2006) 'Evaluation of the application of sodium deoxycholate to proteomic analysis of rat hippocampal plasma membrane', *J Proteome Res*, 5(10), pp. 2547-53.

Zhou, J.Y., Dann, G.P., Shi, T., Wang, L., Gao, X., Su, D., Nicora, C.D., Shukla, A.K., Moore, R.J., Liu, T., Camp, D.G., 2nd, Smith, R.D. and Qian, W.J. (2012b) 'Simple sodium dodecyl sulfate-assisted sample preparation method for LC-MS-based proteomics applications', *Anal Chem*, 84(6), pp. 2862-7.

Ziegler-Heitbrock, L., Ancuta, P., Crowe, S., Dalod, M., Grau, V., Hart, D.N., Leenen, P.J., Liu, Y.J., MacPherson, G., Randolph, G.J., Scherberich, J., Schmitz, J., Shortman, K., Sozzani, S., Strobl, H., Zembala, M., Austyn, J.M. and Lutz, M.B. (2010) 'Nomenclature of monocytes and dendritic cells in blood', *Blood*, 116(16), pp. e74-80.

Zimmer, A., Bouley, J., Le Mignon, M., Pliquet, E., Horiot, S., Turfkruyer, M., Baron-Bodo, V., Horak, F., Nony, E., Louise, A., Moussu, H., Mascarell, L. and Moingeon, P. (2012) 'A regulatory dendritic cell signature correlates with the

clinical efficacy of allergen-specific sublingual immunotherapy', *J Allergy Clin Immunol*, 129(4), pp. 1020-30.

Zubarev, R.A., Kelleher, N.L. and McLafferty, F.W. (1998) 'Electron Capture Dissociation of Multiply Charged Protein Cations. A Nonergodic Process', *Journal of the American Chemical Society*, 120(13), pp. 3265-3266.

Zuo, X. and Speicher, D.W. (2000) 'A method for global analysis of complex proteomes using sample prefractionation by solution isoelectrofocusing prior to two-dimensional electrophoresis', *Anal Biochem*, 284(2), pp. 266-78.